

**The Design and Synthesis of Diazepine Inhibitors as
Novel Anti-Cancer Agents**

A thesis submitted to Cardiff University for the degree of
Doctor of Philosophy

by

PARINAZ HAMIDI

BSc, MSc

Welsh School of Pharmacy, Cardiff University

2006

UMI Number: U584079

All rights reserved

INFORMATION TO ALL USERS

The quality of this reproduction is dependent upon the quality of the copy submitted.

In the unlikely event that the author did not send a complete manuscript and there are missing pages, these will be noted. Also, if material had to be removed, a note will indicate the deletion.



UMI U584079

Published by ProQuest LLC 2013. Copyright in the Dissertation held by the Author.
Microform Edition © ProQuest LLC.

All rights reserved. This work is protected against
unauthorized copying under Title 17, United States Code.



ProQuest LLC
789 East Eisenhower Parkway
P.O. Box 1346
Ann Arbor, MI 48106-1346

DECLARATION AND STATEMENTS

Declaration

This work has not previously been accepted in substance for any degree and is not being concurrently submitted in candidature for any degree.

Signed... *P. Hamidi*(candidate)

Date ... *31/10/06*

STATEMENT 1

This thesis is the result of my own investigations, except where otherwise stated.

Other sources are acknowledged by footnotes giving explicit references. A bibliography is appended.

Signed... *P. Hamidi*(candidate)

Date ... *31/10/06*

STATEMENT 2

I hereby give consent for my thesis, if accepted, to be available for photocopying and for inter-library loan, and for the title and summary to be made available to outside organisations.

Signed... *P. Hamidi*(candidate)

Date ... *31/10/06*

ABSTRACT

Cancer is a new growth that arises from abnormal and uncontrolled division of cells that may go on to invade and destroy surrounding tissues. The eukaryotic cell cycle consists of a complex sequence of events that regulates cell division and responses to DNA damage. These processes rely upon several key enzymes, including the cyclin dependent kinases (CDKs), checkpoint kinases (Chk2) and poly(ADP-ribose)polymerase-1 (PARP-1).

CDKs are a family of protein kinases that control progression of the cell cycle, and are themselves regulated by a complex network of activating and inhibitory mechanisms. The vital importance of CDKs in regulating of the cell cycle, emphasise their importance as anti-cancer drug targets. CDKs inhibitors compete with the natural substrate ATP in a competitive manner. Hymenialdisine and kenpaullone have been identified as novel and potent CDK inhibitors both containing an unusual azepinone scaffold.

Checkpoint kinase 2 (Chk2) is a novel target for anti-cancer drug design. The enzyme mediates cell proliferation in response to DNA damage by inducing cell cycle arrest, which facilitates the DNA repair pathways. Chk2 inhibition has been recognised as a potential target for the chemopotentialisation of current anti-cancer treatments. Few Chk2 inhibitors are known, kenpaullone has been identified as a novel and selective ATP competitive Chk2 inhibitor ($IC_{50} = 0.8 \mu M$). Debromohymenialdisine (DBH) also containing an azepinone scaffold has also been reported to inhibit Chk2.

Poly(ADP-ribose)polymerase-1 (PARP-1) is activated in response to DNA damage, and inhibition can potentiate cancer chemotherapy and radiotherapy. A PARP-1 inhibitor in combination with a cytotoxic agent should enhance drug activity by blocking the repair capabilities of PARP-1 in cancer cells.

Although many types of inhibitors have been identified for each of these three enzymes, compounds containing a seven-membered lactam ring have been identified as key inhibitors for CDKs/Chk2/PARP-1. This study is entered upon developing the synthesis for a series of novel inhibitors of these three enzymes containing the essential lactam pharmacophore in their structures. The compounds synthesised in this study were assessed by a number of biological assays showing moderate or good growth or catalytic inhibitory activity against CDKs and PARP-1 respectively, while assays against Chk2 showed no inhibition.

ACKNOWLEDGEMENTS

My first and most earnest acknowledgement must go to my supervisor Dr Alex White for his continuous guidance, encouragement and support throughout. In every sense, none of this work would have been possible without him.

Many thanks also to the staff of the Welsh School of Pharmacy for their advice and encouragement, technicians for their helps, Tenovus, and KUDOS Pharmaceuticals Ltd, Cambridge, UK for their efforts in conducting the biological assays.

My gratitude also goes to numerous friends and colleagues for their help and the generous way in which they shared their knowledge. In particular, especial thanks should go to Mathew, Jerome, Nick, Andy and Rupi for their beneficial discussions and enjoyable friendship.

Naturally I owe my parents a great debt of gratitude for being available and supportive when I needed them most.

My final and most heartfelt acknowledgment must go to my husband Behzad. His love, support, encouragement and companionship turned my time in Cardiff into a pleasure. I also should mention my lovely son Farbod, for his understanding and tolerance of his mother's absence on evenings and weekends that were devoted to this thesis.

To my husband

Behzad

CONTENTS

ABSTRACT	iii
ACKNOWLEDGEMENTS	iv
ABBREVIATIONS	ix
1 CHAPTER 1 Introduction	1
1.1 Introduction	1
1.2 The cell and The cell cycle	4
1.2.1 Cells	4
1.2.2 The cell cycle	5
1.2.3 Cell signalling	6
1.2.4 Tyrosine kinases	7
1.2.4.1 Epidermal growth factor (EGFR) and the cell cycle	7
1.2.4.2 EGFR structure and function	7
1.2.4.3 EGFR and signal transduction	8
1.2.5 Cyclin dependent kinases (CDKs)	9
1.2.6 CDK regulatory mechanisms	10
1.2.7 The monomeric CDK	11
1.2.7.1 The ATP binding site of CDKs	12
1.2.8 Natural inhibitory proteins and CDK regulation	13
1.2.8.1 CDKs regulation by INK4 family	14
1.2.8.2 CDKs regulation by Cip/Kip family	14
1.2.8.2.1. The p53 pathway	15
1.2.8.2.2. The Rb pathway	16
1.2.9 Inhibitors of cyclin dependent kinases	17
1.2.9.1 Natural product cyclin dependent kinase inhibitors	19
1.2.9.2 Synthetic cyclin dependent kinase inhibitors	21
1.2.9.3 Non-purine CDK inhibitors	23
1.3 Checkpoints	27
1.3.1 The molecular pathways associated with DNA damage ATM and ATR	28
1.3.2 The checkpoint kinases	29

1.3.3 Cell cycle checkpoints and cancer	30
1.3.4 Chk2 as a therapeutic target.....	31
1.3.4.1 Chemosensitization	31
1.3.4.2 Chemoprotection.....	32
1.3.5 Known Chk2 inhibitors	33
1.4 Poly(ADP-ribose)polymerases (PARPs).....	35
1.4.1 PARP-1: Structure and Function	36
1.4.2 Poly(ADP-ribose)polymerase-2 (PARP-2).....	39
1.4.3 Poly(ADP-ribose)polymerase-3 (PARP-3).....	40
1.4.4 Vault poly(ADP-ribose)polymerase (VPARP).....	40
1.4.5 Tankyrases.....	40
1.4.6 Pharmacological inhibitors of PARPs	41
1.4.7 Chemical inhibitors of PARPs.....	42
1.4.8 The development of existing PARP inhibitors and the PARP-1 active site	42
1.5 Aims of Research.....	46
2 CHAPTER 2 Cell Cycle Inhibitors, Results and Discussion.....	50
2.1 Efficient benzodiazepin-2-one synthesis (Bachman and Helsey, 1949)	51
2.1.1 Synthesis of N-5 benzodiazepin-2-one derivatives.....	51
2.1.1.1 Attempts to enhance the reactivity of the electrophile.....	53
2.1.1.2 An amide protecting strategy for the synthesis of benzodiazepin-2-one analogues (Annoura and Tatsuoka, 1995).....	55
2.1.1.2.1. Synthesis of the protected lead compound analogues	56
2.2 Lipophilic modification to benzodiazepine-2-one scaffold	66
2.2.1 The synthesis of modified benzodiazepin-2-one.....	66
2.2.1.1 Attempts to synthesis of modified benzodiazepin-2-one analogues	67
2.3 Synthesis of dibenzodiazepin-2-one analogues.....	68
2.3.1 Synthesis of the protected lead compound analogues	73
2.4 Synthesis of benzodiazepinone-5-one analogues	81
2.4.1 Synthesis of the protected lead compound analogues	81
2.5 Attempted synthesis of an alternative pharmacophore.....	96
2.6 Conclusions.....	102
2.7 Nomenclature	103

3	CHAPTER 3	PARP Inhibitors, Results and Discussion	106
	3.1	Introduction	106
	3.2	Synthesis of imidazodibenzodiazepinones	110
	3.2.1	Modification of 1'-aryl substituents	122
	3.2.2	Attempted carboxylic acid reduction	123
	3.3	Conclusions	134
	3.4	Nomenclature	135
4	CHAPTER 4	Biological Results and Discussion	137
	4.1	Growth inhibition assay	137
	4.1.1	Reference compound	138
	4.1.2	Benzodiazepin-2-one analogues	139
	4.1.3	4-Aminodibenzodiazepin-2-one analogues	142
	4.1.4	7-Aminobenzodiazepin-5-one analogues	144
	4.2	Checkpoint Kinase 2 (Chk2) enzyme assays	145
	4.3	PARP inhibition assays	147
	4.4	Biological Conclusions	151
	4.5	overall Conclusion	152
5	CHAPTER 5	Experimental Procedures	154
	5.1	Spectral Characterization	154
	5.1.1	NMR Spectroscopy	154
	5.1.2	Thin Layer Chromatography	155
	5.1.3	Column Chromatography	155
	5.1.4	Mass Spectroscopy	155
	5.1.5	Infrared Spectroscopy	155
	5.1.6	Melting Point	156
	5.1.7	Chemicals and Solvents	156
	5.1.8	Molecular modelling methodology	156
	5.2	General Procedures	157
	References		216
	Appendix A		240

ABBREVIATIONS

3-AB	3-Aminobenzamide
ADP	adenosine diphosphate
ATM	Ataxia-telangiectasia, mutated
ATP	Adenosine triphosphate
ATR	Ataxia-telangiectasia and Rad3-related
aq	aqueous
Bn	Benzyl
Bu	Butyl
br	broad
BRCA1	Breast cancer 1
br s	broad singlet
br t	broad triplet
CAK	CDK activating kinase
cdc25	cell division cycle 25
CDI	<i>N, N</i> -carbonyldiimidazole
CDK	Cyclin dependent kinase
CDKI	Cyclin dependent kinase inhibitory protein
Chk	Checkpoint kinase
Cip	CDK interacting protein
d	doublet
dd	double doublet
ddd	double double doublet
DCM	Dichloromethane
DMA	Dimethyl acetamide
DMAP	4-Dimethylaminopyridine
DMF	<i>N, N</i> -Dimethylformamide
DMSO	Dimethyl sulfoxide
DNA	2'-Deoxyribonucleic acid
DSB	Double strand breaks
E2F	Transcription factor

EDCI	1-(3-Dimethylaminopropyl)-3-ethylcarbodiimide hydrochloride
Et	Ethyl
G ₀	Dormant cell phase
G ₁	Gap phase one
G ₂	Gap phase two
GI ₅₀	growth inhibition 50%
h	Hour
HRMS	high resolution mass spectrometry
HU	Hydroxy urea
IC ₅₀	Inhibitory Concentration (50%)
INK4	inhibitors of CDK4 and CDK6
IR	Ionising radiation
IUPAC	international union of pure and applied chemistry
Kip	kinase inhibitory protein
m	Multiplet
M	Mitosis
M ⁺	Molecular ion
Me	methyl
MOE	molecular operating environment
mvp	major vault protein
NBS	N-bromo succinamide
NCI	National Cancer Institute
NMR	Nuclear magnetic resonance
NOE	nuclear overhauser enhancement
NOESY	nuclear overhauser enhancement spectrometry
p18	Protein inhibitor of CDK4
p19	Protein inhibitor of CDK4
p16 ^{INK4}	Protein inhibitor of CDK4
p15 ^{INK4}	Protein inhibitor of CDK4
p21	Protein inhibitor of CDK2
p27	Protein inhibitor of CDK2
p53	Product of the p53 tumour suppressor gene
PARG	poly(ADP-ribose)glycohydrolase

PARP	poly(ADP-ribose)polymerase
PDB	Protein data bank
Ph	phenyl
Petrol	Petroleum ether fraction (boiling at 60-80 °C)
ppm	Parts per million
pRb	Retinoblastoma protein
R	Alkyl or aryl group or restriction point
s	Singlet
SAR	Structure activity relationship
SEM	2-(Trimethylsilyl)ethoxymethyl
S _N 1	Substitution, nucleophilic, unimolecular
S _N 2	Substitution, nucleophilic, bimolecular
S _N Ar	Substitution, nucleophilic, aromatic
S phase	Synthesis phase
t	Triplet
TBAF	Tetrabutylammonium fluoride
TBAI	Tetrabutylammonium iodide
TBDMS	tertiary-butyl dimethyl silyl
TEA	Triethylamine
tert	tertiary
THF	Tetrahydrofuran
TLC	Thin layer chromatography
UV	Ultraviolet light
VPARP	vault poly(ADP-ribose)polymerase

CHAPTER 1

INTRODUCTION

1.1 INTRODUCTION

Cancer is a major cause of poor health and illness in all countries of the world. Each year 10.9 million people worldwide are diagnosed with cancer and there are 6.7 million deaths from the disease. It is estimated that there are 24.6 million people alive who have received a diagnosis of cancer in the last five years. However, there are large geographic differences in the incidence of cancer. These differences have often helped researchers understand more about how cancer can be caused by cultural and environmental factors. So an individual risk of developing cancer depends on many factors, including smoking behaviour, diet and genetic disorder. Overall, it is estimated that more than one in three people will develop some form of cancer during their lifetime, with one in four dying from their disease (<http://www.cancerresearchuk.org.html>, accessed 1st September 2005).

There are many classes of anti-cancer drugs including alkylating agents, DNA-targeting drugs, hormones and enzyme inhibitors. All current treatments are limited by effectiveness and side effects, and exploring new biological targets in cancer treatment is important to

develop more effective cancer treatments. The enzymes that regulate the cell cycle and DNA repair are currently under investigation as novel targets in the treatment of cancer. Deregulation of cellular mechanisms such as those controlling cell cycle progression or DNA damage contribute to the development of cancer (Morgan, 1995; Sielecki *et al.*, 2000). Almost all tumours are usually caused by cumulative effects of several mutations in a somatic cell over time which explains why the incidence of cancer generally increases with age. It is estimated that three to seven independent mutations are required (Guo and Hay, 1999).

There are several ways to treat cancers including surgery, radiotherapy and chemotherapy; the main agents currently used in chemotherapy include agents that damage DNA or disrupt DNA synthesis. Cellular responses to DNA damage constitute an important field in cancer biology (Kastan and Bartek, 2004) with potential for the design of novel therapeutic agents.

The most frequently mutated gene in human cancer has been found to be the p53 tumour suppressor gene, which is a key regulator of the cell cycle and of genome stability. This in turn will lead to deregulated control of cell cycle checkpoints, which can result in the replication of damaged DNA (Elledge, 1996; Sherr, 1996). In response to DNA damage, mammalian cells activate checkpoint regulators, to delay cell cycle progression (Tominaga *et al.*, 1999).

The cell cycle is a vital process in the body, controlling cell division and ensuring accurate duplication of genetic material. In all eukaryotic organisms it is essential that the cell cycle transitions are coordinated precisely. In cancer cells this process fails to function normally, resulting in uncontrolled cell proliferation (Ho and Dowdy, 2002).

The cyclin dependent kinases (CDKs) are a group of serine threonine kinases, which control the transition between cell cycle phases. Since cancer cells are more likely to be proliferating than non-transformed cells, the proteins that drive and control cell cycle progression are potential drug targets for anti-cancer agents. CDKs may therefore be important therapeutic targets in cancer therapy (Garrett and Fattaey, 1999; Meijer, 1996). As the majority of protein kinases belong to the same superfamily of proteins, specificity

is a major issue (Cohen, 1999; Garrett and Fattaey, 1999). However, recent development of ATP competitive protein kinase inhibitors which show high potency and specificity indicate the important role that chemical inhibitors of CDKs may play in the suppression of cell division (Garrett and Fattaey, 1999).

Progression through the cell cycle is also controlled by various surveillance mechanisms that block or delay transitions until each phase of the cell cycle is accurately completed. Recent studies in yeast, as well as in mammalian cells, have shown that these control pathways, termed checkpoints, are found in all phases of the cell cycle. Integrity of the checkpoint pathways is critical for genomic integrity (Hartwell, 1992) as well as for the repair and survival of cells exposed to DNA-damaging agents and replication inhibitors (Yu *et al.*, 2002). Cells can respond to DNA damage by activating checkpoints that delay cell cycle progression, allowing time for DNA repair. There is considerable data to suggest that DNA damage is a major contributor to the development of human cancers, it is reasonable to speculate that alterations in these pathways increase the risk of cancer developing (Kastan and Bartek, 2004). Chemical inhibitors of the G₂ phase DNA damage checkpoint may be used as tools to understand better how the checkpoint is regulated and may be used to sensitize cancer cells to DNA-damaging therapies (Curman *et al.*, 2001). Inhibitors of checkpoint regulators have the potential to increase the efficacy of DNA-damaging anti-cancer therapies by selectively increasing the sensitivity of tumour cells with checkpoint and repair defects (Zhou and Bartek, 2004). Checkpoint kinase 2 (Chk2) is a checkpoint regulator and a novel, relatively unexplored target for anti-cancer drug design. This enzyme blocks cell proliferation in response to DNA damage by inducing G₂/M cell cycle arrest; this is believed to facilitate the DNA repair process, and could be a promising target for future cancer therapy strategies (Bartek *et al.*, 2001).

Poly(ADP-ribose)polymerase-1 (PARP-1) has become an important target in cancer therapy. It is a DNA-strand break sensor activated by radiotherapy and chemotherapies that target tumour DNA (Oliver *et al.*, 2004). It initiates repair of the damage inflicted by these therapies. Interruption of this process by pharmacological inhibition of PARP-1 would limit the ability of the tumour cells to repair their damaged DNA and, therefore, increase the effects of cancer radiotherapy and DNA damaging chemotherapy (Southan and Szabo, 2003).

The discussion so far has highlighted three major enzymes, namely cyclin dependent kinases (CDKs), checkpoint kinases (Chk2) and poly(ADP-ribose)polymerases (PARPs), that are all potential targets for the treatment of cancer. Each will be explained in greater depth in the following sections.

1.2 THE CELL AND THE CELL CYCLE

1.2.1 Cells

The importance of the cell as the fundamental unit of life was first fully understood in the mid-nineteenth century, based upon the idea that both plants and animals are made of cells with the extraordinary ability to create copies of themselves by growing and dividing in two (Nurse, 1998). Therefore, new cells can arise only by the division of pre-existing cells (Murray and Hunt, 1993). To be able to reproduce new cells the existing ones must replicate their chromosomes and then separate into two daughter cells (Alberts *et al.*, 1998), Chapter 17. These daughter cells were found to closely resemble their parent and each other, and were able to repeat the process.

The adult human being is constituted of 50 trillion living cells all of which originated from the initial fertilized egg. Every second our body undergoes approximately 20 million cell divisions to compensate for continuous cell loss and death (Gray *et al.*, 1999). In the late 1970s and 1980s, in light of advances in molecular biology, scientists better understood the very basics of cell composition and this provided a frame-work for further investigation into the molecular details of cells and the cell cycle; the particular sequence of events that lead from one to two daughter cells (Nurse *et al.*, 1998).

1.2.2 The cell cycle

The cycle of duplication and division of the contents of the cell is known as the cell cycle (Alberts *et al.*, 1998), Chapter 18. The eukaryotic cell cycle is divided into four phases, G₁, S, G₂ and M and is controlled by the input of growth factor signals (Figure 1.1).

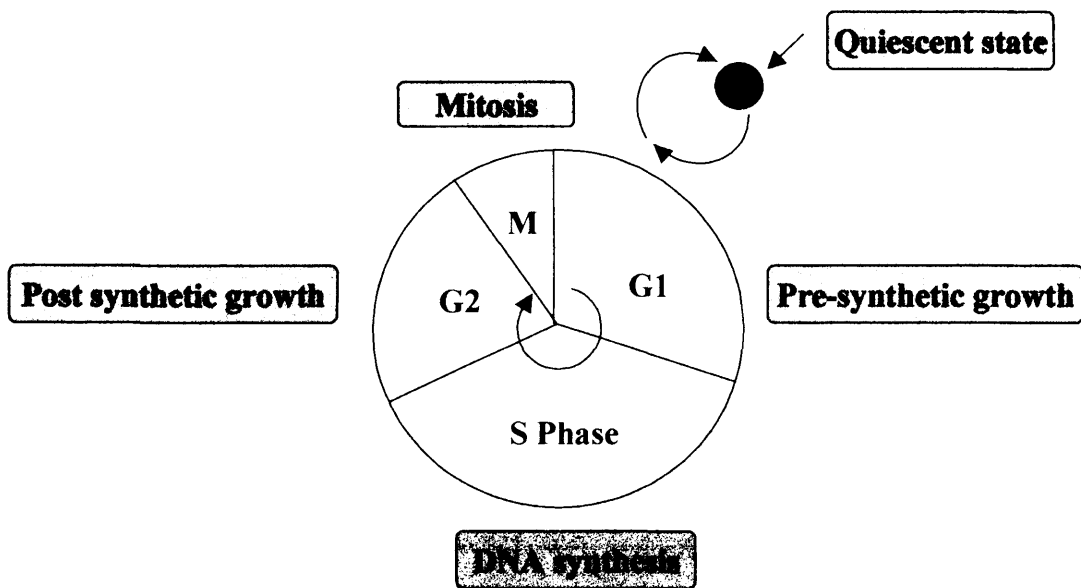


Figure 1.1 The four phases of the eukaryotic cell cycle.

The cell cycle is an ordered, tightly regulated process with multiple checkpoints that control extracellular growth signals, cell size, and DNA integrity to ensure that the events of the cell cycle take place in the correct sequence (Ho and Dowdy, 2002). Failure of these checkpoints to arrest the cell after inappropriate chromosome replication and segregation is a hallmark of cancer (Hartwell and Kastan, 1994; Swanton, 2004). The most significant event is M phase, consisting of mitosis (nuclear division) and cytokinesis (cell separation) (Crews and Mohan, 2000; Johnson and Walker, 1999).

In a mammalian cell, M phase takes about an hour, which is only a small fraction of the whole cell cycle period. M phase represents actual cell division, the time between two M phases is called interphase, which is the period during which both cell growth and DNA synthesis occurs in preparation for cell division (Crews and Mohan, 2000; Johnson and Walker, 1999).

Interphase is further subdivided into the remaining three phases of the cell cycle (Cooper, 2000). S phase, during which DNA synthesis and cell enlargement occurs, is flanked by two gap phases G_1 and G_2 . The G_1 phase, is a preparatory phase during which the enzymes necessary for DNA synthesis are produced and the cell mass increases in order to support division. In the G_2 phase the cell prepares for mitosis with two complete sets of chromosomes. In addition to G_1 , S, G_2 and M, the term G_0 is used to describe cells that have exited the cell cycle and become quiescent (Johnson and Walker, 1999). Most of the cells within a healthy organism are in this non-dividing (quiescent) state. In quiescent cells, DNA has not yet duplicated. Upon appropriate external stimulation, G_0 cells can enter the cell cycle into early G_1 , also cycling cells present in early G_1 can exit into G_0 in the lack of external growth stimulus (Zetterberg *et al.*, 1995). The cell cycle is very responsive to extracellular signals, such as growth factors, which usually control progression through the G_1 phase in the cell cycle.

Cancer cells differ from normal cells because they often receive excessive growth factor signalling, are therefore locked in the cell cycle and subjected to increased cell division.

1.2.3 Cell signalling

For multicellular organisms to remain functional it is essential that growth, differentiation, and metabolism of cells is regulated by a wide variety of signalling molecules, including proteins, amino acids and hormones (Alberts *et al.*, 1994).

One of the key groups of extracellular stimuli are growth factors, which act on the cell cycle and mitosis via transmembrane signal transduction (Sherr, 1993). There are essentially two pathways by which extracellular signals can effect a response. Firstly, the extracellular signalling molecule (ligand) can bind to a specific protein (receptor) on the target-cell surface and, secondly, the signalling ligand can enter the target cell to activate it by binding to a receptor within the cell. For the signalling ligand to diffuse across the plasma membrane it must be small and hydrophobic. Once the signal has passed through the plasma membrane of the target-cell, by either method, the message is relayed by

intracellular signal cascades across the cell interior and an alteration in cell behaviour results (Alberts *et al.*, 1994; Hinterding *et al.*, 1998).

1.2.4 Tyrosine kinases

The epidermal growth factor receptor (EGFR) subfamily is one of the best studied tyrosine kinase receptors (Fry, 1999; Noonberg and Benz, 2000).

Tyrosine kinases are integral components of the signal transduction pathways used by cells to maintain normal growth and differentiation, they are proteins involved in both normal cell growth and transformed cells. Several different families of tyrosine kinases have been identified, many of which transmit extracellular signals from receptors on the cell surface into the cytoplasm, using signal transduction cascades which end in the nucleus as a signal to divide or arrest. In rapidly proliferating cancer cells, tyrosine kinases and signal pathways are often deregulated, resulting in increased signalling to the cell cycle and uncontrolled growth. Comprehensively reviewed by (Raymond *et al.*, 2000).

1.2.4.1 Epidermal growth factor (EGFR) and the cell cycle

The relationship between EGFR and the cell cycle has been primarily identified by examining the effects of specific EGFR targeting agents on cancer cells. Suppression of specific growth signalling by various therapeutic agents results in cell cycle arrest in many tumour cells, and several studies have demonstrated an alteration of cell cycle regulatory molecules following EGFR blockade (Yanlui and Grandis, 2002).

1.2.4.2 EGFR structure and function

EGFR is present in most cell types and has ligand-dependent intracellular tyrosine kinase activity (Raymond *et al.*, 2000; Velu, 1990). It is composed of three major regions: an N-

terminal extracellular region, a hydrophobic transmembrane region, and a C-terminal intracellular region, which contains the tyrosine kinase domain. The role of the extracellular region, a ligand-binding site, is to bind various ligands or growth factors, but mainly EGF and transforming growth factor α (TGF- α). The intracellular domain of the receptor has enzymic, or more specifically, tyrosine kinase, activity (Gill and Lazar, 1981; Gross *et al.*, 1991; Osada and Saji, 2003).

1.2.4.3 EGFR and signal transduction

When a ligand, e.g. EGF or TGF- α , binds to the extracellular ligand-binding site of EGFR, receptor dimerization takes place and the intracellular tyrosine kinase is activated, resulting in the binding of an ATP molecule (Figure 1.2). This results in tyrosine autophosphorylation of the receptor subunits, activation of catalytic activity, and generation of phosphorylated tyrosine residues (Fabbro *et al.*, 2002; Raymond *et al.*, 2000).

After ligand induced activation, EGFR can bind to a number of intracellular proteins involved in signal transduction cascades. This phosphorylates and activates proteins called transcription factors, which enter the nucleus and initiate gene expression, resulting in various responses including cell division. As a consequence of this process, extracellular signals are transmitted to the cell nucleus (Raymond *et al.*, 2000).

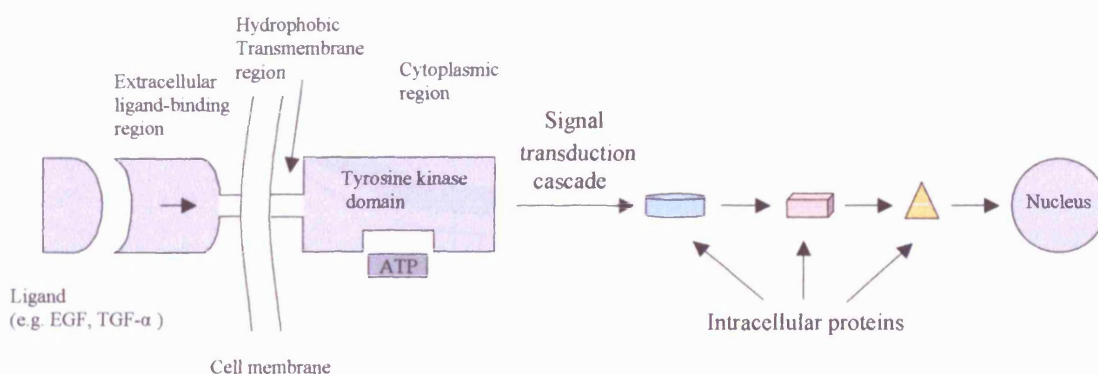


Figure 1.2 Schematic representation of EGFR and its function.

1.2.5 Cyclin dependent kinases (CDKs)

The control of the cell cycle in higher eukaryotes is carried out by a specific family of protein kinases, enzymes that regulate progression through G₁, S, G₂ and M phase of the cell cycle. (Knockaert *et al.*, 2002; Nugiel *et al.*, 2001; Schultz *et al.*, 1999). Cyclin dependent kinases are responsible for the phosphorylation of intermediates essential for progression of the cell cycle, and catalyse the transfer of a phosphate group from their substrate, ATP, to a particular amino acid side chain on their target: a protein implicated in cell cycle progression. CDK levels do not fluctuate throughout the cell cycle, but their activity is controlled by interaction with cyclin protein partners (Figure 1.3), the levels of which do vary within the cell cycle (Jeffery *et al.*, 2001; Murray, 2004). Although cyclin binding is the primary determinant of CDK function, other regulatory subunits and protein kinases also modulate CDK activity, which will be discussed shortly.

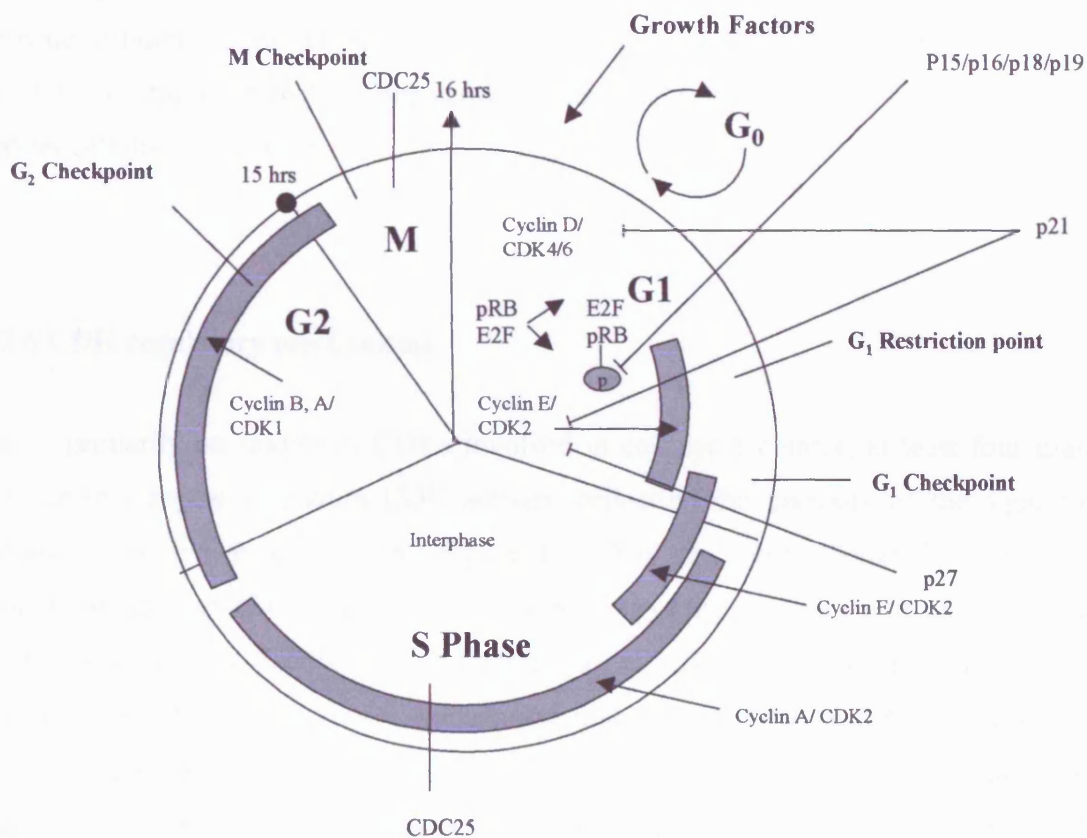


Figure 1.3 Detailed function of the mammalian cell cycle (Yanlui and Grandis, 2002).

Under appropriate external growth factor stimulation, cells which are quiescent in G_0 , can enter the cell cycle into early G_1 , likewise cycling cells present in early G_1 can exit into G_0 from the lack of extracellular signals (Ho and Dowdy, 2002). In early-mid G_1 , extracellular signals modulate the activation of CDK4 and CDK6 by expression of D-type cyclins, which is a requirement for G_0 - G_1 transition and entry into a new round of cell division (Knockaert *et al.*, 2002; Sherr, 1994).

The point of irreversible commitment between late G_1 phase and entry into S phase and another round of cell division, is termed the restriction point (Zetterberg *et al.*, 1995). Entry into S phase is coincident with activation of CDK2 by the sequential degradation of cyclin E and expression of cyclin A, which is essential for the replication of DNA (Roberts and Heichman, 1994).

Following completion of DNA synthesis, CDK1 combines with cyclin A or B in G_2 to activate cell division (Solomon *et al.*, 1990). This completes the cell cycle and is followed by exit from mitosis into G_1 . Cells can then either enter quiescence in G_0 , or commit to further cell division in G_1 /S.

1.2.6 CDK regulatory mechanisms

Based primarily on studies of CDKs involved in cell cycle control, at least four major mechanisms appear to govern CDK activity, reflecting the diversity of the signalling pathways that converge on them (Figure 1.4) (Morgan, 1995; Pavletich, 1999). The primary mechanism of CDK activation is the binding of the cyclin subunit, as the isolated CDK has no activity. Cyclin binding imports partial activity to the kinase, for complete activation most CDKs requires phosphorylation of the CDK/cyclin complex at a conserved threonine residue by cyclin activating kinase (CAK) (Fisher and Morgan, 1994; Kaldis *et al.*, 1996). The fully active kinase, as well as the activation process, can be turned off by interaction with two families of cell cycle inhibitory proteins. Members of the Cip family bind to and inhibit the active cyclin/CDK complex (Johnson and Walker, 1999; Sherr and Roberts, 1995). Members of the INK4 family use an indirect process. They bind to the isolated CDK and prevent its association with the cyclin and thus its

activation (Obaya and Sedivy, 2002; Pavletich, 1999). However, they can also bind to and inhibit the pre-formed CDK/cyclin complex without dissociating the cyclin, suggesting that may have multiple mechanisms of action (Pavletich, 1999; Serrano, 1997).

An understanding of these structural modifications, and the nature of other CDK regulatory interactions, is vital in the design of potential anti-cancer agents aimed at cell cycle inhibition.

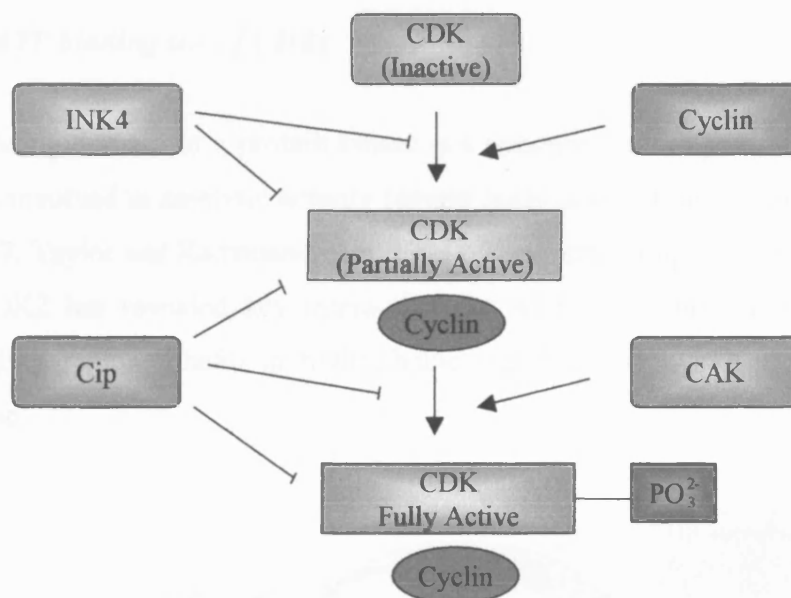


Figure 1.4 Summary of CDK regulation (Pavletich, 1999).

1.2.7 The monomeric CDK

Although the tertiary structure of CDK2 is similar to that of other protein kinases there are two regions that differ from the general kinase structure (Pavletich, 1999). One is an α -helix, present in other kinases, but which has a unique amino acid sequence, PSTAIRE, in the cyclin-dependent kinases (Noble and Endicott, 1999; Noble *et al.*, 1997; Pavletich, 1999). The other is a regulatory loop (the T-loop) that contains the activating phosphorylation site, threonine 160. In the inactive, monomeric, form of CDK this loop and Thr 160 is buried. This conformation is known as the closed conformation (Pavletich, 1999), as the residues present in the active site are incorrectly positioned with respect to

the triphosphate moiety of ATP for catalysis to occur. Although the inactive form of CDK2 does not allow correct orientation of the ATP phosphate groups it is still able to bind ATP (Brown *et al.*, 1999a; Brown *et al.*, 1999b). CDK2 is activated by two events: binding of a cyclin and phosphorylation on Thr160, both dramatically affect the structure and the conformation of the protein (Jeffrey *et al.*, 1995; Russo *et al.*, 1996).

1.2.7.1 The ATP binding site of CDKs

The ATP binding domain of a protein kinase is a common feature present in all kinases. The residues involved in catalytic activity remain fairly constant among different kinases (Hunter, 1987; Taylor and Radzianoandzelm, 1994). X-ray crystallographic analysis of ATP bound to CDK2 has revealed key interactions of ATP with Glu81 and Leu83 in the adenine binding region, Phe80 in hydrophobic region I and Lys33 in the phosphate binding region.

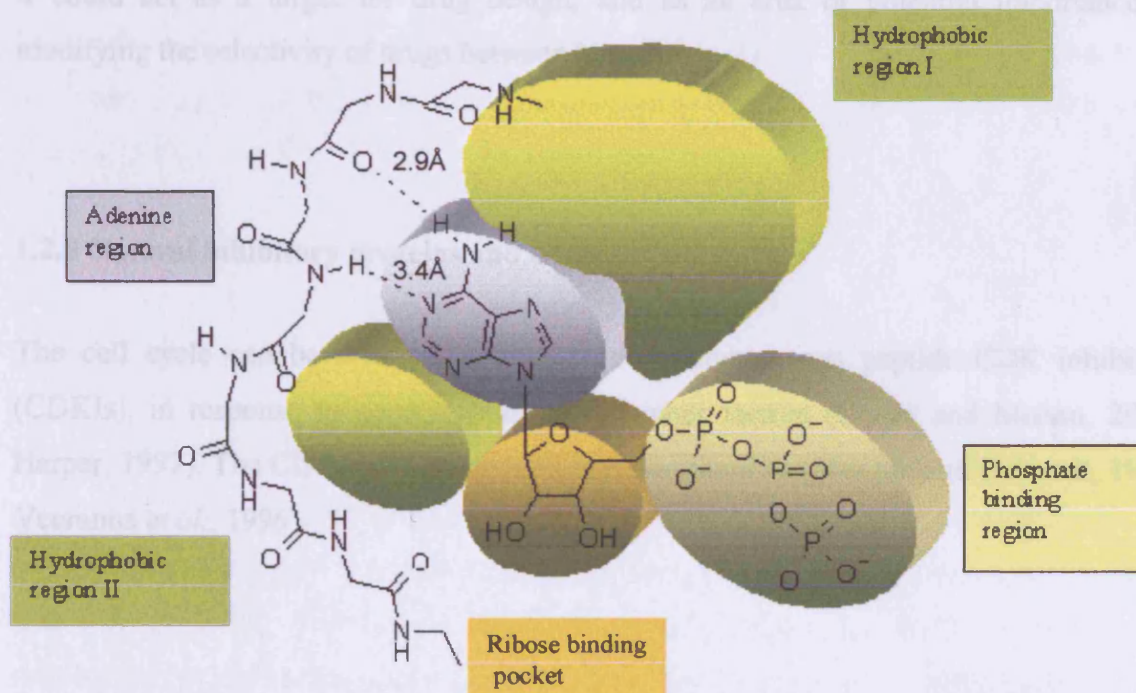


Figure 1.5 A pharmacophore diagram of the CDK2 ATP binding site. Hydrogen bonding interactions in the adenine binding site are shown by a dotted line, labelled with the interatomic distance in Å (Toledo *et al.*, 1999).

The adenine ring of ATP is bound at the bottom of the active site cleft. Two hydrogen bonds are observed between the protein, from the backbone NH of Leu83 to N-1 of the purine and from the backbone carbonyl of Glu81 to the 6-NH₂ of adenine (Figure 1.5). The entrance to the pocket is surrounded by a number of hydrophobic residues (not shown), which create mainly van der Waals interactions with the purine ring (Schulze-Gahmen *et al.*, 1996).

The other region important for the orientation and binding of ATP is the ribose binding pocket, which is mainly hydrophilic. The phosphate binding region is exposed to solvent and plays a role in the transfer of inorganic phosphate (Traxler and Furet, 1999).

The ATP binding site also consists of two hydrophobic pockets deeper into the kinase structure not occupied by ATP (Figure 1.5). The first hydrophobic pocket extends in the plane of the adenine N7 nitrogen of ATP. In CDK2, Phe80 occupies this position. The second hydrophobic pocket is exposed to solvent (Traxler and Furet, 1999). In spite of the fact that this pocket apparently plays no role in the binding and catalytic activity of ATP, it could act as a target for drug design, and as an area of potential importance in modifying the selectivity of drugs between kinases.

1.2.8 Natural inhibitory proteins and CDK regulation

The cell cycle can be arrested at any stage by endogenous peptide CDK inhibitors (CDKIs), in response to genetic damage and other factors (Crews and Mohan, 2000; Harper, 1997). The CDKIs can be divided into two families (Morgan and Debonadt, 1994; Veeranna *et al.*, 1996).

1.2.8.1 CDKs regulation by INK4 family

Members of the INK4 family consist of p15, p16, p18 and p19, which exclusively bind to CDK4 and CDK6 and prevent creation of CDK4 or 6/cyclinD complexes (Johnson and Walker, 1999).

CDK4 and CDK6/cyclinD complexes are highly involved in the hyperphosphorylation of pRb and effect the transition from G₁ into S phase. The CDKIs p15, p16, p18 and p19 prevent the phosphorylation of pRb, inhibiting the release of the E2F transcription factor required for S phase (Bartek *et al.*, 1996; Sherr, 1993).

Many tumour cells have p16 defects. In tumour cells where p16 is inactivated, Rb, a vital factor for transition from G₁ into S phase, is dephosphorylated, and in turn, inhibits the release of the E2F transcription factor. Hence, p16 appears to play a unique role regulating Rb. (Johnson and Walker, 1999; Koh *et al.*, 1995; Okamoto *et al.*, 1994; Serrano *et al.*, 1993).

Due to the specificity of the INK4 family for CDK4 and 6 with cyclinD complexes, these inhibitors only block progression through the restriction point in G₁ (Cooper, 2000; Vidal and Koff, 2000).

1.2.8.2 CDKs regulation by Cip/Kip family

Members of the Cip/Kip family can act on most CDK/cyclin complexes and even on some kinases other than the CDKs (Johnson and Walker, 1999). p21 was identified as the first member of this family which includes p27 and p57 (Hengst and Reed, 1996; Johnson and Walker, 1999). They inhibit the activities of CDKs at the G₁/S checkpoint and prevent the hyperphosphorylation of Rb (Harper, 1997; Harper *et al.*, 1993; LaBaer *et al.*, 1997 Johnson, 1999 #298). They insert into the ATP binding site, blocking ATP binding as well as binding to the CDK/cyclin complex (Pavletich, 1999; Russo *et al.*, 1996).

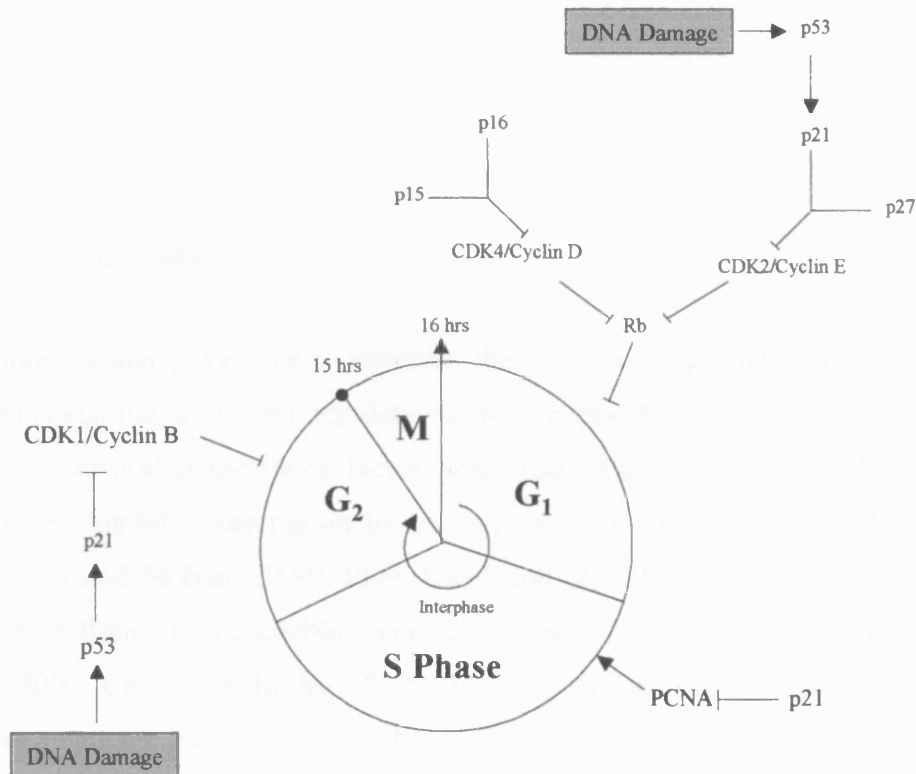


Figure 1.6 Induction of p21 by DNA damage (Crews and Mohan, 2000).

p21 is induced by the p53 tumour suppressor gene, which is activated in response to DNA damage. p21 inhibits cell proliferation and activates DNA repair (Johnson and Walker, 1999). Induction of p21 blocks cell cycle progression by CDK inhibition and inhibition of DNA replication by interacting with PCNA, an elongation factor for DNA polymerase δ , required for DNA synthesis (Figure 1.6) (Buolamwini, 2001; Eldeiry *et al.*, 1993; Gartel *et al.*, 1996; Johnson and Walker, 1999).

1.2.8.2.1. The p53 pathway

The p53 gene was the first tumour suppressor gene to be identified and is altered in many human cancers (Pecorino, 2005). It can be activated by signals such as cell stress and DNA damage, and can trigger several crucial cellular responses that suppress tumour formation. In response to stress signals, p53 can cause cell cycle arrest or DNA damage repair. The ability to arrest the cell cycle by induction of p21 is one of the central

functions of p53 in response to DNA damage which gives the opportunity to repair the damage prior to the next round of replication, thus damaged DNA will be prevented from being replicated and passed on to daughter cells (Pecorino, 2005).

1.2.8.2.2. The Rb pathway

The retinoblastoma protein (Rb) regulates the cell cycle by inhibiting the G₁/S phase transition (Pecorino, 2005). Rb regulates G₁ progression by binding to and regulating the activity of a critical transcription factor called E2F in its hypophosphorylated form and this complex inhibits transcription by binding to DNA (Bramson *et al.*, 2001; Cooper, 2000; Crews and Mohan, 2000). Phosphorylation of pRb by CDK/cyclin D complexes releases E2F from Rb thus enabling gene expression (Figure 1.7) (Bramson *et al.*, 2001; Cooper, 2000; Crews and Mohan, 2000; Johnson and Walker, 1999). Whereas cyclin E positively regulates E2F activity, cyclin A participates in a negative feedback loop for E2F regulation (Bramson *et al.*, 2001).

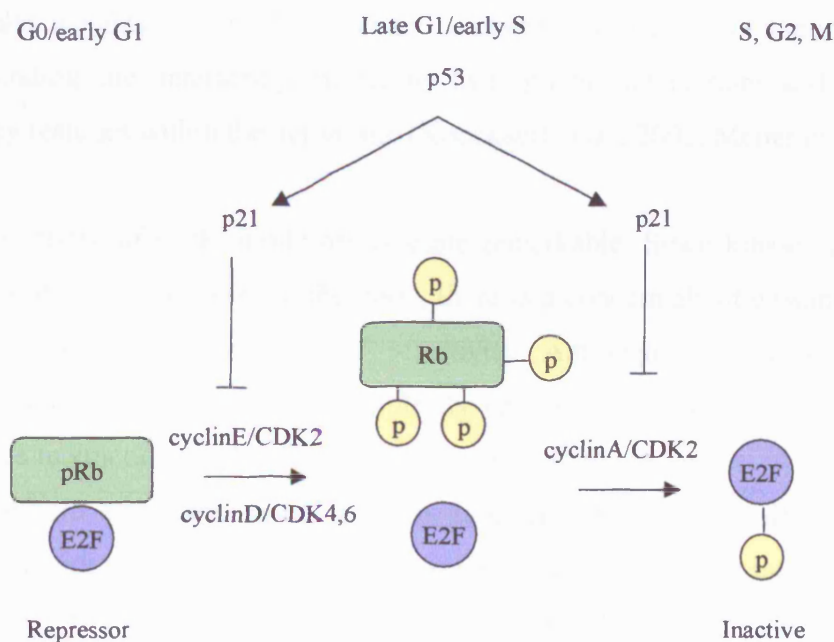


Figure 1.7 Regulation of E2F transcriptional activity through the cell cycle (Johnson and Walker, 1999).

1.2.9 Inhibitors of cyclin dependent kinases

Uncontrolled cell cycle progression, which is the hallmark of cancer, often involves the deregulation of CDKs or cyclins in human cancers, and has presented numerous opportunities for an extensive search for potent and selective inhibitors of cyclin dependent kinases. Sources of small-molecule inhibitors are very varied, and include natural products (from microorganisms, plants, etc), and purely synthetic compounds, some being active at nanomolar concentrations. Isolation of a lead compound allows for the development of a structure activity relationship (SAR). Although several possible targets for inhibition exist within the CDK/cyclin complex, the most existing advances have been small molecule inhibitors that competitively inhibit ATP. These will be discussed in more detail below and each compound represents a potential starting point for the establishment of a SAR, to guide the design of selective and more potent inhibitors (Coleman *et al.*, 1997; Gray *et al.*, 1999; Knockaert *et al.*, 2002; Meijer *et al.*, 1997; Meijer *et al.*, 2000; Walker, 1998).

ATP-binding pocket inhibitors of CDKs are varied chemically and structurally, but they all share some common properties. They are flat hydrophobic heterocycles with low molecular weights (<600). They act by competing with ATP for binding in the kinase ATP binding site, interacting mostly by hydrophobic interactions and hydrogen bonds with key residues within the active site (Knockaert *et al.*, 2002; Meijer *et al.*, 1999).

The selectivity of CDK inhibitors is quite remarkable. Since kinases are vital to the function of many processes in the body, there is a concern about unwanted side effects from compounds with a lack of selectivity. Although the structural reasons for selectivity of inhibitors are not completely understood, selectivity is probably due to exclusive interactions with amino acid residues that do not interact with ATP (Meijer *et al.*, 1999). In accordance with the structural data from co-crystallization of various inhibitors with CDK2, amino acids that are essential for inhibitor interaction have been discovered. The inhibitors usually contain a planar heterocyclic ring, and two or three hydrogen bonds are consistently seen between the inhibitors and the Glu81 and Leu83 residues of CDK2 (Meijer *et al.*, 1999). The backbone carbonyl and amide NH group of Leu83 act, respectively, as a H-bond acceptor and a H-bond donor to the inhibitors,

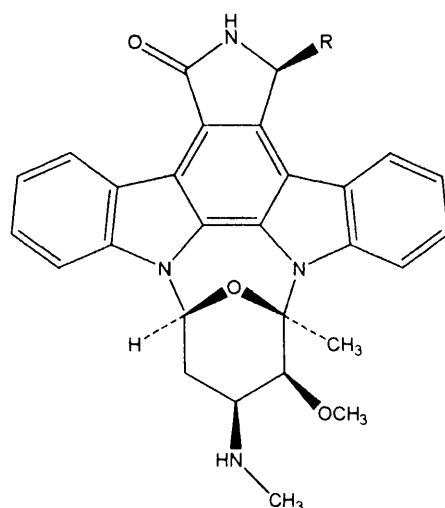
whereas the backbone carbonyl of Glu81 acts as a H-bond acceptor (Knockaert *et al.*, 2002).

Table 1.1 Chemical inhibitors of CDKs: IC₅₀ (concentration required to inhibit 50% of enzyme activity) against CDK1/cyclin B, CDK2/cyclin A and CDK4/cyclin D1.

Inhibitor	IC ₅₀ (μM)		
	CDK1/cyclin B	CDK2/cyclin A	CDK4/cyclin D1
Staurosporine (1)	0.004	0.007	>10
UCN-01 (2)	0.031	0.03	0.032
Flavopiridol (3)	0.3	0.28	0.4
6-Dimethylaminopurine (5)	120	-	-
Olomoucine (6)	7	7	>1000
Roscovitine (7)	0.65	0.7	>100
Indirubin (8)	10	2.2	12
5-Chloroindirubin (9)	0.4	0.75	-
Indirubin-3-monoxime (10)	0.18	0.44	3.33
Indirubin-5-sulphonic acid (11)	0.055	0.035	0.3
Paullone (12)	7	0.68	>100
Kenpaullone (13)	0.4	0.68	-
Hymenialdisine (14)	0.022	0.07	0.6

The different families of CDK inhibitors have varied potency, selectivity and cellular effects and their specificity against different protein kinases indicates that a purine nucleus, as found in ATP the natural substrate, is not a requirement for protein kinase inhibition (Coleman *et al.*, 1997; Meijer, 1996; Walker, 1998). Table 1.1 outlines inhibition data and these inhibitors will be discussed as follows:

1.2.9.1 Natural product cyclin dependent kinase inhibitors

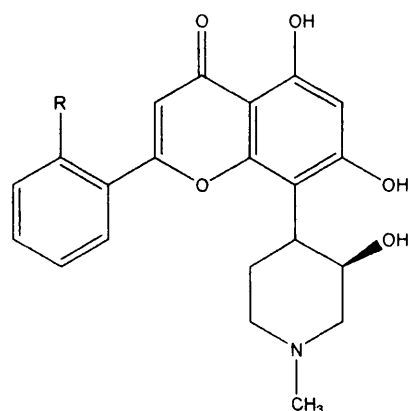


1, R=H, Staurosporine
2, R=OH, UCN-01

Staurosporine (1), a microbial alkaloid, and its analogue UCN-01 (2), are extremely potent, non selective inhibitors of a range of serine/threonine and tyrosine kinases (Coleman *et al.*, 1997; Meijer, 1995, , 1996).

The crystal structure of staurosporine bound to monomeric CDK2 revealed that the molecule is highly complementary to the ATP binding site of CDK2, and it appears to behave as a competitive inhibitor for ATP binding (Noble and Endicott, 1999). Staurosporine (1), is a non-specific kinase inhibitor, which makes it difficult to elucidate fully the cellular mechanism of action. Despite the lack of selectivity, they are both potent inhibitors of CDK1/cyclin B and CDK2/cyclin A (Table 1.1) (Meijer, 1996).

UCN-01 (2) blocks cell cycle progression, promotes apoptosis and although it is very non-selective and inhibits a wide range of kinases is currently in phase II trials (Akinago *et al.*, 2000).

Flavopiridol/Deschloroflavopiridol (Flavonoids)

3, R=Cl, Flavopiridol
4, R=H, Deschloroflavopiridol

Flavopiridol (**3**) was shown to arrest cells in G₁ phase and at the G₂/M boundary. Therefore, CDKs were considered as its molecular target, inhibition (competitive with ATP) of CDKs 1, 2 and 4 *in vitro*, and co-crystallization of a flavopiridol derivative in the ATP binding pocket of the enzyme confirmed direct interaction with CDKs (Fischer and Lane, 2000; Sausville, 2003).

The crystal structure of a complex between CDK2 and inhibitor **4** showed that the flavone portion of the inhibitor binds to the adenine binding pocket of the CDK (PezerRoger *et al.*, 2002). Moreover, the position of the piperidine group enables the inhibitor to make contacts with the enzyme where the ribose and phosphate groups sit.

The promising preclinical effects seen with flavopiridol have led to phase I/II clinical evaluation of the drug. Initial results show good tolerance of the drug, that safe concentration needed for CDK inhibition can be achieved, resulting in some anti-cancer effects (Fischer and Lane, 2000; Garrett and Fattaey, 1999; Sausville, 2003). Flavopiridol is reported to have cytotoxic activity against a wide range of cancer cell lines and has demonstrated its efficacy in several clinical trials (Wirger *et al.*, 2005)

1.2.9.2 Synthetic cyclin dependent kinase inhibitors

Many of compounds that have been tested for activity against CDKs have been based on a purine core. It was suggested that these types of compounds would most closely resemble ATP in the CDK active site (Figure 1.8) (Noble and Endicott, 1999).

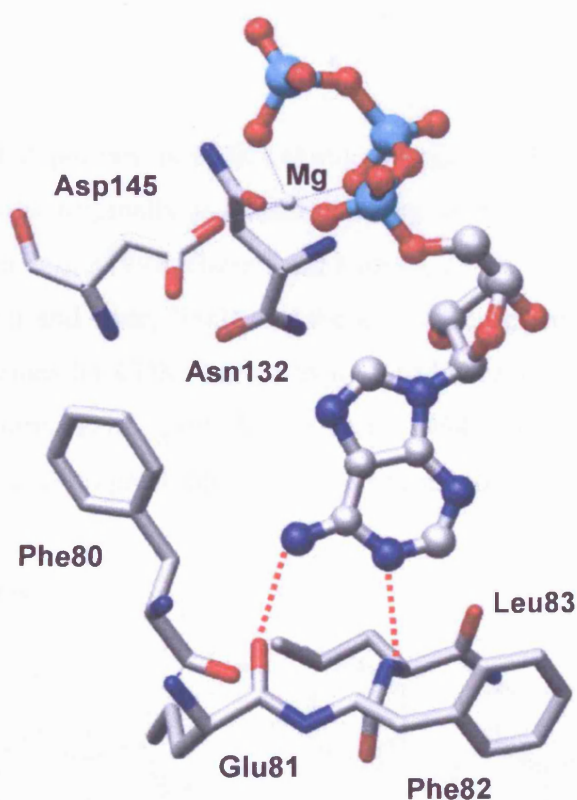
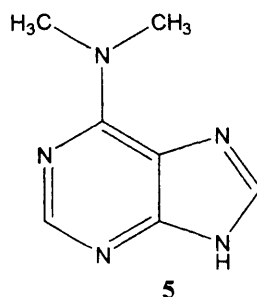
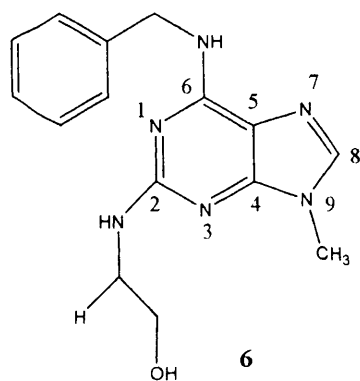


Figure 1.8 Interactions between ATP and CDK2 backbone residues Glu81 and Leu83.

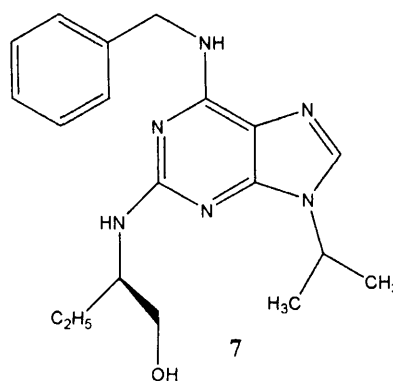
Based on crystal structure studies and depending on the nature of the substituents, the ATP binding pocket is tolerant of a number of different purine derivatives. It appears that only one hydrogen bond interaction is conserved between all purine inhibitors, which is equivalent to the hydrogen bond interaction between N1 of ATP and Leu83 (Noble and Endicott, 1999).

Dimethylaminopurine

The study of substituted purines as CDK inhibitors began with 6-dimethylaminopurine (DMAP) (**5**), which was originally synthesized as an analogue of the natural product puromycin (De Azvedo *et al.*, 1997; Garrett and Fattaey, 1999). DMAP was found to be a CDK1 inhibitor (Fischer and Lane, 2000), and the least specific protein kinase inhibitor of this series with IC_{50} values for CDKs higher than 40 μ M (PezerRoger *et al.*, 2002; Rialet and Meijer, 1991; Veeranna *et al.*, 1996; Vesely *et al.*, 1994). The weak inhibitory activity of dimethylaminopurine led to great interest into purine analogues as potential inhibitors.

Olomoucine/Roscovitrine

Olomoucine



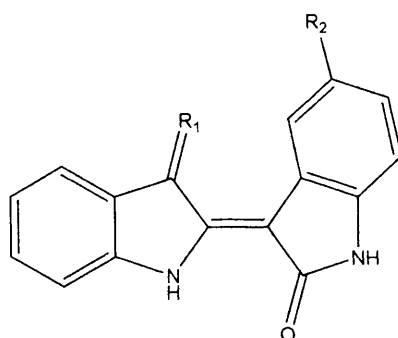
Roscovitrine

Further investigations of purine analogues led to olomoucine (**6**) and roscovitrine (**7**). Olomoucine showed an increased selectivity for CDK1 and CDK2 but only moderate activity. It also displayed selectivity as it is a poor inhibitor of CDK4 (Table 1.1) (Meijer, 1995; Sielecki *et al.*, 2000). Therefore, extensive synthetic work into purine derivatives identified roscovitrine as an alternative derivative, which showed a 10-fold increase in activity for CDK1 ($IC_{50} = 0.65 \mu$ M) compared to olomoucine (Kavanaugh and Williams, 1996). The 2- and 9-substituents in both are increased in size and structure activity

relationship studies (SARs) indicated that a benzyl group at C-6 or the lipophilic substituent at N-9 dramatically increased enzyme inhibition. These results were confirmed in part by examination of the binding modes of olomoucine/roscovitrine in the CDK2 ATP binding site by X-ray crystallography (De Azvedo *et al.*, 1997; Schulze-Gahmen *et al.*, 1995). They are both specific for CDK1, 2 and 5, but are very weak inhibitors of CDK4. Roscovitrine is a relatively potent inhibitor of CDK1/cyclin B and CDK2/cyclin A (Table 1.1) (Meijer *et al.*, 1997; PezerRoger *et al.*, 2002; Veeranna *et al.*, 1996; Vesely *et al.*, 1994). Roscovitrine contains a single chiral centre and it has been demonstrated that the (R)-stereoisomer is two-fold more potent than the (S)-stereoisomer (Meijer *et al.*, 1997). Cell-cycle analysis has shown that olomoucine and roscovitrine arrest cells in the G₁ and G₂ phases (Garrett and Fattaey, 1999).

1.2.9.3 Non-purine CDK inhibitors

Indirubins



- 8**, R₁=O, R₂=H, Indirubin
9, R₁=O, R₂=Cl, 5-chloroindirubin
10, R₁=NOH, R₂=H, Indirubin-3'-monoxime
11, R₁=O, R₂=SO₃H, Indirubin-5-sulfonic acid

Recent investigations have brought to light an interesting new range of CDK inhibitors obtained from traditional Chinese medicine. Indirubin (**8**) is the active ingredient of a plant used in traditional Chinese medicine to treat various chronic diseases. Since indirubin shows poor solubility and absorption, several analogues have been produced (Hossel *et al.*, 1999). Indirubin and its analogues (Atkinson *et al.*, 2002; Bramson *et al.*, 2001; Draetta and Eckstein, 1997) are very specific inhibitors of CDKs, blocking cell proliferation at late G₁ and G₂/M phase and show very little activity against other protein

kinases. Indirubin blocks all CDKs equally while some indirubin derivatives were shown to have a preference for CDK1, CDK2 and CDK5. Higher antitumour activity was observed in animal models for 5-chloroindirubin (**9**) (Table 1.1) (Hoessel *et al.*, 1999). The synthesis of indirubin-3-monoxime (**10**) and indirubin-5-sulfonic acid (**11**) has also been carried out, both showing an increase in inhibition against CDK1/cyclin B compared to indirubin.

The crystal structures of both indirubin-3-monoxime (**10**) and indirubin-5-sulfonic acid (**11**) in complex with monomeric CDK2 have been obtained. Both bind within the ATP binding site and show a similar binding mode, with the lactam amide nitrogen of the inhibitor donating a hydrogen bond to the oxygen of Glu81, the NH of Leu83 donating a hydrogen bond to the lactam amide oxygen, and the indole NH acting as a hydrogen bond donor to the carbonyl oxygen of Leu83.

Paullones

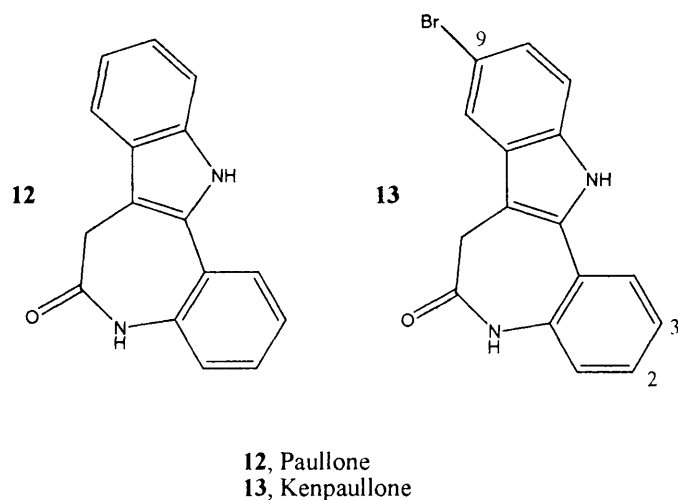


Table 1.2 CDK1/cyclin B inhibitory activity of paullone analogues (Schultz *et al.*, 1999).

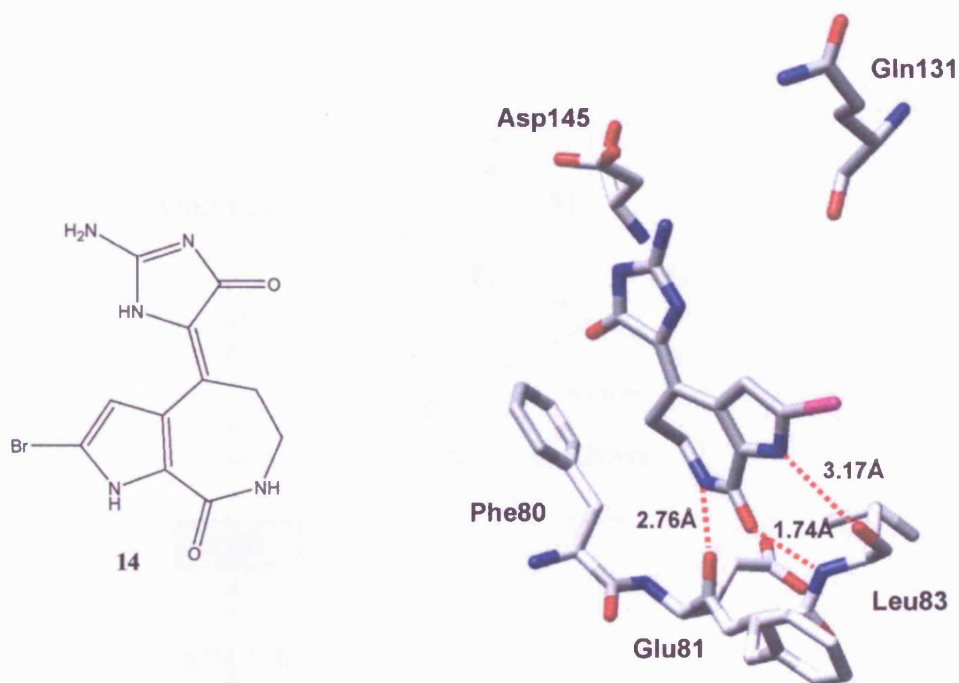
Substitution on paullone scaffold	IC ₅₀ CDK1/cyclin B (μM)
9-H	7.0
9-Br	0.4
9-Cl	0.6
9-CN	0.024
9-NO ₂	0.035
9-CF ₃	0.4
2, 3-di-OCH ₃	4.3

The paullones (**12**) were discovered using COMPARE, an NCI (National Cancer Institute) algorithm that detects similarities in the pattern of compound action against

human tumour lines compared to a compound of known activity, in this case flavopiridol. Paullones act as competitive inhibitors of ATP binding; based on molecular modelling studies, paullones make contacts in the ATP binding site similar to those observed in the crystal structure of other CDK2-bound inhibitors (Zaharevitz *et al.*, 1999a). The potency of kenpaullone (**13**) is quite high ($IC_{50} = 400$ nM) and it has less effect on other protein kinases (IC_{50} values in the μ M range). It is a selective inhibitor of CDK1, 2 and 5 over CDK4. Kenpaullone has also been shown to inhibit the growth of tumour cells in culture and causes altered cell cycle progression, comprehensively reviewed (Zaharevitz *et al.*, 1999b). Several analogues of kenpaullone have been synthesized by modifying the paullone scaffold in a search for CDK inhibitors with improved potency and antitumour activity (Table 1.2) (Schultz *et al.*, 1999).

Investigation of structure activity relationships based on molecular modelling studies and biological data for a considerable number of analogues revealed that a lactam ring, a free indole nitrogen, and a substituent in the 9-position were necessary parts of the paullone pharmacophore. An obvious relationship was found between the kinase inhibitory activity and the electron withdrawing property of the substituent in the 9-position (Schultz *et al.*, 1999).

A computer model of kenpaullone bound to the active site of CDK2 gave a greater insight into how further activity could be gained from the paullone series (Kunick *et al.*, 2000). The model suggested that substituents in the 2-position could be accommodated in the access channel to the ATP binding site. It was supposed that polar groups at the terminal of a carbon chain could form favourable interactions with amino acid side chains present in the vicinity of the binding site, or interact with solvent molecules. The bromine can also form hydrophobic interactions with Phe80 (Evans *et al.*, 1983).

Hymenialdisine

Hymenialdisine (**14**) is a compound which was isolated from a marine sponge and contains a lactam, bromopyrrole and guanidinone heterocycles (Meijer *et al.*, 2000). It acts as an ATP competitive inhibitor and the crystal structure of the CDK2/hymenialdisine complex shows three hydrogen bonds to the conserved Glu81 and Leu83 residues of CDK2, as observed in other CDK/inhibitor structures. It is a very potent inhibitor of CDK1/cyclin B, CDK2/cyclin A and CDK5/p35 (Table 1.1). Interestingly, it shows high inhibitory activity against three other protein kinases presumably involved in Alzheimer's disease: glycogen synthase kinase-3 β (GSK-3 β), casein kinase 1 (CK1) and CDK5, with IC₅₀ values of 10 nM, 35 nM and 28 nM, respectively. The inhibitory activity of hymenialdisine related natural compounds as well as some synthetic analogues of hymenialdisine have been tested against CDK1/cyclin B, however none were found to be more active than hymenialdisine itself. The nature of the selectivity of hymenialdisine is of great interest, as the range of targets and protein kinases that this inhibitor interacts with within a cell is quite limited, comprehensively reviewed by (Meijer *et al.*, 2000). By contrast with kenpaullone, the bromine atom of hymenialdisine is directed outward from the cleft towards the solvent.

1.3 CHECKPOINTS

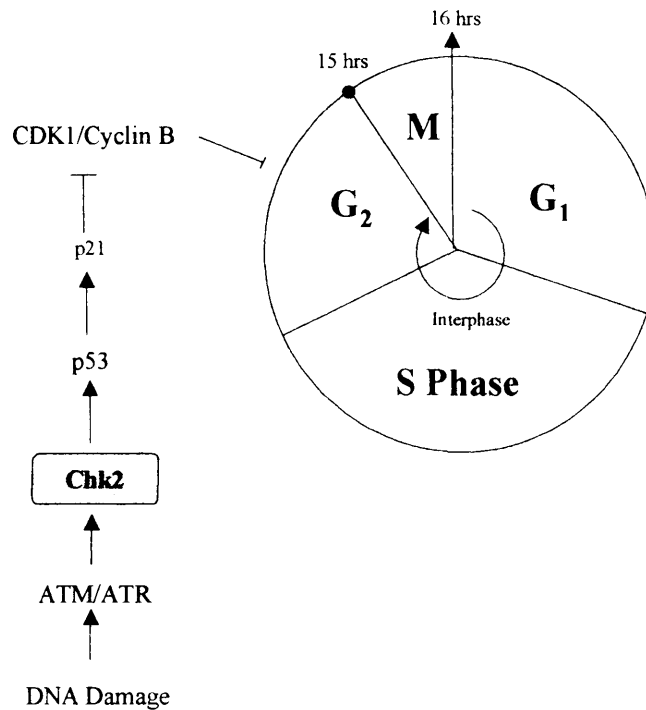


Figure 1.9 Activation of the G₂-checkpoint following DNA damage.

Progression through the cell cycle is regulated by further mechanisms that block or delay transitions to make sure that each phase of the cell cycle is precisely completed (Yu *et al.*, 2002). These mechanisms are vital for regulation of the cell cycle once the cell has passed the restriction point (Bartek and Lukas, 2001; PlanasSilva and Weinberg, 1997; Ringo, 2004). Recent studies in yeast and mammalian cells have revealed that these control pathways, called checkpoints, are found at all phases of the cell cycle. Integrity of checkpoint pathways is vital for the repair and survival of cells exposed to DNA-damaging agents (Yu *et al.*, 2002). A key regulator of the cell cycle at the G₂/M transition is the serine/threonine checkpoint kinase 2 (Chk2) (Bartek and Lukas, 2001; Zhou and Elledge, 2000). Many cancer cells have mutations in genes involved in the G₁ checkpoint because of alterations of the Rb and p53 pathways (Yao *et al.*, 1996). Only exceptionally do some cancer cells show the G₂ checkpoint defects in addition to G₁ checkpoint (Kawabe *et al.*, 1997). Therefore, the G₂ checkpoint appears particularly important for cancer cells and targeting the G₂/M checkpoint could be an effective strategy for enhancing the cytotoxicity of DNA damaging agents (Yu *et al.*, 2002).

Following DNA damage, Chk2 (and functionally related Chk1) are activated by upstream kinases ATM and ATR. The checkpoint kinases inhibit critical proteins required for cell cycle progression and result in cell cycle arrest at the G₂/M checkpoint (Ward *et al.*, 2001). Small molecules that can inhibit the checkpoint kinases may enhance the efficacy of DNA damaging chemotherapeutics or radiation therapy (Yu *et al.*, 2002; Zhou *et al.*, 2003).

1.3.1 The molecular pathways associated with DNA damage ATM and ATR

ATM and ATR are central components of the DNA damage response in mammals (Elledge, 1996; Zhou and Elledge, 2000). They are sometimes referred to as “sensor kinases” for DNA damage (Pommier *et al.*, 2005). They are members of the phosphoinositide 3-kinase (PI3K) family, which are extremely large protein kinases with predicted molecular mass of 350 and 301 kDa. respectively. They phosphorylate numerous substrates to achieve their physiological goals and can be activated instantaneously following exposure to appropriate genomic stress (Kastan and Bartek, 2004; Kastan and Lim, 2000). The function of pathway involving ATM is better understood than that involving ATR owing to ATM mutations in human disease like Ataxia telangiectasia and as it is not essential for normal cell cycle progression or cellular differentiation (Kastan *et al.*, 1992; Shiloh and Kastan, 2001). ATM seems to become engaged in signalling pathways at any point in the cell cycle primarily following the introduction of double strand breaks (DSBs) caused by ionisation radiation (IR) and similar genotoxic agents, whereas ATR responds to single strand DNA and damage to DNA replication forks (Falck *et al.*, 2001; Nyberg *et al.*, 2002; Zhou and Bartek, 2004; Zhou and Elledge, 2000). Both homologues share a number of substrates and therefore display overlapping roles, however, the way in which ATM and ATR are regulated is still widely unknown. Activation of ATM and ATR lead to the phosphorylation/activation of the checkpoint effectors (CDC25A and CDC25C, p53, BRCA1), via phosphorylation/activation of the chk1 and chk2 kinases, (Pommier *et al.*, 2005). This pathway is illustrated in Figure 1.10.

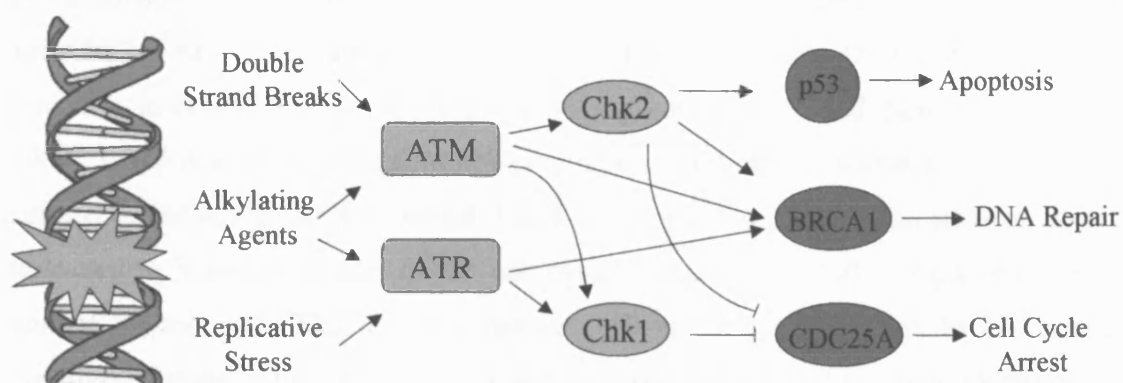


Figure 1.10 A summary of the DNA damage response network.

BRCA1 is a vital tumour suppressor gene whose inactivation increases the risk of breast and ovarian cancers (Rahman and Stratton, 1998). Cells deficient in BRCA1 show hypersensitivity to IR and DNA cross-linking agents (Bhattacharyya *et al.*, 2000; Moynahan *et al.*, 1999; Wang *et al.*, 2001).

1.3.2 The checkpoint kinases

The checkpoint kinases Chk1 and Chk2 are two serine/threonine kinases that are structurally unrelated but share some overlapping substrate specificity (Zhou and Elledge, 2000). Chk1 and Chk2 are small size proteins compared to the PI3Ks, as they share a range of substrates, they perform major roles for cell cycle arrest/checkpoint activation, DNA repair, and DNA damage-induced transcription (Bartek and Lukas, 2003). Chk1 is a checkpoint kinase in mammals and regulates G₂/M and S phase cell cycle checkpoints. It is absent or minimal in quiescent and differentiated cells (Kaneko *et al.*, 1999; Lukas *et al.*, 2001). Like ATR, Chk1 is essential for cell viability and is activated by phosphorylation at Ser345 and Ser317 in response to different types of DNA damage like IR (Ionization Radiation), UV (Ultraviolet) and HU (Hydroxylurea) (Xiao *et al.*, 2003). Although structurally distinct, Chk2 shares overlapping substrate specificity with Chk1 and can phosphorylate substrates such as CDC25A and CDC25C *in vitro* (Chaturvedi *et al.*, 1999; Madani *et al.*, 2002; O'Neill *et al.*, 2002). Cell cycle progression is blocked by Chk1 when replication is inhibited, and by Chk2 when double-strand breaks (DSBs) exist. Furthermore, Chk2 activation led to cell cycle arrest in G₁/S, S and G₂/M phase after

DNA damage (Falck *et al.*, 2001). However, fundamental differences exist between Chk1 and Chk2. Chk2 is activated primarily by ATM in response to DSB, whereas Chk1 is primarily activated by ATR in response to replication-associated damage (Liu *et al.*, 2000). Chk2 is a stable protein, which is expressed and can be activated throughout the cell cycle, including G₀. By contrast, Chk1 is an unstable protein, and its expression is restricted to S and G₂ phases of the cell cycle (Lukas *et al.*, 2001). As a result of the normal function of Chk2 in DNA damage checkpoints, and its link to Li-Fraumeni syndrome disease (with a mutated p53 tumour suppressor), Chk2 has been identified as a promising pharmacological target for anti-cancer drug design.

1.3.3 Cell cycle checkpoints and cancer

One of the most important features of aberrant checkpoint control in cancer, is the link between the CDKIs and p53. The detection of DNA damage at one of the cell cycle checkpoints (G₁/S, G₂/M) activates the p53 suppressor gene which stimulates the synthesis of a range of CDKIs and gives the cell time to repair the malfunction (Elledge, 1996; Sherr, 1996). However, it is well known that the p53 gene is defective in a wide range of human cancers (Greenblatt *et al.*, 1994). This in turn will lead to aberrant control of cell cycle checkpoints and result in the replication of damaged DNA. As the checkpoint and repair pathways facilitate cellular responses to DNA damage, and because there is reasonable information indicating that DNA damage is a major contributor to the development of human cancers, it is possible that alterations in these pathways increase the risk of cancer developing (Kastan and Bartek, 2004). Development of the checkpoint pathway that works independently of the p53 pathway provides an alternative route by which cancer cells can mediate DNA repair and survive. This not only highlights the importance of the checkpoints in normal cells but also emphasises the role the checkpoint kinases play within cancer cells.

1.3.4 Chk2 as a therapeutic target

Numerous investigations have suggested that Chk2 is vital for the maintenance or arrest at the DNA damage induced G₂ checkpoint. The G₁ checkpoint is defective in many cancer cells, which implies the importance of the G₂ checkpoint in pharmacological studies. The G₂ checkpoint and Chk2 acts as the primary target of anti-cancer agents such as UCN-01 (2), and leads to a synergistic action with ionising radiation and currently used anti-cancer drugs, comprehensively reviewed by (Pommier *et al.*, 2005) in G₁ defective cells. UCN-01 is a non-specific kinase inhibitor that has been recently identified as a Chk1 and Chk2 inhibitor (Pommier *et al.*, 2005; Yu *et al.*, 2002). Observations such as these lead the efforts into understanding the molecular mechanisms and pharmacology of Chk2. In further support of Chk2 as a therapeutic target, the ATM/Chk2 pathway responds almost instantaneously to double strand breaks caused by radiotherapy and similar agents (Bartek *et al.*, 2001). One would therefore expect that the initial response to DNA damage, as a result of anti-cancer treatments would be mediated via a Chk2 pathway.

BRCA1, as a substrate for Chk2, has been implicated in the DNA damage response suggesting that Chk2 inhibition may block this pathway leading to arrest of cell division within tumours and subsequent cell death (Lee *et al.*, 2000). P53 is another substrate linked to Chk2 (Bell *et al.*, 1999; Chehab *et al.*, 2000). Chk2 inhibition in p53 capable tumour cells will prevent cell arrest at the G₁ and G₂ checkpoint and block mediation of repair factors by p53 (Zhou and Sausville, 2003).

Continuing research in pharmacology will confirm if the Chk2 enzyme is an attractive target for drug discovery, and several pharmaceutical companies are searching for small molecule inhibitors of this kinase.

1.3.4.1 Chemosensitization

The sensitisation of tumour cells to chemotherapy or radiotherapy is known as chemosensitization or radiosensitization respectively (Zhou and Bartek, 2004). Caffeine, an ATM inhibitor, treatment has been used as a research tool in many biological

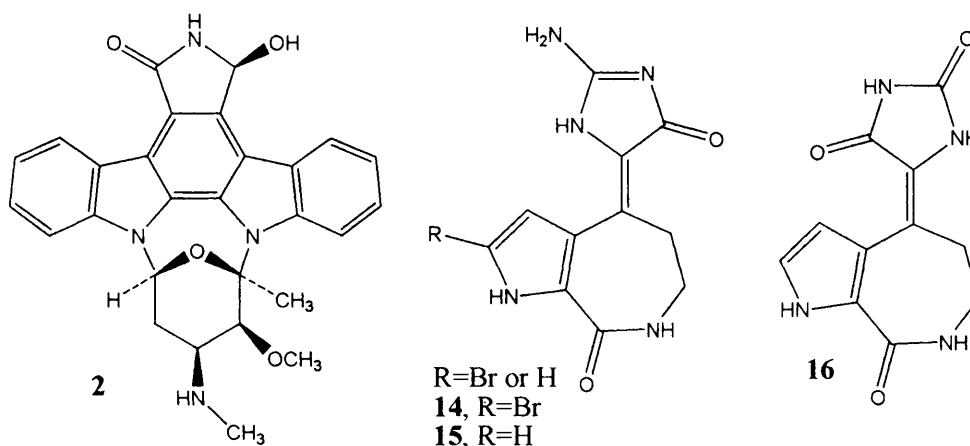
evaluations. Following radiation damage, caffeine prevents Chk2 phosphorylation by ATM inhibition, and has led to the principle of sensitisation (Suganuma *et al.*, 1999). This has now been showed by a few compounds. UCN-01, inhibits Chk1 predominantly by abrogating G₂ cell cycle arrest following DNA damage where p53 is mutated (Graves *et al.*, 2000). It has been shown to potentiate the cytotoxicity of a number of anti-cancer agents, encouraging a combination therapy approach for treating cancer. It is currently in clinical trials.

1.3.4.2 Chemoprotection

Chemoprotection or radioprotection refers to the protection of normal cells from the toxicity of cancer chemotherapeutic agents or radiotherapy (Zhou and Bartek, 2004). A few studies question whether the role of Chk2 in the DNA damage response network is redundant. Chk2 appears to mediate p53 in apoptosis in response to DSBs (Zhou and Sausville, 2003; Zhou and Bartek, 2004). This observation has proposed Chk2 as a novel chemoprotective target; inhibition of Chk2 may improve the side effects of dose-limiting anti-cancer therapies such as radiotherapy. Blockade of the apoptotic pathway, via Chk2 inhibition, in healthy cells may reduce intolerable side effects such as diarrhoea, vomiting and hair loss.

To summarise, the points above demonstrate that the inhibitors of checkpoint kinases may selectively increase the chemosensitivity of cancer cells with checkpoint and repair defects or selectively increase the chemoprotection of normal cells, enhancing the efficacy of DNA-damaging cancer therapies. Therefore the availability of selective inhibitors would validate these therapeutic hypotheses (Zhou and Bartek, 2004).

1.3.5 Known Chk2 inhibitors



Very limited reports of small molecules which inhibit Chk2 are available in the literature (Arienti *et al.*, 2005). The indolocarbazole UCN-01 (**2**) (Yu *et al.*, 2002) and the marine natural product debromohymenialdisine (DBH) (**15**) (Wan *et al.*, 2004) are the only characterized inhibitors of the Chk2 kinase. UCN-01 was reported to be a potent inhibitor of Chk2 (10 nM) but inhibits a variety of other kinases involved in the cell cycle control, making this compound and other similar indolocarbazoles, poor tools for exploring the pharmacology of specific Chk2 inhibition (Pommier *et al.*, 2005; Sordet *et al.*, 2003). UCN-01 can inhibit both Chk2 and Chk1, however its activity with respect to checkpoint kinases works predominantly through Chk1 (Yu *et al.*, 2002).

Debromohymenialdisine was reported to inhibit both Chk1 ($IC_{50} = 3 \mu\text{M}$) and Chk2 ($IC_{50} = 3.5 \mu\text{M}$) while inhibiting the G_2 checkpoint and sensitising cancer cells to DNA damaging agents (Curman *et al.*, 2001). Interestingly, debromoaxinohyantoin (DBAH, **16** a related marine natural product isolated in similar fractions to HYM (**14**) and DBH) showed no G_2/M checkpoint inhibition, suggesting there are exact requirements for orientation of the carbonyl group and indicating that precise molecular design could be used to synthesize molecules with high selectivity towards a particular checkpoint kinase.

We have recently identified the CDK inhibitor kenpaullone (**13**), to be a potent small molecule inhibitor of Chk2 ($IC_{50} = 0.8 \mu\text{M}$). It has a similar structure to HYM, DBH and DBAH containing a seven membered lactam ring and a bromine substituent, which might be contributory to its potent activity.

The structure of Chk2 is currently unknown. A homology model of the Chk2 kinase has been developed (see Appendix A). Kenpaullone has been docked within the ATP binding site to develop a SAR study of the Chk2 active site (Figure 1.11).

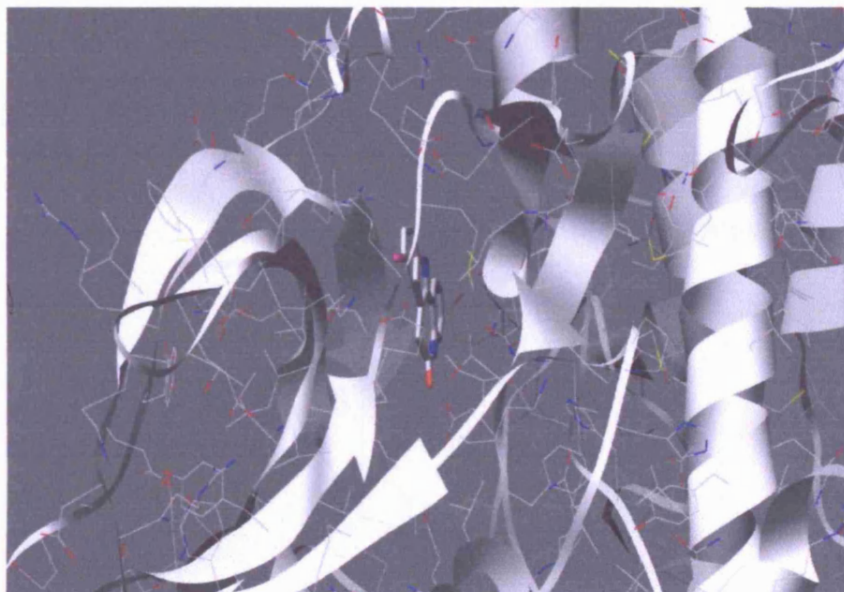


Figure 1.11 Kenpaullone (**13**) docked into the Chk2 homology model.

Compounds that inhibit Chk2 and the G₂ checkpoint may be useful tools to assess the value of this target in cancer therapy to enhance the effectiveness of DNA-damaging agents in tumours with a defective G₁ DNA damage checkpoint, such as those with mutated p53 (Pommier *et al.*, 2005; Sordet *et al.*, 2003).

To exploit the G₂/M checkpoint as a novel target for cancer therapeutics we wish to identify potent and specific inhibitors of the signalling kinase Chk2 using lactam-based DBH and kenpaullone lead compounds to identify Chk2 structure activity relationships and the requirements for selectivity.

1.4 POLY(ADP-RIBOSE)POLYMERASES (PARPs)

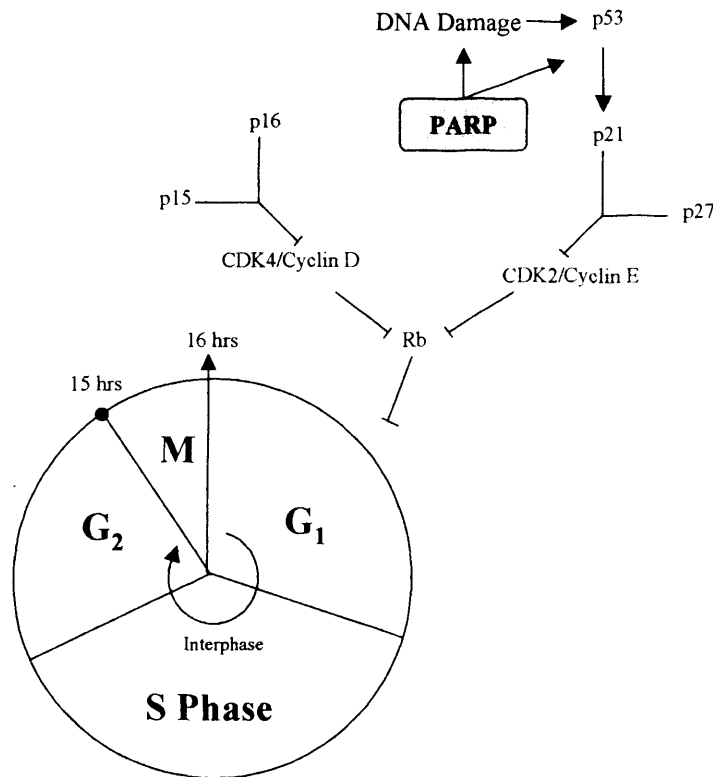


Figure 1.12 PARP control of DNA damage.

Poly(ADP-ribose)polymerases (PARPs) are members of a large family of enzymes, which are usually involved in poly(ADP-ribosyl)ation of DNA binding proteins. They use NAD^+ as a substrate to transfer ADP-ribose onto glutamic acid residues of target proteins, a reaction that functions as a DNA damage sensor and is induced by ionising radiation (IR), oxidative stress, and DNA damaging anti-tumour drugs (D'Amours *et al.*, 1999; Smith, 2001). Poly(ADP-ribose)polymerase-1 (PARP-1) is the principle and best known member of the PARP enzyme family consisting of PARP-1 and several recently identified novel poly(ADP-ribosyl)ating enzymes.

Although poly(ADP-ribosyl)ation is barely noticeable in resting cells, it is increasingly induced in cells confronted with DNA damaging agents. Therefore in the absence of DNA damage, PARP is not required for cell survival. Numerous studies have shown that PARP knockout mice are completely healthy, and appear unaffected by this lack of enzyme (Wang *et al.*, 1995). If PARP has no involvement in physiological processes, then

inhibiting the enzyme is unlikely to induce major toxicity. PARP is therefore an attractive target for anti-cancer drug design (White *et al.*, 2000).

1.4.1 PARP-1: Structure and Function

Poly(ADP-ribose)polymerase-1 (PARP-1), also known as poly(ADP-ribose)synthetase (PARs) and poly(ADP-ribose)transferase (PADPRT), is a nuclear enzyme present in all eukaryotes. It is a 116 kDa protein comprising of three main domains: the N-terminal DNA-binding domain containing two zinc fingers, the automodification domain, and the C-terminal catalytic domain (Southan and Szabo, 2003). The catalytic function of PARP-1 relates to its role as a DNA-damage sensor and signalling molecule mentioned earlier. The enzyme initially recognizes and binds to a site of DNA damage. PARP-1 contains a pair of zinc fingers to recognize single and double-stranded DNA. Binding to damaged DNA stimulates PARP-1 to catalyse the synthesis of ADP-ribose polymers from its substrate nicotinamide adenine dinucleotide (NAD⁺) (Figure 1.13), with release of nicotinamide (Benjamin and Gill, 1981).

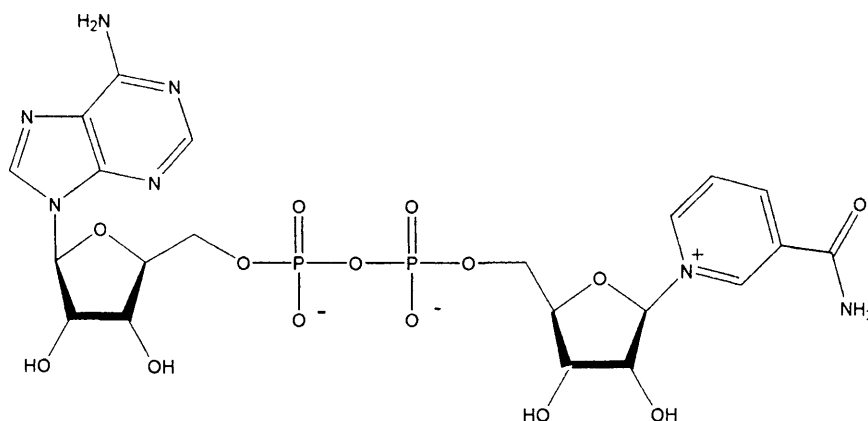


Figure 1.13 Structure of Nicotinamide Adenine Dinucleotide (NAD⁺).

NAD⁺ is used to synthesize branched ADP-ribose polymers that are covalently attached to acceptor proteins, including histones, transcription factors and primarily PARP-1 itself (Davidovic *et al.*, 2001; Virag and Szabo, 2002) (Figure 1.14).

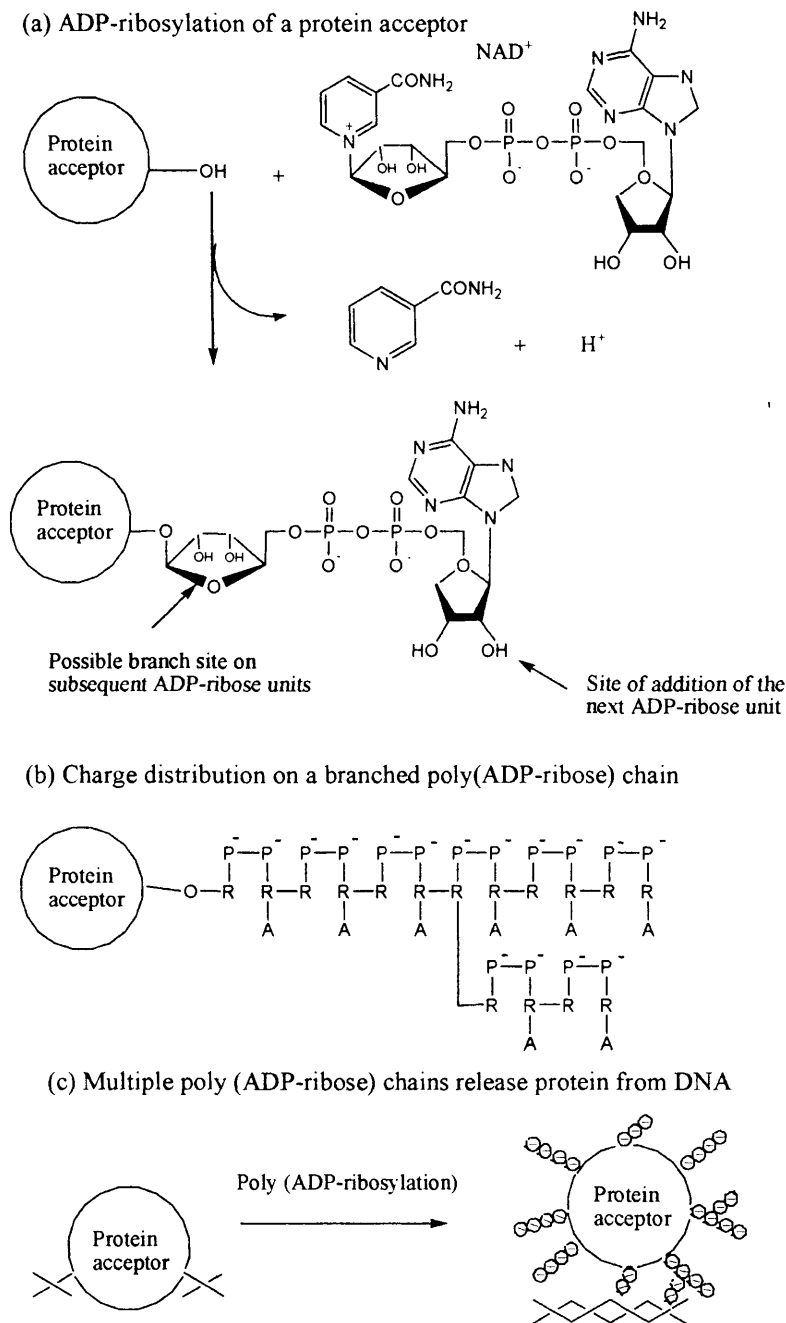


Figure 1.14. (Diagram obtained from Smith, 2001) (a) ADP-ribosylation of a protein using NAD^+ as a substrate. ADP-ribose is transported from NAD^+ to a glutamic acid residue on a protein acceptor by the action of PARP-1. This complex can then act as an acceptor for the accumulation of a further ADP-ribose. (b) Long, linear and branched chains of negatively charged ADP-ribose polymers are thus synthesized. (c) Numerous polymers can alter the properties of the protein acceptor. Poly (ADP-ribosylation) of a protein bound to DNA can inhibit DNA binding through electrostatic repulsion of the negatively charged polymer (Smith, 2001)

The size of the branched polymer varies from a few to 200 ADP-ribose units (Virag and Szabo, 2002). However, branched and short polymers are degraded more slowly than long and linear polymers (Hatakeyama *et al.*, 1986; Malanga and Althaus, 1994). As the polymer gradually accumulates more negative charge by the sequential addition of ADP units, because of its high negative charges, the covalently attached ADP-ribose polymer affects the function of target proteins by preventing any interaction with other anionic molecules such as DNA (Virag and Szabo, 2002).

More than 30 nuclear substrates of PARPs have been identified *in vivo* and *in vitro* (Althaus and Richter, 1987). Among these substrates, the major and most abundant acceptor of poly(ADP-ribosylation) is the enzyme itself, representing a major regulatory mechanism for PARP-1 resulting in the down-regulation of enzyme activity. In addition to PARP-1, histones are also the second major acceptor of poly(ADP-ribose) (Virag and Szabo, 2002).

Poly(ADP-ribosylation) is a dynamic process, with the polymer having a short *in vivo* half life (less than 1 minute) due to the catabolic actions of two particular enzymes (Whitacre *et al.*, 1995). Poly(ADP-ribose)glycohydrolase (PARG) and ADP-ribosyl protein lyase are involved in the catabolism of poly (ADP-ribose). Branched short polymers are degraded more slowly than long and linear polymers. Additionally, the nicotinamide released during the polymerisation reaction exerts an inhibitory effect on PARP-1 thus allowing for a negative feedback mechanism.

Essentially, poly(ADP-ribosylation) contributes to DNA repair and the preservation of the genome. When DNA is only moderately damaged, PARP-1 contributes in the DNA repair process and the cell survives. However, in the case of extensive DNA damage, excessive activation of PARP-1 causes the over-consumption of NAD^+ and consequently ATP (needed for synthesis of NAD^+), thus the consequential culmination is cell dysfunction or necrosis (Shieh *et al.*, 1998). Subsequently this is implicated in the pathogenesis of several diseases where cellular damage occurs including stroke, myocardial infarction and diabetes. Thus, PARP-1 can be considered a viable target for pharmacological development against conditions such as these, in addition to enhancing the efficacy of DNA-damaging anti-cancer agents (Bowman *et al.*, 2001).

Until recently, poly(ADP-ribosyl)ation was believed to result from the function of a single enzyme. One of the first clues indicating the presence of multiple PARPs was the observation of some residual PARP activity in PARP-1 deficient cells (Shieh *et al.*, 1998; Virag and Szabo, 2002). Intensive research commenced to identify the enzymes responsible for this activity. Four new PARPs possessing poly (ADP-ribosyl)ation activity were identified: PARP-2, PARP-3, vault-PARP (VPARP) and tankyrase (Smith, 2001) with the original member of the PARP enzyme family becoming known as PARP-1. The homology between these proteins is limited to the C-terminal domain of PARP-1, called the PARP homology domain, with no relationship outside this region between the five PARPs. Tankyrase contains the smallest PARP domain sufficient for PARP activity (Smith, 2001). Although the biological and pharmacological significance of these other PARP enzymes is not well understood at present, interesting data about their structure and properties has already been determined.

1.4.2 Poly(ADP-ribose)polymerase-2 (PARP-2)

Poly(ADP-ribose)polymerase-2 (PARP-2) bears the closest resemblance to PARP-1. It has approximately 60% homology in the catalytic PARP domain (Ame *et al.*, 1999). Relative to PARP-1, the DNA-binding of PARP-2 is distinct from PARP-1 and could signify different substrate specificities for these two proteins. The automodification domain is missing in PARP-2. Moreover, PARP-2 is capable of autopoly(ADP-ribosyl)ation, however, it can not poly(ADP-ribosyl)ate histones, which are prototypical PARP-1 substrates, comprehensively reviewed by (Virag and Szabo, 2002). PARP-2, contributes to the residual poly(ADP-ribose) activity observed in PARP-1 knockout cells after treatment with DNA-damaging agents, indicating a biological role for PARP-2 in response to DNA-damage (Smith, 2001).

1.4.3 Poly(ADP-ribose)polymerase-3 (PARP-3)

PARP-3 is the smallest member of the PARP family and also is the least studied PARP thus far, consisting of a unique N-terminal domain of 39 amino acids followed by the PARP homology domain. The catalytic site of PARP-3 has 39 % homology with PARP-1. It is not well understood if this protein shares properties with PARP-1 and PARP-2 such as a nuclear localization, DNA-binding activity, or response to DNA damage. These properties might be enclosed by the unique N-terminal domain or by the PARP homology domain itself (Smith, 2001).

1.4.4 Vault poly(ADP-ribose)polymerase (VPARP)

Vault PARP has been identified in the vault complex, a ribonucleoprotein particle that is expressed in many eukaryotes. Their biological role is still unknown but believed to be nuclear transport proteins. Vault PARP has been found to associate with and poly(ADP-ribosyl)ate the major vault protein (mvp). Unlike other PARPs, this enzyme is not activated by damaged DNA and has only 29% homology at the PARP catalytic domain. *In vitro* studies with purified vault proteins indicate that MVP and VPARP act as acceptors for ADP-ribosylation. Thus poly(ADP-ribosyl)ation could regulate changes in vault confirmation, such as opening and closing the vaults to allow entry and exit of transport molecules, comprehensively reviewed by (Kickhoefer *et al.*, 1999).

1.4.5 Tankyrases

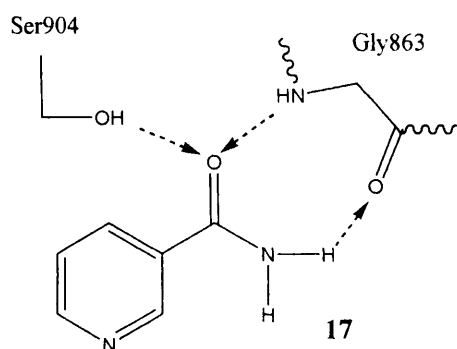
Tankyrase is an enzyme with homology to the highly conserved enzyme, poly(ADP-ribose)polymerase (PARP-1), which is limited to the catalytic domain of PARP-1. Tankyrase is capable of the (ADP-ribosyl)ation of itself and the telomeric-binding protein TRF1 (Smith *et al.*, 1998). TRF1, regulates telomere length by inhibiting the action of telomerase at the ends of telomeres (Harley, 1991). The modification of TRF1 by tankyrase allows access for the enzyme telomerase, which is responsible for maintaining telomere length (Smith and de Lange, 2000). Telomeres are protective caps at the ends of

chromosomes (Blackburn, 1991) that decrease in length following each cell division (Harley *et al.*, 1990). After a certain number of cell divisions telomeres reach a critical length initiating cellular senescence (Harley, 1991). The maintenance of telomere length is therefore crucial for tumorigenesis and telomerase activity has been detected in most tumours (Neidle and Parkinson, 2002).

1.4.6 Pharmacological inhibitors of PARPs

Inhibition of DNA repair by pharmacological inhibition of PARP would limit the ability of the tumour cells to repair their damaged DNA and, therefore, increase the effects of cancer chemotherapy (Southan and Szabo, 2003). Small molecule inhibitors bind to the conserved NAD⁺-binding site of the enzyme, although this site is conserved in all PARPs, there is sufficient diversity in amino acid sequence between proteins to predict the improvement of isozyme-specific inhibitors. This observation could be quite useful to predict the therapeutic potential of individual PARPs (Smith and de Lange, 2000). PARP specific inhibitors could be developed for use in conditions such as diabetes, stroke and myocardial infraction as these are pathological diseases affected by PARP-1 (Zhang *et al.*, 1999). However, the clinical possibilities of interest within the scope of this project are the potential use of the PARP-1 inhibitors in anti-cancer therapy. These could be used in conjunction with a chemotherapeutic drug to obstruct DNA repair and hence resistance development in PARP-1 up-regulated cancer cells brought about by the ability of a tumour cell to repair induced damage (Smith, 2001).

1.4.7 Chemical inhibitors of PARPs



Most PARP inhibitors act as competitive inhibitors of the enzyme by interfering with NAD^+ binding to the catalytic domain of the enzyme. One can conclude that a fairly consistent structural relationship exists between NAD^+ and the inhibitors. Based on the crystal structure information of PARP-1, it is obvious that the majority of PARP inhibitors are based on the benzamide pharmacophore, which mimics the conformation of nicotinamide (17) moiety of NAD^+ due to the fact they are designed to interact with the same active site residues (Jagtap and Szabo, 2005).

The residues of PARP-1 that provide hydrogen-bonding interactions with these inhibitors are completely conserved in PARP-2. In PARP-1 the amide group of these inhibitors interacts with the backbone atoms of Gly863, and the side chain of Ser904 additional non-polar π - π interactions with Tyr907 and, to some degree, Tyr896 which lines the other side of pocket and provides further binding interactions (Jagtap and Szabo, 2005). Additional inhibitor specificity has been correlated with the formation of additional H-bonds either to a catalytic glutamate, Glu988, or to the hydroxyl group of Tyr907 (Figure 1.15) (Oliver *et al.*, 2004).

1.4.8 The development of existing PARP inhibitors and the PARP-1 active site

During the past decade, structure-based design and an increased knowledge of the molecular details of the active site of PARP-1 have been useful in the discovery of highly potent PARP inhibitors. Most PARP inhibitor compounds fall into the categories of bi-

and tricyclic heterocyclic scaffolds. Recent investigations have been pointed to the synthesis of tri- and tetracyclic PARP inhibitor scaffolds. The general knowledge of the SARs of these benzamide pharmacophore based PARP inhibitors has directed the synthesis of highly potent novel inhibitors (Peukert and Schwahn, 2004; Southan and Szabo, 2003). Reviewing the published data illustrates a consistent orientation of each inhibitor in almost identical positions in the PARP-1 active site (Figure 1.15).

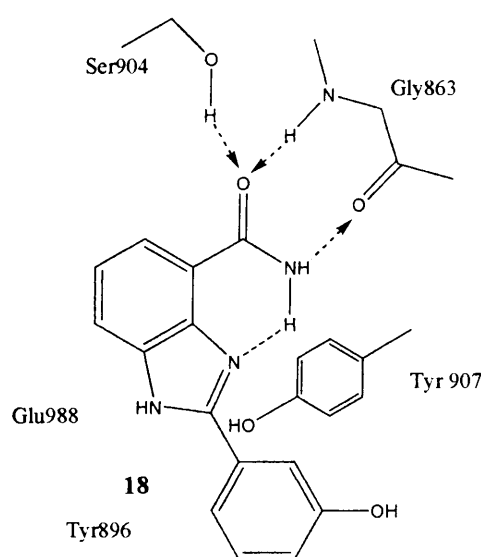
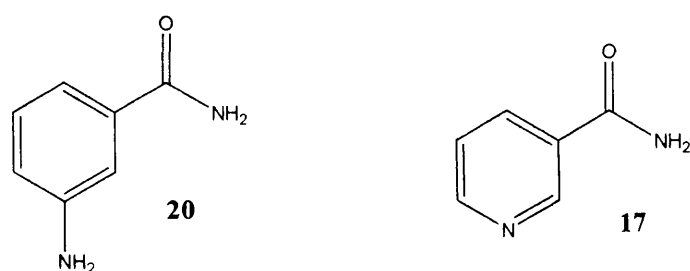


Figure 1.15 NU1058 complexed with the catalytic domain of PARP.

A common structural feature for PARP inhibitors is an aromatic amide or the amide group placed in a polyaromatic heterocyclic skeleton to generate a fused aromatic lactam or an amide restrained by an intramolecular hydrogen bond, see **18** in Figure 1.15 (Virag and Szabo, 2002).

Early structure activity relationship (SAR) studies revealed nicotinamide and various 3-substituted benzamides such as 3-aminobenzamide (**20**) to be some of the first effective PARP-1 inhibitors. They have IC_{50} values of approximately 30 μ M in an isolated PARP-1 enzyme assay. Being a natural compound, nicotinamide (**17**) with an $IC_{50} = 9 \mu$ M (Suto *et al.*, 1991) acts as a substrate for other NAD^+ metabolising enzymes. Structurally similar compounds such as benzamide, pyrazinamide and substituted benzamides, in particular 3-aminobenzamide also demonstrated inhibition of PARP-1 (Southan and Szabo, 2003).



These studies revealed the importance of the carboxamide group within the compound. Yet poor efficacy, specificity and sometimes inadequate water solubility, is a complication in the clinical testing of these compounds (Southan and Szabo, 2003). One possible reason for the lack of effectiveness of these compounds is that the amide bond of the nicotinamide or 3-aminobenzamide is free to rotate relative to the plane of the aromatic ring and is not restricted to the biologically active 'planar' conformation. Therefore, the synthesis of isoquinolinones in which the amide bond was incorporated in an anti-configuration within an aliphatic ring system was reported (Figure 1.16). (Griffin *et al.*, 1995; Griffin *et al.*, 1998). The anti-isomer **21** has an IC₅₀ 0.41 μM and the IC₅₀ of syn-isomer **20** is approximately 8 μM (Suto *et al.*, 1991).

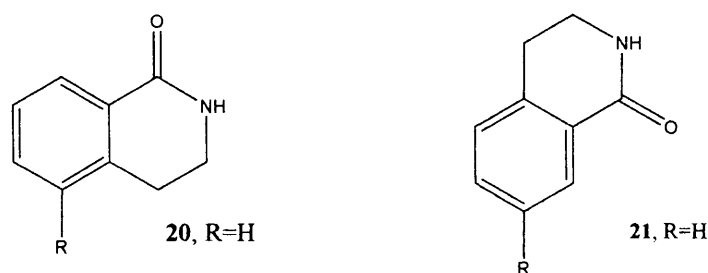


Figure 1.16 Structures of isoquinolinones (anti- and syn-configuration).

As restriction of the carboxamide into the favourable conformation should result in increased inhibitory potency, a series of benzimidazole-4-carboxamides compounds were synthesised that favoured the active conformation by intramolecular hydrogen bonding between the amide proton and a heterocyclic nitrogen (Figure 1.17) (Southan and Szabo, 2003).

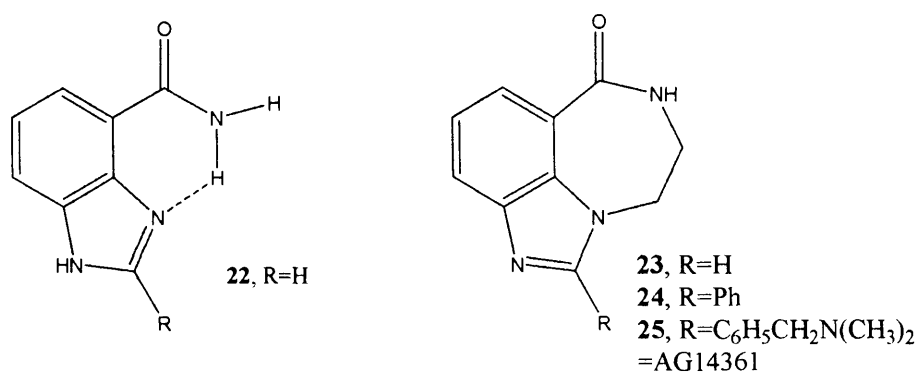


Figure 1.17. Examples of ring open and cyclized PARP inhibitors.

These compounds (**22**, **23**) show more potency, both with an IC₅₀ about 300 nM, more active compared to the monocyclic carboxamides.

The strategy of cyclizing an open benzamide structure by the synthesis of 7-membered rings (Figure 1.17) is one of the best approaches to design new PARP inhibitors. All lactam derivatives that contain a carboxamide group in an anti-(or syn-) configuration within a ring structure are reasonably more effective than their ring open amide analogues (Suto *et al.*, 1991).

Studies indicate that a phenyl group at the 2-position of the benzimidazole (Figure 1.17) improves efficacy (Southan and Szabo, 2003).

AG14361 (**25**) is a lactam-based PARP-1 inhibitor. An important feature within this molecule is the addition of the benzyldimethylamine group at the R-position of compound **25**. This drug has also undergone a reasonable degree of clinical testing; hence making it a useful compound for comparisons (SARs).

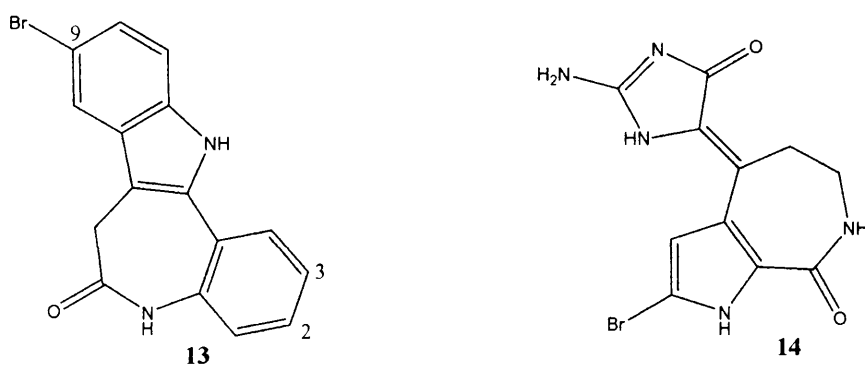
This PARP-1 inhibitor embraces the overall favourable pharmacological properties of high potency (K_i < 5nM), specificity, stability, and *in vivo* activity all of which that are necessary for its application in humans (Calabrese *et al.*, 2004).

1.5 AIMS OF RESEARCH

The cell cycle, including checkpoints, and the DNA damage response are all important therapeutic targets for the treatment of cancer. Although many types of inhibitors have been identified in each of these areas, compounds containing a seven-membered lactam ring have been identified as key inhibitors for CDKs/Chk2/PARP-1. This thesis aims to investigate the medicinal chemistry of this pharmacophore against various biological targets and develop synthetic routes for compounds of interest. Hence, the aims of this research can be divided into three sections:

- Design of novel cell cycle inhibitors
- Design of novel cell cycle checkpoint inhibitors
- Design of novel DNA repair inhibitors

The first aim was to synthesize novel inhibitors of the cyclin dependent kinases (CDKs). The starting point of this project was centred upon developing the synthesis based on the essential lactam pharmacophores in kenpaullone (**13**) and hymenialdisine (**14**) (Figure 1.17).



Both kenpaullone and hymenialdisine inhibit CDK1/cyclin B ($IC_{50} = 0.4, 0.02 \mu M$ respectively) and CDK2/cyclin A ($IC_{50} = 0.68, 0.07 \mu M$ respectively) in low micromolar concentrations. The main aim was to develop a synthetic route to synthesise compounds that could be used to explore the SARs associated with novel lactam based hymenialdisine/kenpaullone related CDK inhibitors. Based on details of the interaction of kenpaullone with the CDK active site, the lactam occupies little of the ATP binding pocket volume where the sugar and phosphate groups of the ATP interact, and bulky,

lipophilic groups in this region are of great importance (Arris *et al.*, 2000). This may result in better potency and antitumour activity.

The synthesis of analogues containing a seven-membered lactam ring fused to an aromatic ring will provide diverse selection of potential inhibitors to screen for anti-cancer activity and reinforce the hypothesis that such compounds can be developed as cell cycle inhibitors. The lactam group can form hydrogen bond interactions with the enzyme with the conserved residues Glu81 and Leu83. In addition, these compounds contain a free NH at the 5-position (Figure 1.18). As shown in Figure 1.18, lead compounds **26**, **27** and **28** can be altered in different ways.

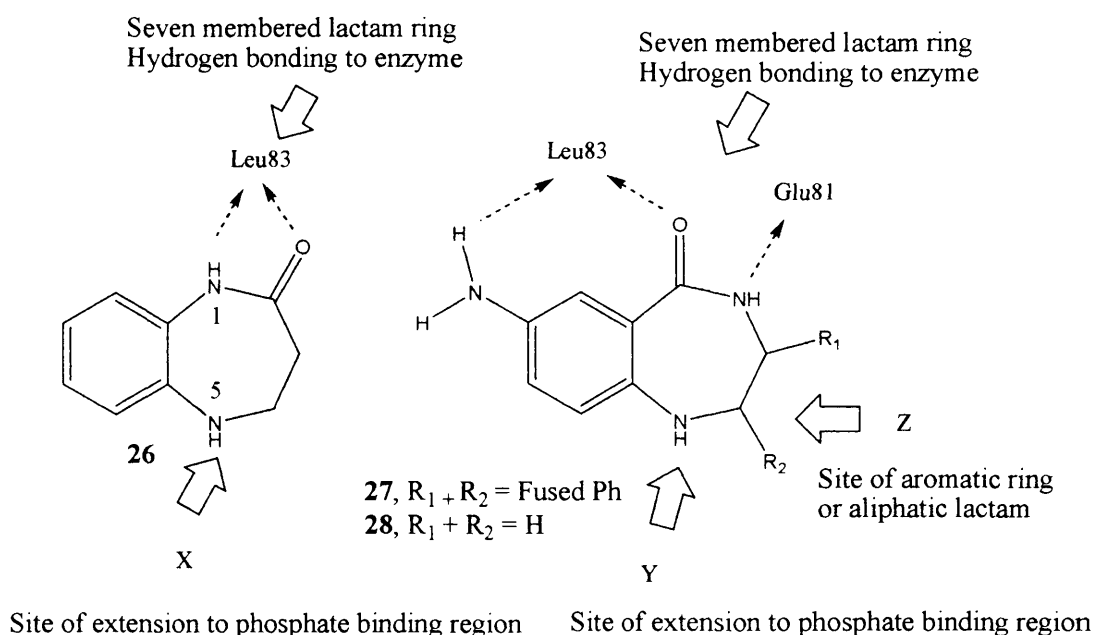


Figure 1.18 SAR determination of compounds **26**, **27** and **28**.

The second aim of this project was to study a series of compounds as a preliminary study for the identification of novel and potent inhibitors for Chk2. Currently there are few published small molecule inhibitors of Chk2, as the Chk2 kinase is yet to be crystallized. To determine if Chk2 is a suitable target for anti-cancer therapeutics based on the lactam pharmacophore, SAR studies would be useful and lead us to develop our synthesized compounds (Figure 1.18). From the studies of the kenpaullone docked within the ATP binding site of the Chk2 homology model and current known Chk2 inhibitors, the bromine atom appears to play an important role in the activity of this compound as it fills

the back of the binding site and may serve as a hydrophobic anchor to put the molecule into place (Figure 1.19). In addition to the bromine, the amide group is predicted to form hydrogen-bonding interactions with an aspartate residue (Figure 1.20).

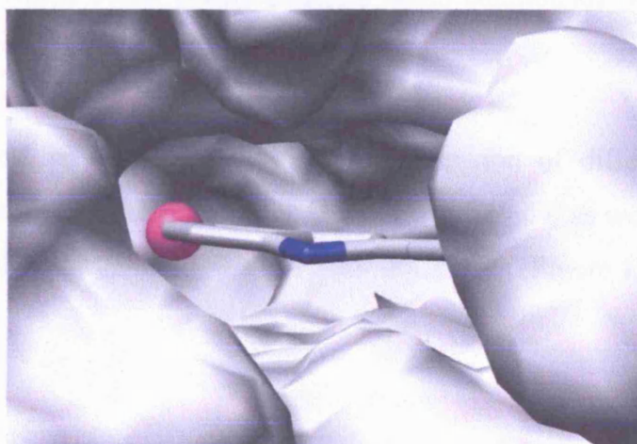


Figure 1.19 The ATP binding pocket of the Chk2 model, bromine is presented as a sphere.

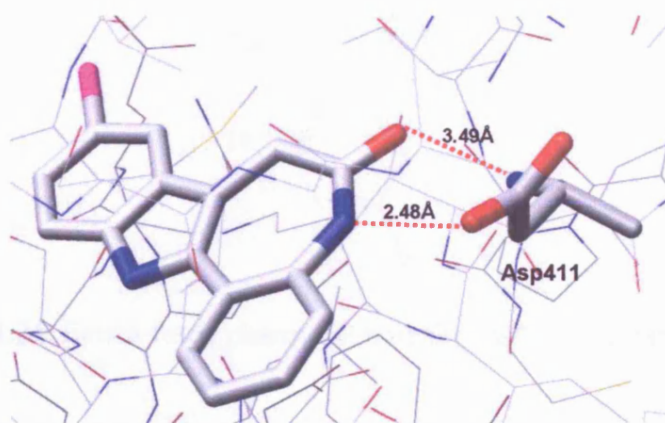


Figure 1.20 Lactam interactions of kenpaullone with Chk2 aspartate.

The third aim was to synthesize novel inhibitors of PARP-1, by investigating novel modifications to a known lactam pharmacophore and introducing various additional substituent groups to improve PARP-1 inhibition. The benzo-fused pharmacophore (**29**) has recently been patented (Lubisch *et al.*, 2003) and is an interesting option to improve PARP-1 inhibition. It comprises an aromatic ring extension that could potentially provide the platform for further active site interactions. Numerous derivatives of this structure,

mostly concerned with the variation of phenyl imidazole ring segment, were analysed in this patent (Lubisch *et al.*, 2003) with generally promising activity. However with the aid of molecular modelling several new ideas were hypothesised for prospective pharmacophore modifications, through the addition of substituent groups at the X-, Y- and Z-positions, which could permit possible novel compounds with novel interactions between the inhibitor and the PARP-1 active site.

The important feature of this scaffold is the extension of different groups to allow exploration of additional interaction with Gly863 and Ser864, as well as other amino acid residues previously untargeted in PARP-1 inhibitor design (Figure 1.21).

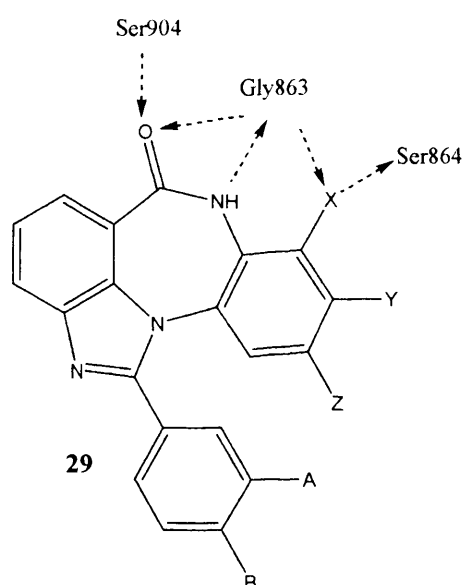


Figure 1.21 Benzo-fused pharmacophore for PARP-1 inhibition.

To search for interactions within the enzyme active site, this project aimed to devise and prepare novel dibenzo-derivatives with emphasis on aromatic substituents that could enhance the intermolecular binding with amino acid residues within the PARP-1 active site, and build up SARs for this series of compounds. The synthesis and biological evaluation of the various benzo-derivative compounds is described in this thesis.

CELL CYCLE INHIBITORS, RESULTS AND DISCUSSION

Small molecule inhibitors targeting cyclin dependent kinases (CDKs), have been the focus of extensive interest in cancer research. Although a number of small molecule inhibitors have been identified, they frequently lack potency and/or specificity. Efforts are underway to uncover inhibitors that selectively target specific CDKs and to develop these as a new generation of antitumour drugs. In order to develop the methodology required for the synthesis of seven-membered lactam pharmacophore found in kenpaullone (**13**) and hymenialdisine (**14**), and to generate non-purine based CDK inhibitors, benzodiazepin-2-one (**26**) was selected as a scaffold and initial synthetic target. The synthesis and biological activity of some of these compounds has been previously reported. N-5 is the main group of this compound where substitution can occur (Figure 2.1).

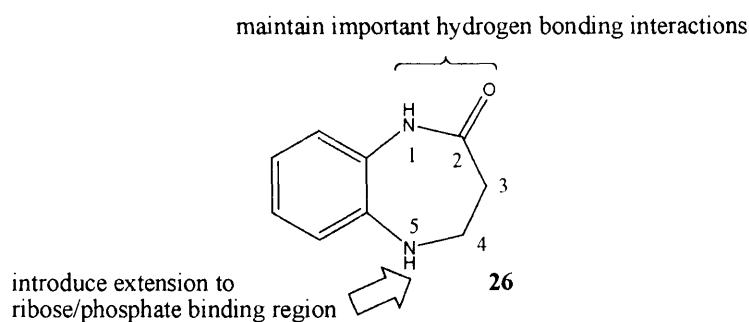
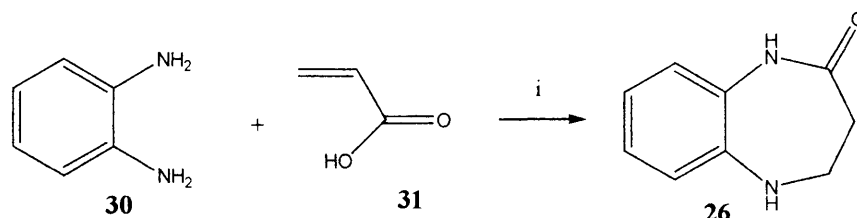


Figure 2.1 The main substitution site previously investigated on the benzodiazepin-2-one scaffold.

2.1 EFFICIENT BENZODIAZEPIN-2-ONE SYNTHESIS (Bachman and Helsey, 1949)

A concise synthesis was reported by treating 1,2-phenylenediamine (**30**) with aqueous acrylic acid (**31**), followed by heating in concentrated hydrochloric acid (Bachman and Helsey, 1949) (Scheme 2.1). The resulting product, isolated as an off-white solid, was used for most syntheses described in this chapter with no further purification. Although the yields for this reaction were low, 37 % was the greatest achieved, the synthesis involved cheap, commercially available starting materials and was performed on a large scale (up to 15 g). **26** is surprisingly water-soluble (clogP = 0.6) and problems extracting this material during the work-up of the reaction may account for the low yields observed in the synthesis.

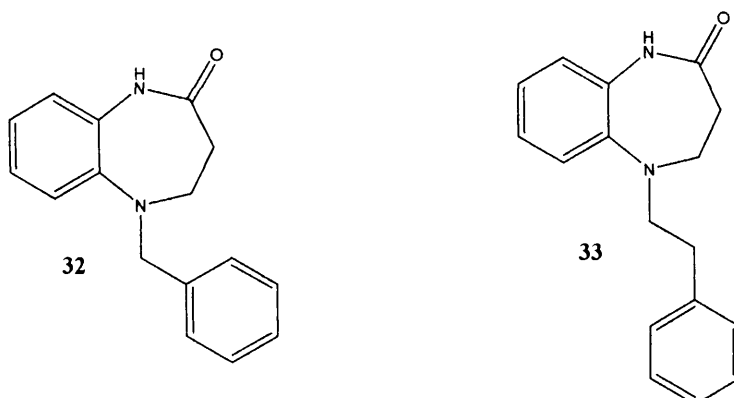
Scheme 2.1



i) Acrylic acid (60 %), conc. hydrochloric acid, reflux, 37 %.

2.1.1 Synthesis of N-5 benzodiazepin-2-one derivatives

By analogy to kenpaullone (**13**) it is expected that the amide group of previously reported CFU58 (**26**) will interact with Glu81/Leu83 in the active site of CDK2, and extensions to the pharmacophore will be possible from the amine N-H. Therefore, in order to investigate the extent of hydrophobic interactions made by the N-5 substituent within the active site of the CDKs, 5-benzylbenzodiazepin-2-one (**32**, CFU38) and 5-phenethylbenzodiazepin-2-one (**33**, CFU46) were synthesised previously within the group.



The GI_{50} values obtained for these compounds (assays were conducted by the Tenovus group) suggested that they are more active than CFU58 (**26**), which was expected since their extensions should occupy the cleft of the active site (Table 2.1). It appears that hydrophobic extensions into the active site cleft are beneficial to biological activity and the slightly improved activity of CFU46 (**33**) compared to CFU38 (**32**) suggests a longer extension is better.

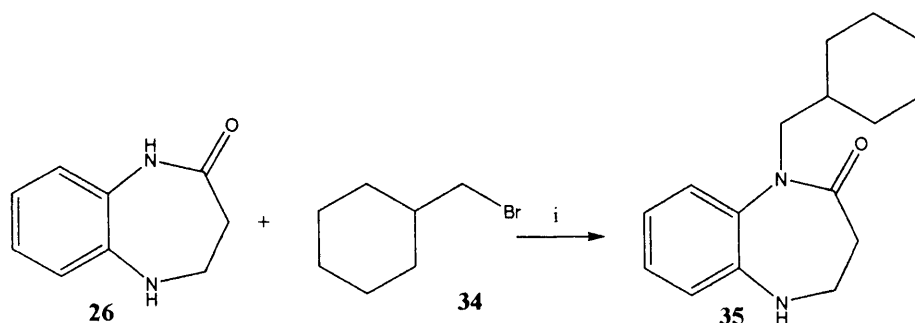
Table 2.1 Growth inhibition (MCF7) results.

Compound	CFU	GI_{50} (μ M)
26	58	>100
32	38	188
33	46	141

To study structure-activity relationships in the active site cleft, the synthesis of saturated ring analogues, which may have alternative interactions with the active site of CDKs was proposed.

These analogues may be prepared by similar methodology. CFU58 (**26**) was treated with cyclohexylmethyl bromide (**34**) to give CFU40 (**35**) (Scheme 2.2). In spite of the predicted lower reactivity of the amide nitrogen, this reaction was regioselective to the amide nitrogen. No amine substituted products could be identified from the reaction.

Scheme 2.2



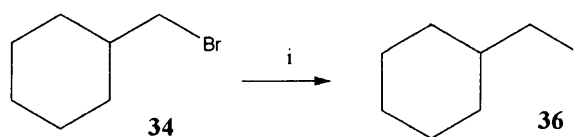
i) NaH, DMF, 32 %.

Since cyclohexylmethyl bromide (34) is quite sterically hindered, and this reacts with the amide nitrogen adjacent to a relatively bulky carbonyl group, this suggests the N-5 amine centre is more hindered for reaction with the incoming electrophile.

2.1.1.1 Attempts to enhance the reactivity of the electrophile

Considerable effort was made to synthesize mono-substituted analogues selective to the amine N-5 position of CFU58 (26) using iodide derivatives, as iodide is a better leaving group than bromide and increased reactivity may overcome the steric problem. The Finklestein reaction was the best method for preparing suitable iodo derivatives: commercially available cyclohexylmethyl bromide was treated with sodium iodide producing the desired compound in high yield with no need for further purification (Scheme 2.3).

Scheme 2.3



i) NaI, acetone, reflux, 100 %.

Hence, CFU58 (**26**) was reacted with cyclohexylmethyl iodide (**36**) in the presence of sodium hydride at room temperature, but the product isolated after purification by column chromatography (beside starting material) was mono-substituted selectively on the amide nitrogen (Scheme 2.4). In this compound, the precise N-alkylation was determined by the presence of amine signals in the ^1H NMR (δ 5.15). Further evidence for the amide substitution in compound **35** was provided by the two dimensional NOESY spectrum, an NMR experiment used to detect protons with close proximity, generally 2-4Å, falling off rapidly as the inverse sixth power of the distance apart of the nuclei. NOE interactions were observed between the amine peak at δ 5.15 and protons in the aromatic region and the adjacent CH_2 peak. There were also NOE interactions between the cyclohexylmethyl CH_2 peak and the aromatic proton (Figure 2.2).

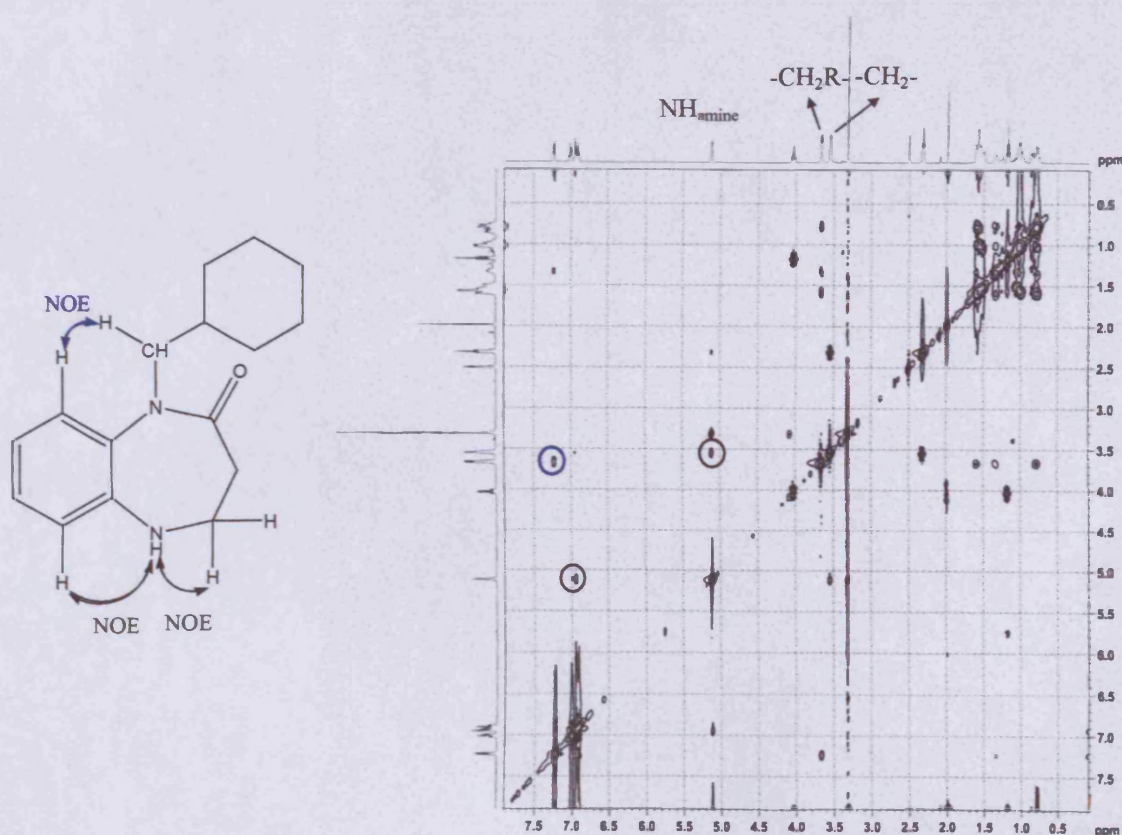
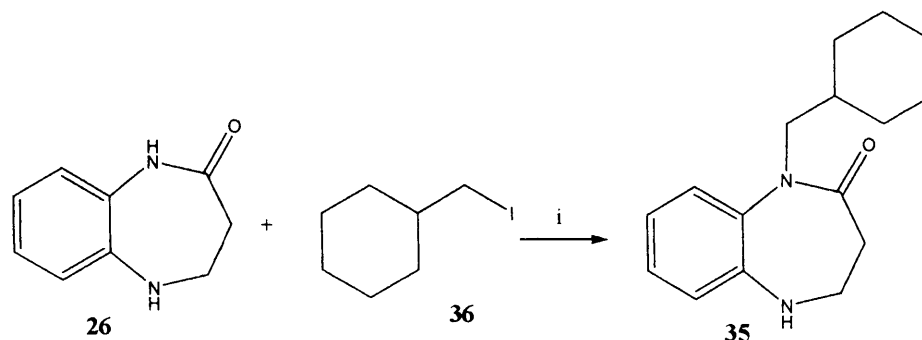


Figure 2.2 The Nuclear Overhauser effects observed in compound **35**.

Scheme 2.4



i) NaH, DMF, 40 %.

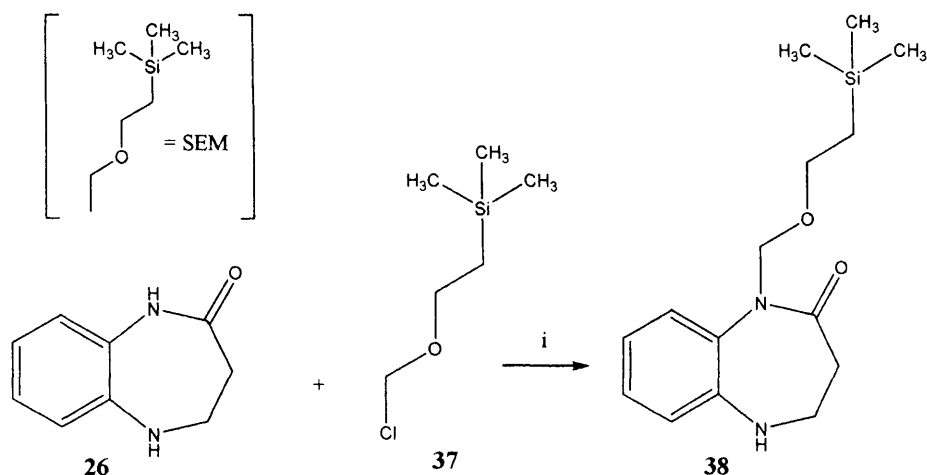
This suggests that the electrophile's steric hindrance has a greater effect than the increased reactivity due to the iodide leaving group, however, the approach requires further investigation.

2.1.1.2 An amide protecting strategy for the synthesis of benzodiazepin-2-one analogues

(Annoura and Tatsuoka, 1995)

One of the major problems with the previous method had been the steric bulk of the alkylating reagent, suppressing addition at the amine nitrogen and resulting in addition at the amide nitrogen. Therefore, the use of an alternative procedure was considered, in which a less bulky, amide protecting group was inserted at an early stage of the synthesis. The rationale was that since the amide appeared to be readily substituted it should be easy to incorporate a protecting group selectively at this position. 2-(Trimethylsilyl)ethoxymethyl chloride (37) was chosen as a robust silyl protecting group, which is readily cleaved by fluoride. Additionally, the electrophilic centre of the silylating reagent is a primary carbon atom resembling the previously used alkylating reagents but with low steric bulk (Scheme 2.5). The protected product 38 was shown to have the correct N-substitution by NMR, due to the presence of a peak at δ 5.12 for the amine proton, and the lack of the amide peak at approximately δ 9.

Scheme 2.5



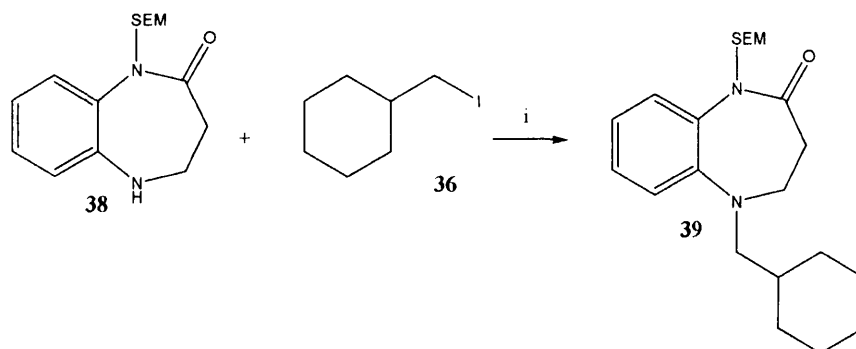
i) NaH, DMF, 16 %.

A low yield for the SEM protected compound (**38**) was observed. Unexpectedly the yield was even lower compared to CFU40 (**35**), as the SEM-Cl looked to be less hindered than cyclohexylmethyl bromide at the electrophilic carbon. The reason for the low yield of compound **38** was unclear.

2.1.1.2.1. Synthesis of the protected lead compound analogues

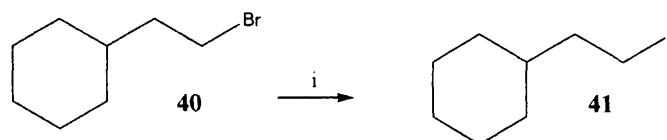
With the protecting group in place, compound **38** was treated with cyclohexylmethyl iodide (**36**) in the presence of potassium carbonate (a strong base) to deprotonate the amine in DMF. This reaction was successful in alkylation of the N-5 amine nitrogen (Scheme 2.6).

Scheme 2.6



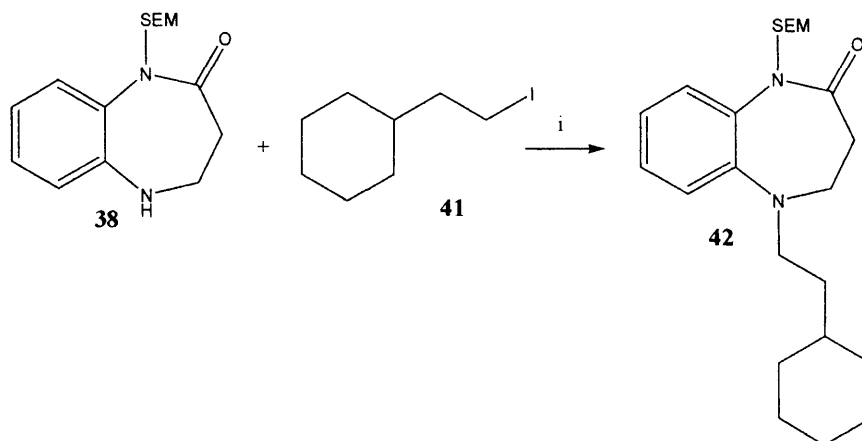
i) K_2CO_3 , DMF, 150 °C, 30 %.

As previously explained, the Finklestein reaction was reused to activate an alternative electrophile, (2-bromoethyl)cyclohexane (**40**), by converting to (2-iodoethyl)cyclohexane (**41**) in presence of sodium iodide (Scheme 2.7).

Scheme 2.7

i) NaI, acetone, reflux, 90 %.

This method could now be used to investigate how introducing various substituents at the N-5 position would affect biological activity. For this purpose, following an analogous procedure to that attempted for the synthesis of **39**, compound **38** was treated with (2-iodoethyl)cyclohexane (**41**) in presence of potassium carbonate in DMF to produce the compound **42** (Scheme 2.8).

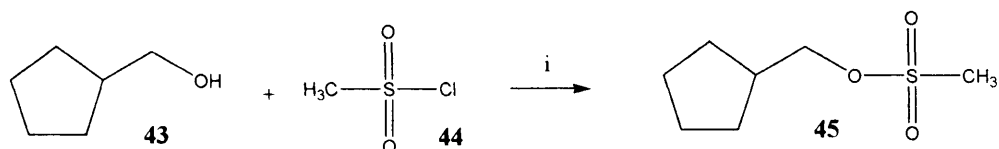
Scheme 2.8

i) K₂CO₃, DMF, 150 °C, 36 %.

In order to vary the ring size for structure activity purposes, methylcyclopentanol was a commercially available reagent that could be readily converted into a suitable alkylating reagent. This was achieved by treating methylcyclopentanol (**43**) with methanesulfonyl

chloride (**44**) to yield the mesylate derivative, a good leaving group and thus converting the alcohol into a powerful alkylating reagent (Scheme 2.9).

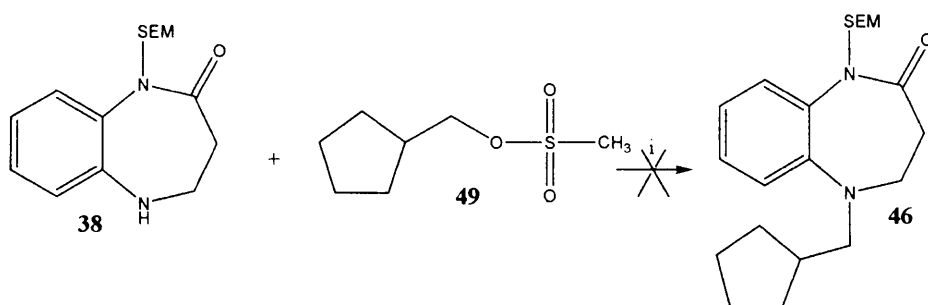
Scheme 2.9



i) TEA, THF, 100 %.

SEM protected lactam **38** was heated with the activated mesylate **45** in presence of potassium carbonate in DMF, but surprisingly no reaction occurred. This was presumably due, again, to the bulkiness of the reagents at the point of reaction (Scheme 2.10).

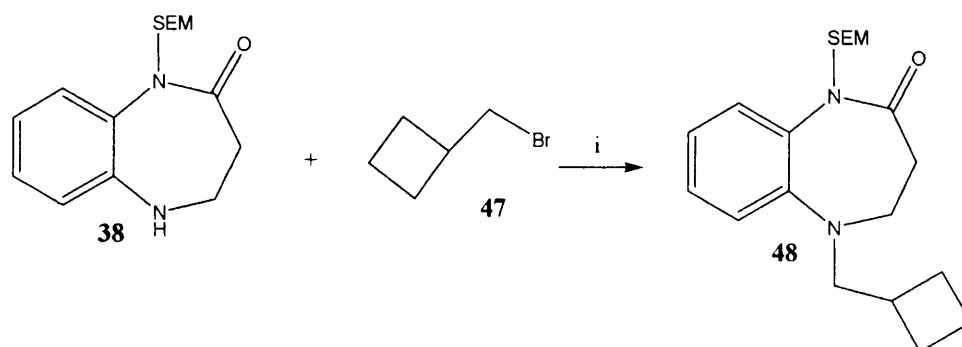
Scheme 2.10



i) K₂CO₃, DMF, 150 °C, 0 %.

In order to investigate the effect on activity of the smaller aliphatic rings which may be better accommodated in the binding pocket, the commercially available cyclobutylmethyl bromide (**47**) was used. To do so, following an analogous procedure to that previously used, compound **38** was treated with cyclobutylmethyl bromide in presence of potassium carbonate in DMF to produce the compound **48** (Scheme 2.11).

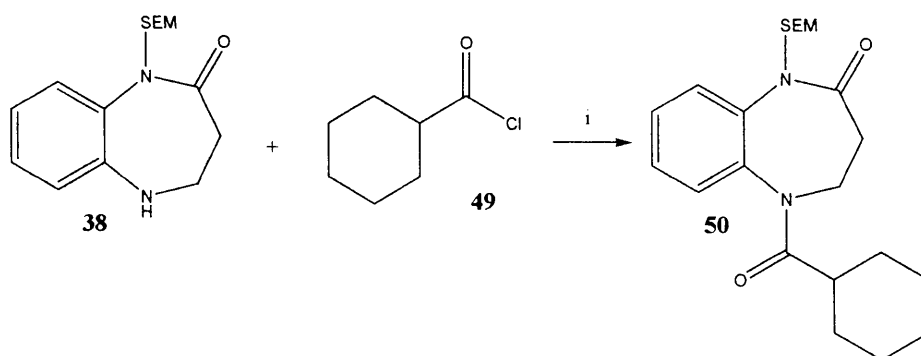
Scheme 2.11



i) K_2CO_3 , DMF, 150 °C, 45 %.

An alternative alkylating reagent was cyclohexoyl chloride (**49**), due to its higher reactivity as an electrophile. The reaction was performed in the presence of sodium hydride at room temperature to produce the compound **50** in an improved yield compared to the use of halide or mesylate derivative (Garin *et al.*, 1987; Puodziunaite *et al.*, 1997) (Scheme 2.12).

Scheme 2.12



i) NaH, pyridine, CH_2Cl_2 , 50 %.

The final step needed to recover the target compounds is the cleavage of the 2-(trimethylsilyl)ethoxymethyl (SEM) protecting group. This is reported to proceed with 1M tetrabutylammonium fluoride solution at reflux (1M in TBAF) (Whitten *et al.*, 1986). Compounds **39**, **42**, **48** and **50**, were treated with 1M TBAF/THF solution at reflux to furnish the desired products **52**, **53**, **54** and **55** respectively (Scheme 2.13). The yields were unexpectedly poor for silyl deprotection. The silicon not being bonded directly to the

nitrogen might have impeded the reaction, since silyl removal is followed by the decomposition of the N-methylhydroxy intermediate shown in Figure 2.3.

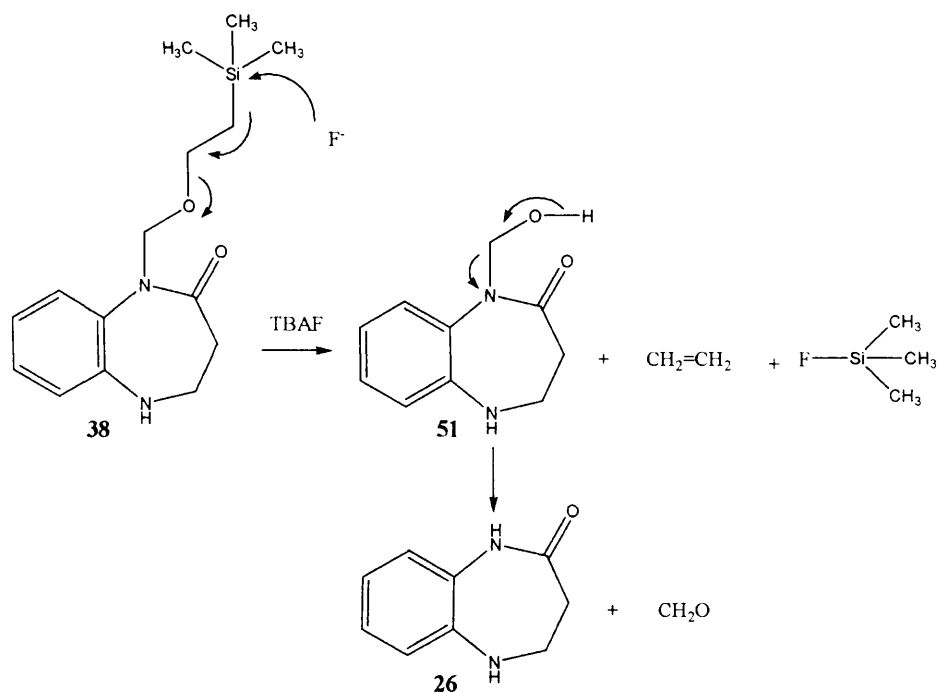
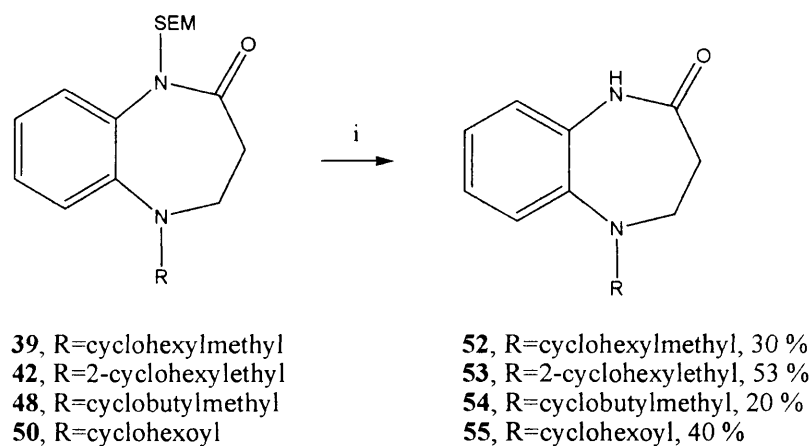


Figure 2.3 Proposed steps in the SEM deprotection.

Scheme 2.13



i) 1M TBAF/THF solution, reflux.

Molecular modelling studies of compound **62** (page 63) bound to CDK2 revealed that the presence of Asp86 in the ribose-binding pocket provided a residue for potential interaction. Furthermore, this residue has been exploited by other CDK2 inhibitors.

An overlay of **62** and olomoucine (**6**) bound to monomeric CDK2 (Figure 2.4) revealed that both inhibitors bind to the same residues within the ATP binding site, but with one less hydrogen bond interaction formed by compound **62** compared to olomoucine. Therefore, it was hypothesised that the introduction of an alcohol functional group into the N-5 substituent could mimic the ethyl hydroxy group of olomoucine and lead to favourable interactions with residues in the ribose-binding domain thereby providing greater activity and the possibility of introducing further activity.

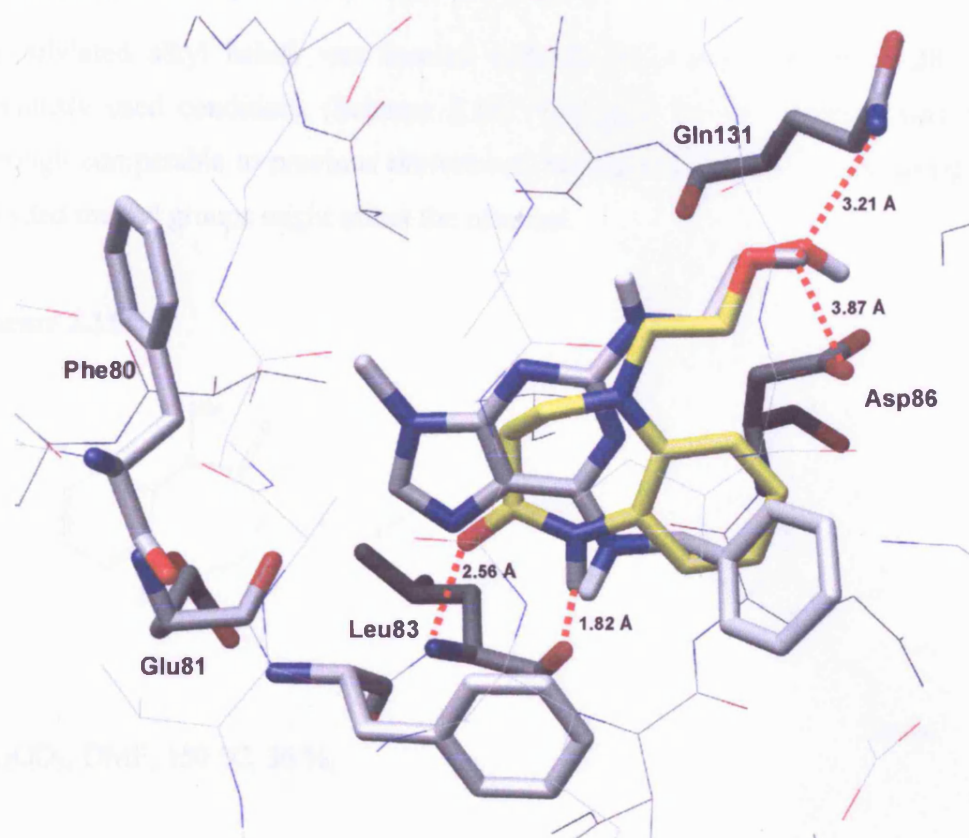
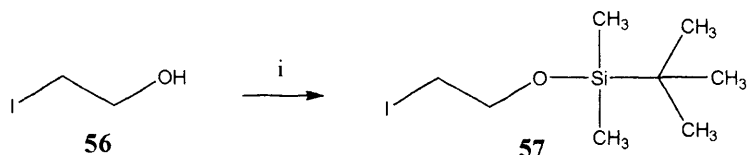


Figure 2.4 Overlay of olomoucine (grey sticks) and compound **62** (yellow sticks) bound to the active site of CDK2. (Oxygen is shown in red, nitrogen in blue).

To introduce these functional groups, the established method could be used, using a suitable alkyl halide. However, it would be necessary to protect the hydroxyl group of the alkyl halide in order to protect possible side reactions. The chosen protection group was *tert*-butyldimethylsilyl chloride (TBDMS-Cl), a well-known silyl protecting group for alcohols that is easy to introduce: reaction of **56** with TBDMS-Cl in the presence of imidazole in DMF had excellent yields of 98 % (Scheme 2.14).

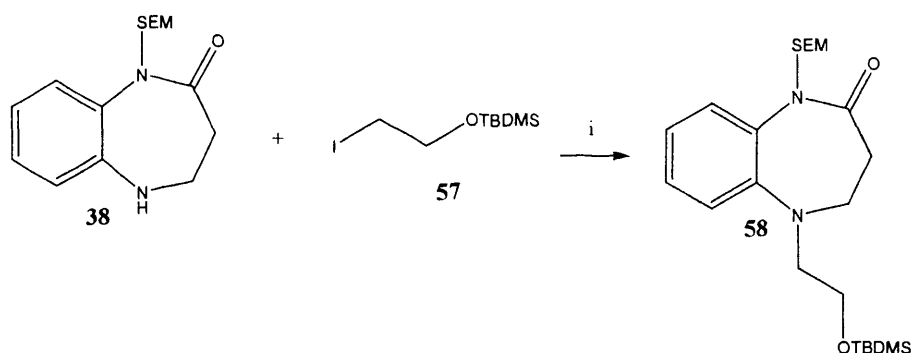
Scheme 2.14



i) TBDMS-Cl, imidazole, DMF, 98 %.

The silylated alkyl halide was reacted with the SEM-protected amide **38** under the previously used conditions (Scheme 2.15). The yield for this reaction was moderate, although comparable to previous derivatives, but the steric hindrance resulting from the crowded methyl groups might affect the reaction.

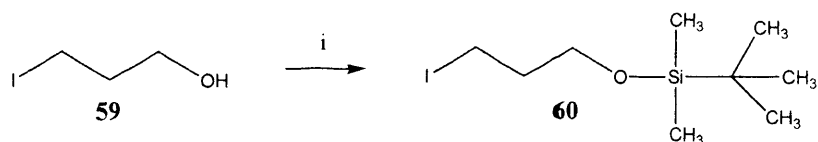
Scheme 2.15



i) K_2CO_3 , DMF, 150 °C, 36 %.

This methodology now allowed an investigation of the effect of increasing the aliphatic chain length of the N-5 substituent, a similar procedure was used to add the hydroxypropyl substituent at N-5 (Scheme 13). Again the protection step was performed before the main reaction to yield the iodopropyl compound **60** (Scheme 2.16).

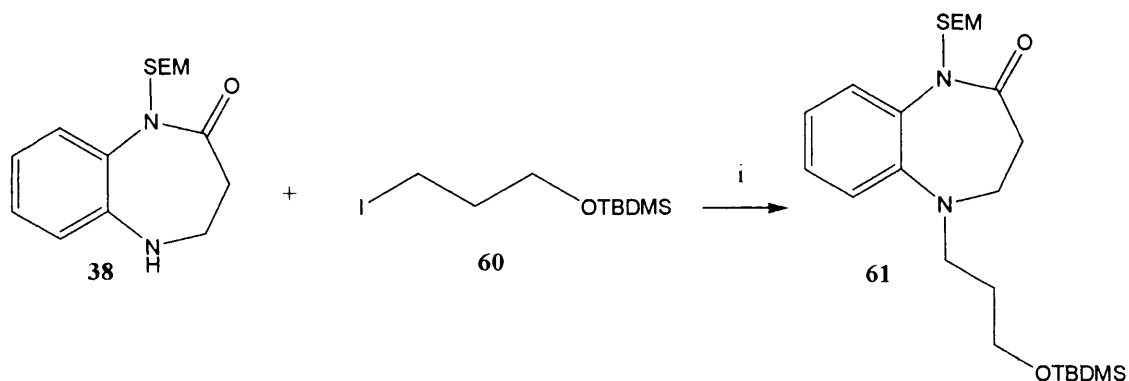
Scheme 2.16



i) TBDMS-Cl, imidazole, DMF, 84 %.

This was reacted with SEM-protected amide **38** under similar conditions as previous, yielding the protected hydroxyl N-propyl compound **61** (Scheme 2.17).

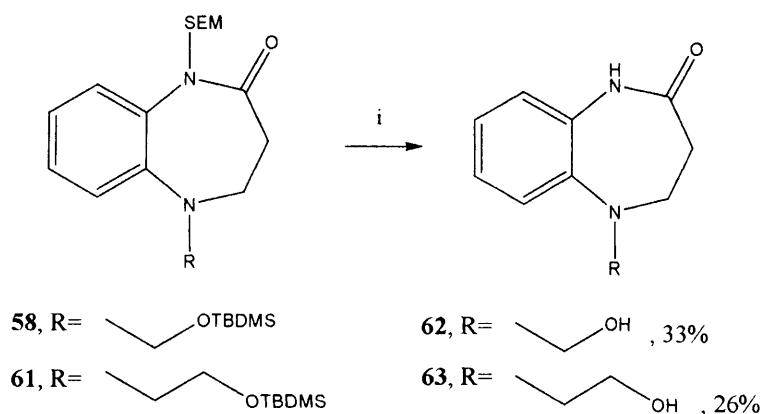
Scheme 2.17



i) K_2CO_3 , DMF, $150^\circ C$, 30 %.

The analogous compounds **58** and **61** contain both O-silyl and C-silyl protecting groups. However, the method used to cleave the SEM protecting group should also be applicable to deprotect the O-TBDMS, group. To do so, compound **58** and **61**, were both treated with 1M TBAF/THF solution at reflux that resulted in simultaneous deprotection of the SEM and TBDMS groups in one pot (Scheme 2.18).

Scheme 2.18



i) 1M TBAF/THF solution, reflux.

The crystal structure of CDK2 complexed with H717 (**64**), an olomoucine-derived highly potent CDK2 inhibitor ($IC_{50} = 48 \text{ nM}$) showed that the purine ring system of H717 binds quite differently from the purine portion of the ATP but in a similar way as olomoucine which is 200-fold weaker ($IC_{50} = 7 \mu\text{M}$, CDK1/cyclin A) (Dreyer *et al.*, 2001). The improved potency of this compound due to the presence of the 4-aminocyclohexylamino group was possibly as a result of an additional interaction between the charged amino group connected to the cyclohexyl ring, which interacts via a salt bridge to Asp145, and a hydrogen bond with Asn132, as observed in the X-ray structure (Figure 2.5).

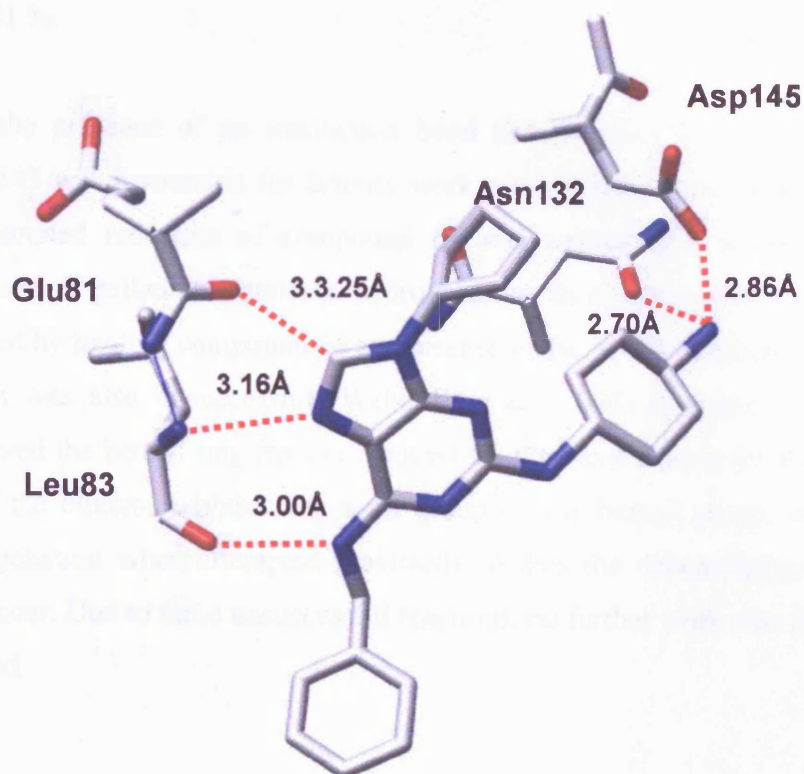
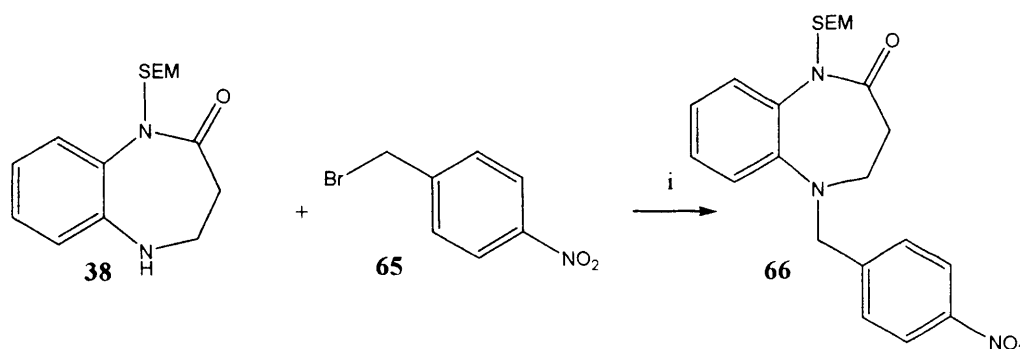


Figure 2.5 The binding orientation of H717 in CDK2. The 4-aminocyclohexyl group is shown interacting with Asn132 and Asp145 .

Therefore, in an alternative attempt to further probe the ATP binding site in the vicinity of the benzodiazepinone N-5 substituent leading to any possible interactions with Asp145 or other residues in the ribose-binding pocket, the preparation of an amine containing analogue was proposed. Initially, the nitrobenzyl derivative of **66** was synthesised. This was done by treating intermediate **38** with 4-nitrobenzyl bromide (**65**) in presence of sodium hydride in DMF (Scheme 2.19).

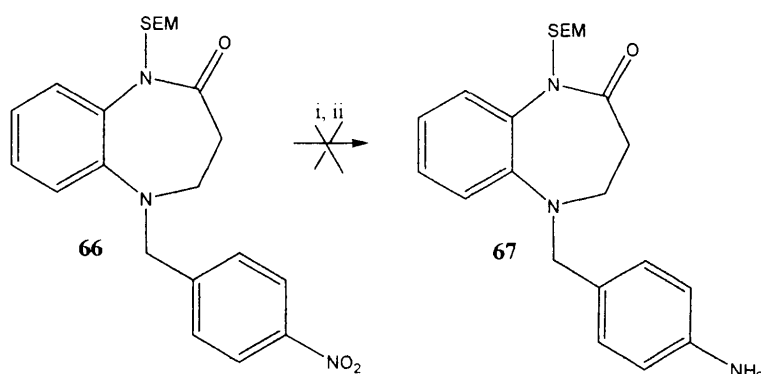
Scheme 2.19



i) NaH, DMF, 51 %.

As discussed, the presence of an interaction bond between the N-5 substituent and Asn132 or Asp145 was favourable for activity work was carried out to reduce the nitro group. The attempted reduction of compound 66 was unsuccessful when using the standard conditions of palladium-catalysed hydrogenation. In an alternative attempt, this reaction was tried by treating compound 66 in presence of Fe/AcOH in ethanol at reflux, but the reaction was also unsuccessful (Webb II *et al.*, 1991) (Scheme 2.20). Both conditions removed the benzyl ring from compound 66. One explanation for this may be the presence of the electron-withdrawing nitro group on the benzyl group, which was stable to hydrogenation when attempted previously, makes the debenzilation reaction more likely to occur. Due to these unsuccessful reactions, no further work was carried out on this compound.

Scheme 2.20



i) H₂, 10% Pd/C, MeOH, 0%. ii) Fe/AcOH, EtOH, 0 %.

2.2 LIPOPHILIC MODIFICATION TO BENZODIAZEPINE-2-ONE SCAFFOLD

Phe80 is an important residue in the active site of CDK2 forming a hydrophobic region deep in the active site of the enzyme. In order to assess the importance of lipophilic interactions with CDK2 modifications to benzodiazepine-2-one scaffold (**26**, CFU58) by incorporation of methyl groups, and the synthesis of the compound **68** was hypothesized (Figure 2.6).

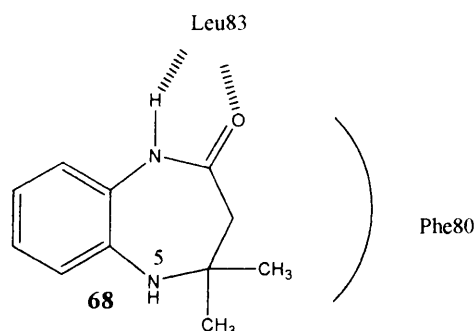
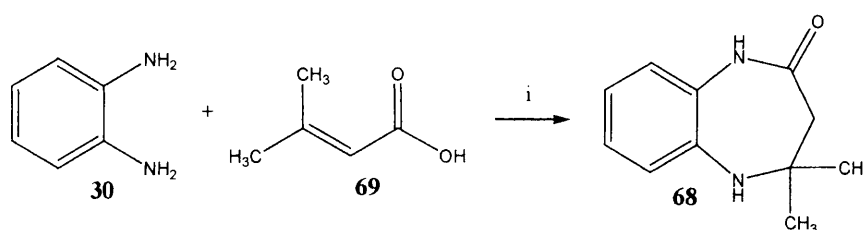


Figure 2.6 Lipophilic modification to benzodiazepinone scaffold.

2.2.1 The synthesis of modified benzodiazepin-2-one

Compound **68** was synthesized by treating 1,2-phenylenediamine (**30**) with methacrylic acid (**69**), and heating in concentrated hydrochloric acid (Bachman and Helsey, 1949) (Scheme 2.21). The desired product was isolated, although the yields for this reaction were low, and most of the starting material remained unreacted. However, the synthesis involved cheap, commercially available starting materials. The presence of the bulky methyl groups on the methacrylic acid may account for the low yields observed in this reaction.

Scheme 2.21



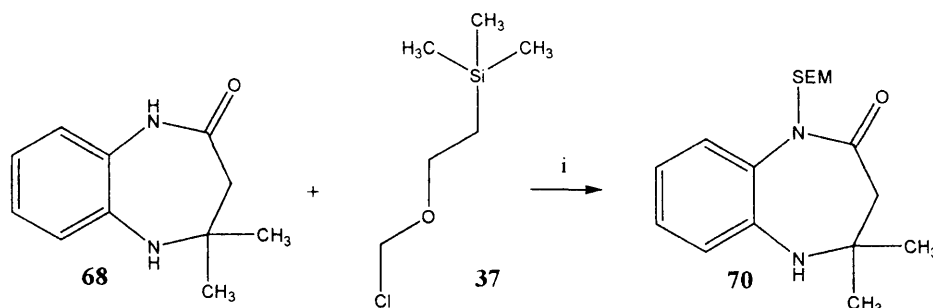
i) Methacrylic acid (60%), conc. hydrochloric acid, reflux, 16 %.

2.2.1.1 Attempts to synthesis of modified benzodiazepin-2-one analogues

As it is seen in Figure 2.6, it is expected that the amide of **68** will interact with Glu81/Leu83 in the active site of CDK2. Furthermore, the methyl groups of the methacrylic acid derivative could have lipophilic interactions with Phe80. Additionally, extensions from the 5-NH of **68** could form further binding interactions within the active site cleft.

As described previously, mono-substitution of compound **68** regioselectively at the N-5 position was required. To avoid formation of the amide substituted by-product, protection of this group was performed using SEM-Cl. The low yield of this reaction was comparable to that obtained previously with analogue **38** (Scheme 2.22). Having the SEM group attached to **70**, improved its physical properties as **70** became more nonpolar and thus easier to purify.

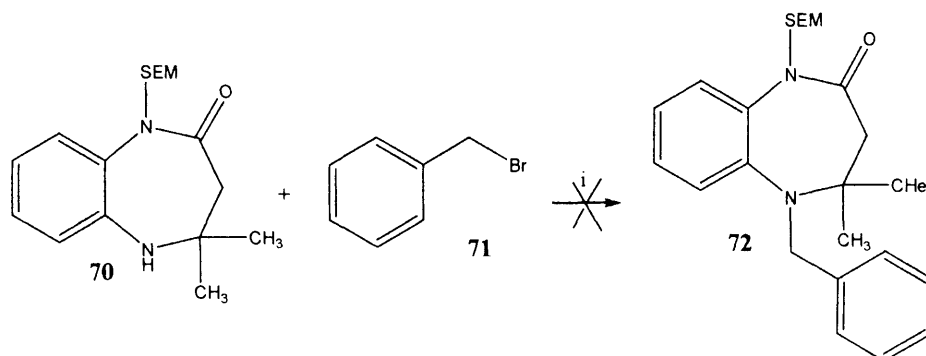
Scheme 2.22



i) NaH, DMF, 18 %.

To continue the determination of SAR, the synthesis of N-5 derivatives was required. The dimethyl compound (**70**) was reacted with benzyl bromide (**71**) (Scheme 2.23), but no reaction occurred and only the starting material was recovered. This was possibly due to the bulkiness of the compound **70** at the N-5 nitrogen, adjacent to two methyl groups.

Scheme 2.23



i) NaH, DMF, 0 %.

Owing to polarity of lead compound (**68**) resulting in difficulty purifying it, no further examples were studied using this method, which is presumably restricted to the use of aliphatic reagents.

2.3 SYNTHESIS OF DIBENZODIAZEPIN-2-ONE ANALOGUES

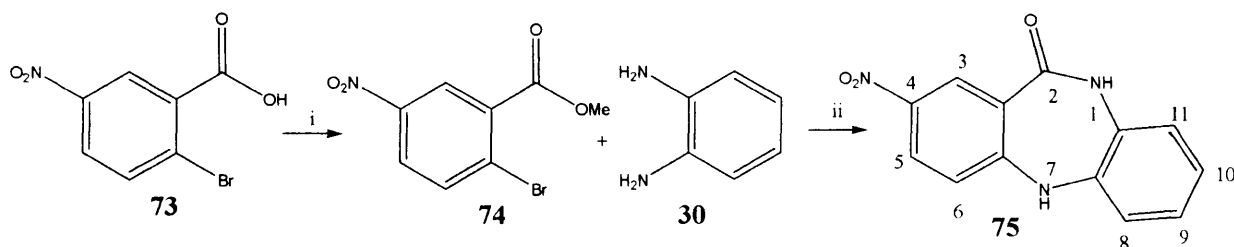
To further explore SAR of the benzodiazepine-2-one system, an additional benzene ring was introduced to give dibenzo analogues. As previously discussed in chapter 1, many known CDK inhibitors form three hydrogen bonds with the backbone residues of the active site.

To compensate for the lack of one intermolecular hydrogen bond seen in the previously made compounds it was believed that an amino group at the 4-position of compound **27** (page 47) could be beneficial for interactions within the ATP binding site of CDK2. Additionally, the amino group could be further substituted with additional functional groups.

It was proposed these compounds could be synthesised by a condensation reaction between **74** and **30** (Scheme 24). Initially, 2-bromo-5-nitrobenzoic acid (**73**) was esterified which afforded compound **74**. Compound **74** was heated with 1,2-

phenylenediamine (**30**) in dimethylacetamide (DMA) at 150 °C for 10 h, yielding the desired compound in good yield (Skalitzky *et al.*, 2003) (Scheme 2.24).

Scheme 2.24



i) Conc.H₂SO₄, MeOH, 100 %. ii) DMA, 150 °C, 51 %.

The reaction undergoes an S_NAr mechanism, the nitro group activates the *para*-bromo promoting the nucleophilic attack of the amine, followed by intramolecular attack of the ester group by the unreacted amine (Figure 2.7). Despite the poor nucleophilicity of the phenylenediamine, the yield was good.

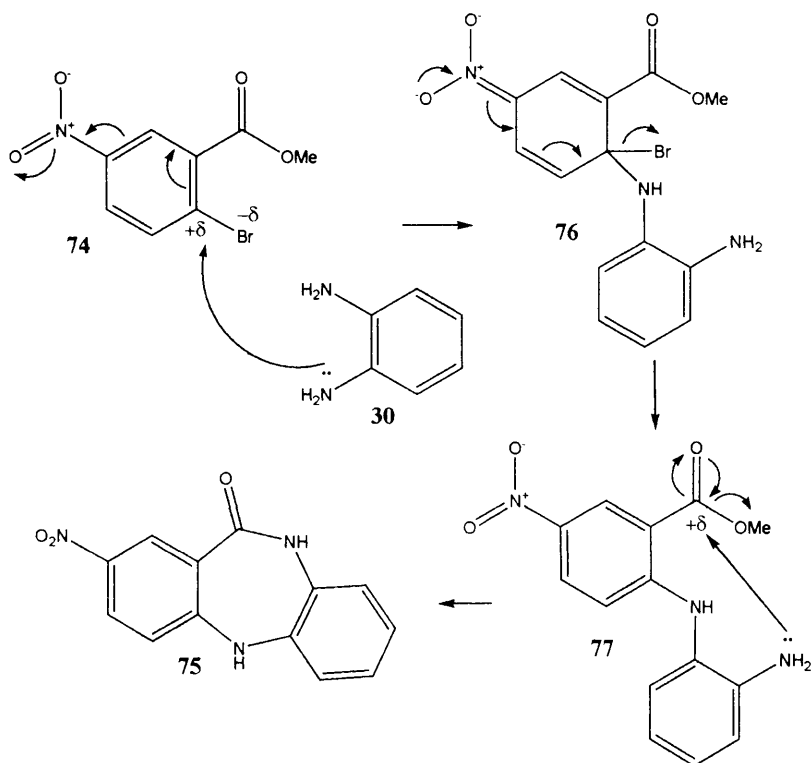
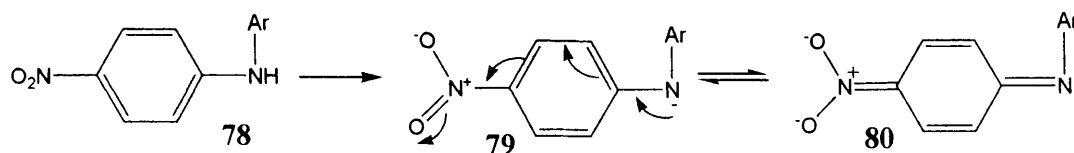


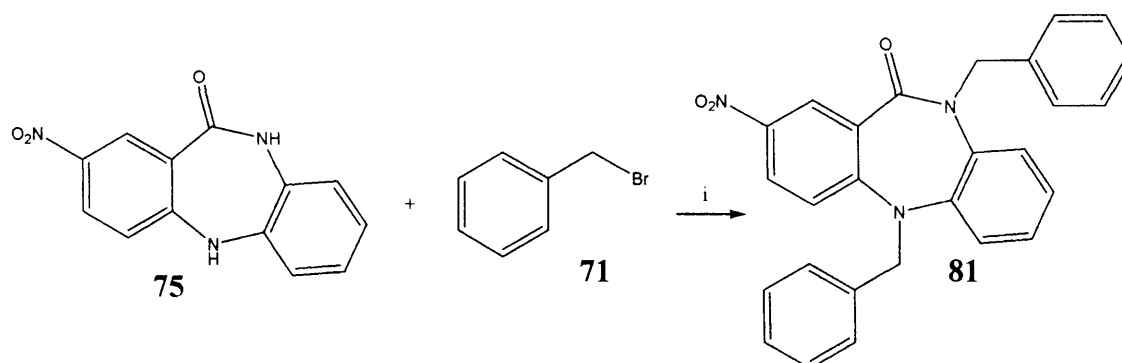
Figure 2.7 The proposed mechanism for cyclization of compound **75**.

Dibenzo compound **75** contains both an amide and amino functional group, so mono-substitution of the amine alone could still be challenging. It was hoped the amine would be more acidic than the amide anion due to stabilisation from the presence of the additional benzene ring and the *para*-nitro group i.e.



Thus, amine substitution was initially attempted without protection of the amide as had been necessary with the previous derivatives. Reacting compound **75** with benzyl bromide in presence of sodium hydride in DMF, yielded the di-substituted product (**81**) shown in Scheme 2.25.

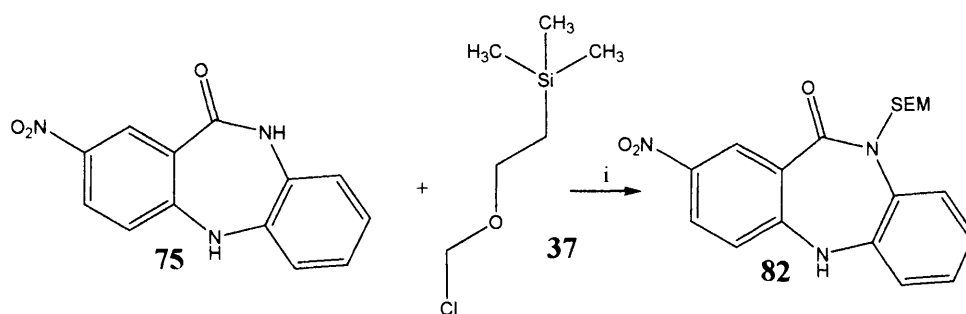
Scheme 2.25



i) NaH, DMF, 19 %.

This suggested that although the amine is more reactive, substitution at the amide N-1 position also occurred readily in the dibenzo series. Therefore, introduction of an amide protecting group was again attempted, using 2-(trimethylsilyl)ethoxymethyl (SEM) chloride. This was synthesized using a similar method as for compounds **38** and **70** (Scheme 2.26).

Scheme 2.26



i) NaH, DMF, 30 %.

The SEM protected amide **82** was obtained in moderate yield, similar to that obtained previously. The correct regioselectivity of **82** was clearly determined by NOESY that showed the NOE interactions between the amine proton and aromatic protons. NOE interactions were also observed between the aromatic proton and CH_2 peak (Figure 2.8).

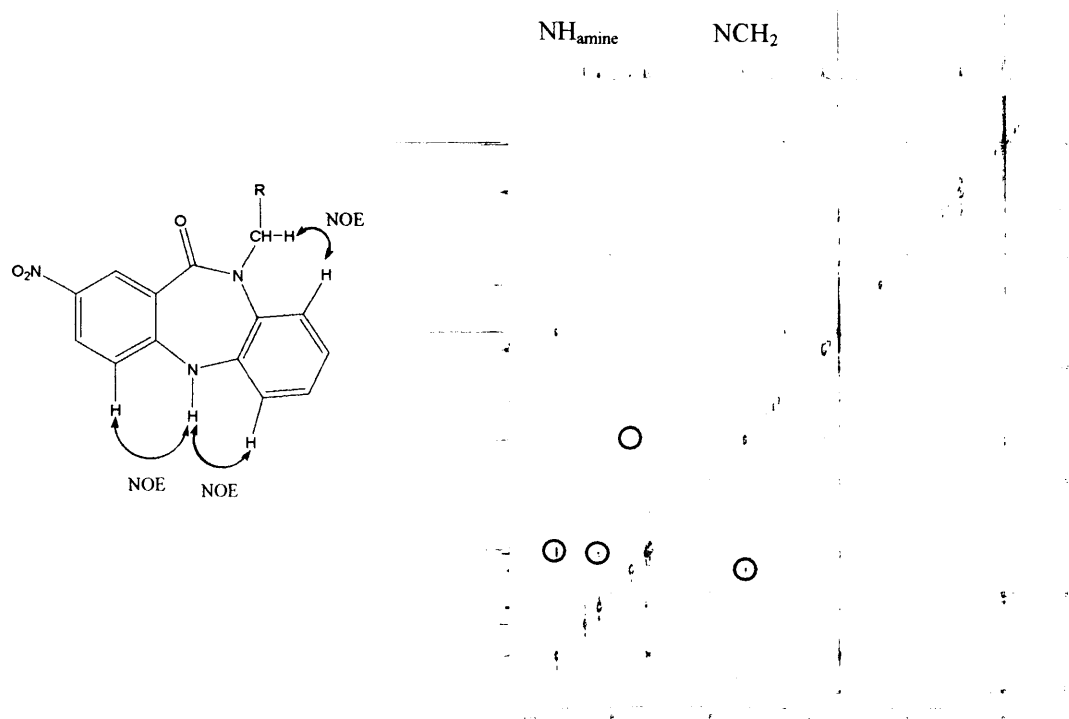
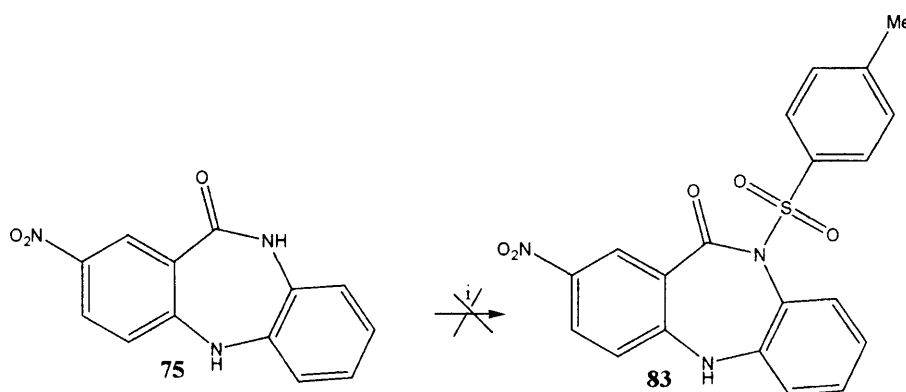


Figure 2.8. The Nuclear Overhauser effects observed in compound **82**.

This compound is a key intermediate, needed for the synthesis of further analogues described in this chapter, so in order to improve the yield of the protection step the introduction of alternative protecting groups like tosyl and *tert*-butyldimethylsilyl Chloride (TBDMS) were also investigated (Scheme 2.27, 2.28).

The synthesis of an N-tosyl derivative was attempted followed by treating **75** with two equivalents of tosyl chloride and potassium *tert*-butoxide in presence of 18-crown-6 to mop up the potassium ion with the aim of protecting the amide NH (Abell *et al.*, 1998; Makosza and Kwast, 1995). However, no product was recovered from this reaction despite the highly reactive nature of the tosyl-chloride reagent.

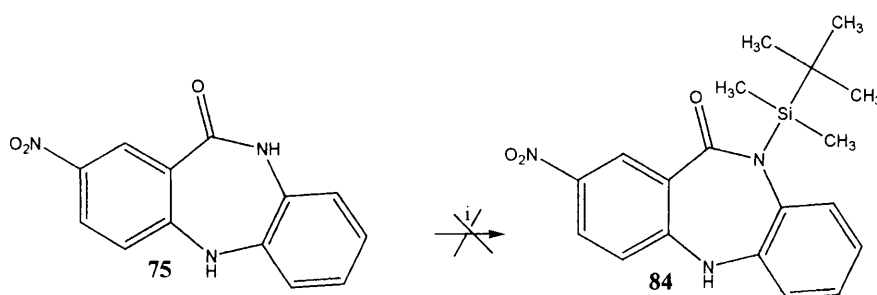
Scheme 2.27



i) Potassium *tert*-butoxide, 18 crown-6, tosyl chloride, THF, 0 %.

Similarly, the synthesis of the amide N-TBDMS compound yielded no product (Scheme 26).

Scheme 2.28



i) TBDMS-Cl, NaH, DMF, 0 %.

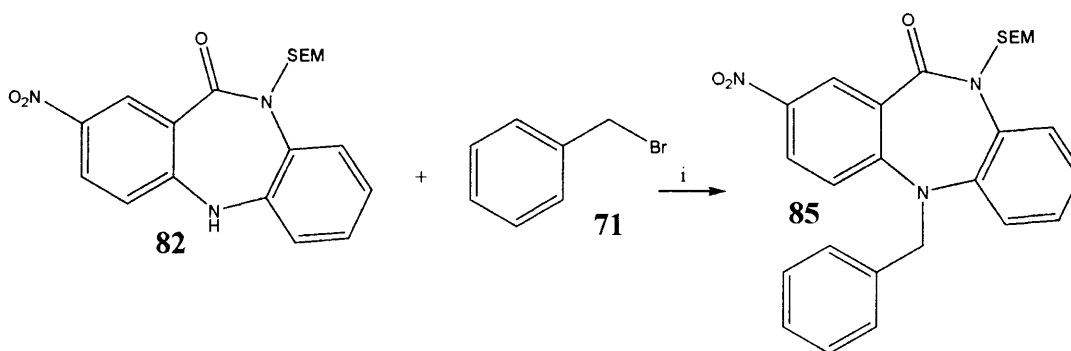
It was thought that the bulkiness of these protecting groups might prevent them reacting with the nitrogen, and this would appear to have been a major factor in these reactions not occurring. Therefore, SEM was found to be the best option in our studies to date, since it contains a primary alkylhalide at the point of reaction.

2.3.1 Synthesis of the protected lead compound analogues

As previously explained, for our proposed compounds to be fully biologically active cell cycle inhibitors, they must be extended into the ATP binding region to form further binding interactions within the active site cleft. N-Benzyl groups have previously been introduced to the benzodiazepin-2-one scaffold and this was also attempted in the dibenzodiazepinone series.

To synthesize **85**, SEM protected compound **82** was treated with benzyl bromide (**71**) in presence of potassium carbonate in DMF, to produce the desired compound in a reasonable yield (Scheme 2.29).

Scheme 2.29



i) K₂CO₃, DMF, 150 °C, 54 %.

O6-(Cyclohexylmethyl)-2-aminopurine (**86**, NU2058) is a known CDK inhibitor (Gibson *et al.*, 2002), that has been synthesized in our laboratory as a control compound in biological studies (Figure 2.9).

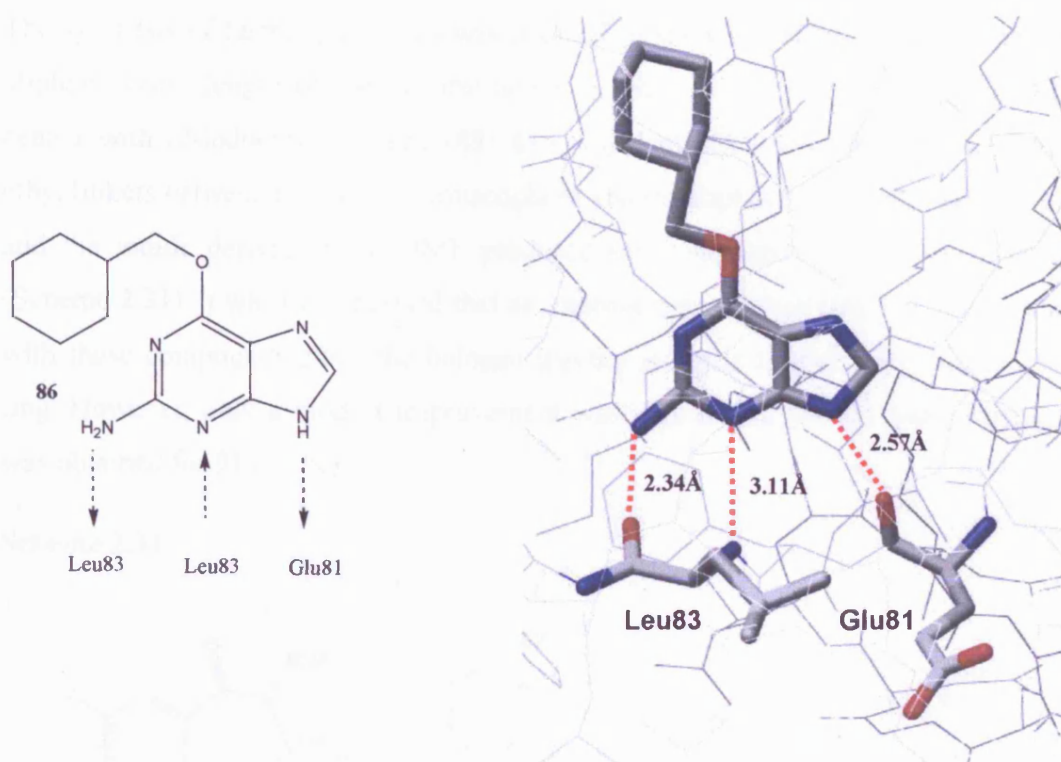
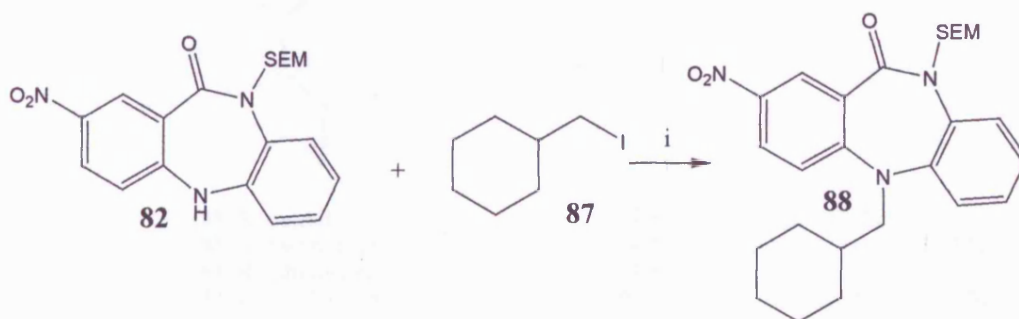


Figure 2.9 The binding orientation of NU2058 (**86**) in CDK2.

Its X-ray structure bound to CDK2 has been reported, and can aid inhibitor design. The O6-substitution of NU2058 (**86**) occupies a similar position to that of the ribose ring of ATP and due to the presence of the aliphatic ring in the molecule, it was thought that the introduction of saturated rings at the N-position of the dibenzodiazepin-2-one may be beneficial for activity compared to the benzylated analogues. So, in order to probe the extent of hydrophobic interactions made by the O6-substituent within the active site of CDK2, the following synthesis was achieved using the cyclohexylmethyl iodide method for compound **88**. The product was obtained in moderate yield (Scheme 2.30).

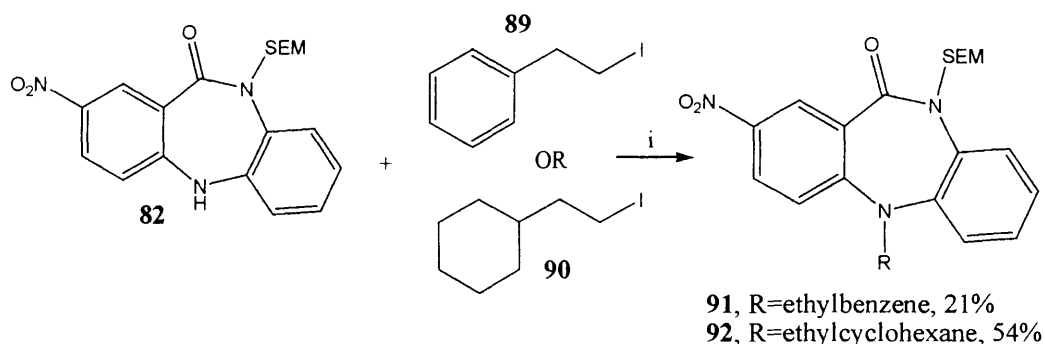
Scheme 2.30



i) K_2CO_3 , DMF, 150 °C, 31 %.

The synthesis of further analogues was planned to study the effect of the increasing the aliphatic chain length of the N-substituents on activity. To do so, compound **82** was heated with (2-iodoethyl)benzene (**89**) and (2-iodoethyl)cyclohexane (**90**) to introduce ethyl linkers between the main pharmacophore and the aliphatic ring. Potassium carbonate and the iodide derivatives in DMF produced the compounds **91** and **92** respectively (Scheme 2.31). It was hypothesised that an improvement in yield may have been achieved with these compounds since the halogen leaving group is further away from the bulky ring. However, only a modest improvement was seen for **92** (54 %) and a poorer yield was obtained for **91** (21 %).

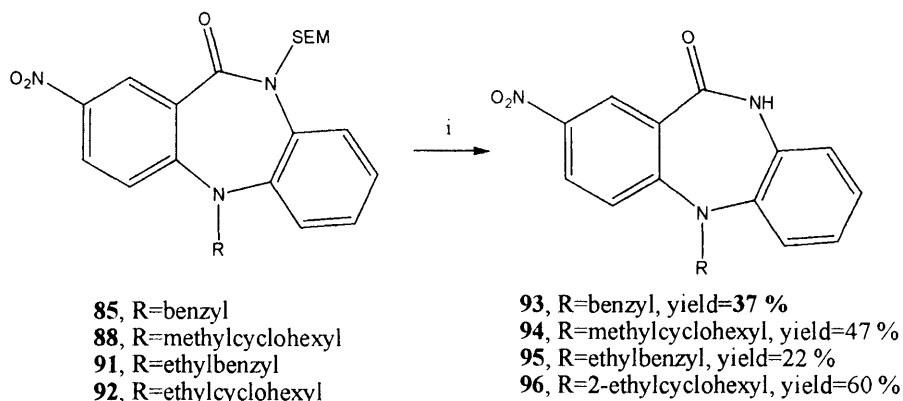
Scheme 2.31



i) K_2CO_3 , DMF, 150 °C.

The removal of the protecting group (SEM) was achieved using the previously reported procedure by refluxing the compounds **85**, **88**, **91** and **92** with tetrabutylammonium fluoride solution (1M TBAF/THF) furnishing the desired compounds as described in Scheme 2.32. A surprising variation in yield was observed for these deprotections.

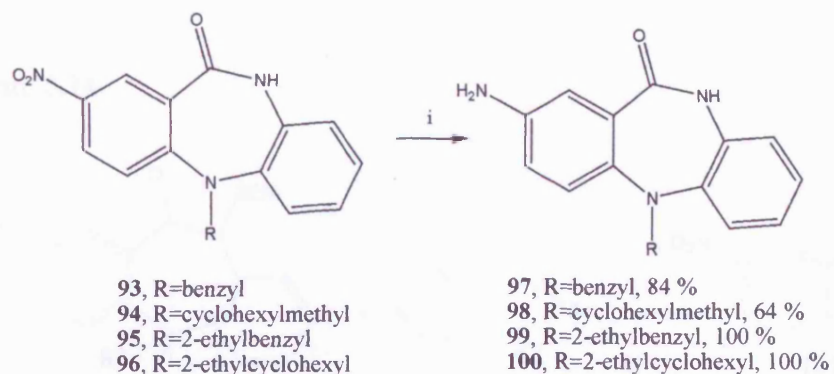
Scheme 2.32



i) 1M TBAF/THF solution, reflux.

Finally the nitro group can be readily reduced to the amino group using palladium-catalysed hydrogenation (Scheme 2.33). The amino group are predicted to form further intermolecular hydrogen bonding interactions with the CDK active site.

Scheme 2.33



i) H₂, 10 % Pd/C, MeOH or DCM.

To investigate whether the extended compounds could be accommodated in the active site of CDK2, 4-aminodibenzodiazepin-2-one extended analogues, were superimposed over NU2058 (**86**) in the crystal structure of CDK2. The initial studies indicated that all the structures would be accommodated by the active site (Figure 2.10). Also showed good alignment with the cyclohexyl ring of NU2058.

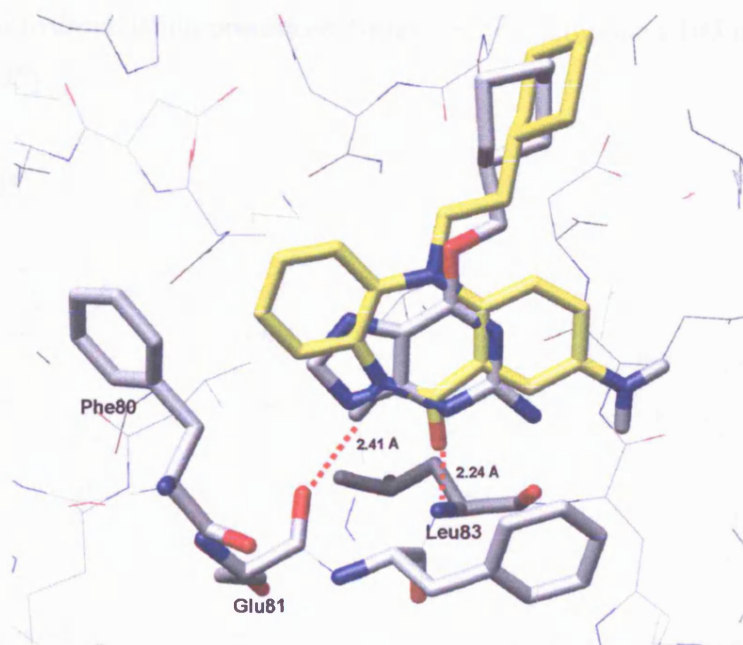
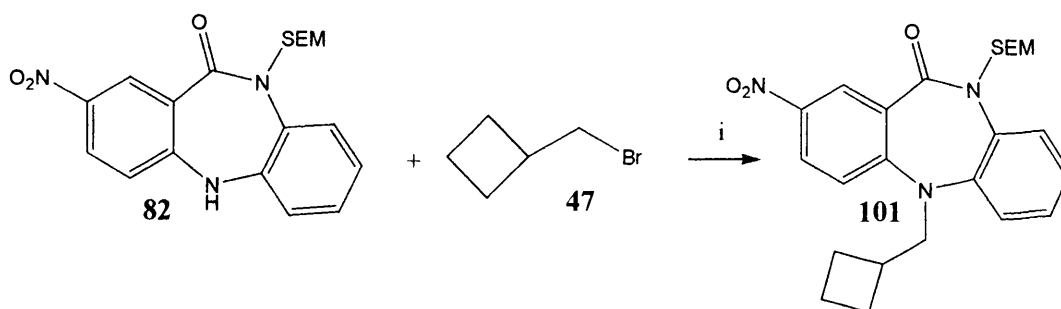


Figure 2.10 Superimposition of NU2058 (grey sticks) and **100** (yellow sticks) in the active site of CDK2.

Extension was also attempted with cyclobutylmethyl bromide (**47**), which was a small hydrophobic modification that may be better accommodated in the active site, in order to investigate the effect of the smaller aliphatic rings upon activity. An analogous reaction to the previously mentioned method was performed to obtain the desired compound (**101**) (Scheme 2.34).

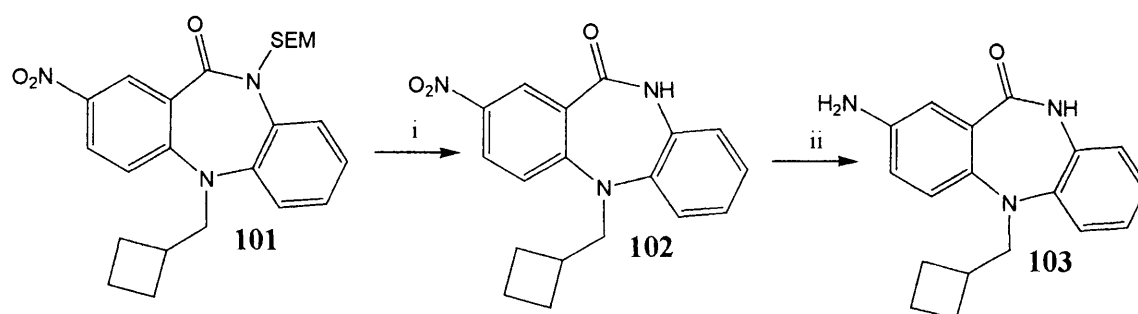
Scheme 2.34



i) K_2CO_3 , DMF, 150 °C, 25 %.

The compound **101** was deprotected by refluxing with 1M TBAF/THF, producing the compound **102** as a yellow solid. The final step was the reduction of the nitro group using the standard hydrogenation procedure, furnishing the compound **103** in quantitative yield (Scheme 2.35).

Scheme 2.35



i) 1M TBAF/THF solution, reflux, 44 % ii) H_2 , 10% Pd/C, DCM, 100 %.

Previous structure activity relationship (SAR) studies indicated that the presence of a benzyl amino substituent and a lipophilic ethyl hydroxy substituent at N-9 of olomoucine

(6), dramatically increased enzyme inhibition. Since these results were confirmed in part by examination of the binding modes of olomoucine/roscovitine in the CDK2 ATP binding site (De Azvedo *et al.*, 1997; Schulze-Gahmen *et al.*, 1995), it was hypothesized that the introduction of a lipophilic methyl group at N-7 and a benzyl group on the 4-amino group could lead to favourable interactions with ATP binding site residues, specially the hydrophobic regions including Phe80, Ile10 or Lys89 (Figure 2.11)

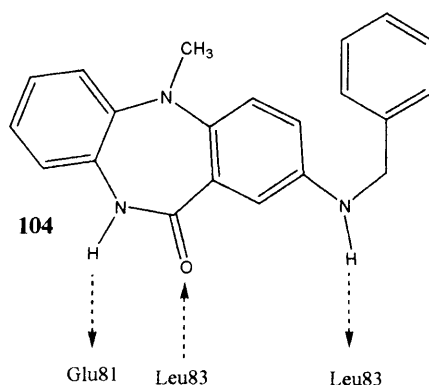
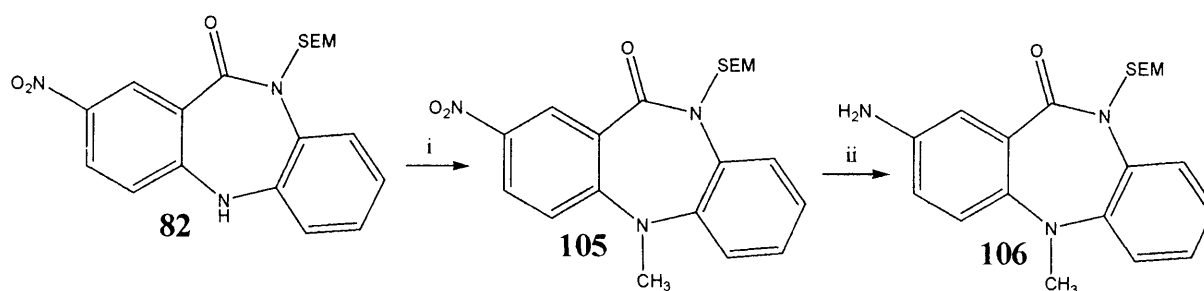


Figure 2.11 Compound **104** interactions with CDK2.

In order to synthesize compound **104**, protected amide compound **82** was treated with methyl iodide in presence of sodium hydride in DMF. The reduction of the nitro group achieved using standard conditions, in order to form the amino group necessary for benzylation (Scheme 2.36).

Scheme 2.36

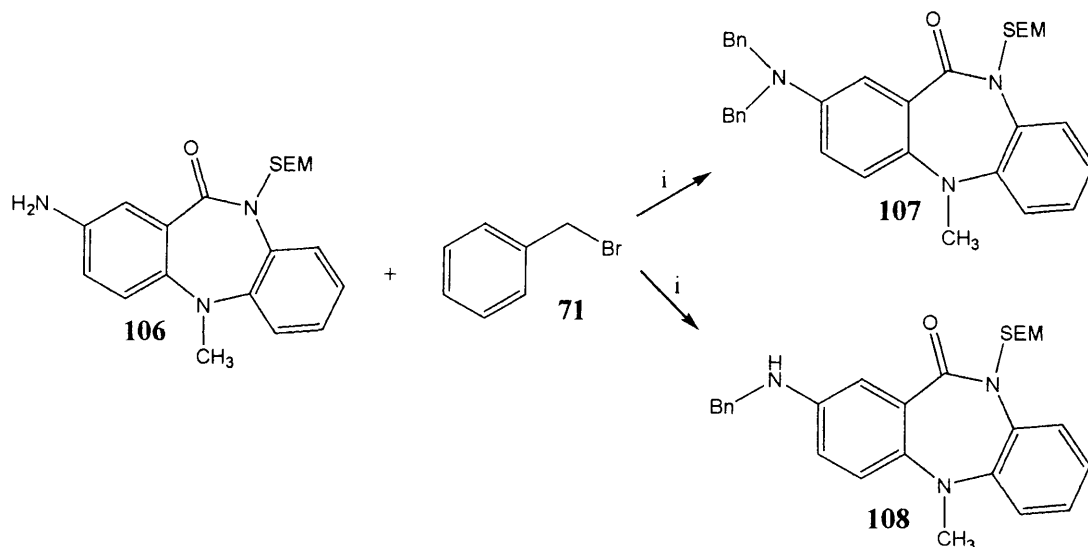


i) CH_3I , NaH , DMF, r.t., 83 % ii) H_2 , 10% Pd/C, DCM, 73 %.

The introduction of the benzyl group on the 4-amino group was achieved using an N-alkylation procedure. Compound **106** was treated with benzyl bromide (**71**) in presence of

potassium carbonate in DMF. However, following purification by column chromatography, the predominant compound obtained was the *N,N*-dibenzylated compound. Increasing the polarity of the eluent led to the isolation of the desired mono *N*-substituted compound in a smaller quantity (Scheme 2.37).

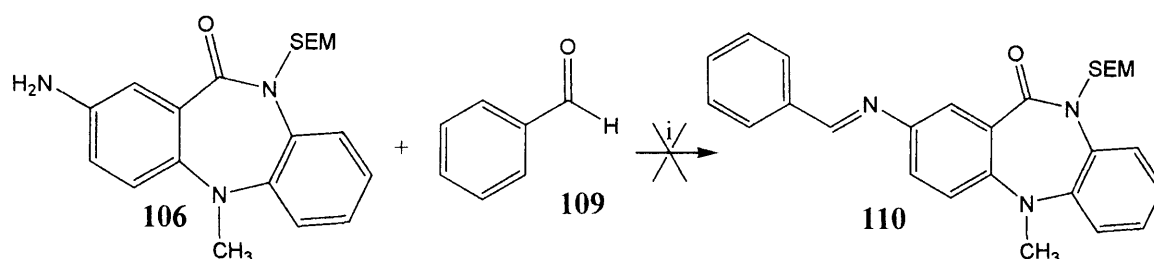
Scheme 2.37



i) K_2CO_3 , DMF, **107**, 56 %, **108**, 12 %.

The synthesis of **108** was attempted via a reductive amination reaction involving the use of benzaldehyde (**109**), to attempt to improve the yield. Compound **106** was treated with benzaldehyde in presence of ethanol and acetic acid (1:1) at reflux for 10 h (Albuschat *et al.*, 2004), but no reaction was achieved (Scheme 2.38).

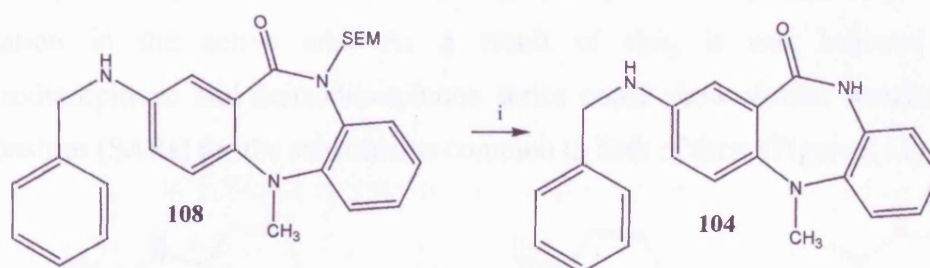
Scheme 2.38



i) EtOH/AcOH (1:1), reflux, 0 %.

These attempts were unsuccessful so the direct benzylation method was repeated for the synthesis of compound **108**. The desired compound (**108**) obtained from that method was enough for final key step, which was the SEM deprotection of compound **108** to form the free amide (Scheme 2.39).

Scheme 2.39



i) 1M TBAF/THF solution, reflux, 41 %.

Once compound **104** was synthesised, it was modelled to investigate its fit in the active site of CDK2 by overlaying with olomoucine (Figure 2.12).

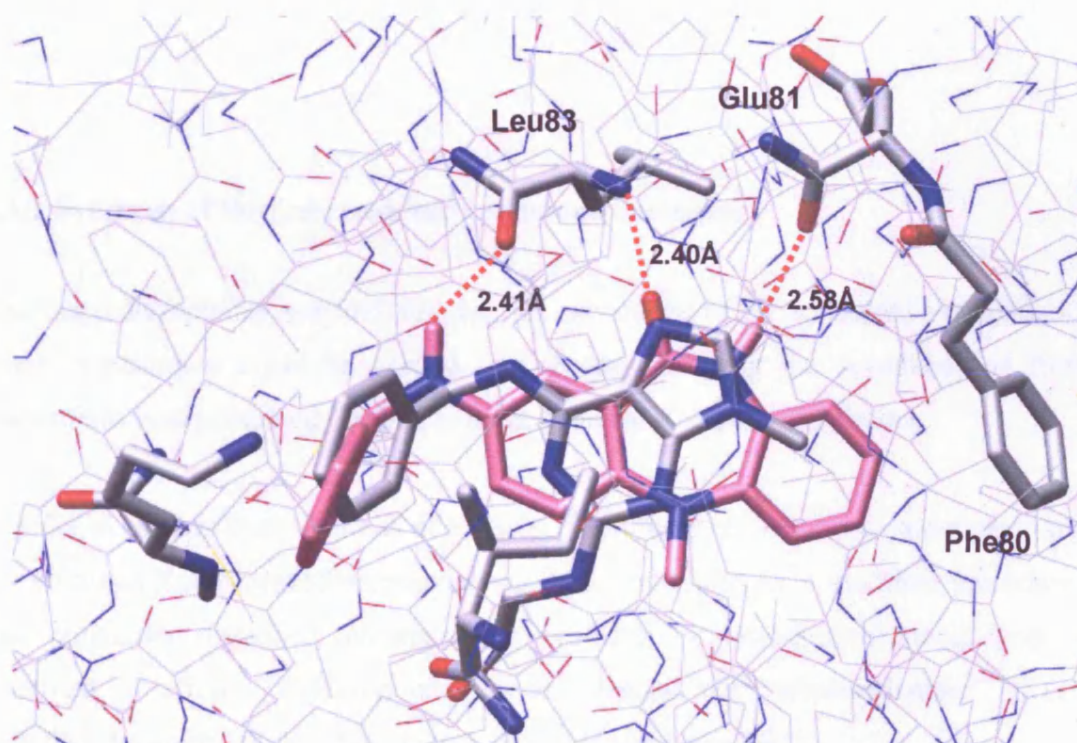


Figure 2.12 Superimposition of olomoucine (grey sticks) and **104** (pink sticks) in the active site of CDK2. (Nitrogens shown in blue, oxygen in red).

2.4 SYNTHESIS OF BENZODIAZEPINONE-5-ONE ANALOGUES

A slightly modified pharmacophore, benzodiazepine-5-one was proposed for investigation.

An overlay of compound **27** and **28** show that both parent compounds bind in the same orientation in the active site. As a result of this, it was believed that the dibenzodiazepinone and benzodiazepinone series could show similar structure activity relationships (SARs) for the substituents common to both of them (Figure 2.13).

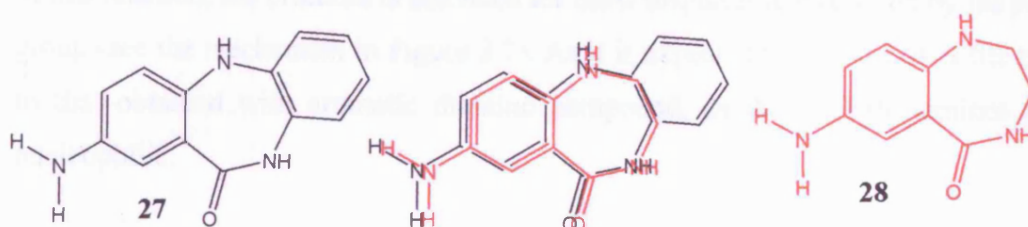


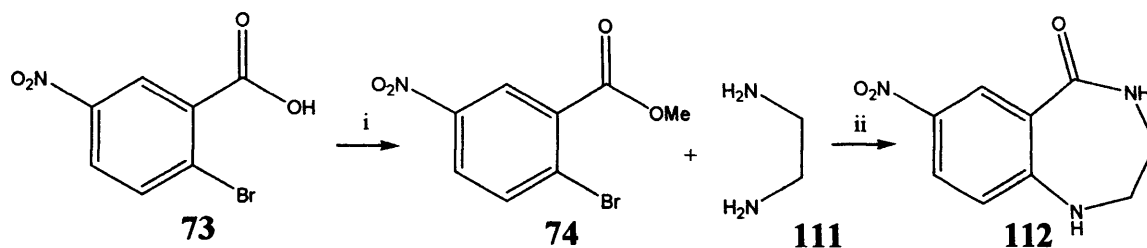
Figure 2.13. Overlay of **27** and **28** showing common groups.

2.4.1 Synthesis of the protected lead compound analogues

The benzodiazepinone scaffold still has the advantage of an additional site (N-amine) where substitution could be carried out, thereby allowing the possibility of further interactions being obtained, leading to more potent and selective inhibitors.

In order to confirm this, synthesis of N-amine substituted analogues was attempted. To do so, precursor 7-nitrobenzodiazepinone was first synthesised by a modified procedure to that previously discussed: commercially available 2-bromo-5-nitrobenzoic acid was esterified to afford **74**. Compound **74** was heated with ethylenediamine (**111**) in dimethylacetamide (DMA) (Skalitzky *et al.*, 2003) (Scheme 2.40).

Scheme 2.40

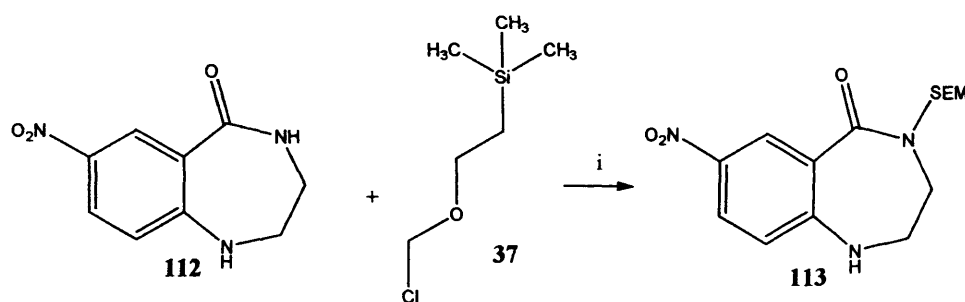


i) Conc. H_2SO_4 , MeOH, 100 %, ii) DMA, 150 °C, 59 %.

In this reaction, the bromine is activated for $\text{S}_{\text{N}}\text{Ar}$ displacement reaction by the *para*-nitro group (see the mechanism in Figure 2.7). As it is expected the yield was better compared to that obtained with aromatic diamino compound, as the aliphatic amines are more nucleophilic.

To N-mono-substitute the amine of compound 112 the method described previously was used, compound 112 was protected by stirring with SEM in presence of sodium hydride in DMF to synthesise 113 (Scheme 2.41).

Scheme 2.41

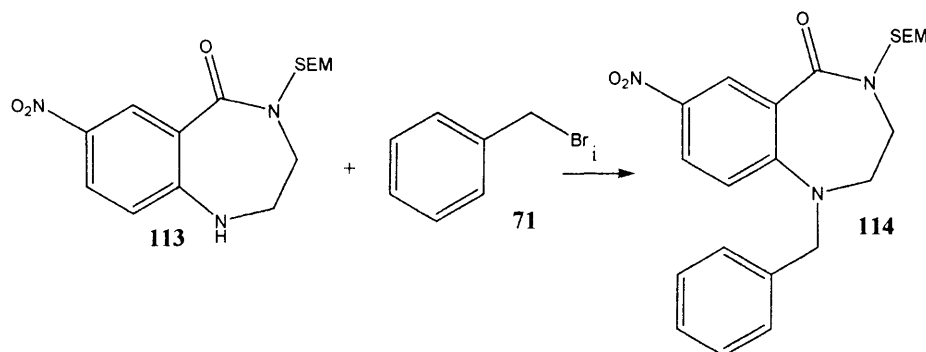


i) NaH, DMF, r.t, 27 %.

The protected compound 113 was shown to have the correct regioselectivity by NMR, due to the presence of a peak at $\delta 8.07$ for the amine proton, and the lack of the amide peak at approximately $\delta 8.5$. The downfield shift for the amine was due to the strong electron withdrawing *para*-nitro group.

To synthesise **114**, protected compound **113** was treated with benzyl bromide (**71**) in presence of potassium carbonate in DMF, yielding the desired compound in a moderate yield (Scheme 2.42).

Scheme 2.42



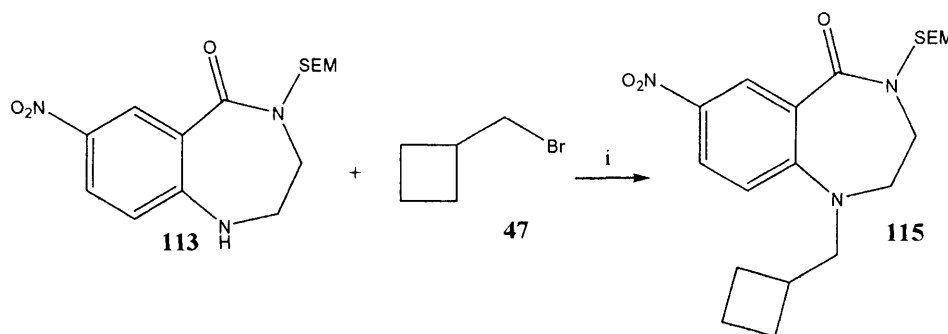
i) K_2CO_3 , DMF, $150^\circ C$, 32 %.

Work was also carried out to investigate the effect of saturation of the ring on activity.

Since the crystal structure of hymenialdisine (**14**) bound to CDK2 revealed that the introduction of cyclobutylmethyl in the N-amine could lead to a better accommodation thereby providing greater activity and possibly further selectivity (Figure 2.15).

So, extension was attempted with cyclobutylmethyl bromide (**47**) in an analogous reaction to the previously mentioned reaction to obtain the desired compound (**115**) in a reasonable yield (Scheme 2.43).

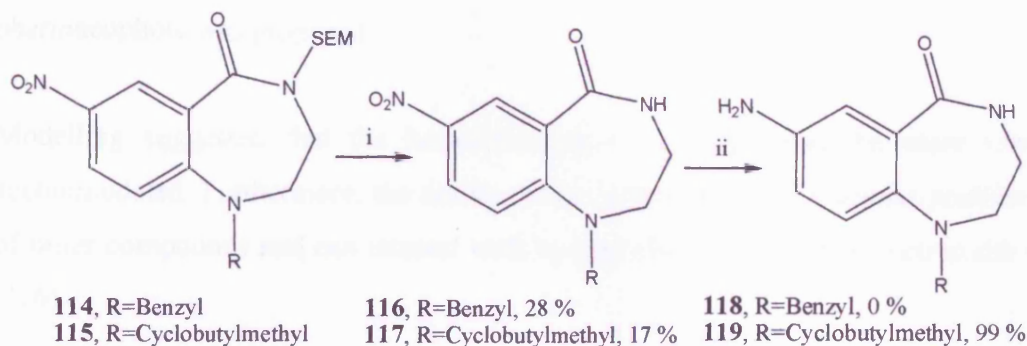
Scheme 2.43



i) K_2CO_3 , DMF, $150^\circ C$, 41 %.

Compounds **114** and **115** were deprotected by refluxing with 1M TBAF/THF, producing the desired compounds **116** and **117** in moderate yield (Scheme 2.44).

Scheme 2.44



i) 1M TBAF/THF solution, reflux, ii) H₂, 10 % Pd/C, MeOH.

The final step was the reduction of the nitro groups using the standard hydrogenation procedure, but for some unknown reasons it did not succeed for compound **118**.

An overlay of hymenialdisine (**14**) and compound **119** bound to CDK2 showed that both bind within the ATP binding site and show a similar binding mode (Figure 2.15).

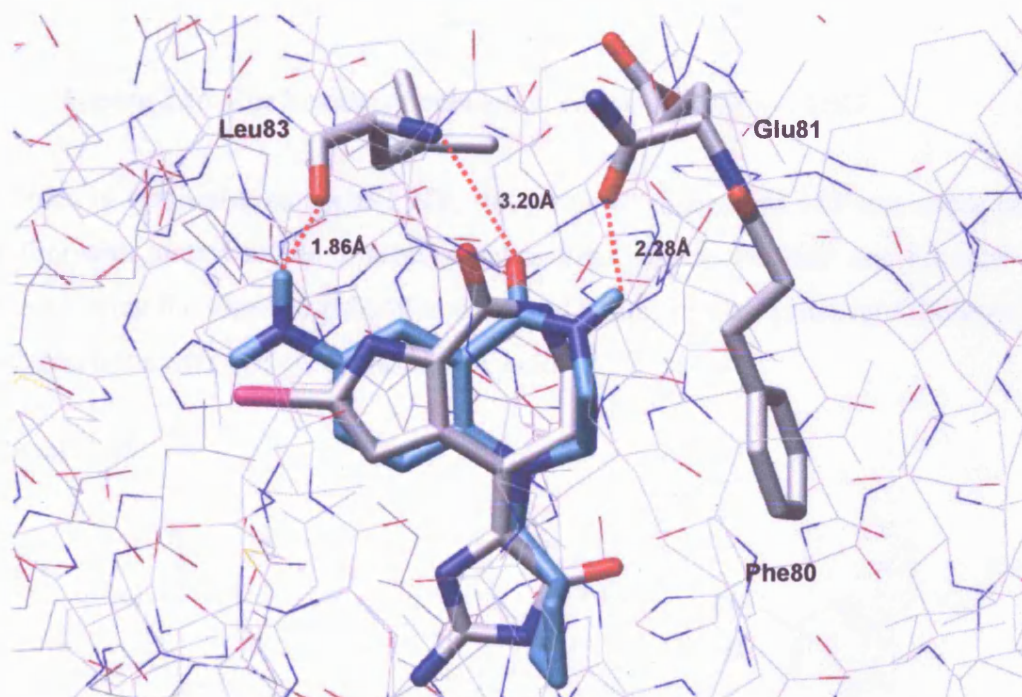


Figure 2.15 Overlay of hymenialdisine (grey sticks) and compound **119** (blue sticks) in the active site of CDK2.

The previous study indicated that the N-benzyl groups of olomoucine and **104** showed good alignment but the fused benzene ring of the dibenzodiazepinone scaffold might be too bulky to be accommodated in the CDK2 active site compared to the methyl group of olomoucine. Therefore, an alternative strategy for the synthesis of a benzodiazepinone pharmacophore was proposed.

Modelling suggested that the benzodiazepine-5-one (**120**) may be more favourably accommodated. Furthermore, the amino methyl group occupies a similar position to that of other compounds and can interact with hydrophobic regions of the active site (Figure 2.16).

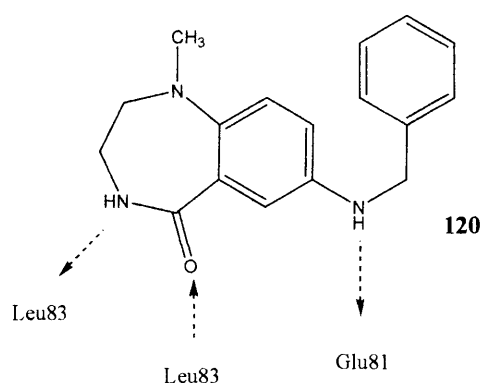
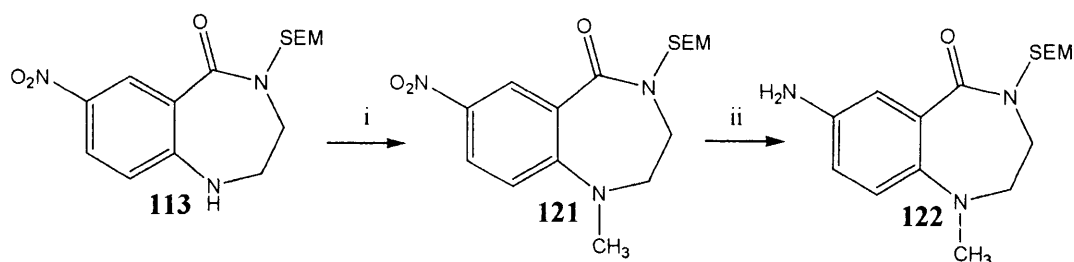


Figure 2.16 The binding orientation of compound **120** in CDK2.

In order to synthesise compound **122**, the protected compound **113** was methylated by treating with methyl iodide in presence of sodium hydride in DMF and the nitro group reduced using the standard palladium catalyzed hydrogenation procedure (Scheme 2.45). Both reactions were achieved in excellent yield.

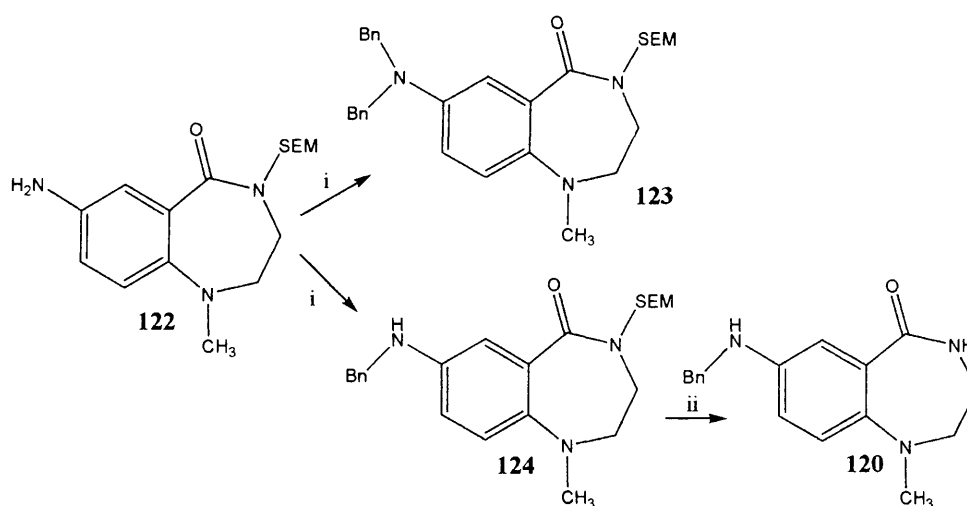
Scheme 2.45



i) MeI, NaH, DMF, r.t, 88 %, ii) H₂, 10% Pd/C, MeOH, 100 %.

The N-7 benzylation of compound **122** was performed using the method used for the synthesis of compound **98**, by stirring the compound **122** with benzyl bromide in presence of sodium hydride in DMF. The *N, N*-dibenzylated compound **123** was obtained following purification by column chromatography as the major product, and the desired compound was obtained by increasing the polarity of the eluent to obtain the minor product. The final step was deprotection of **124** by treating compound **124** in 1M TBAF/THF at reflux, to deprotect the amide functional group (Scheme 2.46).

Scheme 2.46



i) BnBr, NaH, DMF, r.t, **123**, 32 %, **120**, 17 %, ii) 1M TBAF/THF solution, reflux, 40 %.

Compound **120** was modelled in the active site of CDK2 by overlaying with olomoucine (Figure 2.15). Hydrogen bond interactions were seen with Glu81 and Leu83 and the N-benzyl groups of both compounds showed good alignment.

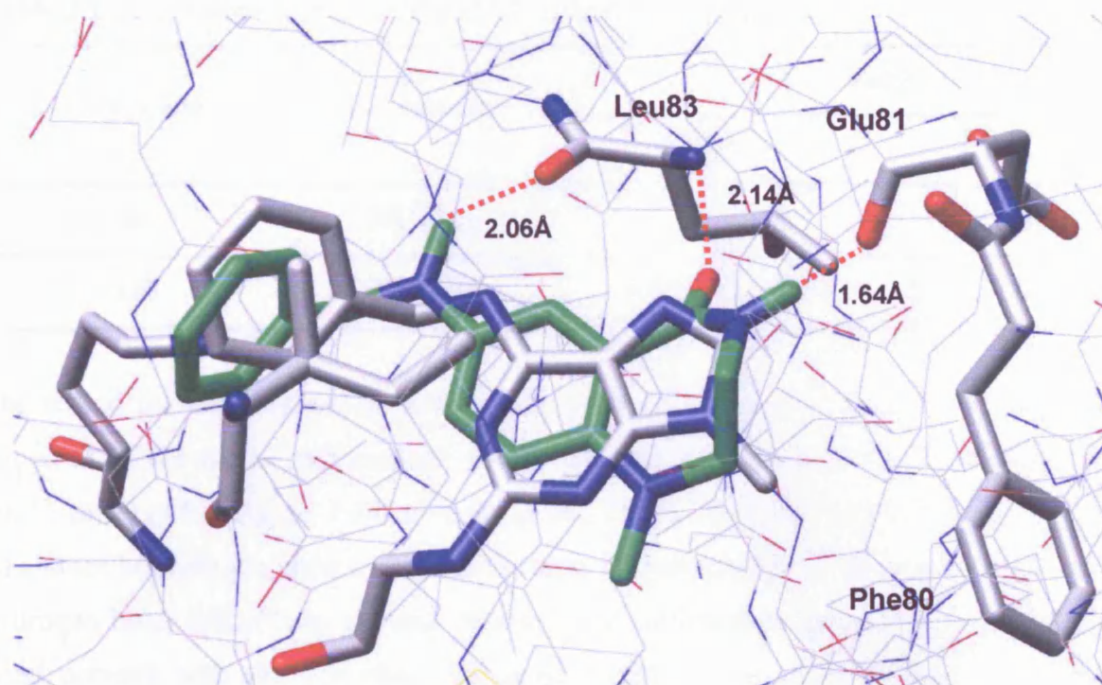
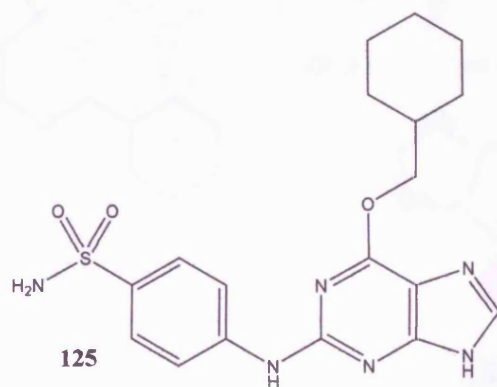


Figure 2.17 Superimposition of olomoucine (grey sticks) with compound **120** (green sticks) in the active site of CDK2.

Literature reports showed that the introduction of substituted phenylamino groups at the 2-position of the purine scaffold could lead to an increase in activity compared to NU2058 (**86**) (Hardcastle *et al.*, 2004). This is best explained by the introduction of a sulfonyl group at the 2-position (**125**, NU6102) (Hardcastle *et al.*, 2004).

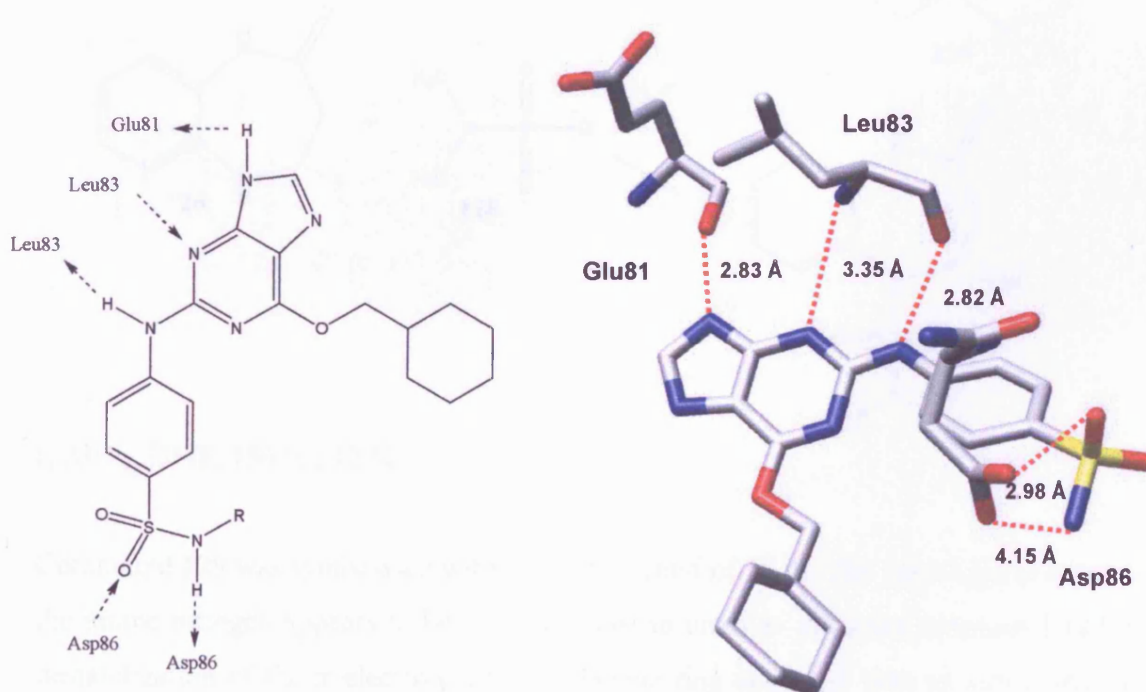


A dramatic increase in activity was observed for NU6102 (**125**) compared with that of the parent compound NU2058 (**86**) (Table 2.2).

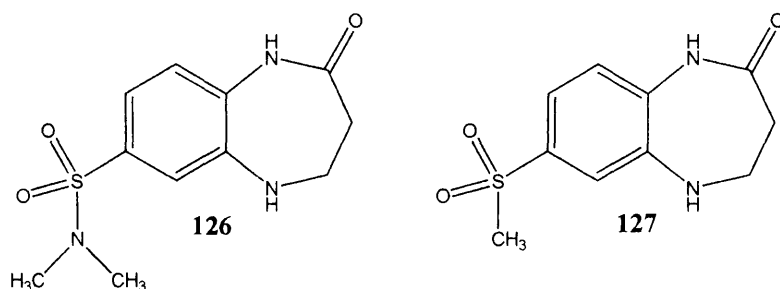
Table 2.2: IC₅₀ Values for NU2058 and NU6102 (Davies *et al.*, 2002).

Compound	NU Number	IC ₅₀ Values	
		CDK1	CDK2
86	NU2058	7 ± 0.7 μM	17 ± 2 μM
125	NU6102	9.49 ± 0.13 nM	5.36 ± 1.01 μM

The reason for this increase in activity was shown by the crystal structure of NU6102 bound to CDK2 and as predicted the purine ring makes the triplet of hydrogen bonds to Glu81 and Leu83 (Figure 2.18) (Davies *et al.*, 2002). However, additional interactions take place between the phenyl ring and the area of hydrophobic residues, and two further hydrogen bond interactions are also formed. The sulfonamide group forms a hydrogen bond network with the side chain group of Asp86. These additional interactions are almost certainly responsible for the increase in potency of NU6102 (**125**) compared to NU2058 (**86**) (Davies *et al.*, 2002).

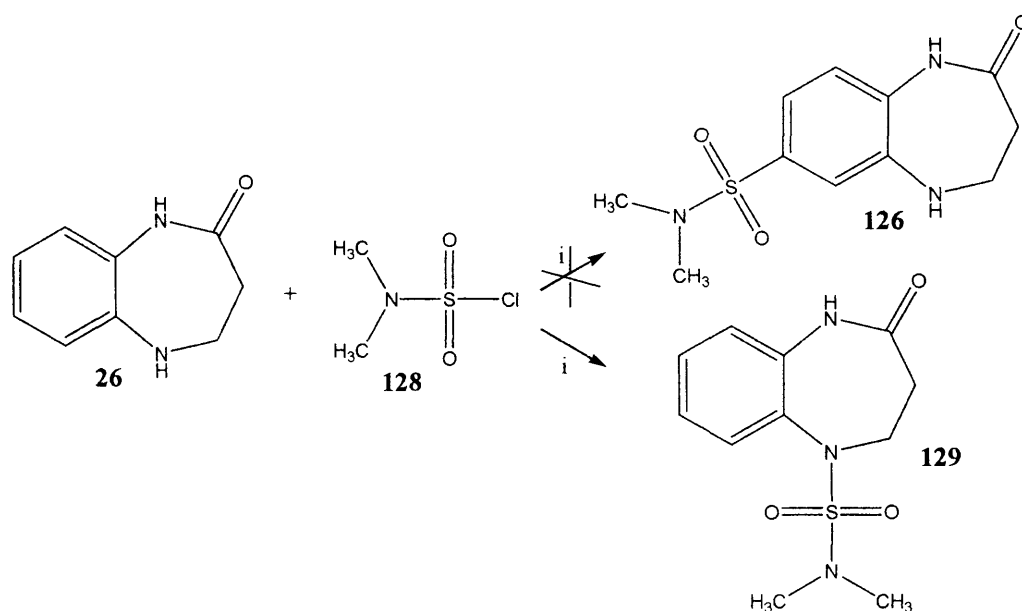
**Figure 2.18** NU6102 (**125**) bound to CDK2 (Davies *et al.*, 2002).

As a result of this, the synthesis of the following substituted sulfonamides based on the lead compound CFU58 (**26**), was attempted:



A Friedel-Crafts method was tried to synthesise the compounds with AlCl₃ and *N,N*-dimethylsulfonyl chloride (**128**). Instead of the desired compound **126**, compound **129** was obtained alternatively (Scheme 2.47).

Scheme 2.47

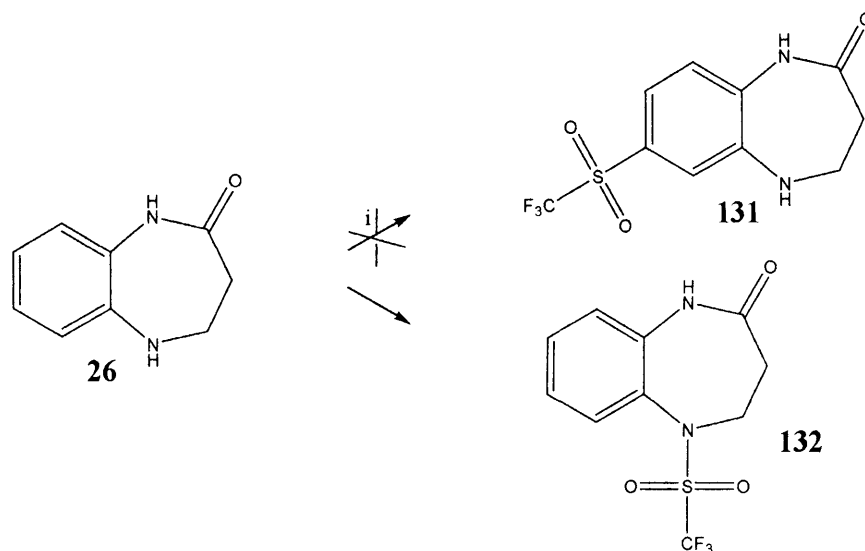


i) AlCl₃, DMF, 150 °C, 12 %.

Compound **129** was synthesised with an overall yield of 12 %. The nucleophilic attack by the amine nitrogen appears to be relatively fast in order to yield the compound **129**, no destabilization of the π electrons of the benzene ring occurred, thus avoiding any side reaction involving the benzene.

Alternatively the following reaction was also tried in order to obtain the desired compound **131** (Peyronneau *et al.*, 2004) (Scheme 2.48).

Scheme 2.48



i) Trifluoromethanesulfonic acid, methylsulfonyl chloride, THF, r.t., 54 %.

This time again compound **132** was produced with an overall yield of 54% as previously discussed. This line of chemistry was stopped here and no further examples were studied in this regard.

The trichlorophenyl substituted pyrazolopyrimidine (**133**) is an alternative CDK inhibitor, the crystal structure determined the binding mode of this inhibitor (Markwalder *et al.*, 2004) (Figure 2.20). It binds in the ATP binding site by forming three hydrogen bonds with Leu83 and Lys33. The tri-chlorophenyl group provides a hydrophobic interaction with either the glycine rich loop or the C-terminal domain (Markwalder *et al.*, 2004).

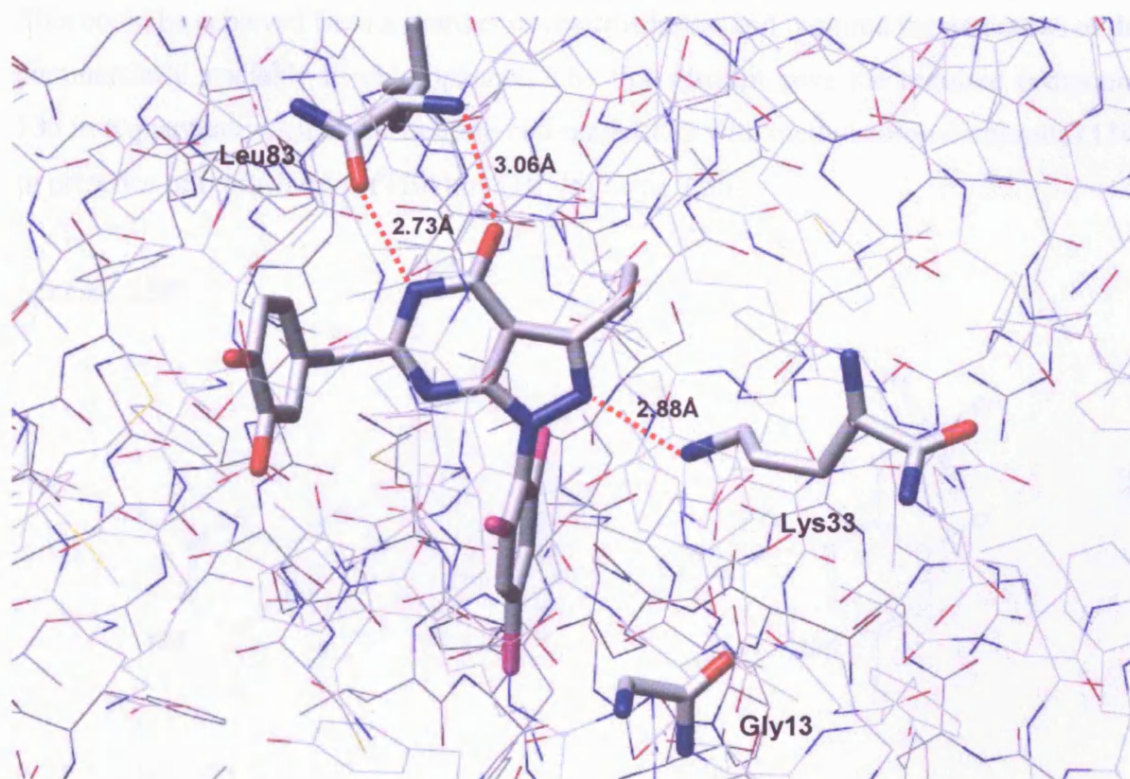
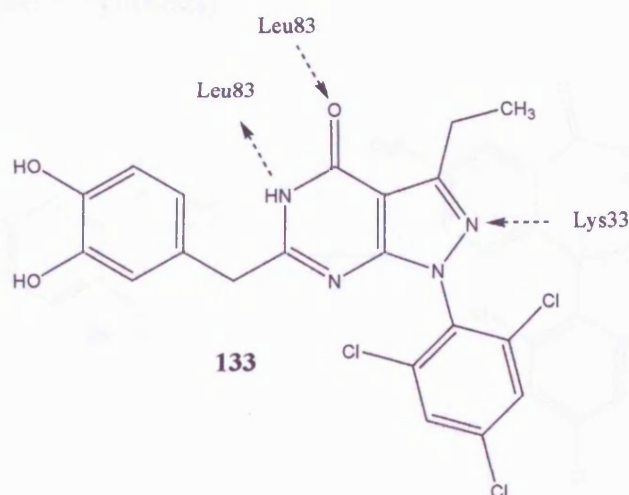
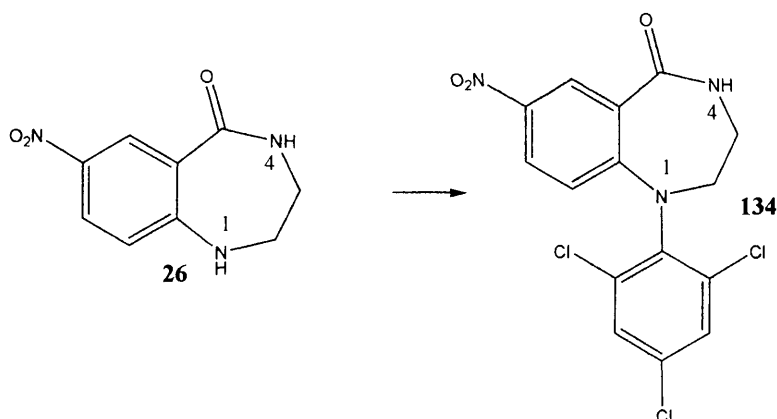


Figure 2.20 Compound 133 bound to CDK2.

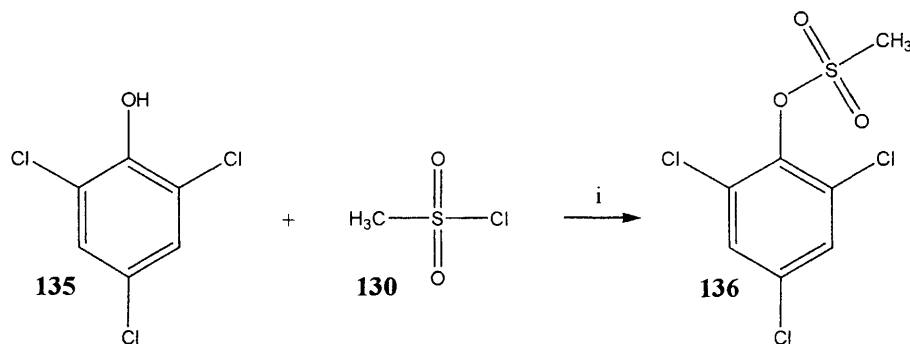
To investigate further the importance of the interactions formed by tri-chlorophenyl group, several attempts were made to introduce the tri-chlorophenyl group to the benzodiazepine-5-one pharmacophore at the 1-position shown in Scheme 2.49.

Scheme 2.49 (General Synthesis)



This could be achieved from a number of intermediates, and required the activation of the commercially available tri-chlorophenol. The first attempt gave the required compound **136** in a quantitative yield, by treating compound **135** with methanesulfonyl chloride (**130**) in presence of triethylamine (TEA) in THF (Scheme 2.50).

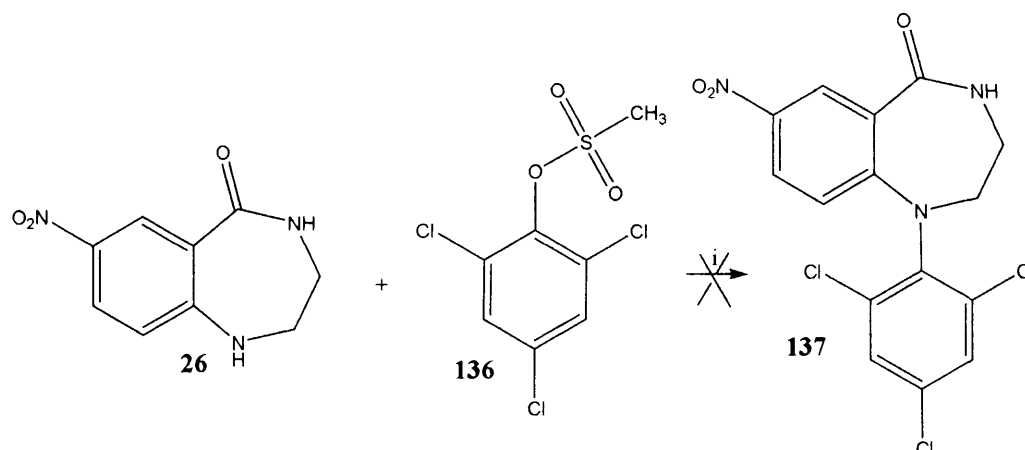
Scheme 2.50



i) TEA, THF, 100 %.

However, subsequent reaction followed by heating compound **26** and **136** in presence of potassium carbonate in DMF was unsuccessful by liberation of the compound **136** to its starting material, tri-chlorophenol (**135**) (Scheme 2.51).

Scheme 2.51

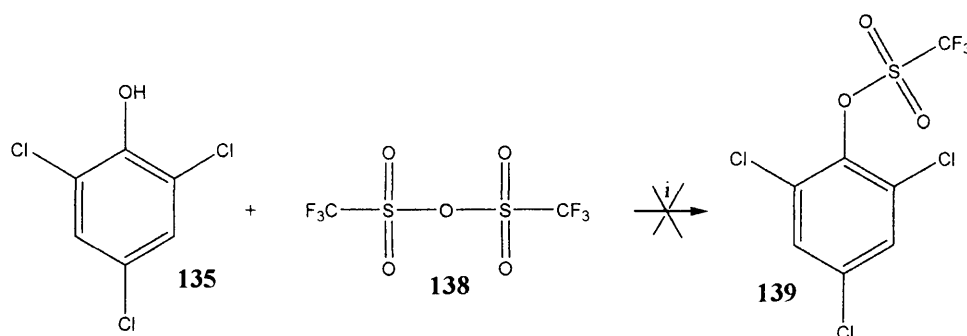


i) K_2CO_3 , DMF, $150\text{ }^\circ\text{C}$, 0 %.

It implies that either the aromatic ring is too sterically crowded to undergo an $\text{S}_{\text{N}}\text{Ar}$ displacement reaction or the tri-chlorophenol anion is possibly more stable than methylsulfonyl anion. The presence of the three chlorine groups on the benzene ring would make the anion even more stable.

Two attempts were made to vary the leaving group to see if by increasing the stability of the intermediate anion, the reaction would go in the required manner. To do so, trichlorophenol was treated with trifluoroacetic anhydride in presence of triethylamine (TEA) in THF (Scheme 2.52), but the reaction failed, due probably to the increased steric bulk of the anhydride, which made the contact of the reagents impossible.

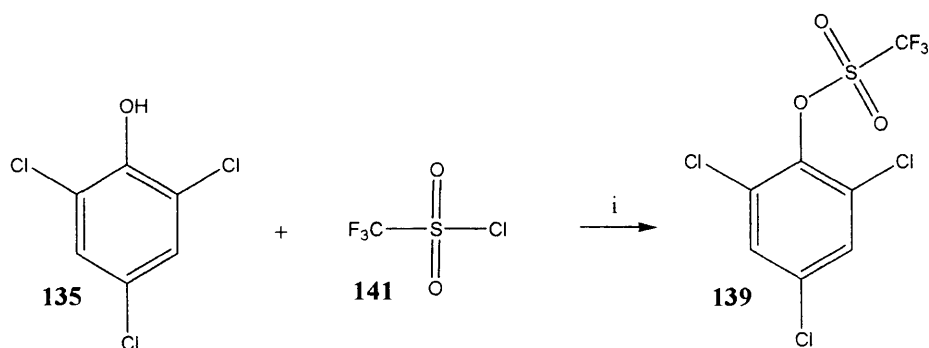
Scheme 2.52



i) TEA, THF, 0 %.

The final attempt gave the required intermediate (**139**) in a quantitative yield (Scheme 2.53).

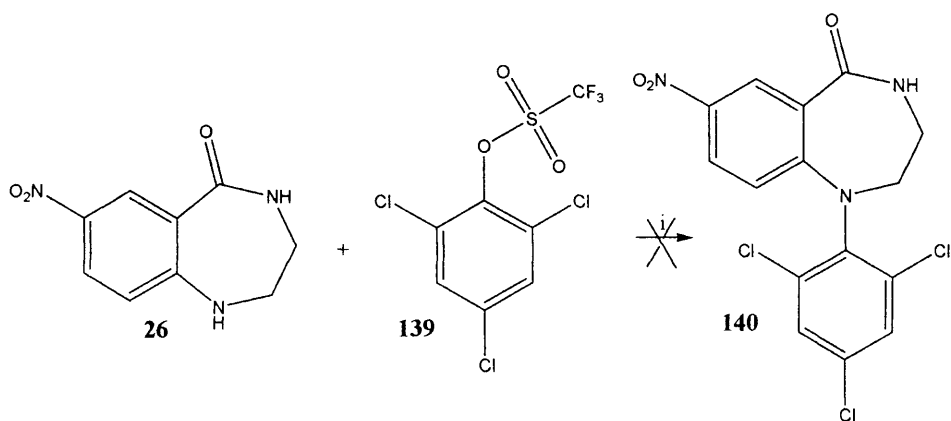
Scheme 2.53



i) TEA, THF, 100 %.

However, when compound **26** was reacted with **139** the same liberation of tri-chlorophenol was observed (Scheme 2.54). It seemed that tri-chlorophenol anion is still more stable than tri-fluoromethanesulfonyl anion or that, the C-O bond is hindered or difficult to break.

Scheme 2.54

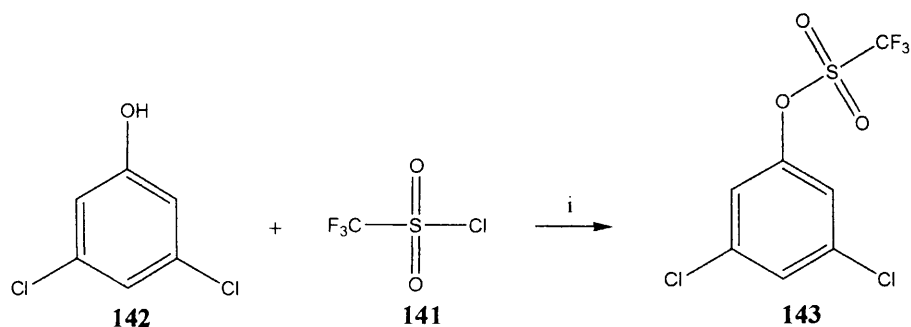


i) K₂CO₃, DMF, 150 °C, 0 %.

The same reaction was also attempted on 3,5-dichlorophenol (**142**) to establish if by using a less substituted phenol the required product could be obtained. In order to do so, the

commercially available 3,5-dichlorophenol was reacted with *tri*-fluoromethanesulfonyl chloride using a similar procedure to yield the intermediate in a good yield (Scheme 2.55).

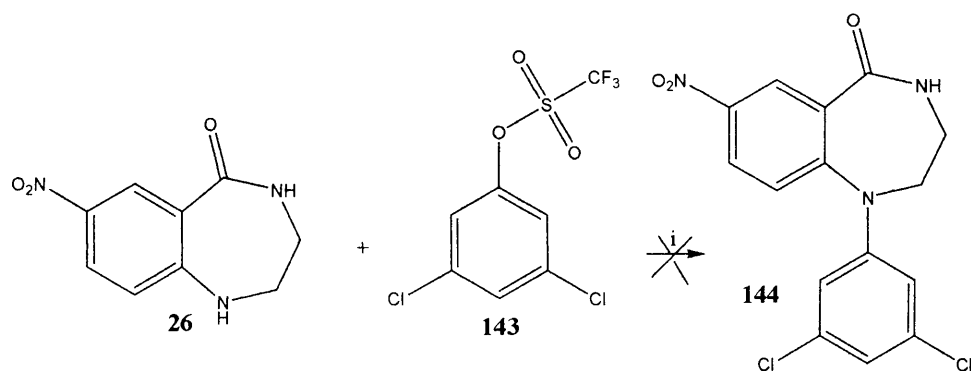
Scheme 2.55



i) TEA, THF, r.t., 60 %.

Finally, compound **26** was treated with **143**, but instead of giving the desired product the same liberation of intermediate (**143**) occurred (Scheme 2.56). It seemed that the steric nature of the compound may not affect in formation of the by-products and the main reason might be the stability of the phenoate anions.

Scheme 2.56



i) K₂CO₃, DMF, 150 °C, 0 %.

2.5 ATTEMPTED SYNTHESIS OF AN ALTERNATIVE PHARMACOPHORE

To improve the interaction of the diazepinone pharmacophore an alternative modification was proposed. The known CDK2 inhibitors hymenialdisine and kenpaullone have a heterocyclic group fused to the azepinone ring in place of the benzo-groups investigated so far in this thesis. Incorporation of a heterocyclic group would provide an extra functional group for hydrogen bonding interactions (Figure 2.21). A pyrrole group is present in hymenialdisine and kenpaullone contains an indole group.

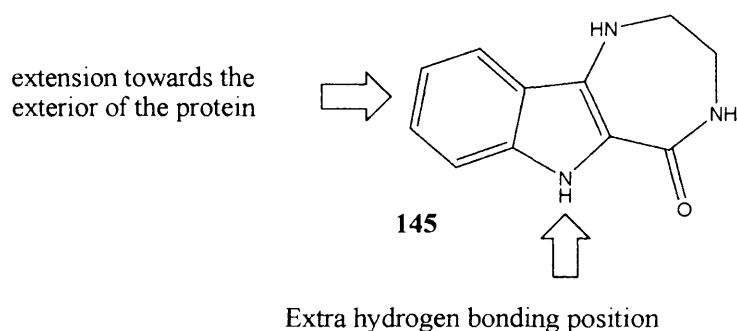
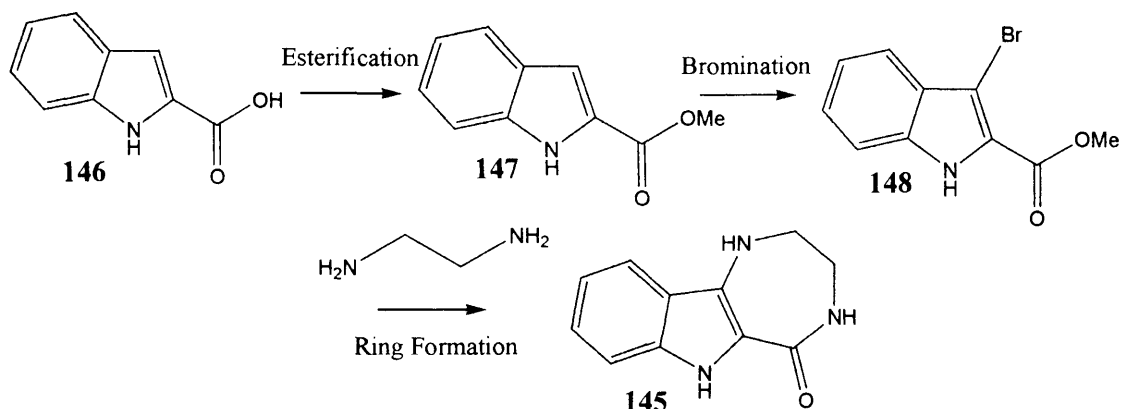


Figure 2.21. The two key areas of the proposed heterocyclic pharmacophore.

The synthesis was proposed from commercially available indole-2-carboxylic acid (146) using a condensation with ethylenediamine in a similar manner to that used previously (Scheme 2.57).

Scheme 2.57 (Outline of Synthesis)

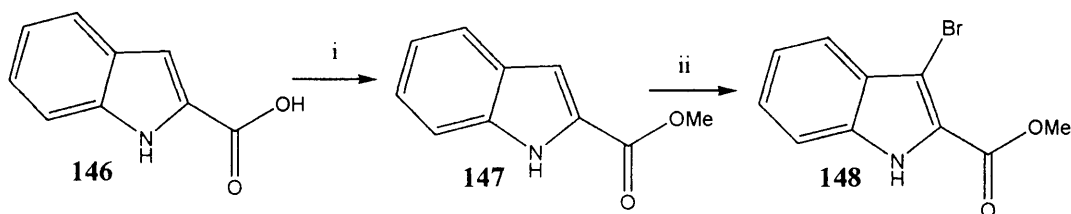


The synthesis of **145** was proposed in three steps: first an esterification reaction to generate methyl indole-2-carboxylate (**147**), secondly bromination of the indole (**147**), and thirdly the condensation to **145**.

The esterification was easy to carry out by refluxing indole-2-carboxylic acid (**146**) in methanol and in presence of concentrated sulfuric acid, to yield the ester in almost quantitative yield (Scheme 2.57).

A reported method of indole bromination using N-bromosuccinimide (NBS) was attempted (Barraja *et al.*, 1999) (Scheme 44). Indoles are preferentially brominated at the 3-position and it was found that bromination occurred exclusively at this position again in very good yield. This brominated compound was the key precursor for the subsequent cyclization step (Scheme 2.58).

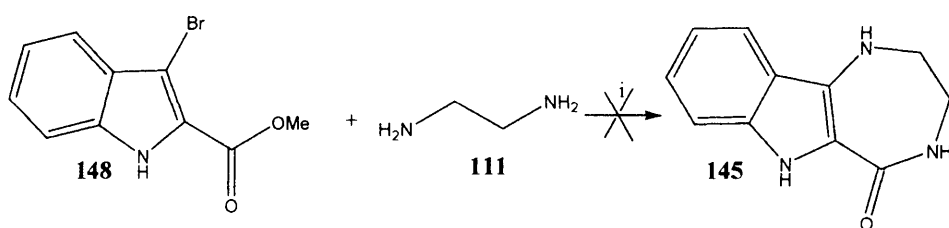
Scheme 2.58



i) Conc. H₂SO₄, MeOH, reflux, 95 %, ii) NBS, DMF, 95 %.

Several attempts were made to achieve the cyclization of the brominated indole ester (**148**). Initially, a simple coupling was attempted by dissolving in DMF in presence of ethylenediamine (**111**) with extensive refluxing. However, no product was isolated from this reaction (Scheme 2.59).

Scheme 2.59



i) DMF, reflux, 0 %.

To improve the method to synthesise compound **145** an alternative procedure was proposed using an activated carboxylic acid. Conversion to the indole acid chloride was followed by treatment with oxalyl chloride, followed by treatment with ethylenediamine .

It is noteworthy that if the reaction was carried out on the indole N-unsubstituted compound (**149**), the unprotected nitrogen would react with a second molecule of the indole acid chloride, and the main product of the reaction was the dimer (**151**) (Figure 2.22).

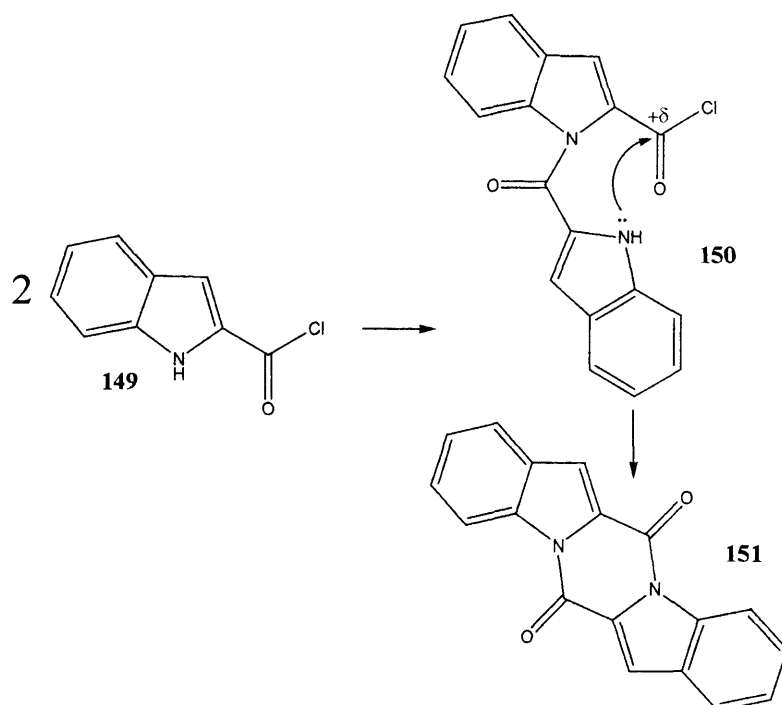
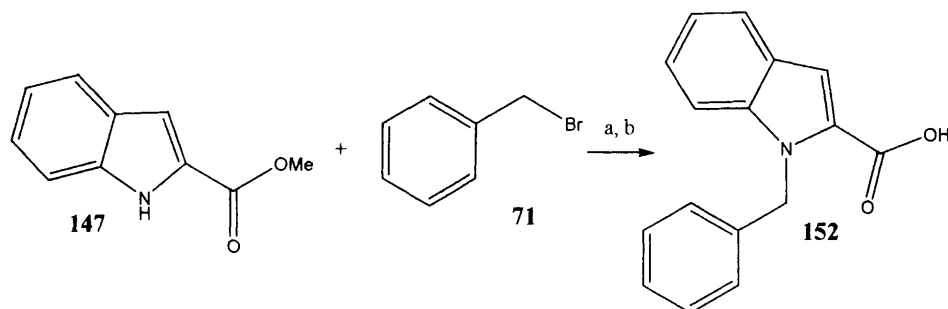


Figure 2.22 Formation of the unwanted side product (**151**) when the amide bond forming reaction is carried out on the free NH indole.

Based on the above theoretical speculation, it was necessary to protect the indole nitrogen for the diazepinone forming reaction to be successful.

Since the benzyl protecting group is stable under a variety of conditions, except for strong acid conditions (Greene and Wuts, 1999), it was thought that this protecting group would be resistant to the conditions used to form the cyclized diazepinone, and could then be removed once reaction was complete. The benzyl group was introduced to the indole NH followed by ester hydrolysis to afford **152** (Scheme 2.60).

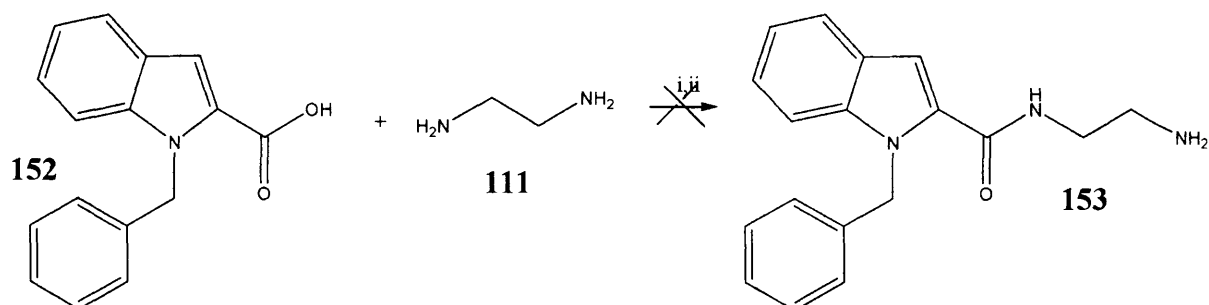
Scheme 2.60



a: i) NaH, THF, ii) THF, b: NaOH (aq), MeOH, 60 °C, 81 %.

The N-protected indole **152** could be activated using oxalyl chloride. It was proposed to react this directly with ethylenediamine to synthesise the amide (**153**), a stable intermediate with one of the bonds for the essential diazepinone having been made (Scheme 2.61). Unfortunately, this reaction was unsuccessful.

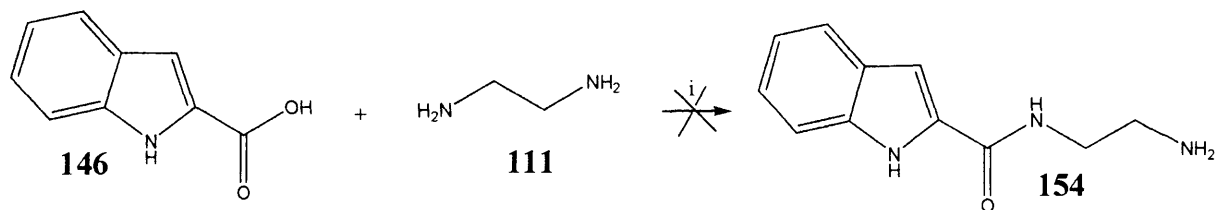
Scheme 2.61



i) TEA, oxalyl chloride, THF, 0 °C, ii) ethylenediamine, THF, 0 %.

A more concise synthesis was tried without the need to protect the indole nitrogen and an alternative synthetic route to form the amide bond was attempted (Sharma and Tepe, 2004) (Scheme 2.62). The synthesis involved using 1-(3-dimethylaminopropyl)-3-ethylcarbodiimide hydrochloride (EDCI) as a coupling reagent, but there was no progress in the reaction.

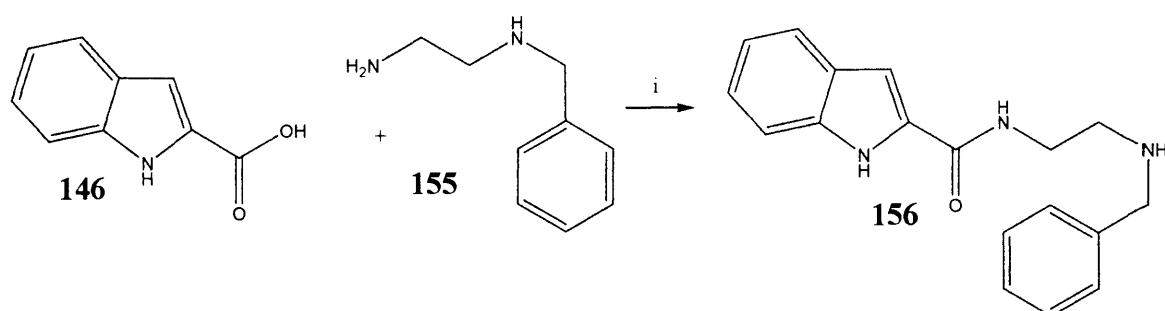
Scheme 2.62



i) EDCI, DMAP, DCM, 0 %.

This was due possibly to the formation of some unwanted reactions by unprotected diamine. *N*-Benzyloxyethylamine, a commercially available protected ethylenediamine, was used as an alternative reagent in the EDCI coupling reaction (Scheme 2.63). This reaction was successful, although a poor yield was obtained after purification.

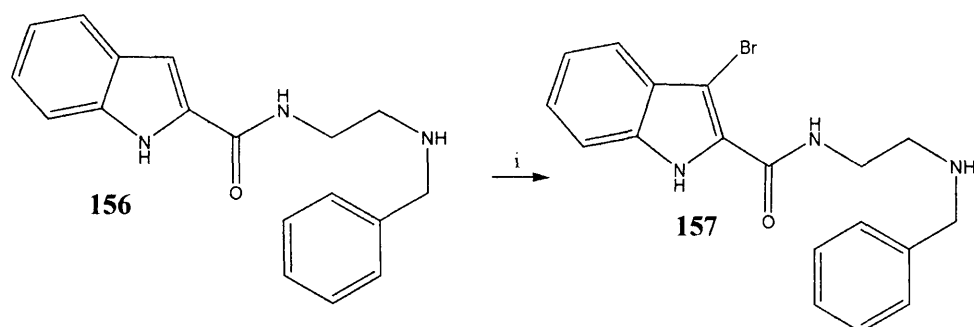
Scheme 2.63



i) EDCI, DMAP, DCM, 18 %.

The next step was bromination of **156**, attempted by treating **156** with *N*-bromosuccinimide (NBS) in DMF (Scheme 2.64), but due to an unclear NMR spectra and mass spectrum it was not possible to identify if the compound had been synthesised.

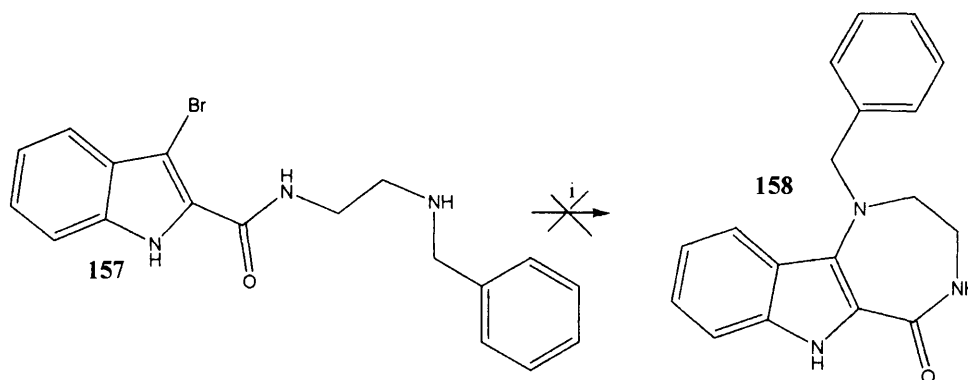
Scheme 2.64



i) NBS, DMF.

However, the compound obtained from the bromination reaction was subjected to cyclization conditions by heating compound **157** in DMF at 150 °C and in presence of copper, but the NMR spectra was still unclear and no product was recovered (Scheme 2.65).

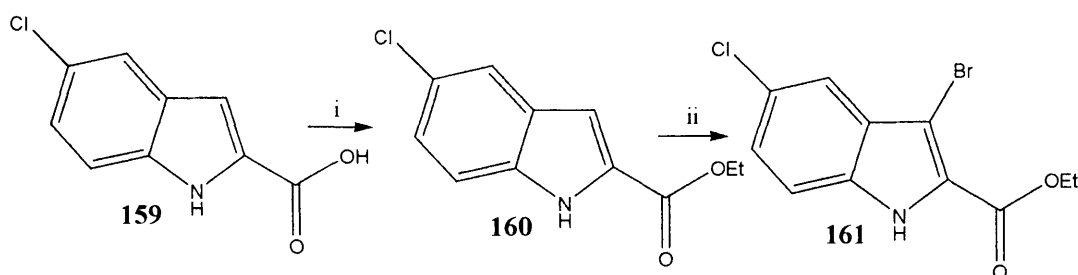
Scheme 2.65



i) Cu, DMF, 150 °C, 0 %.

While the product (**158**) had not successfully been isolated, this method was also attempted with the commercially available chlorinated indole acid (**159**). The esterification was achieved by refluxing the 5-chloro indole-2-carboxylic acid (**159**) in ethanol and in presence of concentrated sulphuric acid, to yield the ester in an excellent yield. Compound **160** was quantitatively brominated using NBS at the 3-position (Scheme 2.66).

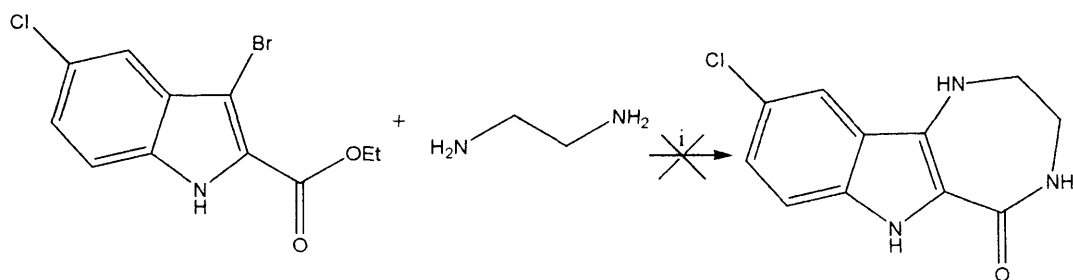
Scheme 2.66



i) Conc. H₂SO₄, EtOH, reflux, 99 %, ii) NBS, DMF, 100 %.

Again, the final cyclization method was not successful, which was attempted by refluxing in DMF in presence of ethylenediamine (**111**) and copper oxide. No product was obtained (Scheme 2.67).

Scheme 2.67



i) CuO, DMF, 150 °C, 0 %.

2.6 CONCLUSIONS

Reasonable methodology has been developed for synthesis of benzo- and dibenzodiazepinones and their rationally extended derivatives. Over all the syntheses investigated, the critical step appeared to be the amide protection step due to the surprisingly similar reactivity of the amide and amine groups resulting in disubstituted compounds. This limiting step considerably reduced the overall yield of the compounds synthesised. Nonetheless, sufficient quantities of compounds were synthesised in order to undertake biological testing.

Ultimately, suitable amide-NH protection was achieved using the SEM group to overcome the regioselectivity problem. Improving the reactivity of the electrophiles (alkylating reagents) by iodination was an alternative approach, which was effective in the synthesis of the desired compounds.

Although we were unable to introduce a variety of groups at the N-1 position of the 7-nitro-benzodiazepine-5-one (**28**), we managed to synthesise a small series N-1 substituted

analogues to be able to establish SARs between these compounds and compounds **26** and **27** analogues.

However, deprotection of the SEM group at the end of the synthesis was not very efficient, small quantities of the desired analogues were formed, further investigations could improve the yield or choice of protecting group.

Several interesting compounds have been synthesised to probe SARs between these compounds.

The synthesis of indolodiazepinone (**145**) and its related analogues were not successful, and further research could study the improved bromination of the indole ring.

2.7 NOMENCLATURE

The synthesised compounds were named using the “Hantzsch-Widman Nomenclature for Heterocyclic rings” combined with the “Fused ring Nomenclature” as described by the International Union of Pure and Applied Chemistry (IUPAC) nomenclature system.



Benzo and 1H, 4H-diazepin-5-one (as the base component) common bond: **[6,7-f]**

Based on this system, compounds were numbered anti-clockwise around the diazepinone ring from N being position 1.

Numbering of the fused rings was as follow:

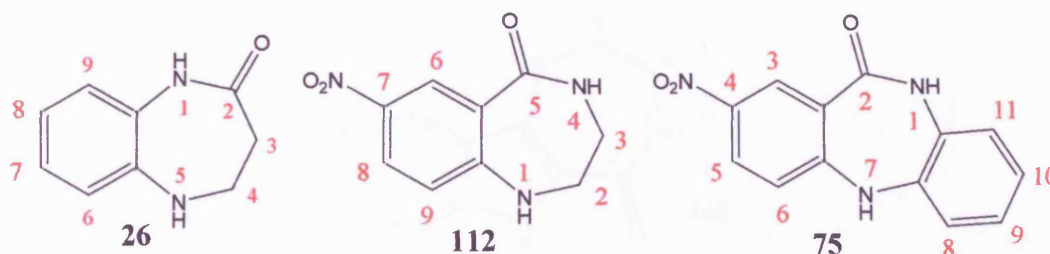


Figure 2.23. Numbering system used for cyclized compounds giving the three heteroatoms the lowest combined numbers.

Therefore, the names were:

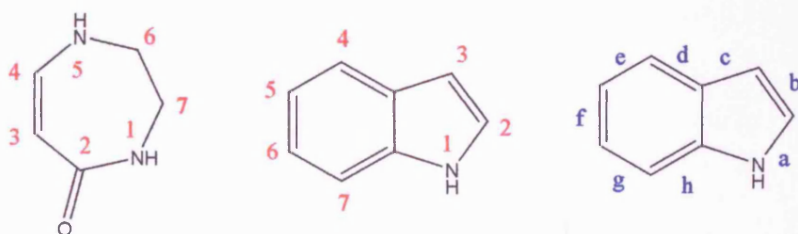
26, 3,4-Dihydro-1*H*,5*H*-benzo[2,3-*b*]diazepin-2-one

112, 2,3-Dihydro-7-nitro-1*H*,4*H*-benzo[6,7-*f*]diazepin-5-one

75, 4-Nitro-1*H*,7*H*-dibenzo[2,3-*b*][6,7-*f*]diazepin-2-one

However, compounds **26**, **112** and **75** were trivially named benzodiazepine-2-one, 7-nitro-benzodiazepine-5-one and 4-nitro-dibenzodiazepine-2-one. These names were used throughout this thesis.

Compound **145** was an alternative group of compounds synthesised and named according to this system.



1*H*,5*H*-Diazepino and **1*H*-indole-2-one** (as the base compound) common bond: [2,3-*b*]

Based on this system, pre-cyclized compounds were numbered anti-clockwise around the indole ring from N being position 1.

Numbering of the fused ring was as follow:

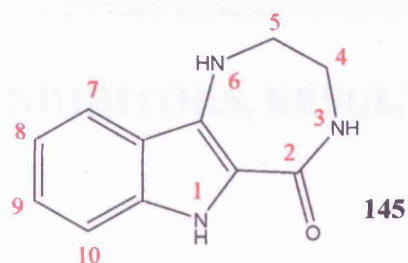


Figure 2.24. Numbering system used for cyclized compound giving the heteroatoms the lowest combined number.

Therefore, the name was:

145, 4,5-Dihydro-3*H*,6*H*-diazepino[2,3-*b*]indole-2-one

This structure was trivially named indolodiazepinone, and is reported by that name throughout this thesis.

PARP INHIBITORS, RESULTS AND DISCUSSION

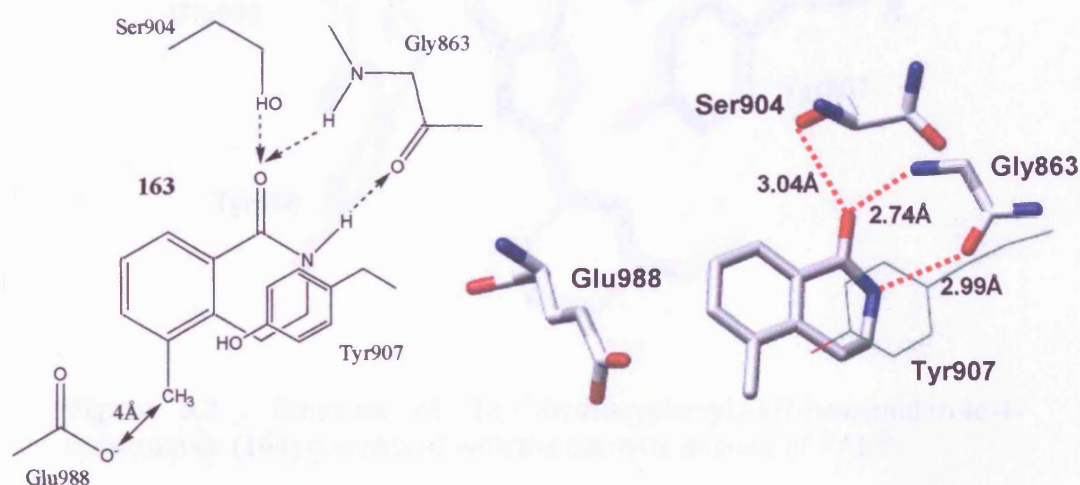
3.1 INTRODUCTION

The first generation of PARP inhibitors such as 3-aminobenzamide (**20**) (Schulze-Osthoff *et al.*, 1995) suffered from poor potency, and non-specific side effects (Piret *et al.*, 1995).

Since this initial report, interest in the use of PARP inhibitors as anti-cancer agents has rapidly expanded. The design of novel PARP inhibitors was greatly accelerated when the x-ray structure of PARP and bound ligands was solved. Due to 100 % homology in the amino acid sequence of the catalytic domain of human and chicken PARP, the crystal structure of the catalytic site of chicken PARP bound to the 3,4-dihydroquinolin-1(2*H*)-one (**163**) gave comprehensive information on the nature of the enzyme-inhibitor interaction (Weinfeld *et al.*, 1997). The inhibitor was bound to the active site by two hydrogen bonds from the carboxamide group to the peptide backbone of Gly863, and a third hydrogen bond from the carbonyl oxygen to the side chain of Ser904 (D'Silva *et al.*, 1999; Weinfeld *et al.*, 1997). This mimics the binding of the nicotinamide portion of NAD⁺, the enzyme's natural substrate. There were also hydrophobic interactions between

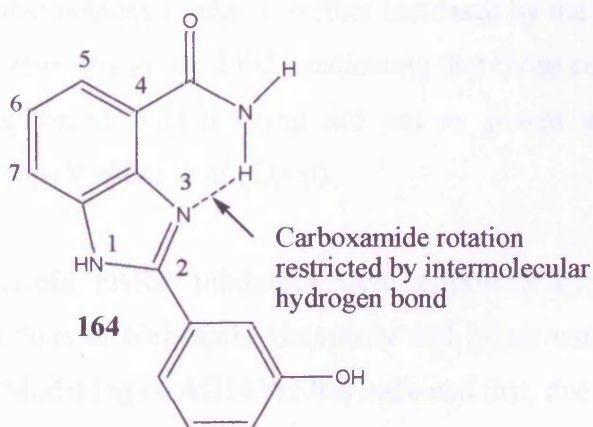
this inhibitor and the adjacent Tyr907. The Glu988 residue, located at a distance of 4Å from a methyl carbon atom, is involved in catalysis (Boulton *et al.*, 1999; Gaken *et al.*, 1996) (Figure 3.1). The positions of binding of all other PARP inhibitors studied by X-ray crystallography are similar.

Figure 3.1 Left: A schematic representation of the enzyme-inhibitor interactions between



PARP catalytic site and 3,4-dihydroquinoline inhibitor. Right: Crystallographic data of the same interaction (Weinfeld *et al.*, 1997).

A series of benzimidazole carboxamides have been developed as potent PARP-1 inhibitors by researchers at Newcastle University. The amide group required for hydrogen bond interactions is held in the correct conformation for hydrogen bond interactions with Gly863 and Ser904 by an intramolecular hydrogen bond. This pharmacophore contains an aryl ring at the 2-position of the benzimidazole that occupies a relatively spacious pocket, containing amino acid residues that could be targeted by further substitution on the aromatic ring (Figure 3.2).



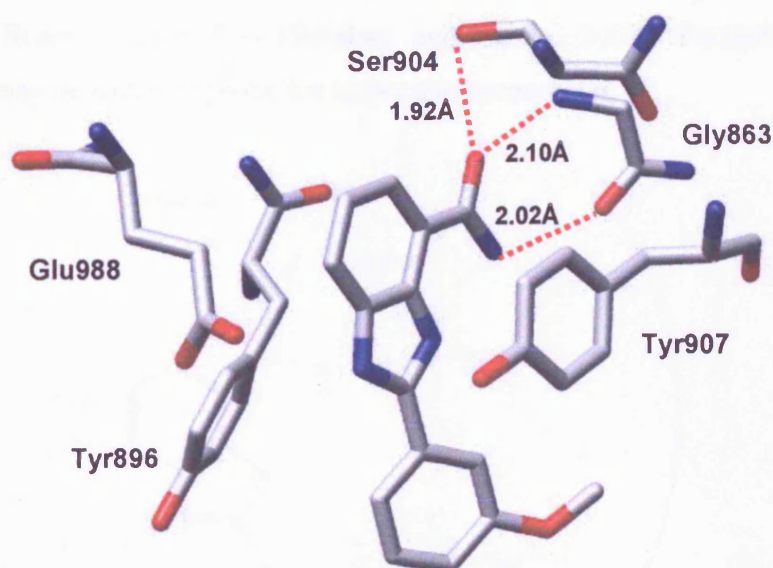


Figure 3.2 Structure of 2-(3'-hydroxyphenyl)-1H-benzimidazole-4-carboxamide (**164**) complexed with the catalytic domain of PARP.

The substituted benzimidazole-4-carboxamides (**164**) were found to be extremely potent PARP inhibitors ($IC_{50} = 0.08\text{--}1.10\ \mu\text{M}$) more so than the 3-substituted benzamides such as 3-aminobenzamide (**20**) ($IC_{50} = 19\ \mu\text{M}$) under the same assay conditions (Anderson and LeesMiller, 1992; Lee *et al.*, 1997).

The study of benzimidazole PARP inhibitors were extended by the synthesis of 7-membered lactam derivatives to totally restrain the amide rotation, and additional aromatic substituents will interact with the PARP-1 active site (Figure 3.3) (Southan and Szabo, 2003). The parent compound (**23**, R=H) has an $IC_{50} = 300\ \text{nM}$ (Ferraris *et al.*, 2002), and it was found that potency could be further increased by the phenyl substituent (R = Ph) ($IC_{50} = 26\ \text{nM}$) (Ferraris *et al.*, 2002), indicating that those compounds with the substituent on the 7-membered (lactam) ring are not as potent as those with the substitution at the 2-position (Webber *et al.*, 2000).

However, the benzimidazole PARP inhibitors were improved by the synthesis of AG14361 (**25**) by researchers at Newcastle University and Pfizer with an ($K_i < 5\ \text{nM}$) (Calabrese *et al.*, 2004). Modelling of AG14361 has indicated that, due to the presence of a spacious pocket in the active site, a dibenzodiazepinone could be incorporated into the

active site of PARP-1 and that an additional fused benzo-ring could increase the inhibitory efficacy (Figure 3.3) (Southan and Szabo, 2003). Furthermore, aromatic substituents may be added to probe for active site interactions.

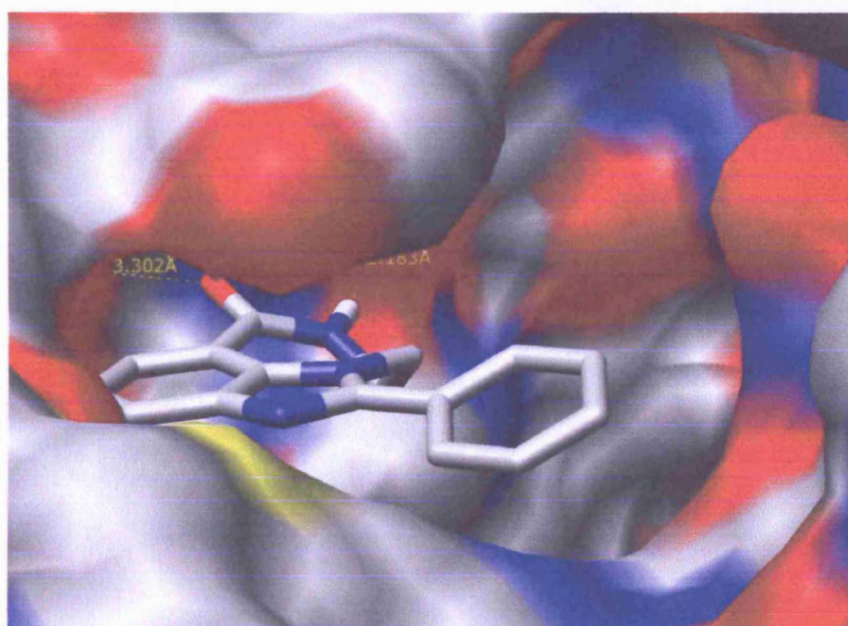
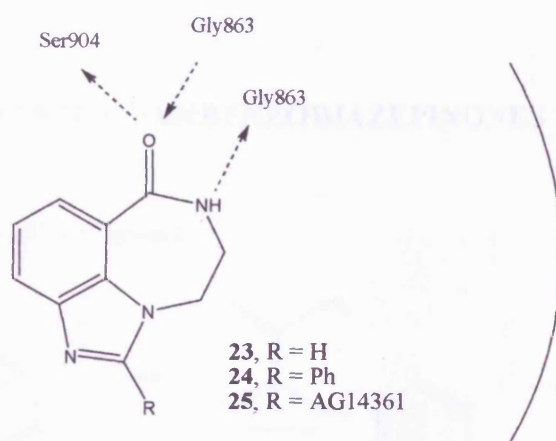


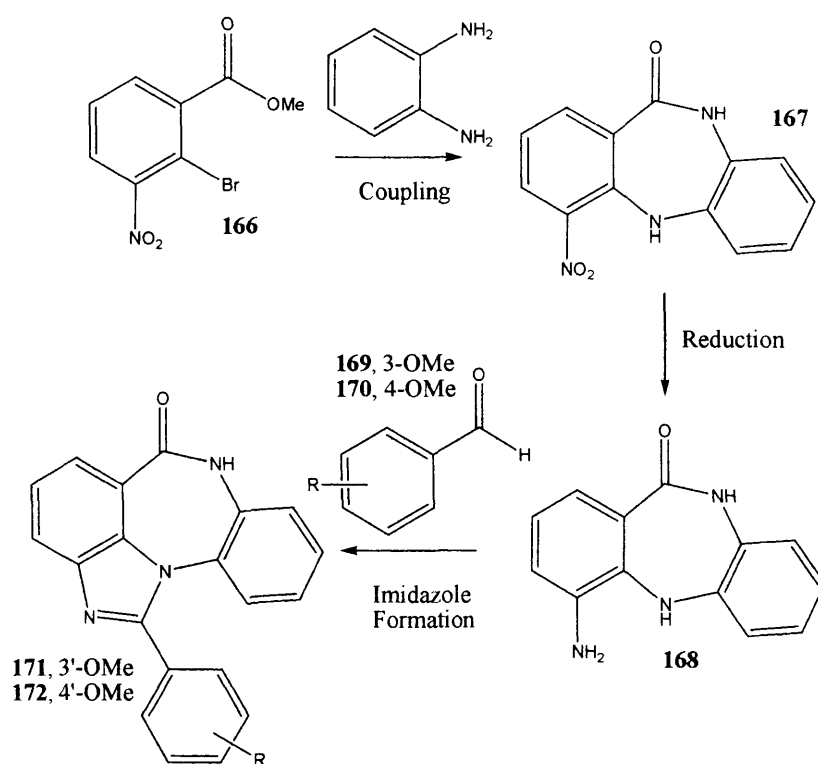
Figure 3.3 Structure of dihydroimidazobenzodiazepin-6(7*H*)-one complexed with the catalytic domain of PARP active site, showing the large active site pocket occupied by the aromatic ring.

The dibenzodiazepinone pharmacophore contains a seven-membered lactam ring for which we have already explored the synthesis. Preparation of these derivatives could allow us to further explore the medicinal chemistry of this group and its use as a novel PARP-1 inhibitor.

In this chapter, the synthesis of imidazodibenzodiazepinone derivatives will be described, followed by discussion of each modification introduced to the main scaffold structure of the lead compound.

3.2 SYNTHESIS OF IMIDAZODIBENZODIAZEPINONES

Scheme 3.1 (Outline of Synthesis)

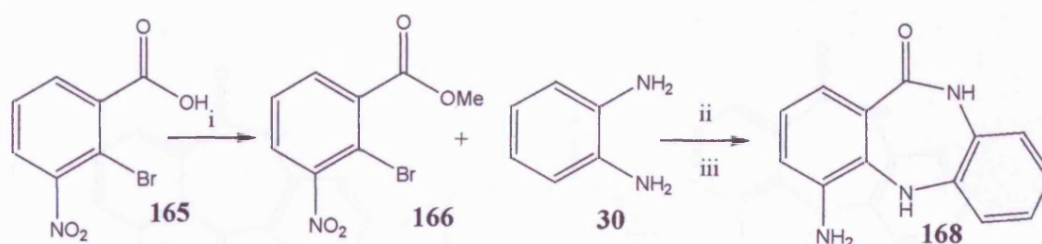


The synthesis of PARP-1 inhibitor precursors used the same methodology as adopted previously, but using the different substitution pattern (**166**). This strategy is possible since the bromine of **166** is activated for substitution by an *ortho*-nitro group (compared to the *para*-nitro group used in previous synthesis).

Esterification of 2-bromo-3-nitrobenzoic acid (**165**) afforded **166**. The next step involved its coupling with 1,2-phenylenediamine (**30**). Compound **166** was heated with 1,2-phenylenediamine in dimethylacetamide (DMA) at 150 °C for 10 h until **167** had been synthesized (Lubisch *et al.*, 2003).

The next step was the reduction of **167** which was performed using 10 % palladium on carbon (10 % Pd/C) in methanol in a pressure vessel under a hydrogen atmosphere of 20-40 p.s.i. This method produced compound **168** cleanly and in quantitative yield (Lubisch *et al.*, 2003) (Scheme 3.2).

Scheme 3.2



i) Conc.H₂SO₄, MeOH, 98 %, ii) DMA, 150 °C, 48%, iii) H₂, Pd/C, MeOH, 100 %.

The NOESY spectrum suggested the right position of amide-NH would be downfield compared to amine-NH (Figure 3.4).

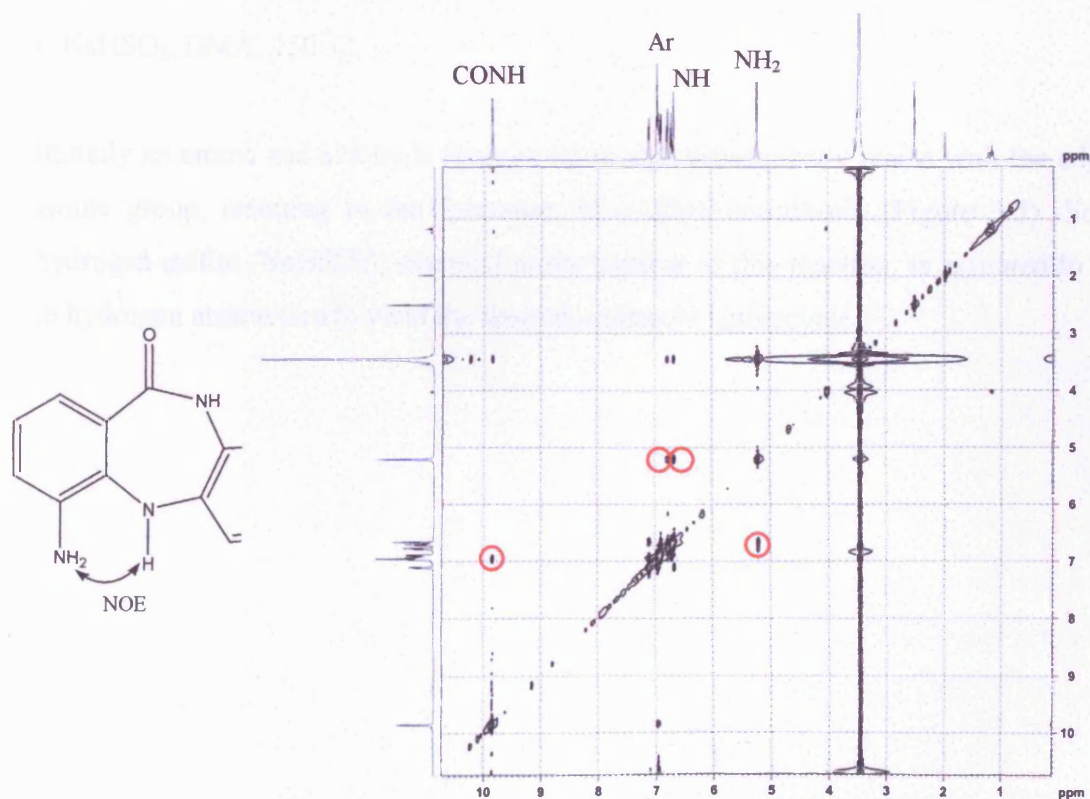
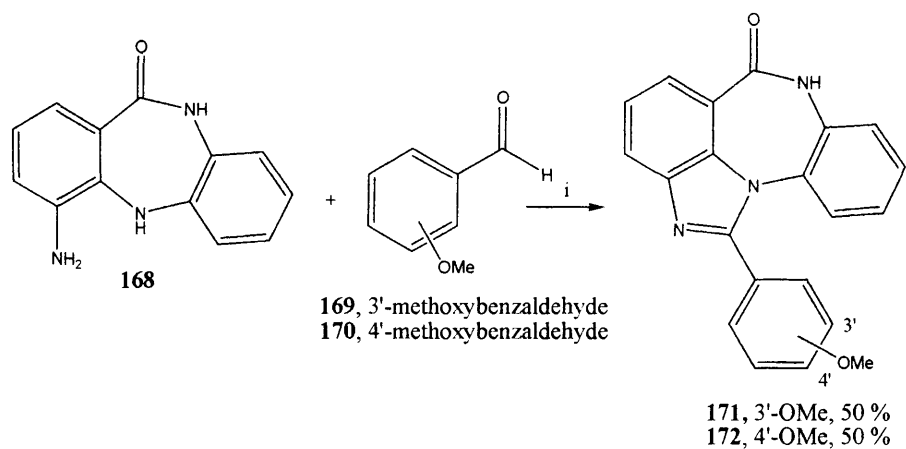


Figure 3.4 Showing NOE interactions between amine-NH and NH₂ and not between amide-NH and NH₂.

The final step of this synthetic pathway involved the formation of the fused imidazole ring via the addition of an aldehyde across the two amine groups. The aldehyde (**169**, **170**) was suspended in DMA along with amine (**168**) and sodium hydrogen sulfite (Scheme 3.3) (Skalitzky *et al.*, 2003) (Lubisch *et al.*, 2003).

Scheme 3.3

i) NaHSO_3 , DMA, 150°C .

Initially an amine and aldehyde form an imine that subsequently reacts with the adjacent amine group, resulting in the formation of a dihydroimidazole (Figure 3.5). Sodium hydrogen sulfite (NaHSO_3), essential to the success of this reaction, is assumed to assist in hydrogen abstraction to yield the desired imidazole heterocycle.

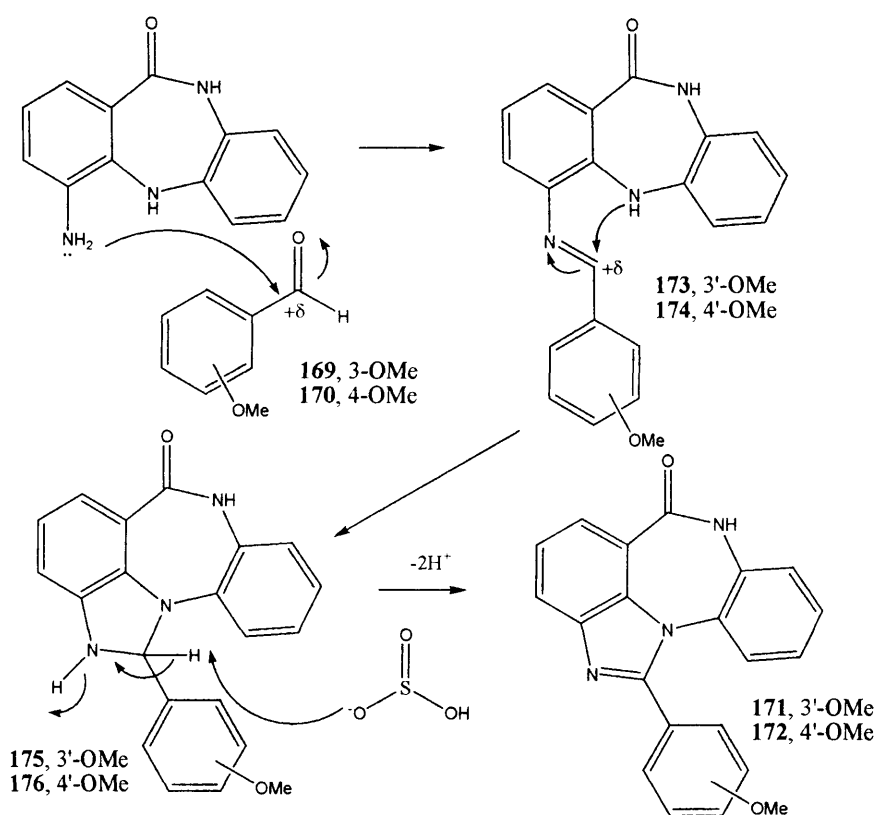


Figure 3.5 Mechanism of imidazole formation.

The aryl group stemming from the imidazole ring with substituents such as methoxy located at the 3'- or 4'-position of the molecule was quite important to consider. The reasoning behind it is that 3'- and 4'-methoxy groups showed good activity in previous SAR studies (White *et al.*, 2000). The chemistry is straightforward, well documented and also the starting materials are commercially available. More importantly, the oxygen group in the ether group acts as a potential H-bond acceptor that may enhance the binding potential of the compound to PARP-1.

The successful preparation of these initial molecules, **171** and **172** demonstrated that imidazodibenzo-derivatives could be simply and practically synthesized within the laboratory with a reasonable yield. This would therefore be helpful towards the design of a more effective and thus valuable molecules based on data obtained regarding the structure activity relationship studies (SARs) of these compounds.

Compound **29**, a PARP-1 inhibitor with fewer groups for intermolecular binding, still shows an IC_{50} of 260 nM. This implies that more developed compounds with additional substitutions at appropriate position to interact with active site residues, could be even more efficacious. Once this has been determined further work can resolve which functional groups are preferable in various positions. The dibenzo analogues allow further investigation of the active site pocket by addition of substituents onto the ring (R') (Figure 3.6).

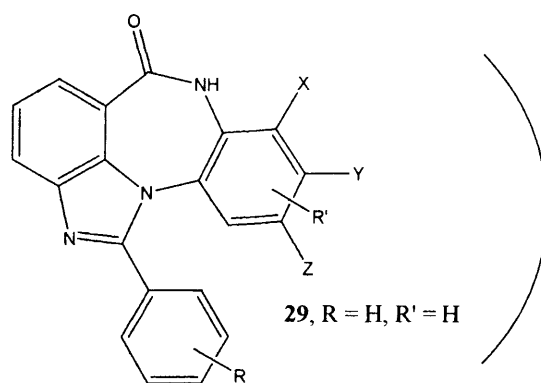
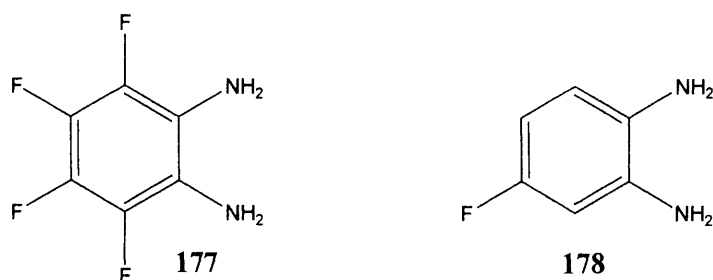


Figure 3.6 Showing the addition of different substituents onto the ring.

The addition of fluorine (an electron-withdrawing group) at the X position of the lead compound (Figure 3.6) was initially considered, as it is a good chemical bioisostere for hydrogen and would be highly polar, thereby enhancing the likelihood of dipole-dipole and could also result in further intermolecular bonding with the PARP-1 active site.

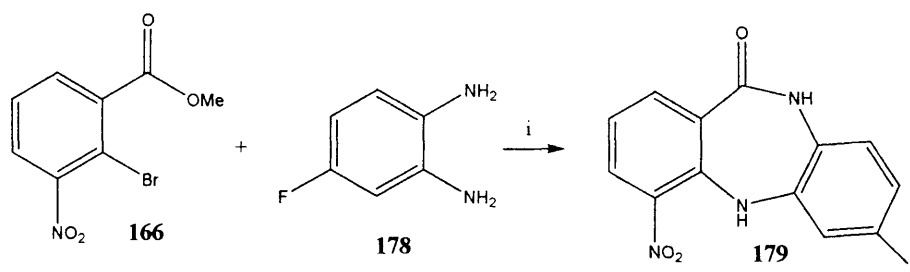
The symmetrical tetrafluorophenylenediamine (**177**) would avoid any problems of regiochemistry and ensure a fluorine atom was positioned at X. However, this compound was not commercially available.



The monofluoro derivative (**178**) could be purchased, and could yield a product with the fluorine at the Y or Z position (Figure 3.7).

In the coupling reaction the same method that had been previously used was reported. To do so, 1,2-diamino-4-fluorobenzene (**178**) was dissolved in DMA and heated for 10 h at elevated temperature (Scheme 3.4).

Scheme 3.4



i) DMA, 150 °C, 100 %.

Being an unsymmetrical precursor, reaction with diamine **178** could possibly result in a mixture of isomers (Figure 3.7). However, one product was obtained from this reaction, in quantitative yield and shown to be a pure, single isomer.

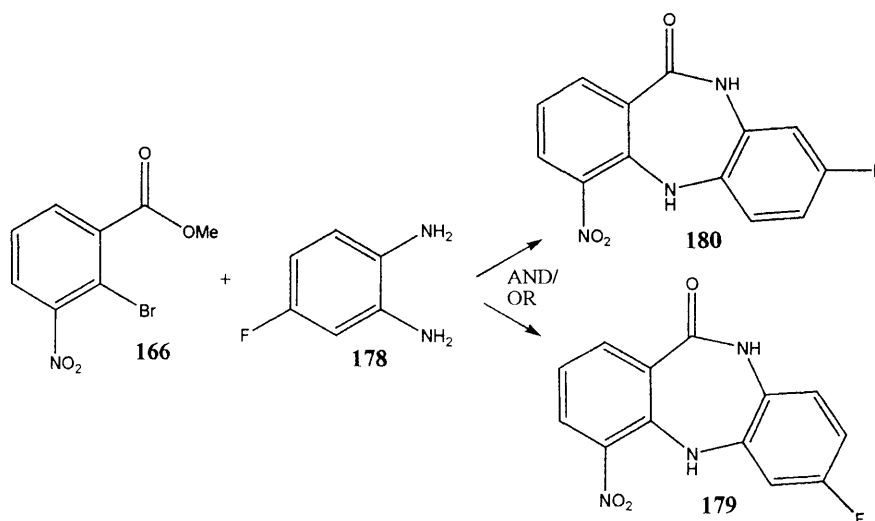


Figure 3.7 Showing the possibility of formation of a mixture of isomers.

A NMR NOESY spectrum confirmed which isomer had been synthesised. A Nuclear Overhauser Effect (NOE) was observed between the 8-H aromatic double doublet peak (extra splitting due to the fluorine atom) and the amine proton located within the lactam ring. Additionally NOE interaction between the amide proton and the 11-H aromatic doublet was observed (Figure 3.8). This is only possible when the fluorine group is located at the 9-position, therefore confirming the regiochemistry of compound **179**.

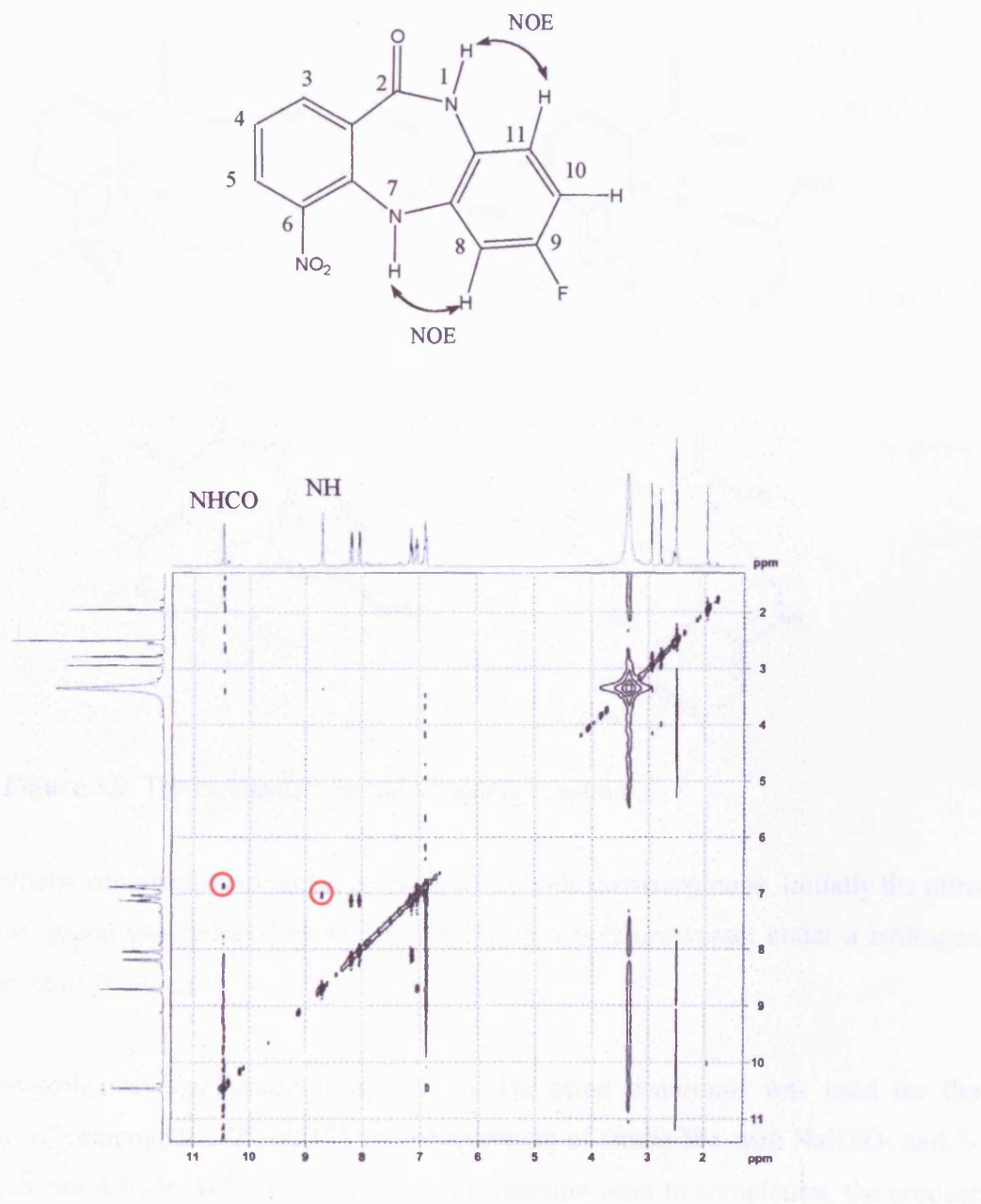


Figure 3.8 Confirming the position of F in **179** using NOE.

The formation of the single isomer can be explained by the nucleophilic properties of the two amines in **178**. The nucleophilicity of the amino group para to the fluorine group will be reduced due to the presence of the electron-withdrawing fluorine group. On the other hand the bromine atom on the compound (**166**) is a good leaving group. Therefore, it is expected that the meta-positioned amino group, being the stronger nucleophile, will react with the bromine initially followed by formation of the amide bond involving with the less nucleophilic amino substituent reacting with the ester group (Figure 3.9).

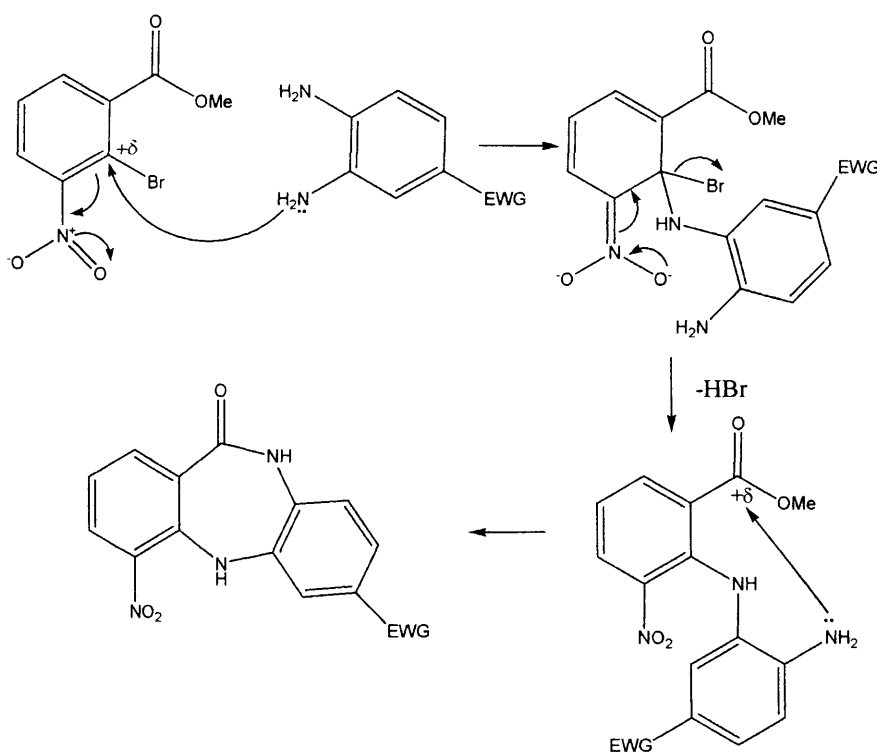
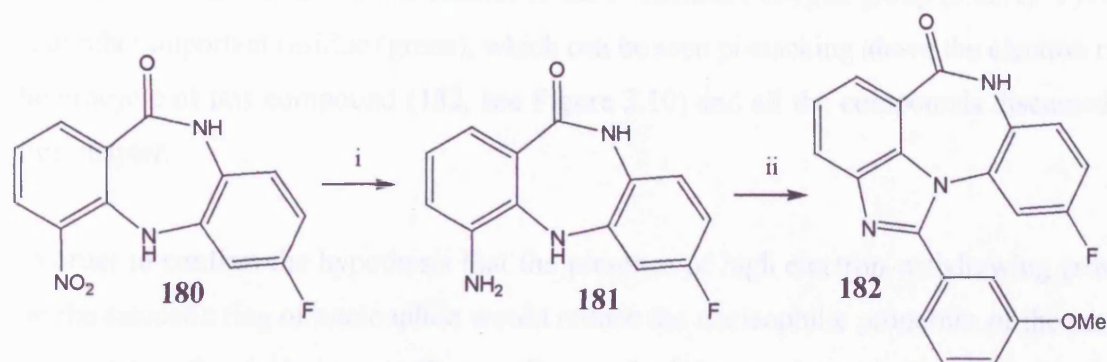


Figure 3.9 The mechanism for the coupling reaction.

The synthesis continued as expected to the imidazole-dibenzoazepinone. Initially the nitro functional group was reduced using 10 % Pd/C in a pressure vessel under a hydrogen atmosphere of 20-40 p.s.i.

The imidazole was synthesised using exactly the same conditions was used for the synthesis of compounds **171** and **172** by the treatment of amine **181** with NaHSO₃ and 3-methoxybenzaldehyde (**169**) in DMA. Once the reaction went to completion, the product was recovered by precipitation from water and recrystallized from methanol to yield the desired compound **182** in an excellent yield of 100 % (Scheme 3.5).

Scheme 3.5



i) H_2 , 10 % Pd/C, MeOH, 60%, ii) 3-methoxybenzaldehyde, NaHSO_3 , DMA, 150°C , 100%.

From the modelling studies of compound **182** one could verify whether a electron-withdrawing group (H-bond acceptor) at the 10-position enhances the degree of inhibition. By comparing the structures of **29**, **171** and **172** it is also expectable that compound **182** will cause greater inhibition of the PARP-1 due to the additional fluorine group, but as can be seen from the following picture there are no close H-bond accepting residues nearby the fluorine to form intermolecular interactions (Figure 3.10).

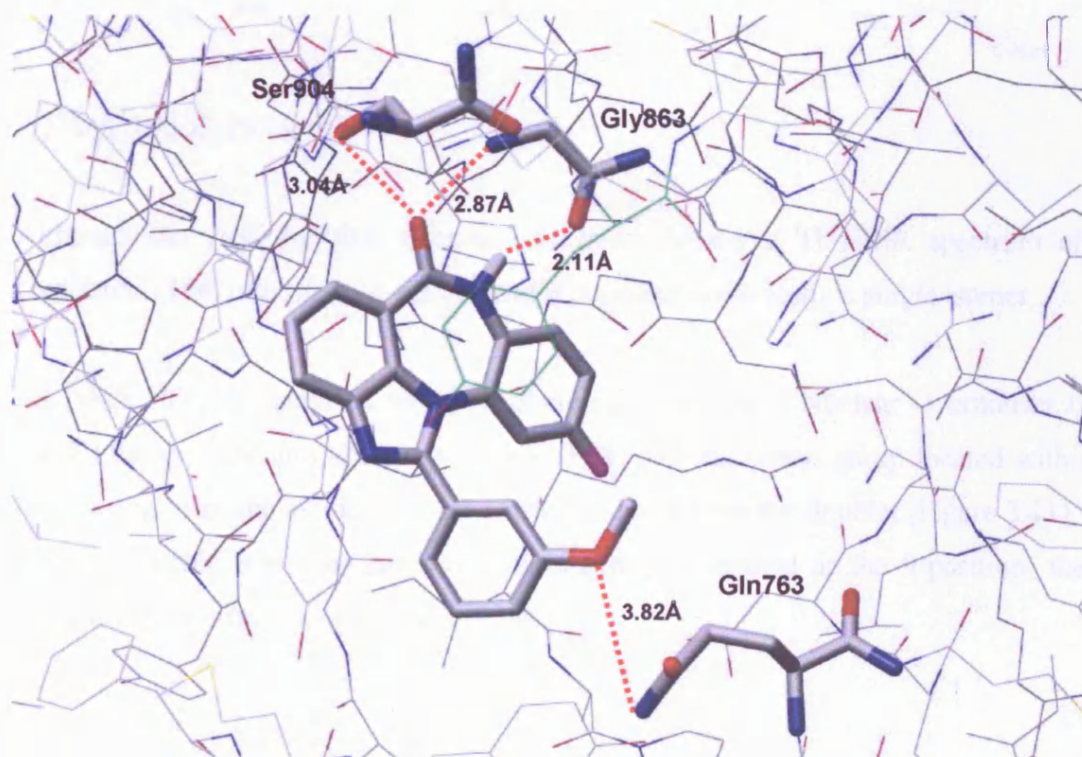
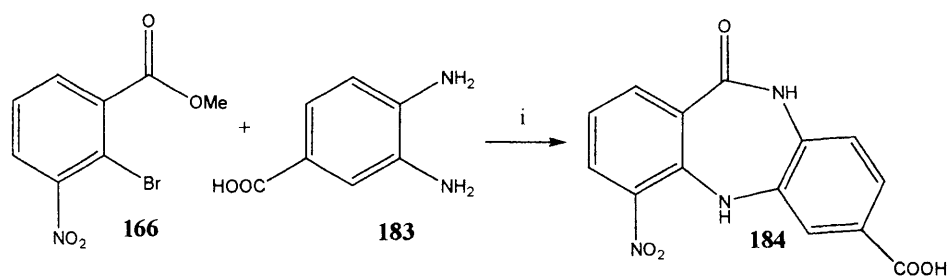


Figure 3.10 The prospective H-bonds of compound **182**, fluorine substituent is in purple.

The conserved residues Ser904 and Gly863 interact with the amide as expected, as well as Gln763 which acts as a H-bond donator to the 3'-methoxy oxygen group (3.82Å). Tyr907 is another important residue (green), which can be seen pi-stacking above the electron rich heterocycle of this compound (**182**, see Figure 3.10) and all the compounds discussed in this chapter.

In order to confirm the hypothesis that the presence of high electron-withdrawing groups on the aromatic ring of nucleophile would reduce the nucleophilic properties of the amine thus creating the single isomer, the coupling method that employed in the synthesis of the fluorine derivative was repeated, with compound **178** being replaced with 3, 4-diaminobenzoic acid (**183**) (Scheme 3.6).

Scheme 3.6



i) DMA, 150 °C, 26 %.

Although the yield for this reaction was much lower, a ^1H NMR spectrum of this compound (**184**) indicated the presence of a pure and importantly a single isomer.

An NMR NOESY spectrum was also obtained, observing a Nuclear Overhauser Effect (NOE) between the aromatic singlet peak (H-8) and the amino group located within the lactam ring. Also the amide interacted with the H-11 aromatic doublet (Figure 3.11). This is only possible when the carboxylic acid group is located at the 9-position, thereby confirming the structure of compound **184**.

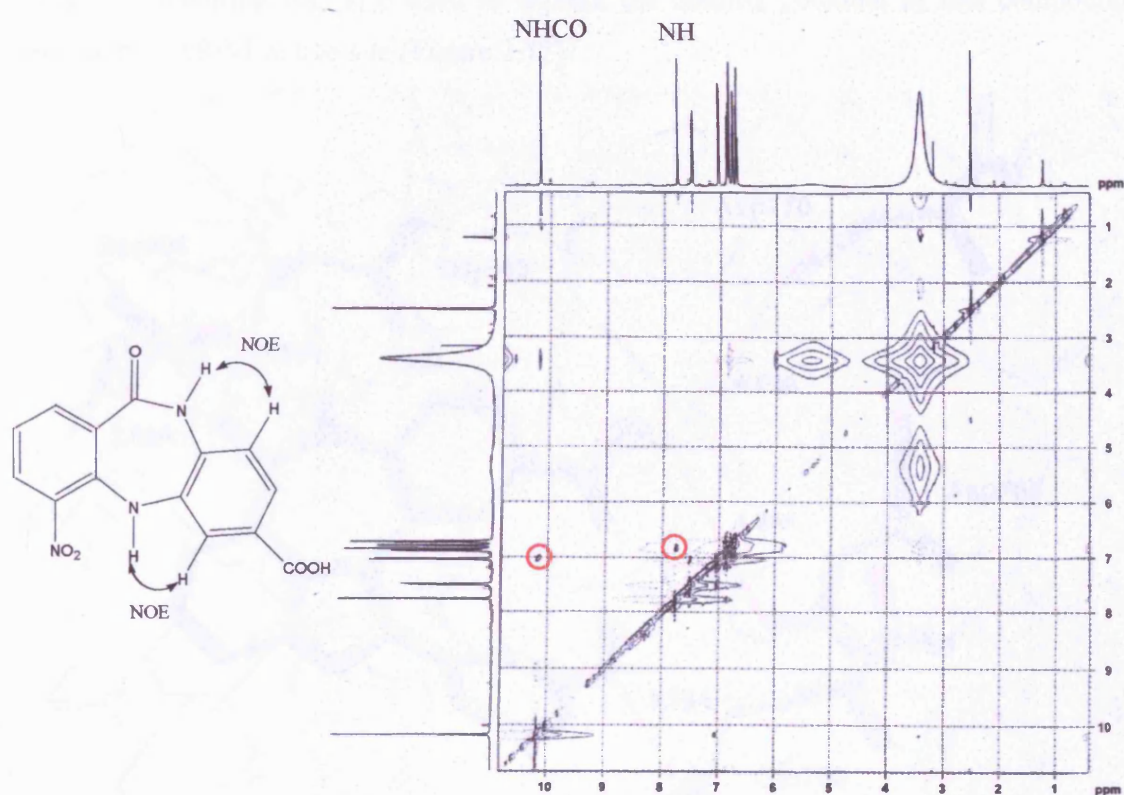
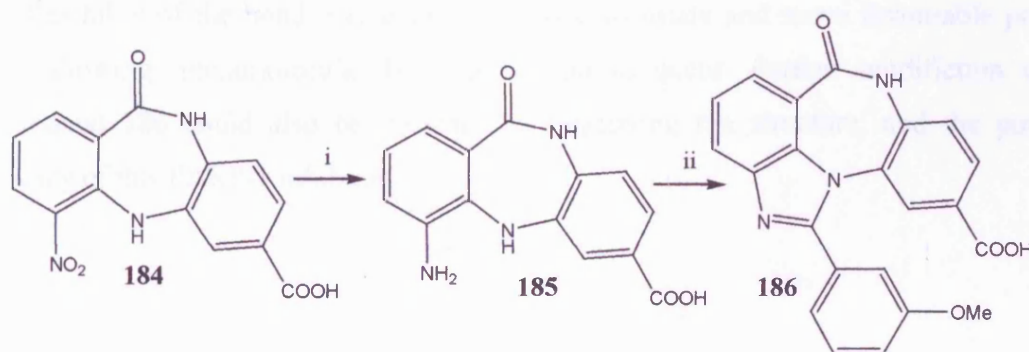


Figure 3.11 Showing NOE interactions between an aromatic singlet peak and amine, and also the amide and aromatic doublet.

The nitro group was readily reduced using the standard hydrogenation procedure. The subsequent amine was reacted with aldehyde **169** to form the imidazole ring. The purification of this, and all similar reactions was quite easy. When the reaction was complete, the crude product was precipitated from water and recrystallized from hot methanol to obtain the pure product (Scheme 3.7).

Scheme 3.7



i) H_2 , 10 % Pd/C, MeOH, 71 %, ii) NaHSO_3 , DMA, 150°C , 55 %.

Molecular modelling was also used to explore the binding potential of this compound (**186**) to the PARP-1 active site (Figure 3.12)

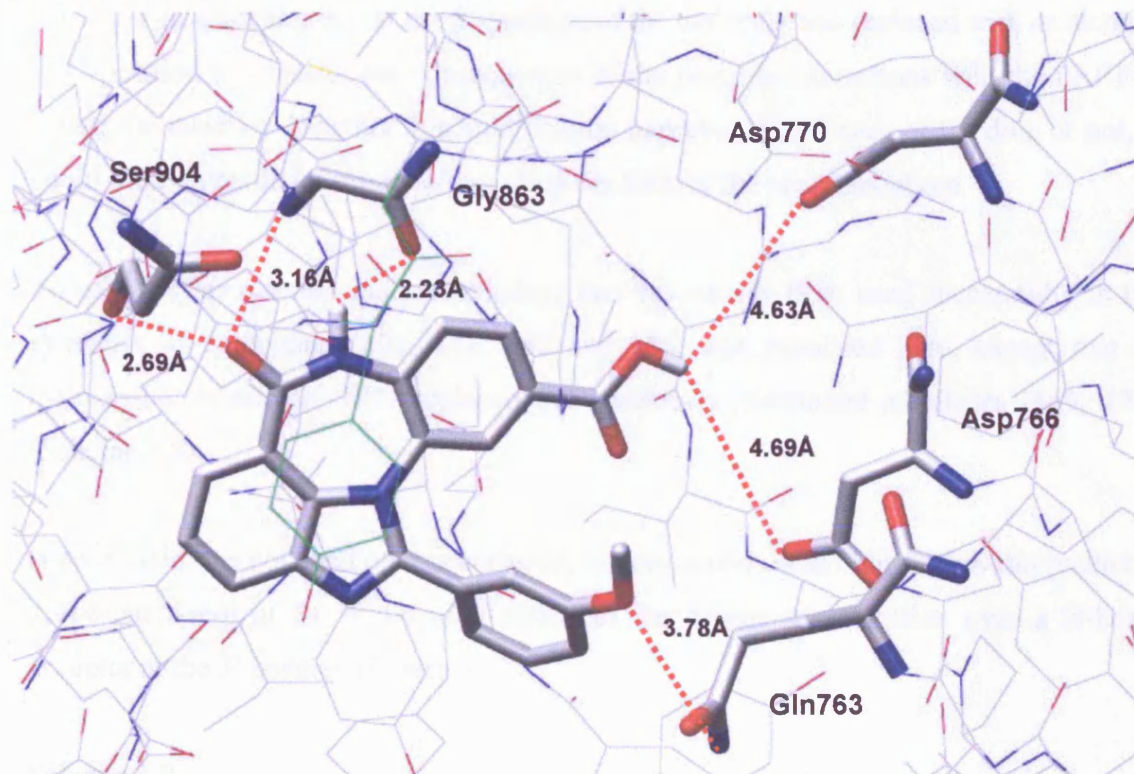


Figure 3.12 The potential H-bonds that could be formed by compound **186** with the enzyme.

When considering the above model, an additional hydrogen bond could be generated due to the presence of the carboxylic acid group at the 9-position. Ser904 and Gly863 interact with the amide as expected. Gln763 could act as H-bond donator by interaction of its NH with the ether group. The Asp770 and Asp766 side-chains may also form a H-bond, even though this distance is outside the optimal range (2.8-3.6 Å), by considering the fact that the flexibility of the bond may enable the bond to rotate and move favourable position thus allowing intermolecular bond formation to occur. Further modification of the compound **186** could also be possible by improving the structure, and the potential efficacy of this PARP-1 inhibitor.

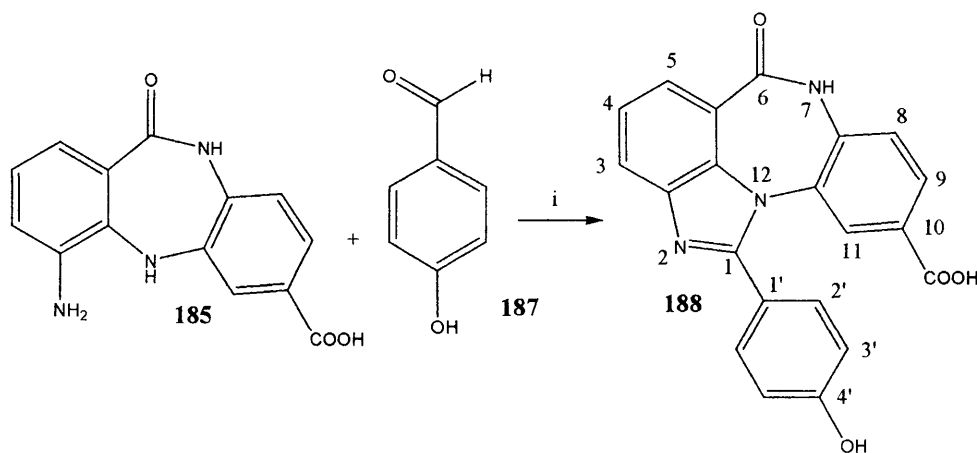
3.2.1 Modification of 1'-aryl substituents

The ether functional group at the 3'-position of the molecule was replaced with an alcohol at 4'-position to consider the consequences of the possible interactions with the PARP-1 active site residues. Whether this modification improves the efficacy of the drug or not, it could offer valuable information regarding the SAR of the pharmacophore.

To achieve this reaction the methodology that has already been used successfully in the synthesis of compounds **171**, **172**, **182** and **186**, was reutilised here, except that 4-hydroxy-benzaldehyde (**187**) replaced the previously mentioned aldehydes (**169**, **170**) (Scheme 3.8).

A poor yield was obtained on this occasion, but molecular modelling studies can predict if a H-bond donor at the 4' position enhances the degree of inhibition over a H-bond acceptor at the 3' position (Figure 3.13).

Scheme 3.8



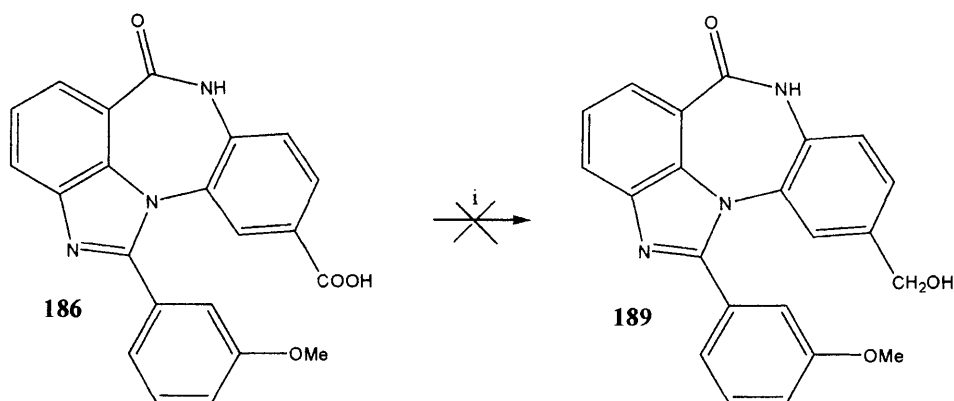
i) NaHSO₃, DMA, 150 °C, 9 %.

thought that a hydrogen bond donor is better located on a ligand rather than a residue within the active site which can be an additional reason for synthesizing such a compound.

Regardless of actual effects of this modification, the obtained information would be useful in structure activity relationship studies.

Compound **186** was treated with lithium aluminium hydride (LiAlH_4) but based on TLC indication there was no progress in the reaction (Scheme 3.9). Although attempts to reduce the acid to an alcohol (**189**) proved unsuccessful, maybe alternative methods were required using alternative reducing agents in the future.

Scheme 3.9



i) LiAlH_4 , THF, 0 %.

The following picture shows hypothetical interactions between the inhibitor and active site residues. As it is obvious in the Figure 3.6, there might be additional interactions with the Asn767 H-bond accepting group as well as Asp766 and Gln763 residues (Figure 3.14).

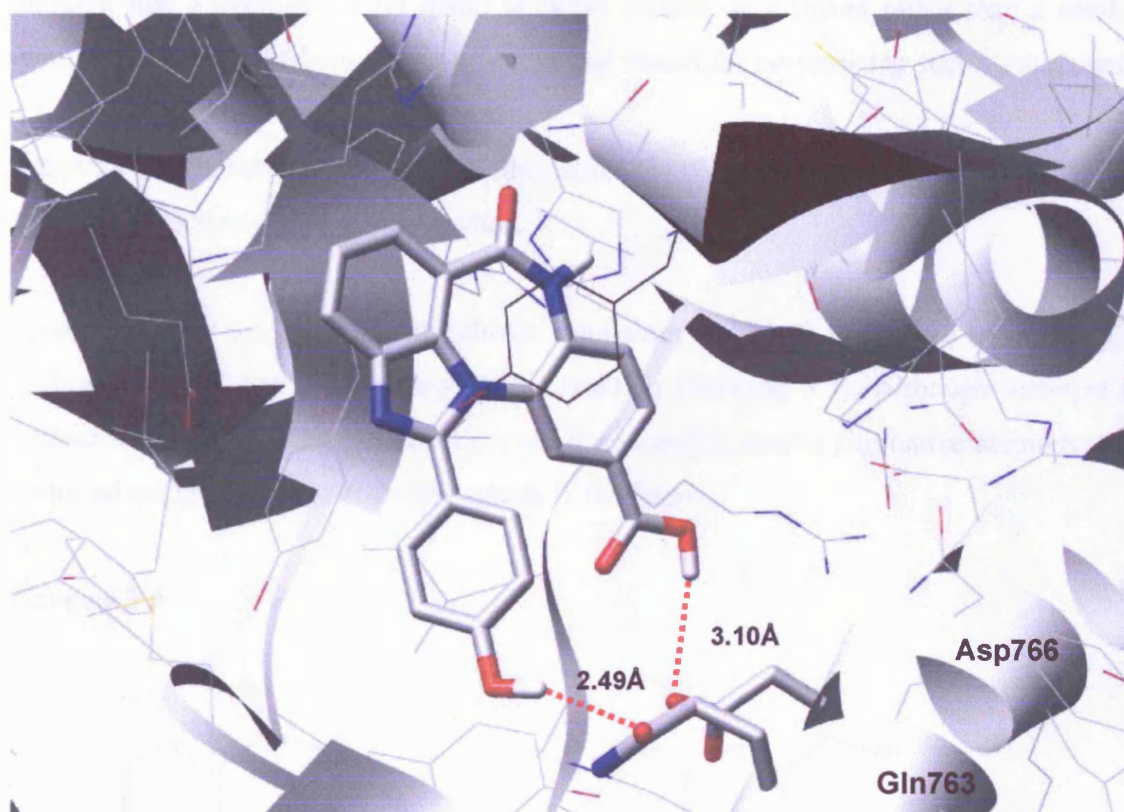


Figure 3.13 The prospective H-bonds from the 4'-hydroxy phenyl substituent of **188**.

The hydroxy group of the alcohol at 4'-position can interact with the Gln763 side-chain differently from the ether, by interaction of the H-bond donating alcohol group with the oxygen acceptor of Gln763. The previously utilised Asp766 backbone residue can also act as a H-bond acceptor. Therefore, one may assume that compound **188** might be as effective as compound **186**.

3.2.2 Attempted carboxylic acid reduction

At physiological pH the acid group is usually ionised hence reducing the hydrogen bonding interactions between the enzyme and the inhibitor due to the potential repelling force between the inhibitor and other negatively charged residues (e.g. possibly an also ionised Asp766). To overcome this problem, it was decided to reduce the carboxylic acid to an alcohol group that may have more favourable interactions with PARP-1. It is also

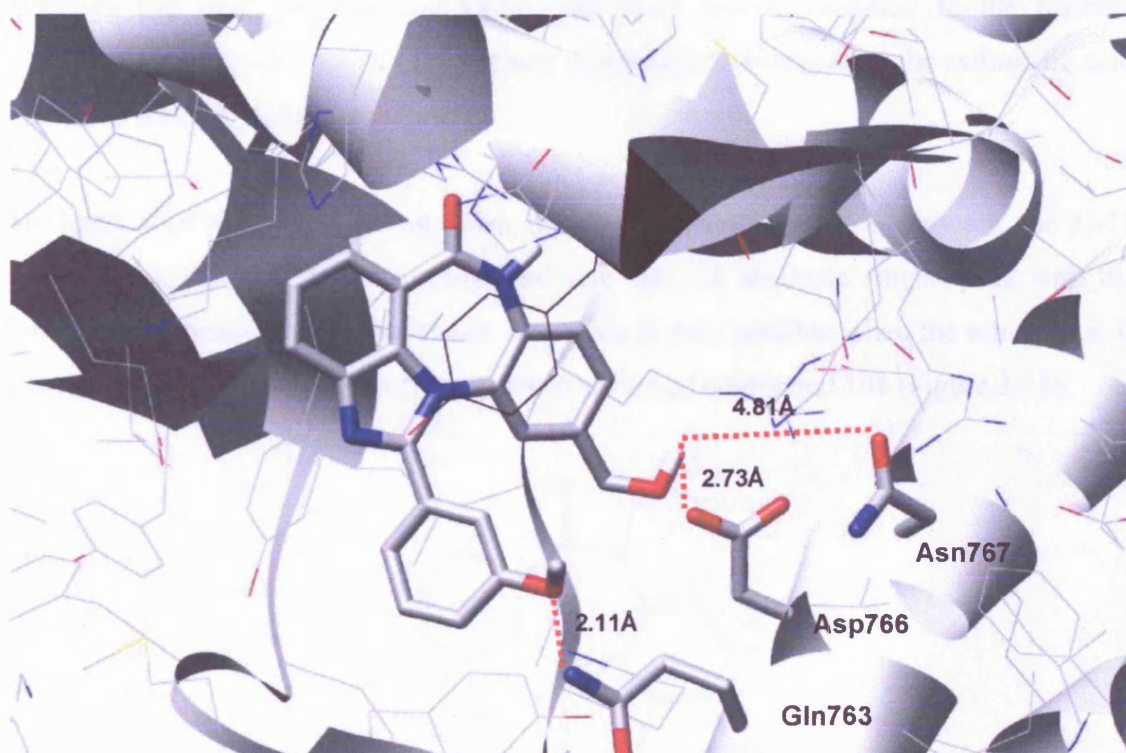
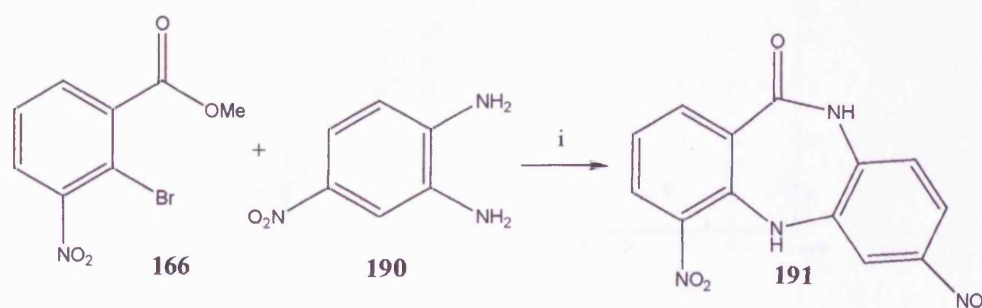


Figure 3.14 The prospective H-bonds formed with 189.

As a further example, the commercially available 1-nitro-3,4-phenylenediamine (**190**) with a highly electron-withdrawing group on the aromatic ring was used, forming the single isomer (**191**). The same method that had been previously employed in the synthesis of the fluorine and carboxylic acid derivatives coupling step was used with compound **191** (Scheme 3.10).

Scheme 3.10



i) DMA, 150 °C, 50 %

Although the yield for this compound was much lower compared to the fluorine derivative coupling compound (179), it was much higher compared to the carboxylic acid derivative coupling (184).

An NMR NOESY spectrum was also obtained indicating a NOE between the H-11 aromatic doublet peak and the amide and also the H-8 aromatic singlet peak with the amino group located within the lactam ring. This is only possible when the nitro group is located at the 9-position, so confirming the structure of compound 191 (Figure 3.15).

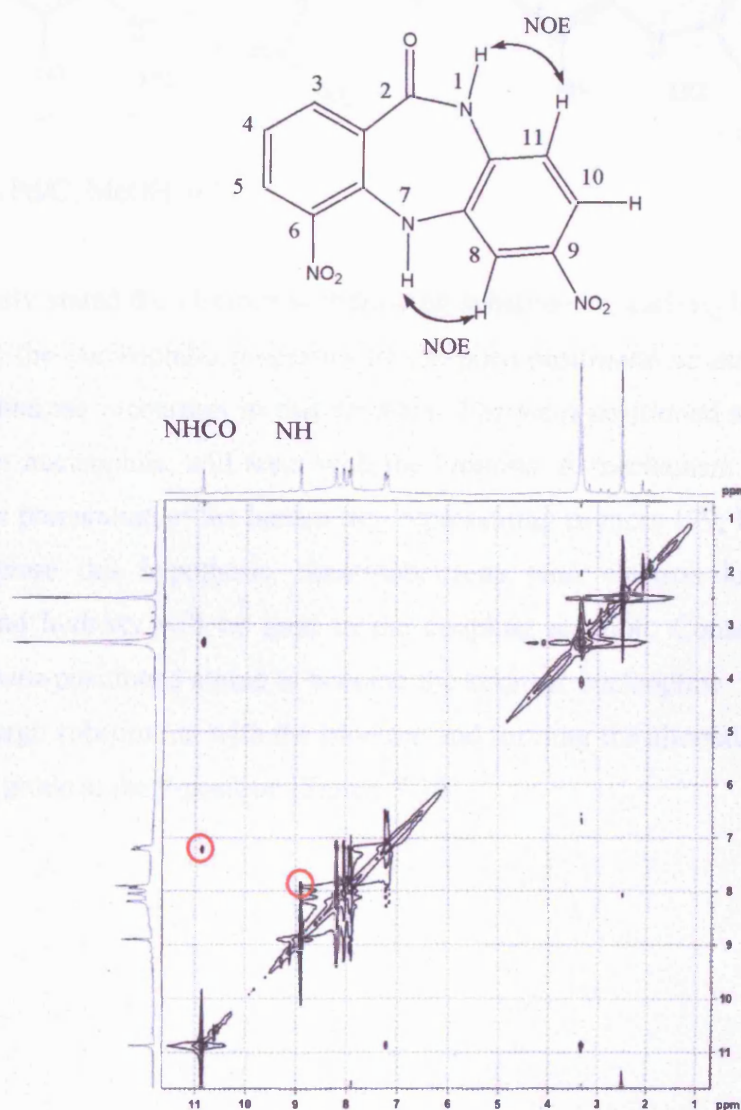
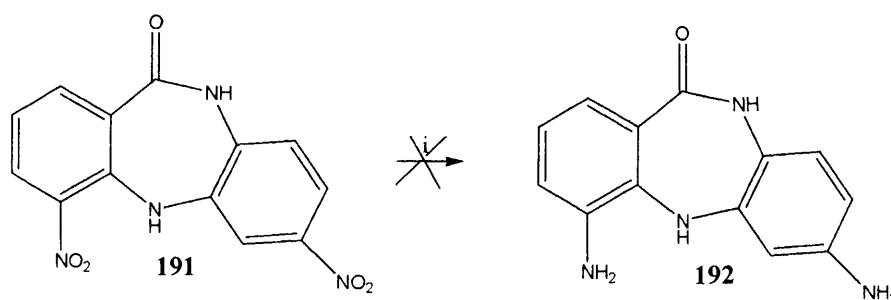


Figure 3.15 Showing NOE interactions between an aromatic singlet peak and amine, and also the amide and aromatic doublet.

However, due to unknown reasons the standard hydrogenation procedure was not successful for compound **191** (Scheme 3.11), so the chemistry of compound **191** was stopped at this stage.

Scheme 3.11



i) H₂, 10 % Pd/C, MeOH, 0 %.

As previously stated the electron-withdrawing substituents, carboxylic acid and fluorine, will reduce the nucleophilic properties of the *para*-positioned amino groups in the 1,2-phenylenediamine precursors in this reaction. The *meta*-positioned amino groups, being the stronger nucleophile, will react with the bromine. A mechanism (Figure 3.9), would result in the preparation of the lactam ring representing isomers **179**, **184**, **191**. In order to further explore this hypothesis, diaminobenzene with electron-donating groups like methoxy and hydroxy will be used in the coupling reaction. Consequently this would cause the *para*-positioned amine to become the stronger nucleophile. This time the amine would undergo substitution with the bromine and forming the alternative isomer, with the substituent group at the 9-position (Figure 3.16).

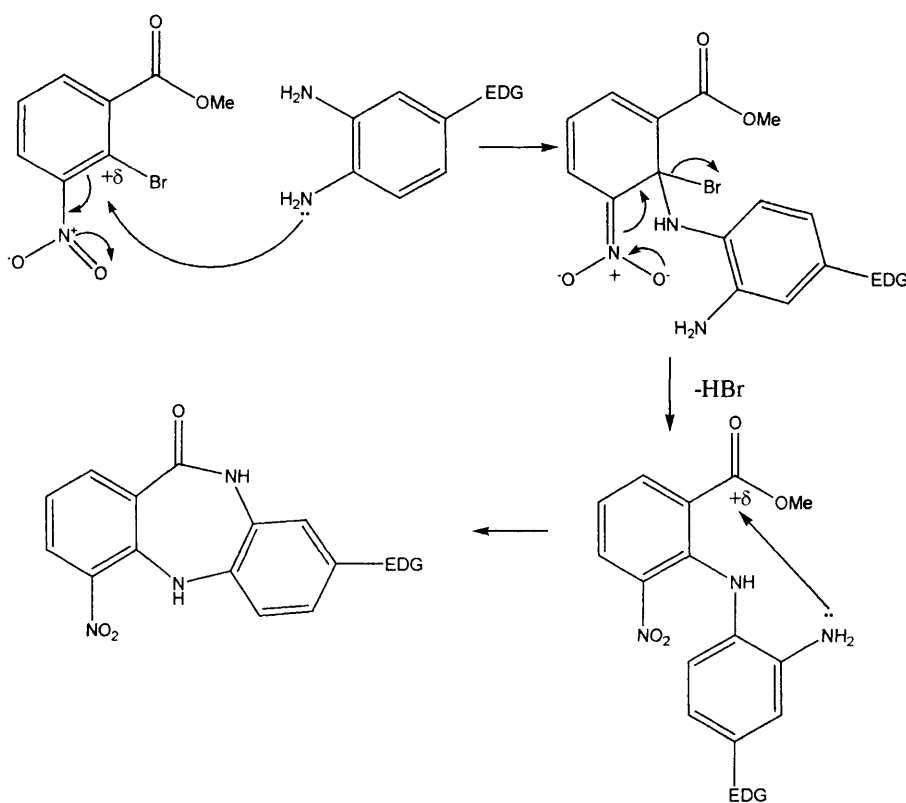
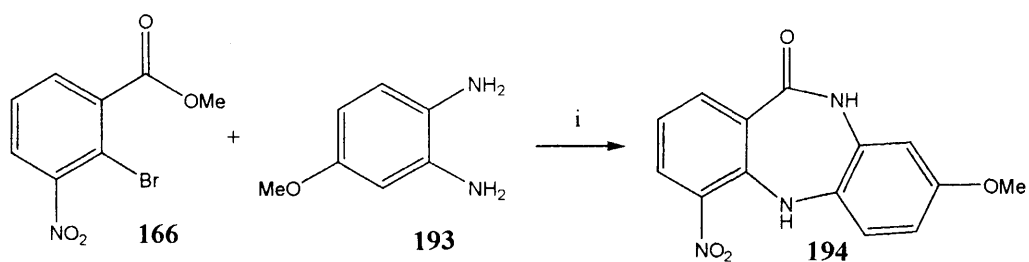


Figure 3.16 The mechanism for the coupling reaction with the substituent amine group at the 4-position.

The commercially available, compound **193** could yield a product with the methoxy group at the Y position (Figure 3.6) as desired.

Using the same method previously used, the mixture **166** and **193** was dissolved in DMA and heated for 10 h, yielding the desired product (Scheme 3.12).

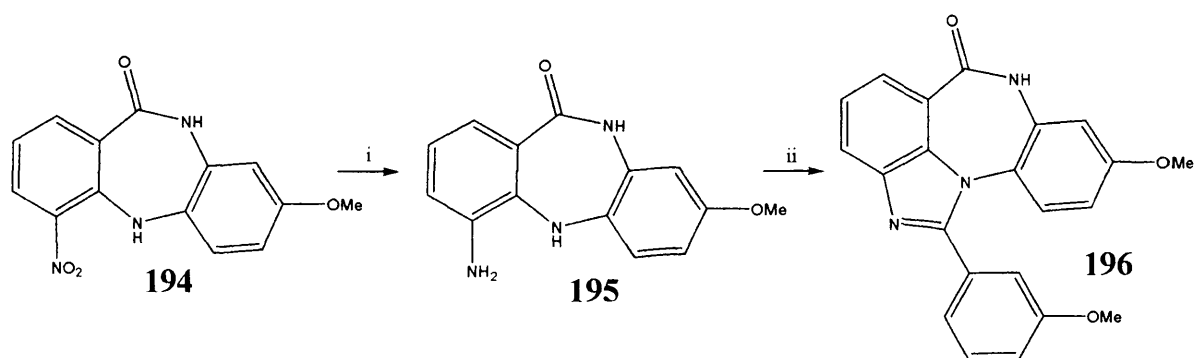
Scheme 3.12



i) DMA, 150 °C, 88 %.

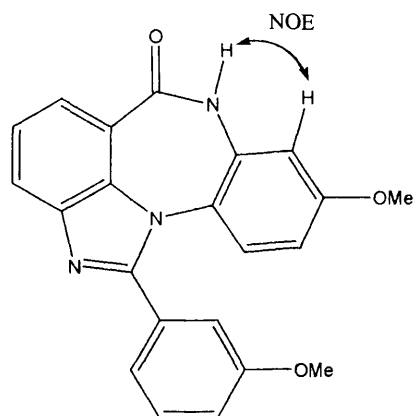
The nitro reduction was achieved by shaking under a hydrogen atmosphere for 3 h with a Pd catalyst. In order to synthesise compound **196**, the amine **195**, NaHSO₃ and 3-methoxybenzaldehyde (**169**) were heated in DMA forming the imidazole ring (Scheme 3.13).

Scheme 3.13



i) H₂, 10 % Pd/C, MeOH, 81%, ii) 3-methoxy benzaldehyde, NaHSO₃, DMA, 150 °C, 39%.

A ¹H NMR spectrum of this compound (**196**) showed the presence of a pure, single isomer. A NMR NOESY spectrum was also obtained, observing Nuclear Overhauser Effects (NOE) between the amide and the H-8 aromatic singlet not an aromatic doublet (Figure 3.17). This is only possible when the electron-donating group is located at the 9-position, thereby forming the compound **196**.



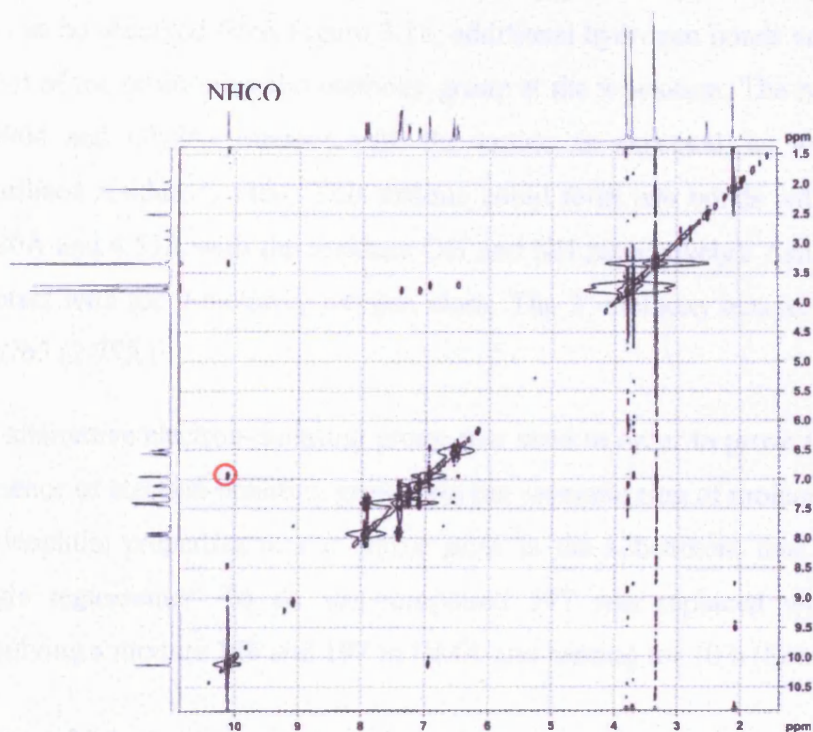


Figure 3.17 NOE interactions between the amide and aromatic singlet.

Additionally it was concluded through the use of molecular modelling, that there would be a satisfactory level of H-bonding to the PARP-1 active site (Figure 3.18).

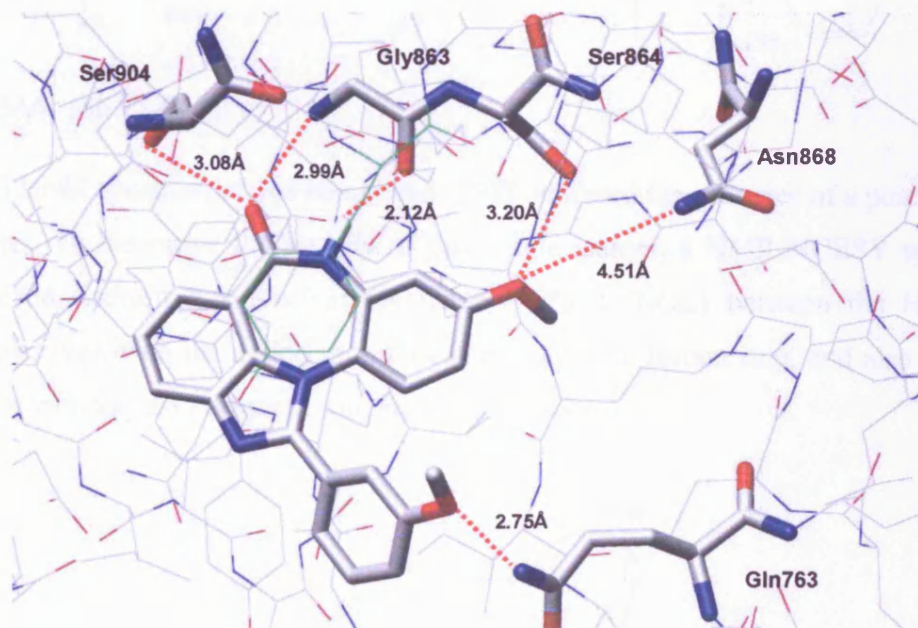
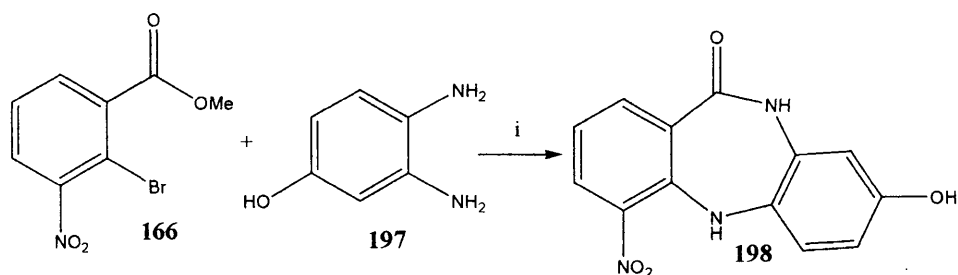


Figure 3.18 The potential H-bonds that could be formed by 196 with the methoxy substituent at 9-position.

As can be observed from Figure 3.18, additional hydrogen bonds could be generated as a result of the positioning the methoxy group at the 9-position. The two conserved residues Ser904 and Gly863 interact with the amide as expected, as well as the previously unutilised residue, Ser864. This residue could form two bonds with the methoxy region (3.20Å and 4.51Å with the residues OH and NH respectively). Asn868 (4.51Å) may also interact with the 9-methoxy oxygen atom. The 3'-methoxy acts as a H-bond acceptor to Gln763 (2.75Å).

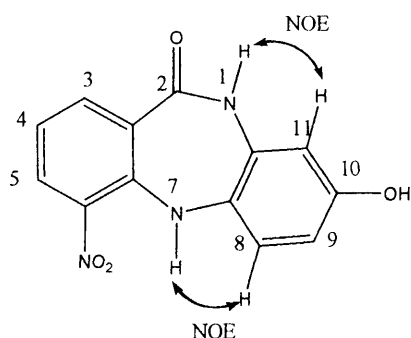
An alternative electron-donating group was used in order to prove the hypothesis that the presence of electron-donating groups on the aromatic ring of molecule would increase the nucleophilic properties of the amine *para* to the substituent thus creating the observed single regioisomer. To do so, compound **197** was replaced with **193**, followed by dissolving a mixture **166** and **197** in DMA and heating for 10 h (Scheme 3.14).

Scheme 3.14



i) DMA, 150 °C, 61 %.

A ^1H NMR spectrum of this compound (**198**) indicated the presence of a pure and a single isomer. To determine the identity of this single isomer, a NMR NOESY spectrum was obtained, indicating a Nuclear Overhauser Effect (NOE) between the H-8 aromatic doublet peak with the amino group located within the lactam ring, and also between the amide with the H-11 aromatic singlet (Figure 3.19).



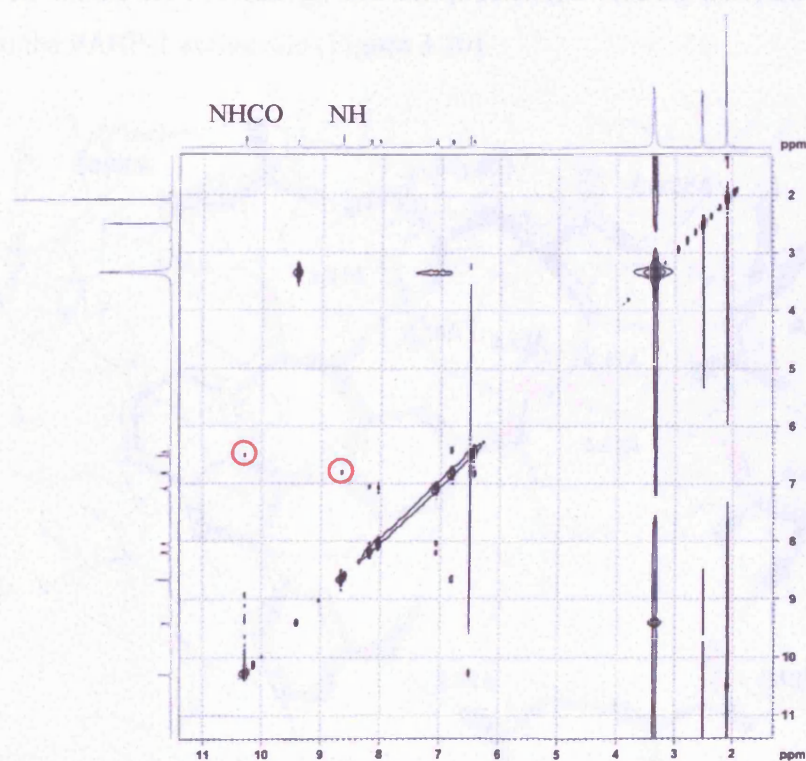
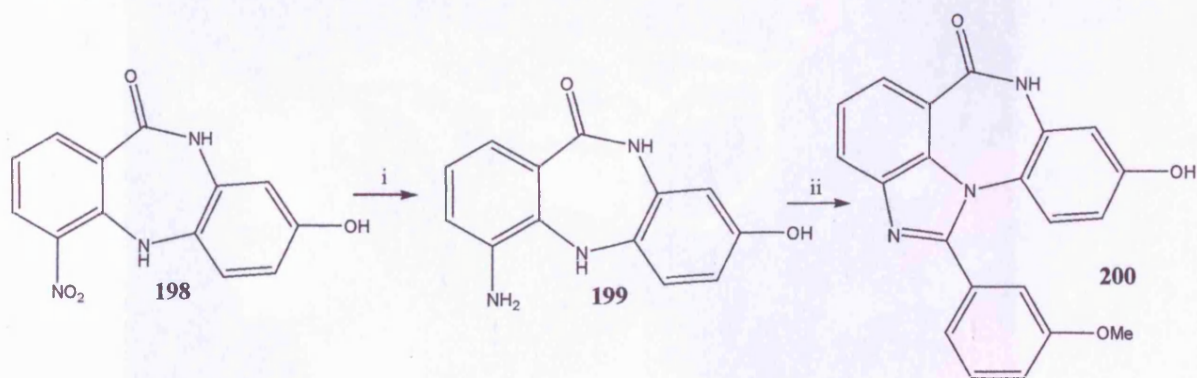


Figure 3.19 Showing interactions between an aromatic doublet and amide, and also between the amide and aromatic singlet.

The reduction of compound **198** was performed using 10% Pd/C in methanol in a pressure vessel under a hydrogen atmosphere for 3 h. This method produced compound **199** cleanly and in good yield. The amine **199**, NaHSO₃ and 3-methoxy-benzaldehyde (**169**) were heated in DMA forming the imidazole (Scheme 3.15).

Scheme 3.15



i) H₂, 10 % Pd/C, MeOH, 79 %, ii) 3-methoxy benzaldehyde, DMA, 150 °C, 20 %.

Using the molecular modelling, one can predict the binding potential of this compound (**200**) to the PARP-1 active site (Figure 3.20).

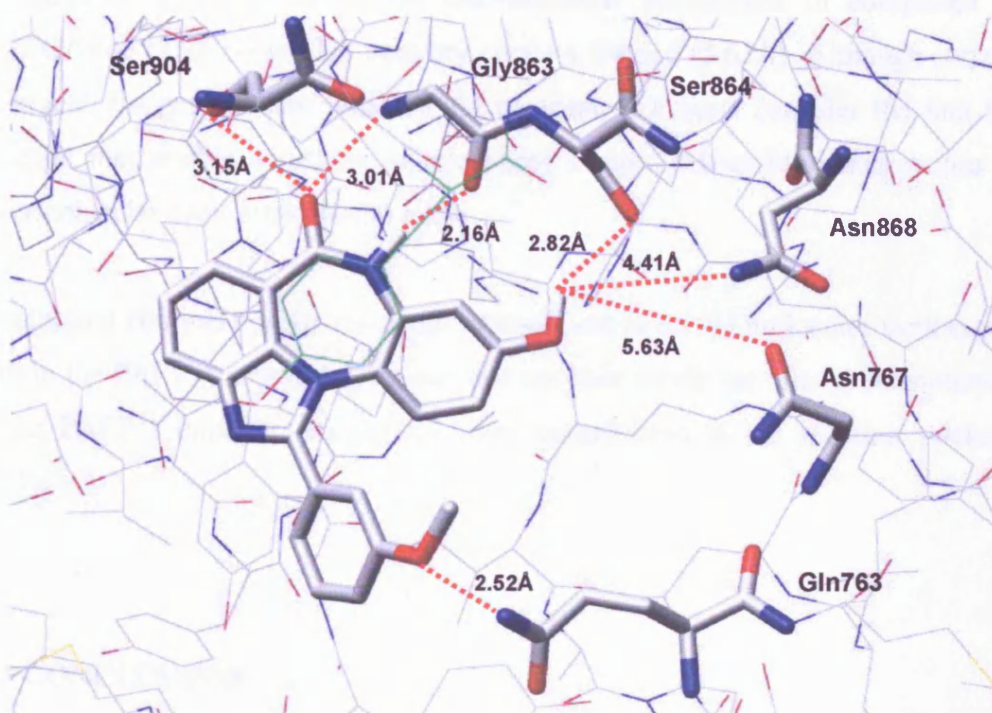


Figure 3.20 The potential intermolecular bonds that **200** may result with the hydroxy located at the 9-position.

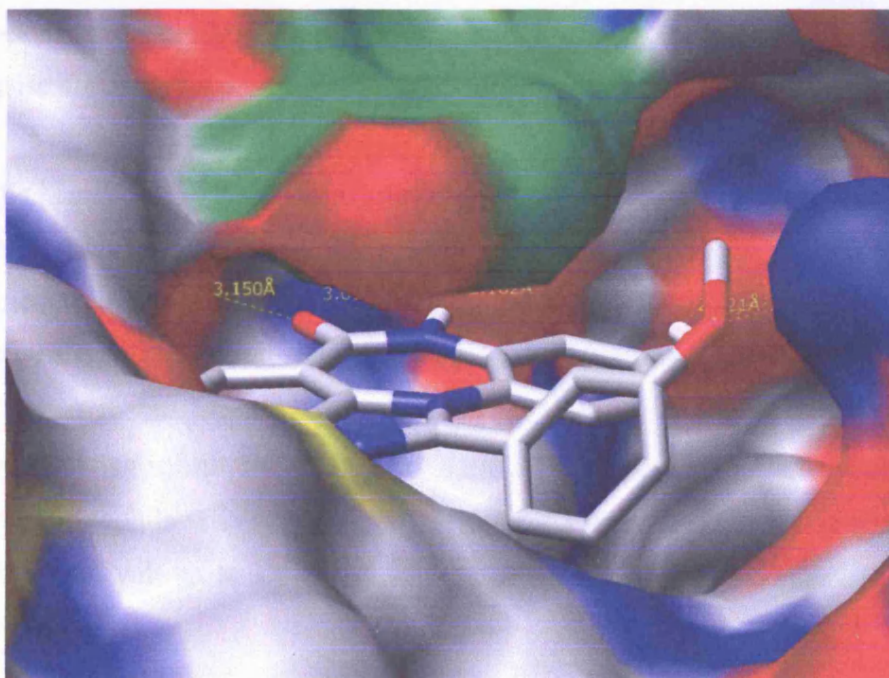


Figure 3.21 Compound **200** within the PARP-1 active site.

This model indicates that several potential hydrogen bonds could be produced as a result of the locating the hydroxy group at the 9-position (**200**). Besides the previously investigated residues involved in intermolecular interactions in compound **196**, the Asn767 side chain could also possibly create a H-bond (5.63Å). Although some of these distances are greater than what would be ideal, one must consider the fact that bond rotation may enable a residue to move into a more favourable position thus allowing intermolecular bond formation to occur.

Compound **200** was considered as an example out of all the molecules synthesised above within the PARP-1 active site, so one can see how nicely the phenyl substituent targeted in an PARP-1 inhibitor design has been accommodated in the spacious pocket (Figure 3.21).

3.3 CONCLUSIONS

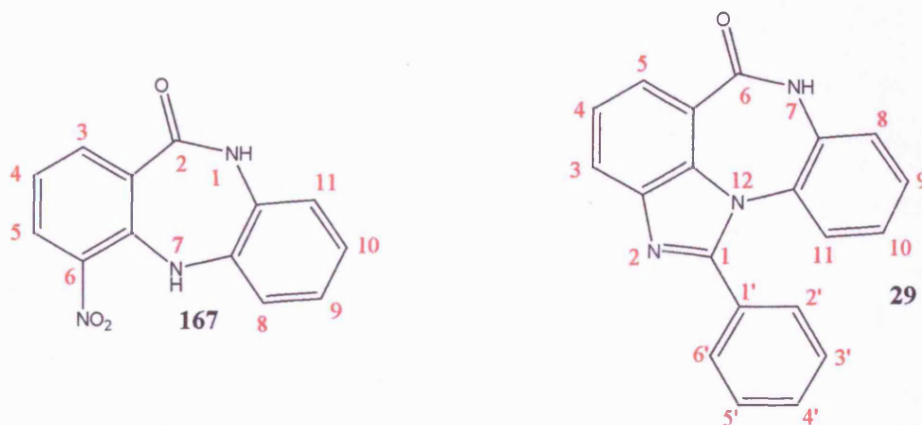
The methodology has been successfully developed for synthesis of the target benzo-derived pharmacophore and its derivatives. The integration of several modifications to the benzo-derived pharmacophore, using a range of substituent groups, is possible to synthesise novel compounds for the inhibition of PARP-1.

With the knowledge of the coupling mechanism (see the text), it is extremely possible that the resultant isomer can generally be predicted by determining the electronic nature of its substituent group. A substituent located on an aromatic ring can effect nucleophilic groups on the ring. Therefore, the presence of an electron-withdrawing group on the ring would reduce the nucleophilicity of the relevant amino group. Alternatively if there is an electron-donating substituent located on the ring, the relevant amine will develop into a stronger nucleophile. The superior nucleophile will react with the bromine initially, thus the substituent will go to an expected position and the resulted isomer can therefore be synthesised.

Benzo, imidazo and diazepin (as the base compound) common bond: **[b] [4,5,1-jk]**

Based on this system, pre-cyclized compounds were numbered clockwise around the diazepinon ring from N-being position 4.

Numbering of the fused rings for compound **167** as previously described and for compound **29** was as follow:



Therefore, the names were:

167, 6-Nitro-1*H*,7*H*-dibenzo[2,3-*b*][6,7-*f*]diazepin-2-one

29, 1-Phenylbenzo[*b*]imidazo[4,5,1-*jk*] [1,4]benzodiazepin-6(7*H*)-one

However, compounds **167** and **29** were trivially named 6-nitrodibenzodiazepin-2-one and 1-phenylbenzoimidazobenzodiazepin-6-one.

BIOLOGICAL RESULTS AND DISCUSSION

The biological activity of the molecules synthesised in this project were evaluated by a number of biological assays. The biological assays of the cell cycle related inhibitors were performed by the Tenovus Centre for Cancer Research in the Welsh School of Pharmacy, Cardiff University. The growth inhibition of these series of compounds were screened against two cancer cell lines. The poly(ADP-ribosyl)polymerase (PARP) assays were conducted by Kudos Pharmaceuticals Ltd, Cambridge, UK. Kudos also conducted assays against Chk2, a new protein kinase implicated in cell cycle control.

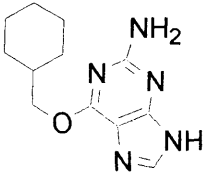
4.1 GROWTH INHIBITION ASSAY

Growth inhibition assays were carried out against the MCF-7 human breast cancer cell line, as well as the A549 human small lung cancer cell line. MCF-7 is derived from epithelial cells in breast carcinoma and is widely used for testing of this nature and were grown in Phenol Red free media. There are no major aberrations apparent in the cell line, and under appropriate conditions they grow well in culture (Solute *et al.*, 1973). A549, largely studied in recent years, is a cell line derived from type II alveolar epithelial cells in lung carcinoma, and is similarly easy to work with in culture (Lieber *et al.*, 1976).

Results are expressed as 50 % growth inhibition (GI_{50}) values. GI_{50} is the concentration required to inhibit 50 % of cell growth compared to an untreated control. Results with a GI_{50} value in excess of 100 μM but showing mild growth inhibition are quoted as % inhibition at 100 μM . Compounds that showed no growth inhibition (0 %) at 100 μM were considered inactive.

4.1.1 Reference compound

Table 4.1 NU2058 as a known cell cycle inhibitor. ^a NT: Not Tested, ^b ClogP calculated using Chem Draw Ultra.

Compound Number	Structure	GI_{50} (MCF-7) μM	GI_{50} (A549) μM	ClogP ^b
O6-(cyclohexylmethyl) 2-aminopurine 86		72	NT ^a	3.5

O6-(Cyclohexylmethyl)-2-aminopurine (**86**, NU2058) is a known inhibitor with an IC_{50} value of 17 μM against CDK2/cyclin A (Gibson *et al.*, 2002), that has been synthesised in our laboratory and assayed under identical conditions to compare the synthesised compounds' potency to this known inhibitor (Table 4.1).

4.1.2 Benzodiazepin-2-one analogues

Table 4.2 Growth inhibition results, ^a NA: Not Active, ^b GI₅₀ assayed on MCF-7 cell line, ^c GI₅₀ assayed on A549 cell line, ^d precipitation observed at 100 μM.

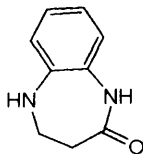
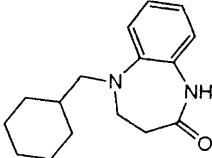
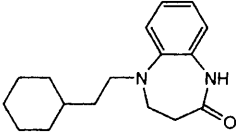
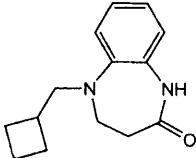
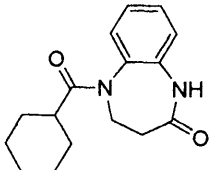
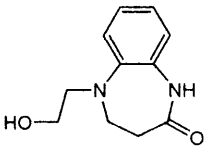
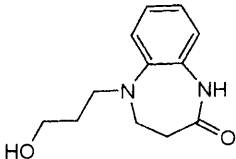
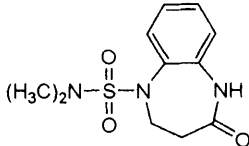
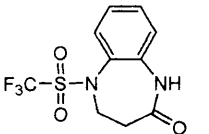
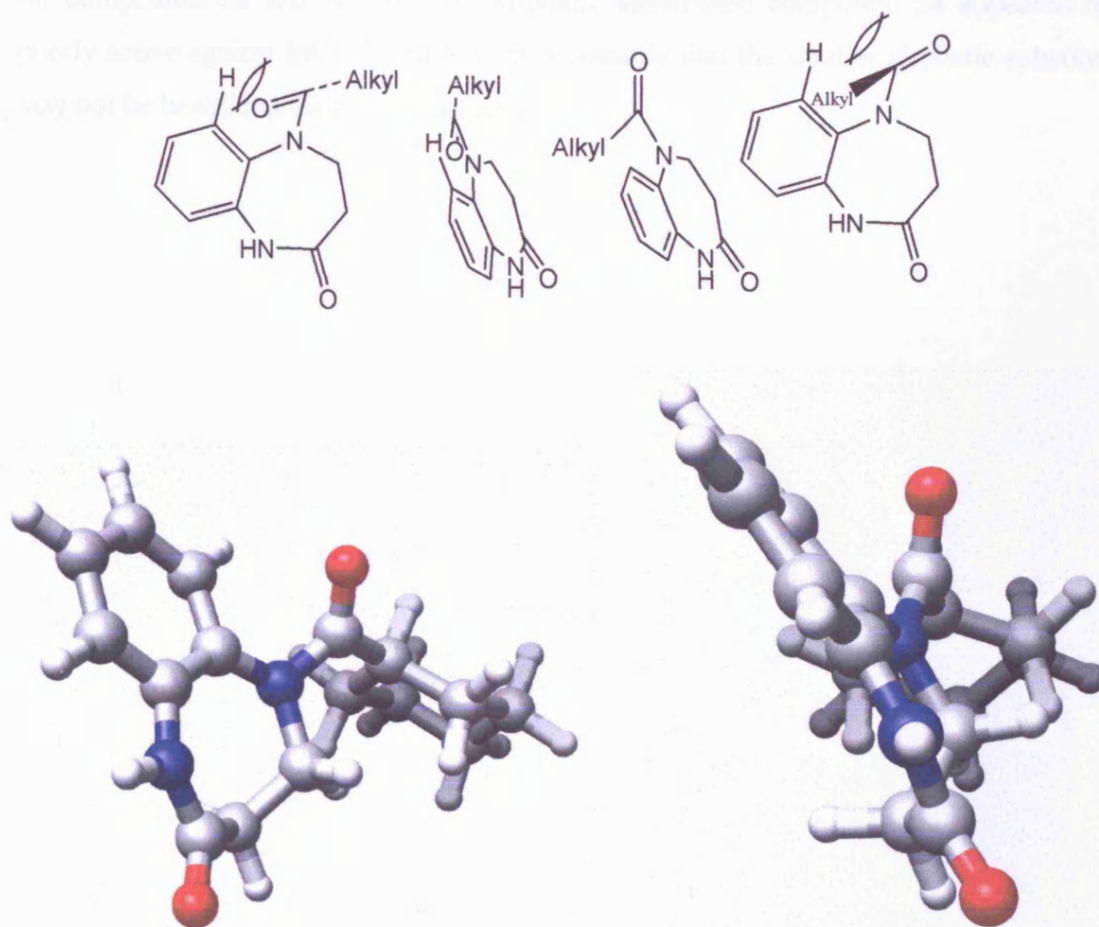
Compound Number	Structure	GI ₅₀ /% inhibition (μM)	ClogP
26		>100 ^b 16 % inhibition at 100 μM	0.6
52		63 ^b	4.0
53		57 ^b	4.5
54		>100 33 % inhibition at 100 μM	2.9
55		NA ^{a, b}	2.4
62		NA ^a	0.5
63		NA ^{a, c}	0.8
129		>100 12 % inhibition at 100 μM ^c	0.4
132		>100 12 % inhibition at 100 μM ^c	1.4

Table 4.2 shows the growth inhibition results obtained for N-5 substituted benzodiazepin-2-one analogues against MCF-7 and A549 cell lines.

The lead compound benzodiazepin-2-one (**26**, CFU58) gave very slight activity; this is expected since we propose that extension from N-5 is needed for biological activity.

Of the compounds tested in this series **55**, **62**, **63**, **129** and **132** were inactive or poorly active in growth inhibition assays. Either they are not CDK substrates or they do not cross the cell membrane. For compound **55**, the relatively bulky carbonyl group makes a large difference to activity, especially when compared with compound **52**. Molecular modelling shows the extra oxygen group, forces the cyclohexyl group out of the plane of the molecule, a conformation that may not be acceptable for active site binding. An additional consequence is that two isomeric forms of compound **55** may be possible.



A similar argument may also apply to compounds **129** and **132**, the bulky sulfonyl groups connected to N-5 may force the compounds into biologically inactive conformations.

Compounds **129** and **132** were also poorly active against the A549 cell line, due possibly to the high polarity of the compounds (ClogP = 0.4 and 1.4 respectively), which may not cross the cell membrane to reach an intracellular target.

Compounds **52** and **53** are the most active compounds of this series that have been identified to date, which were expected due to their substituted N-5 position. These have extensions necessary to fill the cleft of the active site. They have similar cellular activity to the known CDK inhibitor NU2058 (**86**), although this compound has the ability to form an extra hydrogen bond to the active site of the enzyme may improve its binding to CDK2. In common with the purine derivative, it appears that hydrophobic extensions into the active site cleft are beneficial to biological activity. Compound **53** is slightly more active than **52** suggesting that a longer extension may be better. Despite the activity seen for compounds **52** and **53**, the N-5 aliphatic substituted compound **54** appeared to be poorly active against MCF-7 cell line. It is possible that the smaller aliphatic substituents may not be beneficial for biological activity.

4.1.3 4-Aminodibenzodiazepin-2-one analogues

Table 4.3. Growth inhibition results, ^a NA: Not Active, ^b GI₅₀ assayed on A549 cell line

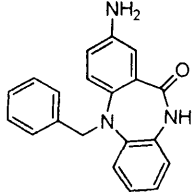
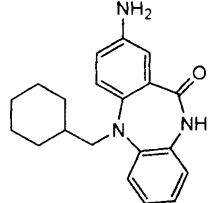
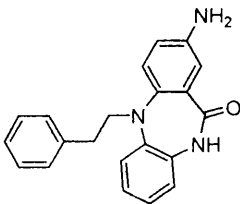
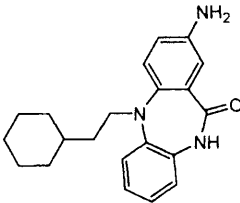
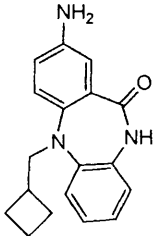
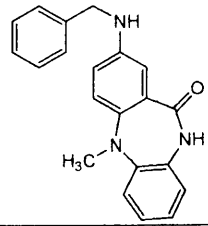
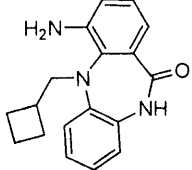
Compound Number	Structure	GI ₅₀ / % inhibition ^b (μM)	ClogP
97		NA ^a	3.7
98		91	4.6
99		83	4.1
100		49	5.1
103		61	3.5
104		12	4.2
201		61	3.5

Table 4.3 shows the growth inhibition results obtained for N-7 substituted dibenzodiazepin-2-one analogues against A549 cell line. All these compounds (except for **97**) show a generally better growth inhibition compared to the benzodiazepin-2-one analogues with calculated logP values being generally higher favouring cell permeation. Increasing the lipophilicity of the compounds by addition of an aromatic ring proves to be efficient as an increase in activity is observed.

Of the six compounds tested, **98** and **99** displayed weak activity against A549 cell line. Interestingly compound **97** was completely inactive and **100** and **103** showed moderate activity against this cell line. Compound **100** was the best of these two, suggesting that a bulky and lipophilic group is an important feature for activity. It was better than **99** favouring a cycloalkane extension or increased lipophilicity. However, despite possessing ClogPs differing by nearly 1.5 units for compound **100** and **104** (about fifteen-fold difference) have more similar GI₅₀ values. This indicates that lipophilicity, above a point, is less important for determining activity.

Compound **104** of all these compounds was the most active (4-fold more active than the nearest compound) against the A549 cell line. This compound was designed, based on the structure of the olomoucine, to observe whether improved activity could be obtained by inserting a benzyl group at the 4-NH₂ position. Olomoucine exhibited greater inhibitory potency due to the presence of a bulky benzyl group at a similar position in its structure. This substituent extends towards solvent, at the mouth of the CDK active site where lipophilic region is present (see Chapter 1). It may be that similar lipophilic contact is observed with compound **104**, as indicated by modelling. It is noteworthy that the ClogP for this compound is still smaller than **100** showing high lipophilicity is not essential for activity.

Finally isomeric compounds **103** and **201** were found to have the same potency indicating that the position of the amino group may not be important for hydrogen bonding and so does not effect in biological activity.

4.1.4 7-Aminobenzodiazepin-5-one analogues

Table 4.4 Growth inhibition results, ^a NA: Not Active, ^b GI₅₀ assayed on A549 cell line.

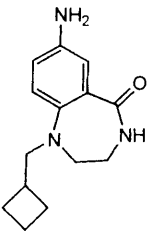
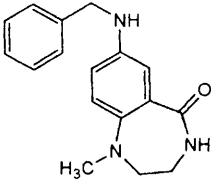
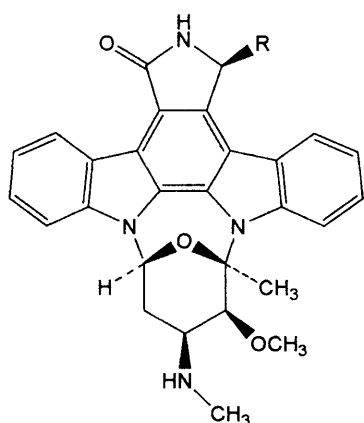
Compound Number	Structure	GI ₅₀ /% inhibition ^b (μM)	ClogP
119		>100 22 % inhibition at 100 μM	1.3
120		NA ^a	2.0

Table 4.4 shows the growth inhibition results obtained for 7-amino-benzodiazepin-5-one analogues against A549 cell line. Compound **119** was poorly active (22 % inhibition at 100 μM) and **120** was inactive. Compound **119** with ClogP = 1.3 seems to be too polar to cross the cell membrane and reach the target. Compound **119** might then interact with proteins situated on the outer surface of the cell producing the slight activity at higher concentrations.

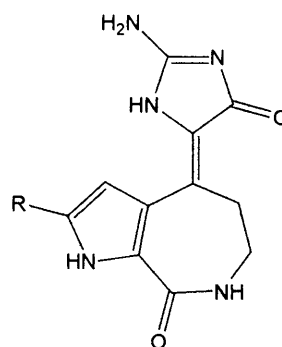
Interestingly, the lack of the second lactam-fused aromatic ring in compound **120** and allowing the compound a better accommodation in the CDK2 active site as suggested by modelling studies resulted in an inactive compound, rather than the predicted increase in activity. Therefore, comparing the biological results of compounds **104** and **120** indicates that the aromatic ring is causing the change in activity between **104** and **120** that provides such a crucial role in the binding of compound **104** to its biological target.

4.2 CHECKPOINT KINASE 2 (CHK2) ENZYME ASSAYS

Some of the compounds which had been synthesised with the objective of inhibiting the cell cycle, were assayed against the Chk2 protein introduced in Chapter 1 as an alternative possible target. Assays were performed according to in-house methods at Kudos Pharmaceuticals Ltd, Cambridge, UK. As a number of CDK2 inhibitors have been shown to be also active against this enzyme, including debromohymenialdisine (**15**) (Tenzer and Pruschy, 2003). The natural product debromohymenialdisine is known to inhibit a few kinases in particular Chk1 and Chk2 enzymes.



1, R=H, Staurosporine
2, R=OH, UCN-01



15, R=H, DBH

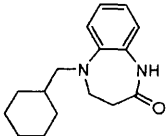
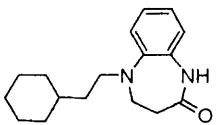
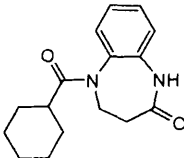
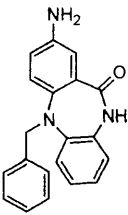
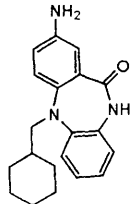
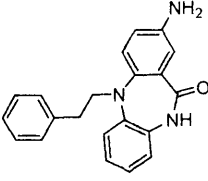
Table 4.5 Inhibition against Chk family enzymes (Tenzer and Pruschy, 2003).

Compound	IC ₅₀ Chk1	IC ₅₀ Chk2
Staurosporine (1)	8 nM	NA
UCN-01 (2)	87-25 nM	1.0 μM
Debromohymenialdisine (15)	3 μM	3.5 μM

However, all the synthesised compounds that were assayed were found to be inactive as Chk2 inhibitors, with IC₅₀ values in excess of 100 μM (Table 4.6). The activity of the DBH (**15**) shows that the aminoimidazolidinone moiety of DBH would be the major feature that plays an important role in inhibition activity of the molecule against the Chk2 enzyme. Extended molecules tested are very lipophilic in contrast to the polar

aminoimidazolidinone of **15**, suggesting that a polar extension would promote some affinity with Chk2.

Table 4.6 Compounds tested against Chk2.

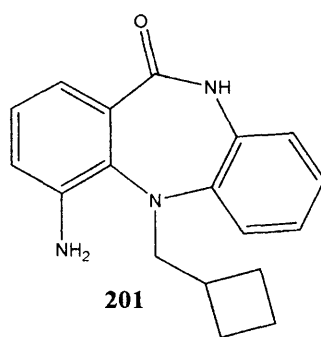
Compound Number	Structure	IC ₅₀	ClogP
52		NA ^a	3.7
53		NA ^a	4.6
55		NA ^a	4.1
97		NA ^a	5.1
98		NA ^a	3.5
99		NA ^a	4.2

4.3 PARP INHIBITION ASSAYS

Assays were carried out against the PARP-1 enzyme and the HeLaB cell line. The HeLaB cell line is derived from a cervical cancer cell and is widely used as they are easy to work with and easy to grow in the culture.

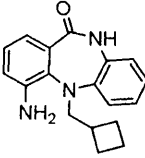
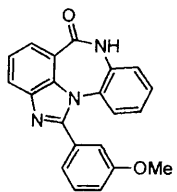
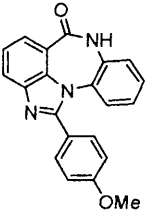

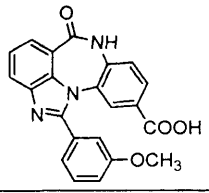
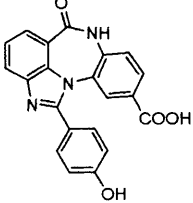
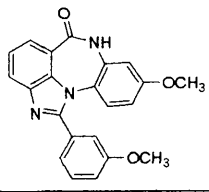
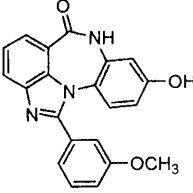
The results were quoted as 50 % Inhibition Coefficient (IC_{50}) of PARP-1 catalytic activity compared to a control and 50 % Potentiation Factor (PF_{50}) of a cytotoxic agent against HeLaB cells. They were determined for every molecule synthesised. IC_{50} is the concentration of inhibitor required to reduce the catalytic activity of the purified PARP-1 enzyme by 50 %, and results with a IC_{50} value greater than 10 μ M were considered to be inactive. PF_{50} is the ratio of the 50 % growth inhibition values of HeLaB cells exposed to the alkylating agent MMS (Methyl Methane Sulfonate) with and without 200 nM of the PARP-1 inhibitor.

6-Amino-7-cyclobutylmethylidibenzodiazepine-2-one (**201**) was used as a control for biological evaluations.

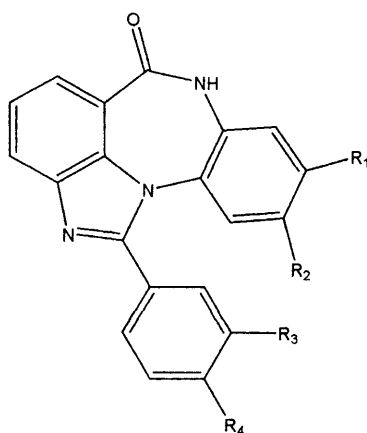


The inhibitors chosen, with their PARP inhibitory IC_{50} values, where available, are shown in Table 4.7.

Table 4.7 PARP-1 inhibitory IC₅₀ values. ^a IC₅₀ assayed on PARP-1.

CFU/Compound	Structure	IC ₅₀ (nM) ^a	PF ₅₀
201		>10,000	0.84
171		225	0.86
172		260	Cellular (HeLaB) toxicity observed in PF ₅₀ control: 30 % cell survival at 500 nM
182		246	0.86
186		114	0.83
188		130	0.81
196		505	1.46
200		236	0.80

Of the compounds tested the un-cyclised compound **201** was inactive ($IC_{50} > 10 \mu M$) against PARP-1, as expected. The reason for that was the presence of the uncyclized free NH_2 -group on the molecule. However, cyclizing the compound to the imidazole derivatives gave a significant increase in activity (**171**, **172**, $IC_{50} = 225 \text{ nM}$, 260 nM , respectively). These molecules with fewer substituent groups for intermolecular binding, showed an inhibitory effect within the nanomolar range which was very encouraging. This implied that more substituted compounds containing an additional substituent at the 9- or 10-position, could potentially be even more efficacious. Therefore, a series of 1-phenylbenzodiazepine-6-ones were synthesised to enable the SAR for substitutions on the benzene ring to be explored. A variety of substituents, with different electronic properties, were introduced at the 9- and 10-positions (**182**, **186**, **188**, **196** and **200**). Inhibition data showed that PARP tolerates a variety of 9- and 10-substituents on the benzene ring and does not distinguish significantly between electronically differing groups. Also the position of the 1-phenyl substituent (3' versus 4') was relatively unimportant for these examples. However, 1-(3'-methoxyphenyl)benzimidazo-10-carboxybenzodiazepine-6-one (**186**, $IC_{50} = 114 \text{ nM}$) was the most active compound among these inhibitors, which was also predictable from its molecular model (Figure 3.12). Comparison of 1-(3'-methoxyphenyl)benzimidazo-10-fluorobenzodiazepine-6-one (**182**, $IC_{50} = 246 \text{ nM}$) with compound **186** showed that compound **182** was about 2-fold less potent than **186**, indicating that there is no favourable hydrogen-bonding interaction between the protein and the 10-fluoro group. The reasoning behind it, was the small size of fluorine substituent, which is too far from the H-bond donating residues in the active site (Figure 3.10). 1-(3'-Methoxyphenyl)benzimidazo-10-hydroxybenzodiazepine-6-one (**200**) and **182** were equipotent ($IC_{50} = 236$ and 246 nM , respectively). However, surprisingly there is a decrease in activity for 1-(3'-methoxyphenyl)benzimidazo-9-methoxybenzodiazepine-6-one (**196**) and it was about 2-fold less potent than **182** ($IC_{50} = 505$, 246 nM , respectively). It is due possibly to the repulsion force created between the relatively bulky methoxy group and active site residues close to it. This implies that small electron-withdrawing groups at the 10-position are more important than bulky H-bond acceptors for intermolecular interactions with the enzyme active site.



The structure activity relationship studies between the synthesised analogues indicates that the presence of the electron-withdrawing groups at R₂ on the aromatic ring was quite important for the biological activity. However, compound **182** (R₂ = F, R₃ = OMe) was twice less potent than the other compounds with electron-withdrawing groups located on their ring at the R₂ position, suggesting that the size and position of the substituent is important for activity. The roughly similar inhibitory activity of compounds **171** and **172** (IC₅₀ = 225 and 260 nM) showed that the position of the substituent (3' versus 4') was relatively unimportant for the PARP-1 biological activity.

The potentiation factor can predict if a PARP-1 inhibitor could potentiate a cytotoxic agent; the clinical rationale for PARP-1 inhibition. The results suggest that there is not a correlation between IC₅₀ and PF₅₀. The best inhibitor identified (**186**) had a PF₅₀ value of 0.83, suggesting no potentiation of MMS induced cytotoxicity in the HeLaB cells. However, the worst inhibitor, compound **196** exhibited the best potentiation, PF₅₀ = 1.46. Similar observations have been seen in other studies. Modest potentiation has been observed for one benzoimidazolebenzodiazepinone PARP-1 inhibitor (**196**), although further testing against other cell lines and various cytotoxic drugs or radiation could yield better results.

4.4 BIOLOGICAL CONCLUSIONS

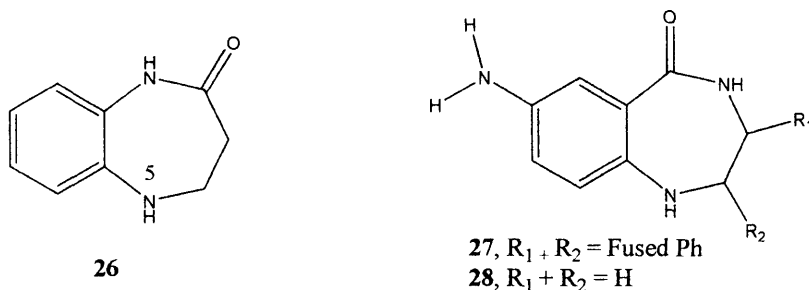
In conclusion, to investigate the seven-membered lactam pharmacophore, a series of compounds have been synthesised as cell cycle inhibitors targeted at CDK2 with a moderate response *in vitro* towards MCF-7 and A549 cell lines. Preliminary biological results suggested that dibenzo- or benzodiazepinones may bind in the ATP binding pocket of CDKs, supporting the modelling studies performed, and providing further evidence for the potential of these series as cell cycle inhibitors. Although we were unable to introduce a variety of groups at the N-1 position of 7-amino-benzodiazepin-5-one (**28**), we did manage to synthesise a small series, and establish SARs between these compounds and benzodiazepin-2-one and 4-amino-benzodiazepin-2-one analogues. The compound showing the best result is compound **104**, which possesses a very good GI₅₀ value.

A related series of the compounds containing the desired pharmacophore have been synthesised for PARP inhibition. Assays show good *in vitro* catalytic inhibition towards PARP-1. There were modest differences in IC₅₀ values for this series of compounds all showed very good activity (ranging from 114-505 nM), but the compound with the best results is compound **186**, which possesses a low IC₅₀ of 114 nM. Reasonable potentiation of a cytotoxic drug achieved by compound **196** (PF₅₀ = 1.46) suggesting a clinical role for this class of compounds in cancer therapy.

The Chk2 enzyme inhibition assays showed no activity for any of the compounds screened (all IC₅₀>100 µM). This result is surprising since other compounds containing the lactam pharmacophore under investigation have been reported to inhibit Chk2 and the same assay identified kenpaullone (**13**) as a potent Chk2 inhibitor (IC₅₀ = 0.44 µM). This suggests very precise requirements for Chk2 binding that are not achieved in the compounds assayed.

4.5 OVERALL CONCLUSIONS

The synthesis of benzodiazepin-2-one (**26**), 4-amino-dibenzodiazepin-2-one (**27**) and 7-amino-benzodiazepin-5-one (**28**) was successfully achieved, and analogues were made from these lead molecules providing the structure activity relationship studies presented in this thesis.



The comparative structure activity relationship between these three series has shown a correlation between them, with slightly higher activity against the MCF-7 and A549 cell line being observed for the 4-amino-dibenzodiazepin-2-one analogues (**27**) than the other two derivatives indicating that the presence of the second fused aromatic ring was quite important for the biological activity. Unexpectedly, synthesis of aliphatic derivatives of the lead compound **28** was more difficult than the aromatic analogues, due possibly to the difficulty of handling these compounds in the laboratory.

Extensions from the ring amine was achieved with aliphatic and aromatic derivatives, although only two analogues were made for 7-amino-benzodiazepin-5-one (**28**) series. Analogues of benzodiazepin-2-one (**26**) containing bulky aliphatic substituents at the N-5 position (**52** and **53**) showed reasonable activity, with only a slight increase in potency being observed compared to 4-amino-dibenzodiazepin-2-one (**27**) analogues.

The amino group of the **27** and **28** scaffolds may hold the potential for the solubility of these series of compounds.

Some of the analogues in these three series of scaffolds were found to be less active or completely inactive against the cancer cell lines. It is believed that this decrease in activity against the cell lines could be due either to the misalignment of the different substituents or not binding to the intended biological target, a CDK. Steric effects may also play a role

in the loss of inhibitory activity. The introduction of a benzyl group at the 4-amino position of the scaffold has produced the most active compound (**104**, $GI_{50} = 12 \mu\text{M}$) in 4-amino-dibenzodiazepin-2-one series to date. However, molecular modelling suggested that the aliphatic compound **120** might be a more suitable fit in the active site of the biological target CDK2.

To conclude, small molecules containing the 7-membered lactam ring pharmacophore displaying good tumour growth inhibition have been synthesised. Other assays on different cell lines would be interesting to investigate. Further experiments are required to evaluate the selectivity of these novel antiproliferative compounds and to see if any other enzymes are targeted by the compounds assayed. The Chk2 enzyme inhibition assay results were all negative, indicating that the compounds tested do not bind to Chk2.

As a third aim of this project, some novel PARP-1 inhibitors were also synthesised enabling the structure activity relationship studies for the analogues made in this project. The compounds synthesised contained a range of substituents allowing structure activity relationships to be established. Analogues with electron-donating groups on their ring were found to be less active against PARP-1, due possibly to the lack of appropriate residue in the vicinity of the molecule in the active site. Meanwhile, the PF_{50} results suggested that there was no correlation between IC_{50} and PF_{50} as the best inhibitor identified (**186**) had the lowest PF_{50} value of 0.83, so further biological investigations are still needed. The dibenzodiazepinone compounds are an interesting pharmacophore for PARP-1 inhibition and the strategy of introducing additional aromatic substituents to promote active site interactions has been beneficial. Although poorer potentiation results were obtained, further experimentation could overcome this.

In accordance a series of nanomolar potent, novel PARP-1 inhibitors containing the seven-membered lactam pharmacophore have been successfully synthesised and analyzed.

Regarding the biological results provided one must conclude that this direction of research remains a significant area for future investigation and there is a great deal of development that could be undertaken to facilitate the progression of the drugs physiological properties.

EXPERIMENTAL PROCEDURES

5.1 SPECTRAL CHARACTERIZATION

5.1.1 NMR Spectroscopy

Proton and carbon-13 nuclear magnetic resonance spectra were recorded on a Bruker Avance DPX300 spectrometer with operating frequencies of 300 MHz and 75 MHz respectively or a Bruker Avance 500 with operating frequencies of 500 MHz and 125 MHz respectively. All ^{13}C NMR spectra were proton decoupled and all proton and carbon nuclear magnetic resonance (^1H NMR and ^{13}C NMR) spectra were obtained in deuterated dimethyl sulphoxide (d_6 -DMSO) except where indicated. Chemical shifts were reported as δ values (parts per million). The following abbreviations are used to describe peak patterns in proton spectra when appropriate: br = broad, s= singlet, d= doublet, t= triplet, q= quartet, m= multiplet; and combinations thereof, e.g. dd (double doublet). Coupling constants (J) are given in hertz (Hz).

5.1.2 Thin Layer Chromatography

Thin layer chromatography (TLC) was performed on commercially available Merck Kieselgel 60F254 plates, using a variety of mobile phases and separated components were visualized using short (254 nm) and long (365 nm) wave ultraviolet light, or by treatment with iodine, vanillin [(60 g Vanillin, 1000 mL 95 % ethanol (aq), 10 mL H₂SO₄ (conc.))] or permanganate dip [(3 g KMnO₄, 20 g K₂CO₃, 5 mL 5 % NaOH (aq), 300 mL water)].

5.1.3 Column Chromatography

Column chromatography was carried out under medium pressure using a hand pump and silica gel 60. Mixtures to be separated were absorbed onto a small amount of silica before loading onto the column or applied as a concentrated solution in the same eluent. Fractions containing the product were identified by TLC and were pooled, and the solvent was removed under reduced pressure.

5.1.4 Mass Spectroscopy

Low resolution electrospray (LRMS) mass spectra were run on a VG platform II Fisons instrument (Fisons, Altrincham, UK) (atmospheric pressure ionisation) or a Bruker microtof in either positive or negative mode using a mobile phase of methanol. High resolution mass spectrometry (HRMS) was performed by the EPSRC National Mass Spectrometry Service Centre, University of Wales Swansea, using electron impact or chemical ionization (EI/CI).

5.1.5 Infrared Spectroscopy

Infrared spectra were recorded on a Perkin Elmer 1600 series FTIR spectrometer as a solid mixture with KBr via a diffuse reflectance accessory.

5.1.6 Melting Point

Melting points (mp) were determined on an electric variable heater (Gallenkamp) and were not corrected.

5.1.7 Chemicals and Solvents

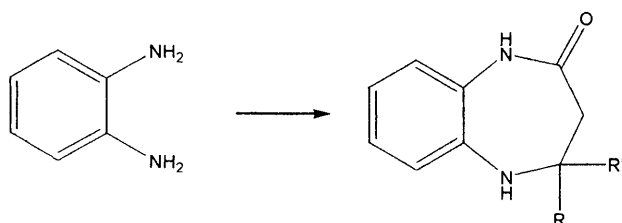
All chemicals used were purchased from Aldrich Chemical Company, Lancaster Synthesis Ltd. or Acros organics (Fisher Scientific Ltd.) and used without further purification. Distilled solvents were stored over 4 Å molecular sieves under an inert gas atmosphere. Petrol refers to petroleum ether 60-80 and sodium hydride refers to 60 % NaH in mineral oil.

5.1.8 Molecular modelling methodology

Ligands were drawn in ChemDraw Ultra (version 7.0.1, CambridgeSoft Corporation) and minimized using the MM2 force field in Chem3D Pro (version 7.0.0, Cambridge Corporation). The structure was then uploaded into Chimera (UCSF, beta version 1) where it was manually superimposed onto the PDB file of a known inhibitor within the hidden protein, thus enabling the compound to be observed in a realistic position within the active site. The inhibitor was removed and the enzyme revealed, allowing details such as H-bond length with the prepared ligand to be calculated. Images used within the report have been generated through Chimera.

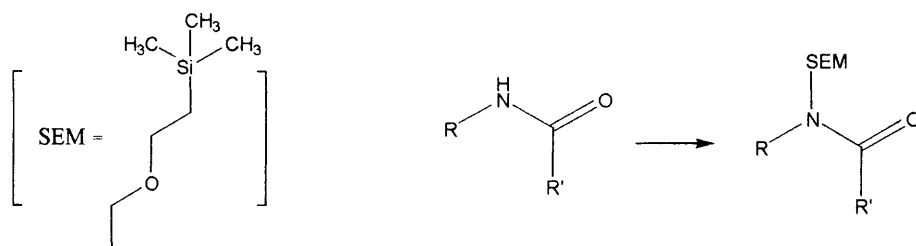
5.2 GENERAL PROCEDURES

Method A – Cyclization I

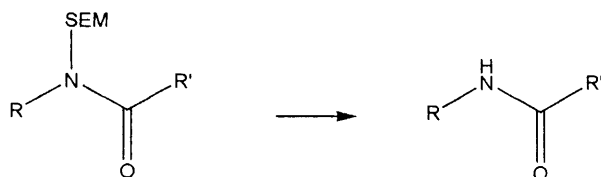


A mixture of 1,2-phenylenediamine, 60 % aqueous acrylic acid or its derivatives, and concentrated hydrochloric acid (0.75 mL) were heated at 100 °C for several hours, cooled, basified with aqueous ammonia to pH = 14, then brine was added. The mixture was extracted with ethyl acetate, followed by drying of the organic fraction over magnesium sulphate (MgSO₄), filtration and evaporation, to recover the product.

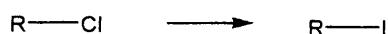
Method B – Amide protection



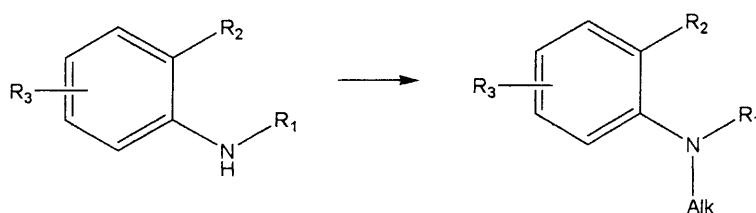
A solution of the amide in DMF (approx. 3mL) under nitrogen was cooled in an ice bath to 0 °C, sodium hydride (1.1 equiv.) was added over a period of 10 min and the reaction was stirred for 1h prior to the addition of 2-(trimethylsilyl)ethoxymethyl chloride (SEM-Cl). The resultant mixture was then warmed to room temperature and stirred overnight. The contents of the flask were concentrated by evaporation, followed by the dropwise addition of water to destroy the sodium hydride. The mixture was extracted with ethyl acetate and the combined organic layers were washed with water, dried over MgSO₄, filtered and evaporated under reduced pressure to recover the product.

Method C – SEM deprotection

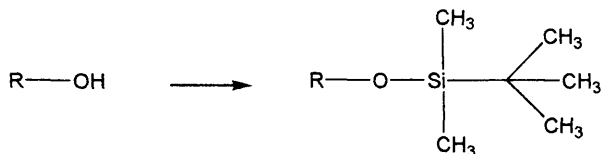
A solution of SEM protected compound in 1M tetrabutylammonium fluoride/THF solution (approx. 5mL) was refluxed for several hours, followed by evaporation to dryness. Water was added to the mixture, extracted with ethyl acetate, dried over MgSO_4 , filtered and concentrated under reduced pressure to recover the product.

Method D – Finklestein reaction

To a solution of alkyl or aryl bromide in acetone was added sodium iodide, after which time the slurry was refluxed for several hours. The acetone was removed by evaporation, followed by addition of water to dissolve the inorganic impurities. The mixture was extracted with ethyl acetate, dried over MgSO_4 , filtered and evaporated to recover the product.

Method E – Amine alkylation/acylation I

A mixture of amine, electrophile and potassium carbonate (5 equiv.), were dissolved in DMF (approx. 3mL) and heated at 150°C for several hours. The mixture was extracted with ethyl acetate or dichloromethane and washed with water. The combined extracts were washed with water, dried over MgSO_4 , filtered and concentrated under reduced pressure, to recover the product.

Method F– Tert-butyldimethylsilyl protection

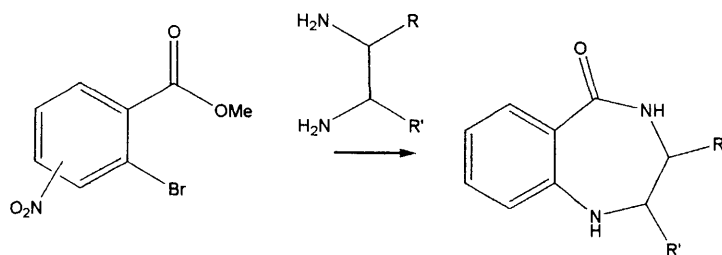
The alcohol was dissolved in DMF (approx. 3mL), followed by addition of imidazole (2.2 equiv.). Tert-butyldimethylsilyl chloride (TBDMS-Cl) (1.2 equiv.) was added dropwise and the reaction was stirred at room temperature for several hours. The mixture was extracted with ether, dried over MgSO_4 , filtered and concentrated under reduced pressure to recover the product.

Method G – Amine alkylation/acylation II

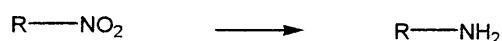
A solution of amine in DMF (approx. 3mL) under nitrogen was cooled in an ice bath to 0 °C. Sodium hydride (1.1 equiv.) was added slowly over a period of 10 min and stirred for 1 h prior to the addition of electrophile. The resultant solution was warmed to room temperature and stirred overnight. Concentration of flask contents by evaporation was followed by the dropwise addition of water to destroy the sodium hydride. The mixture was extracted with ethyl acetate and the combined organic layers were washed with water, dried over MgSO_4 , filtered and evaporated under reduced pressure to recover the product.

Method H – Esterification

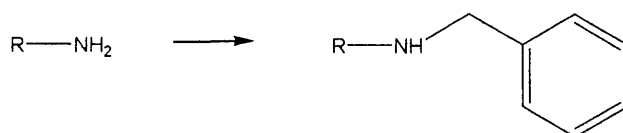
The acid was dissolved in methanol, followed by addition of concentrated sulphuric acid. The resultant mixture was refluxed for several hours. The solvent was removed by evaporation and the resultant residue was washed with saturated aqueous sodium bicarbonate. The aqueous solution was extracted with ethyl acetate, dried over MgSO_4 , filtered and concentrated under reduced pressure to recover the product.

Method I– Cyclization II

A mixture of ester and diamine, was dissolved in DMA (approx. 3mL) forming a dark solution. The solution was heated at 100 °C for several hours, after which time water was added, forming a precipitate. The brown solid was left to stir for 15 mins before being filtered. The brown solid, crude product was left to dry in a desiccator after which time, it was recrystallized from hot methanol.

Method J– Nitro reduction

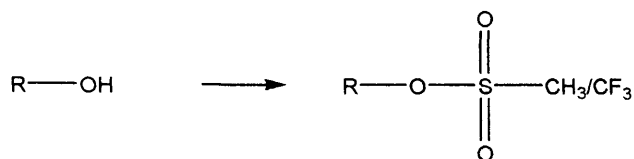
The nitro compound was added to a pressure vessel with 10 % Pd/C catalyst (catalytic amount) in methanol or dichloromethane. The mixture was shaken under a hydrogen atmosphere (20-40 p.s.i) for several hours, after which time it was filtered through Celite and washed with methanol or dichloromethane. The solvent was removed by evaporation to recover the product.

Method K – Amine benzylation

A solution of amine in DMF (approx 3mL) under nitrogen was cooled in an ice bath to 0 °C. Sodium hydride (1.1 equiv.) was added slowly over a period of 10 min and stirred for 1h prior to the addition of benzyl bromide. The resultant solution was warmed to room temperature and stirred overnight. Concentration of flask contents by evaporation was followed by the dropwise addition of water to destroy the sodium hydride. The mixture

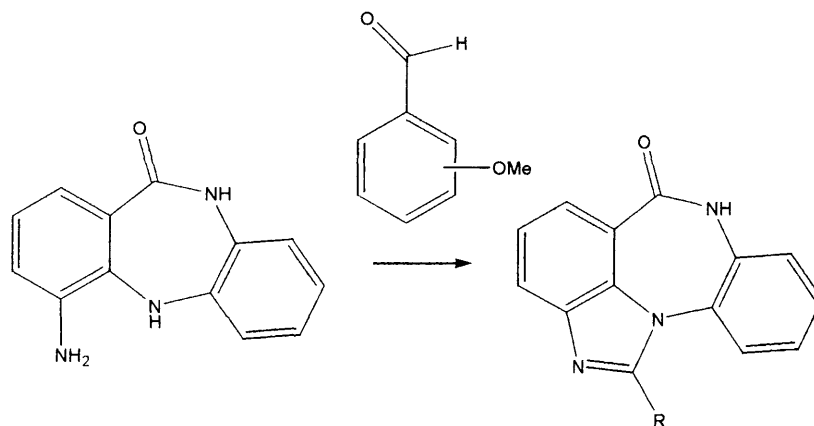
was extracted with ethyl acetate and the combined organic layers were washed with water, dried over MgSO_4 , filtered and evaporated under reduced pressure to recover the product.

Method L. Alcohol protection

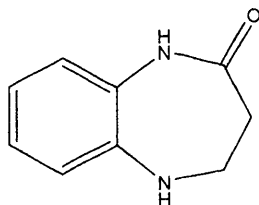


Alcohol and methanesulfonyl chloride or trifluoromethanesulfonyl chloride (1.5-2 equiv.) were suspended in tetrahydrofuran under a nitrogen atmosphere, followed by the addition of triethylamine (TEA) (3 equiv.). The resultant mixture was stirred overnight at room temperature. The solvent was removed by evaporation and the aqueous solution was extracted with dichloromethane or ethyl acetate, dried over MgSO_4 , filtered and concentrated under reduced pressure to recover the product.

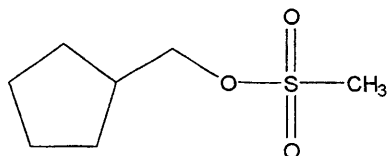
Method M – Imidazobenzodiazepinone formation



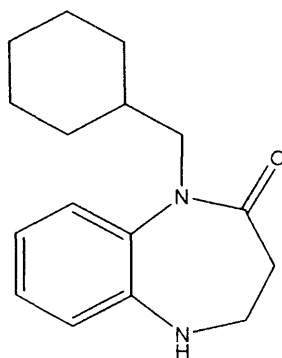
The amine and sodium hydrogen sulfite (1.5 equiv.) was suspended in DMA (approx. 3mL). The aldehyde (1 equiv.) was added dropwise to the reaction mixture, which was subsequently heated at $140\text{ }^\circ\text{C}$ with vigorous stirring for several hours until complete by TLC. Distilled water was added to the resulting solution, and this was left to stir overnight. The precipitate produced was recovered by filtration and dried under vacuum to recover the product.

3,4-Dihydro-1*H*-5*H*-benzo[2,3-*b*]diazepin-2-one, (26) (Bachman and Helsey, 1949)

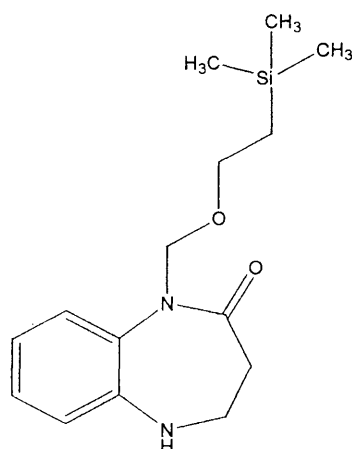
Method A. 1,2-Phenylenediamine (1.00 g, 9.25 mmol), 60 % aqueous acrylic acid (1.7 mL) and concentrated hydrochloric acid (0.75 mL) were heated at 100 °C for 4 h, producing an off-white powder (0.548 g, 37 %); m.p. 140-142 °C (lit (Bachman and Helsey, 1949) 140.5-141.5 °C); ν_{\max} (cm^{-1}) 3227 (NH), 3140 (Ar-H), 3072 (Alkyl-H), 1687 (C=O); δ_{H} 2.47-2.49 (2H, m, $\underline{\text{CH}_2}$), 3.45 (2H, q, $J = 4.8$, $\underline{\text{CH}_2}$), 5.68 (1H, s, $\underline{\text{NH}}$), 6.62 (1H, t, $J = 7.5$, $\underline{\text{H-Ar}}$), 6.75 (1H, d, $J = 7.5$, $\underline{\text{Ar-H}}$), 6.83 (1H, t, $J = 7.5$, $\underline{\text{Ar-H}}$), 6.88 (1H, d, $J = 7.5$, $\underline{\text{Ar-H}}$), 9.40 (1H, s, $\underline{\text{CONH}}$); δ_{C} 37.0 ($\underline{\text{CH}_2}$), 44.6 ($\underline{\text{CH}_2}$), 118.4, 119.3, 122.2, 124.5, 126.1, 140.0, 173.0 ($\underline{\text{C=O}}$); HRMS (ES^+/NH_3) m/z 180.1131[(M+NH₄), 180.1131 calculated for C₉H₁₄N₃O].

Methanesulfonic acid cyclopentylmethanoate (45) (Newcomb and Courtney, 1980)

Method L. Cyclopentylmethanol (0.20 g, 2.00 mmol) and methanesulfonyl chloride (0.46 g, 4.00 mmol) in tetrahydrofuran (10 mL), followed by the addition of triethylamine (TEA) (0.61 g, 6.00 mmol) produced the desired product as a light brown oil (0.38 g, 100 %); ν_{\max} (cm^{-1}) 2945 (Alkyl-H), 1346 (SO₃), 1171 (SO₂-CH₃); δ_{H} 0.94-1.29 (4H, m, Alkyl- $\underline{\text{H}}$), 1.51-1.73 (5H, m, Alkyl- $\underline{\text{H}}$), 3.16 (3H, s, $\underline{\text{CH}_3}$), 4.09 (2H, d, $J = 7.1$, $\underline{\text{CH}_2}$); δ_{C} 25.7, 29.4, 37.7, 39.2, 74.2; MS (ES^-) m/z 178.8 (M⁺), 179.1 (M+H).

3,4-Dihydro-1-(cyclohexylmethyl)-5H-benzo[2,3-b]diazepin-2-one, (35)

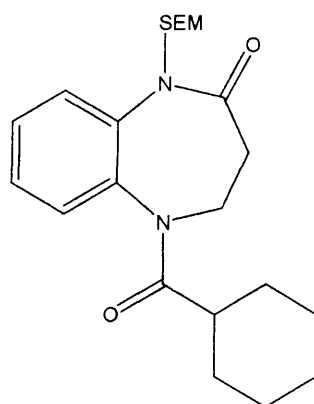
Method B. (**26**) (0.3 g, 1.85 mmol), sodium hydride (0.04 g, 2.47 mmol), cyclohexylmethyl bromide (4.85g, 30.00 mmol) and DMF (3 mL), followed by column chromatography (eluent 3:2 petrol:ethyl acetate) produced a pale yellow oil (0.17 g, 40 %); δ_{H} 0.80-0.87 (3H, m, Alkyl-H), 0.99-1.04 (2H, m, Alkyl-H), 1.18 (1H, t, $J = 7.1$, Alkyl-H), 1.32-1.34 (1H, m, Alkyl-H), 1.50-1.61 (4H, m, Alkyl-H), 2.32 (2H, t, $J = 6.4$, CH_2), 3.54-3.56 (2H, m, CH_2), 3.68 (2H, d, $J = 7.1$, CH_2), 5.12 (1H, s, NH), 6.89-6.95 (2H, m, Ar-H), 7.02 (1H, t, $J = 7.5$, Ar-H), 7.24 (1H, d, $J = 7.5$, Ar-H); δ_{C} 14.1, 20.7, 25.3, 26.0, 28.4, 33.5, 35.8, 49.6, 52.1, 59.7, 121.0, 121.5, 123.3, 125.9, 133.7, 141.9, 171.4; MS (ES^+) m/z 281.2 ($\text{M}+\text{Na}$).

3,4-Dihydro-1-(2-trimethylsilyloxyethyl)-5H-benzo[2,3-b]diazepin-2-one, (38)

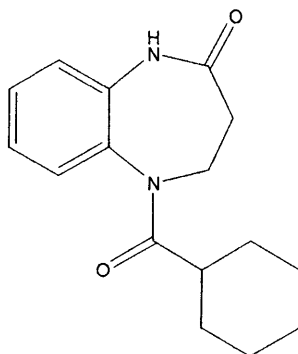
Method B. (**26**) (4.29 g, 26.45 mmol), sodium hydride (0.7 g, 30.00 mmol), SEM-Cl (4.85g, 30.00 mmol) and DMF (6 mL), followed by column chromatography (eluent 2:1 petrol:ethyl acetate) produced a pale yellow oil (3.98 g, 52 %); δ_{H} 0.00 (9H, s, SiCH_3),

0.87 (2H, t, $J = 8.2$, CH_2Si), 2.44 (2H, t, $J = 6.3$, CH_2), 3.54-3.59 (4H, m, $2 \times \text{CH}_2$), 5.10 (2H, s, NCH_2O), 5.24 (1H, br t, NH), 6.95 (1H, t, $J = 7.5$, Ar-H), 7.00 (1H, d, $J = 7.5$, Ar-H), 7.10 (1H, dd, $J = 7.5$, Ar-H), 7.39 (1H, d, $J = 7.5$, Ar-H); δ_{C} 0.0 (SiCH_3), 18.7, 35.0, 50.6, 66.1, 76.9, 122.4, 122.7, 124.0, 127.8, 134.8, 142.0, 173.8 ($\text{C}=\text{O}$); MS (ES^+) m/z 315.1 ($\text{M}+\text{Na}$).

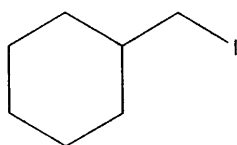
5-(Cyclohexylcarbonyl)-3,4-dihydro--1-(2-trimethylsilylethoxymethyl)benzo[2,3-*b*]diazepin-2-one, (50)



To a solution of 1-(2-trimethylsilylethoxymethyl)-5*H*-benzodiazepin-2-one (**38**) (0.98 g, 3.36 mmol) and pyridine (0.85 g, 10.10 mmol) in chloroform (30 mL) was added cyclohexanecarbonyl chloride (2.36 g, 16.81 mmol). The resultant solution was stirred overnight at room temperature. Water (25 mL) was added and the product was extracted with chloroform (3×50 mL). The organic layers were washed with hydrochloric acid (75 mL, 1 M), dried (MgSO_4), filtered and evaporated to leave the crude residue. Purification by column chromatography using 2:1 petrol:ethyl acetate as eluent, gave the compound as white crystals (0.13 g, 17 %); m.p. 87-89 °C; ν_{max} (cm^{-1}) 2921 (Ar-H), 2859 (Alkyl-H), 1676 ($\text{C}=\text{O}$), 1650 ($\text{C}=\text{O}$), 1282 (SiCH_3); δ_{H} (CDCl_3) 0.00 (9H, s, SiCH_3), 0.88-1.42 (10H, m, Alkyl-H), 1.54 (1H, t, $J = 14.4$, Alkyl-H), 1.67 (1H, d, $J = 13.2$, Alkyl-H), 1.79 (1H, d, $J = 13.2$, Alkyl-H), 2.02 (1H, t, $J = 11.3$, Alkyl-H), 2.35-2.38 (1H, m, Alkyl-H), 3.37-3.41 (1H, m, Alkyl-H), 3.52-3.57 (2H, m, Alkyl-H), 4.67 (1H, t, $J = 13.2$, Alkyl-H), 4.93 (1H, d, $J = 10.1$, NCHO), 5.26 (1H, d, $J = 10.1$, NCHO), 7.40-7.42 (2H, m, Ar-H), 7.54 (1H, t, $J = 6.1$, Ar-H), 7.66 (1H, d, $J = 7.9$, Ar-H); δ_{C} (CDCl_3) 0.0 (SiCH_3), 19.6, 26.6, 26.9, 27.0, 30.5, 31.3, 35.2, 43.3, 49.1, 68.1, 77.3, 125.6, 128.7, 130.3, 130.8, 135.8, 142.1, 173.1 ($\text{C}=\text{O}$), 177.9 ($\text{C}=\text{O}$); MS (ES^+) m/z 425.0 ($\text{M}+\text{Na}$).

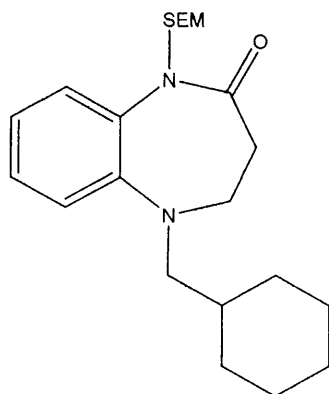
5-(Cyclohexanecarbonyl)-3,4-dihydro--1H-benzo[2,3-b]diazepin-2-one, (55)

Method C. (**38**) (0.93 g, 2.35 mmol) and 1 M tetrabutylammonium fluoride/THF solution (6 mL) were refluxed for 3 h, followed by column chromatography (eluent 1:1 petrol:ethyl acetate) to produce the title compound as a white solid (0.026 g, 40 %); m.p. 202-204 °C; ν_{max} (cm^{-1}) 3025 (NH), 2946 (Ar-H), 2859 (Alkyl-H), 1676 (C=O), 1615 (C=O); δ_{H} (CDCl_3) 0.85-1.74 (10H, m, Alkyl-H), 2.05 (1H, s, COCH), 2.62 (2H, m, CH₂), 3.43-3.50 (1H, m, CH), 4.86-4.96 (1H, m, CH), 7.11-7.39 (4H, m, Ar-H), 7.61 (1H, s, NH); δ_{C} (CDCl_3) 25.7, 25.9, 30.3, 33.8, 42.1, 47.2, 123.2, 126.5, 129.5, 129.7, 134.1, 136.3, 173.8 (C=O), 177.0 (C=O); HRMS (ES^+) m/z 290.1865 [(M+NH₄), 290.1863 calculated for C₁₆H₃₈N₂O₃].

Cyclohexylmethyl iodide, (36) (Kropp and Pienta, 1983; Ogle *et al.*, 1983)

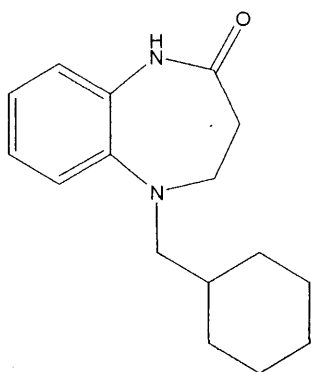
Method D. Cyclohexylmethyl bromide (3.00 g, 16.95 mmol), sodium iodide (6.00 g, 40.03 mmol) and acetone (70 mL) were refluxed for 15 h producing the title compound as a dark oil (4.37 g, 100 %); δ_{H} 0.91-1.81 (11H, m, Alkyl-H), 3.20 (2H, d, CH₂); δ_{C} 5.5, 26.5, 32.9, 38.9, 41.6.

5-(Cyclohexylmethyl)-3,4-dihydro-1-(2-trimethylsilyloxyethyl)benzo[2,3-*b*]diazepin-2-one, (39)



Method E. **(38)** (1.03 g, 3.53 mmol), **(36)** (1.20 g, 5.30 mmol), potassium carbonate (2.43 g, 17.67 mmol) and DMF (3 mL) were heated at 150 °C for 10 h, followed by column chromatography (eluent: 2 % ethyl acetate:petrol) to yield the desired compound as a clear oil (0.41 g, 30 %); ν_{max} (cm^{-1}) 2920 (Alkyl-H), 1685 (C=O), 835 (SiCH₃); δ_{H} 0.00 (9H, s, SiCH₃), 0.86 (2H, t, J = 8.2, SiCH₂), 1.16-1.78 (11H, m, Alkyl-H), 2.34 (2H, t, J = 6.0, CH₂), 2.88 (2H, s, CH₂), 3.33 (2H, s, CH₂), 3.53 (2H, t, J = 8.2, CH₂), 5.14 (2H, s, NCH₂O), 7.13 (1H, t, J = 7.7, Ar-H), 7.19 (1H, d, J = 7.7, Ar-H), 7.28 (1H, t, J = 7.7, Ar-H), 7.45 (1H, d, J = 7.7, Ar-H); δ_{C} 0.0, 18.6, 26.9, 27.7, 30.8, 32.0, 35.3, 35.9, 57.7, 60.2, 66.6, 68.0, 76.1, 121.9, 124.2, 124.4, 128.1, 138.7, 144.4, 173.6 (C=O); MS (ES⁺) m/z 411.1 (M+Na), 799.1 (2M+Na).

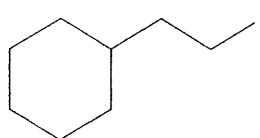
5-(Cyclohexylmethyl)-3,4-dihydro-1H-benzo[2,3-*b*]diazepin-2-one, (52)



Method C. **(39)** (0.37 g, 0.95 mmol) and 1 M tetrabutylammonium fluoride/THF solution (6 mL) were refluxed for 5 h, followed by column chromatography (eluent: 3:2

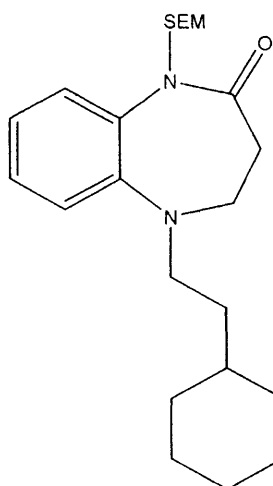
petrol:ethyl acetate) to produce the title compound as a pale yellow solid (0.13 g, 53 %); m.p. 119-121 °C; ν_{\max} (cm^{-1}) 3206 (NH), 2921 (Alkyl-H), 1679 (C=O); δ_{H} 0.81-1.22 (5H, m, Alkyl-H), 1.53-1.72 (6H, m, Alkyl-H), 2.28 (2H, t, $J = 6.6$, CH_2), 2.88 (2H, t, $J = 7.2$, Alkyl-H), 3.37 (2H, t, $J = 6.6$, CH_2), 6.92-7.09 (4H, m, Ar-H), 9.38 (1H, s, NHCO); δ_{C} (CDCl_3) 26.4, 27.2, 31.6, 34.3, 35.7, 56.3, 60.3, 121.2, 122.4, 122.7, 126.4, 133.0, 143.0, 174.7 (C=O); HRMS (ES^+) m/z 259.1805 [(M+H), 259.1804 calculated for $\text{C}_{16}\text{H}_{23}\text{N}_2\text{O}$].

Cyclohexylethyl iodide, (41) (Kropp and Pienta, 1983)



Method D. Cyclohexylethyl bromide (3.00 g, 16.00 mmol), sodium iodide (6.00 g, 40.03 mmol) and acetone (70 mL) were refluxed for 15 h producing the title compound as a brown oil (2.40 g, 90 %); δ_{H} 0.87-1.72 (13H, m, Alkyl-H), 3.30 (2H, t, CH_2I); δ_{C} 5.6, 26.5, 26.9, 32.9, 38.9, 41.6.

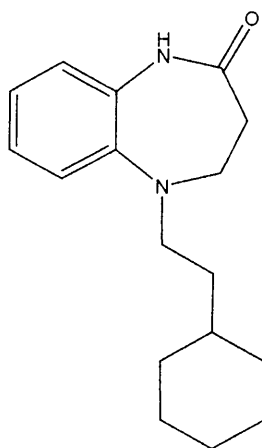
5-(Cyclohexylethyl)-3,4-dihydro-1-(2-trimethylsilylethoxymethyl)benzo[2,3-*b*]diazepin-2-one, (42)



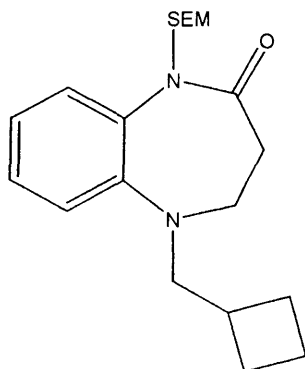
Method E. (38) (0.95 g, 3.26 mmol), cyclohexylethyl iodide (1.16 g, 4.89 mmol), potassium carbonate (2.25 g, 16.30 mmol) and DMF (3 mL) were heated at 150 °C for 9 h, followed by column chromatography (eluent: 9:1 petrol:ethyl acetate) to yield the desired compound as a pale yellow oil (0.47 g, 36 %); δ_{H} 0.00 (9H, s, SiCH_3), 0.84-1.73 (13H, m,

Alkyl-H), 2.34 (2H, t, $J = 6.4$, CH_2), 3.08 (2H, br s, CH_2), 3.45-3.49 (2H, m, CH_2), 3.56 (2H, t, $J = 8.2$, CH_2), 4.31 (2H, t, $J = 5.1$, CH_2), 5.13 (2H, s, NCH_2O), 7.14 (1H, t, $J = 7.9$, Ar-H), 7.18 (1H, d, $J = 7.9$, Ar-H), 7.29 (1H, t, $J = 7.9$, Ar-H), 7.45 (1H, t, $J = 7.9$, Ar-H); δ_{C} 0.0, 18.6, 27.1, 27.6, 34.3, 35.1, 35.4, 36.0, 36.7, 51.2, 57.8, 59.8, 66.1, 75.9, 122.0, 124.3, 124.5, 128.1, 138.8, 144.0, 173.6 ($\text{C}=\text{O}$); MS (ES^+) m/z 425.1 ($\text{M}+\text{Na}$).

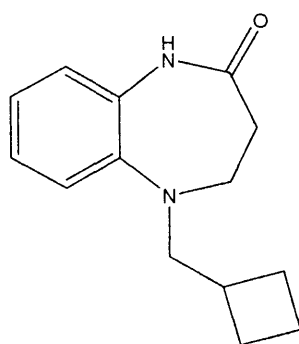
5-(Cyclohexylethyl)-3,4-dihydro-1H-benzo[2,3-b]diazepin-2-one, (53)



Method C. (**42**) (0.40 g, 0.99 mmol), and 1 M tetrabutylammonium fluoride/THF solution (5 mL) were refluxed for 12 h. Column chromatography (eluent 9:1 petrol:ethyl acetate, increasing to 7:3 petrol:ethyl acetate) produced the title compound compound as a white powder (0.08 g, 30 %); m.p. 142-145 °C; ν_{max} (cm^{-1}) 2923 (NH), 2846 (Alkyl-H), 1675 ($\text{C}=\text{O}$); δ_{H} 0.86-1.67 (13H, m, Alkyl-H), 2.28 (2H, t, $J = 6.8$, CH_2), 3.07 (2H, t, $J = 7.4$, CH_2), 3.38 (2H, t, $J = 6.8$, CH_2), 6.92-7.10 (4H, m, Ar-H), 9.42 (1H, s, NH); δ_{C} 26.1, 26.5, 33.1, 34.1, 34.8, 35.5, 50.4, 56.0, 120.6, 122.0, 122.2, 125.3, 134.0, 142.0, 172.8 ($\text{C}=\text{O}$); HRMS (ES^+) m/z 273.1961 [(M+H), 273.1962 calculated for $\text{C}_{17}\text{H}_{25}\text{N}_2\text{O}$].

5-(Cyclobutylmethyl)-3,4-dihydro-1-(2-trimethylsilyloxyethyl)benzo[2,3-b]diazepin-2-one, (48)

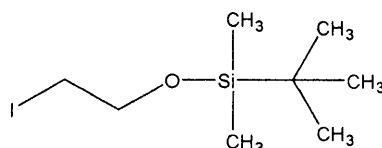
Method E. **(38)** (0.67 g, 2.30 mmol), cyclobutylmethyl bromide (68g, 9.20 mmol), potassium carbonate (1.60 g, 11.49 mmol) and DMF (3 mL) were heated at 150°C for 11 h. The mixture was extracted with dichloromethane, followed by column chromatography (eluent 9:1 petrol:ethyl acetate) to yield the desired compound as a pale yellow oil (0.37 g, 45 %); δ_{H} 0.00 (9H, s, SiCH₃), 0.83-2.05 (7H, m, Alkyl-H), 3.06 (2H, d, CH₂), 3.63 (2H, m, CH₂), 3.92 (2H, d, CH₂), 4.13 (4H, m, CH₂), 5.13 (1H, brs, NH), 5.33 (1H, s, NCH₂O), 7.00-7.42 (4H, m, Ar-H); MS (ES⁺) m/z 383.1 (M+Na).

5-(Cyclobutylmethyl)-3,4-dihydro-1H-benzo[2,3-b]diazepin-2-one, (54)

Method C. **(48)** (0.17 g, 0.47 mmol) and 1 M tetrabutylammonium fluoride/THF solution (5 mL) were refluxed for 11 h. Column chromatography (eluent 9:1 petrol:ethyl acetate, increasing to 4:2 petrol:ethyl acetate) produced the title compound as a pale yellow oil (0.022 g, 20 %); ν_{max} (cm⁻¹) 3008 (NH), 2970 (Alkyl-H), 1675 (C=O); δ_{H} 1.69-2.51 (5H, m, Alkyl-H), 1.83-1.88 (2H, m, CH₂), 2.00-2.05 (2H, m, CH₂), 2.33 (2H, t, J = 6.7 Hz, CH₂), 3.14 (2H, d, J = 7.2 CH₂), 6.97-6.99 (2H, m, Ar-H), 7.08-7.14 (2H, m, Ar-H), 9.44

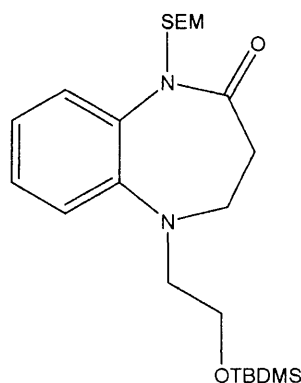
(1H, s, NH); δ_C 19.0, 27.4, 34.3, 34.6, 55.8, 59.7, 121.0, 121.7, 122.5, 126.4, 132.8, 143.1, 174.7 (C=O); HRMS (ES⁺) m/z 231.1490 [(M+H), 231.1492 calculated for C₁₄H₁₉N₂O].

***Tert*-butyl(2-iodoethoxy)dimethylsilane (57)** (Desroches *et al.*, 2003)



Method F. (56) (2.00 g, 11.63 mmol), imidazole (1.74 g, 25.59 mmol) and *tert*-butyldimethylsilyl chloride (TBDMS-Cl) (2.10 g, 13.96 mmol) in DMF (3 mL) produced the product as a yellow oil (3.25 g, 98 %); δ_H 0.00 (6H, s, SiCH₃), 0.81 (9H, s, CCH₃), 3.73 (2H, t, J = 6.2 Hz, CH₂), 3.92 (2H, t, J = 6.2 Hz, CH₂); δ_C -3.00 (SiCH₃), 9.42 (CCH₃), 18.2 (CCH₃), 25.7 (CH₂I), 63.6 (CH₂O); MS (ES⁺) m/z 300.8 (M⁺).

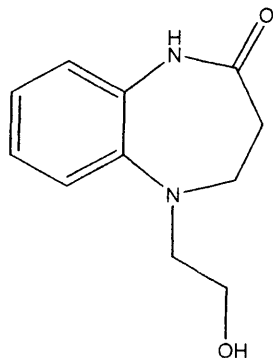
5-[2(*Tert*-butyldimethylsilyloxy)ethyl]-3,4-dihydro-1-(2-trimethylsilyloxy methyl)benzo[2,3-*b*]diazepin-2-one, (58)



Method E. (38) (1.28 g, 4.39 mmol), *tert*-butyl(2-iodoethoxy)dimethylsilane (1.89g, 6.59 mmol), potassium carbonate (3.03 g, 21.96 mmol) and DMF (4 mL) were heated at 150 °C for 13 h. Column chromatography (eluent 9:1 petrol:ethyl acetate) yielded the desired compound as a pale yellow oil (0.72g, 36 %); δ_H 0.05 (15H, s, SiCH₃), 0.89 (9H, s, CCH₃), 2.35 (2H, t, J = 6.8, CH₂), 3.22-3.25 (2H, m, CH₂), 3.42-3.47 (2H, m, CH₂), 3.57 (2H, t, J = 8.1, CH₂), 3.63 (2H, t, J = 5.8, CH₂), 3.73 (2H, t, J = 6.5, CH₂), 4.55 (2H, s, NCH₂O), 7.14 (1H, t, J = 7.5, Ar-H), 7.23-7.28 (2H, m, Ar-H), 7.47 (1H, dd, J = 1.3, 8.0,

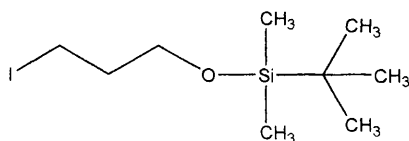
Ar-H); δ_C -1.8, 0.0, 19.2, 27.2, 35.3, 56.0, 57.7, 60.1, 63.9, 66.2, 121.9, 124.0, 124.4, 128.2, 138.5, 144.2, 173.5 (C=O); MS (ES⁺) m/z 473.3 (M+Na).

3,4-Dihydro-5-(2-hydroxyethyl)-1H-benzo[2,3-b]diazepin-2-one, (62)



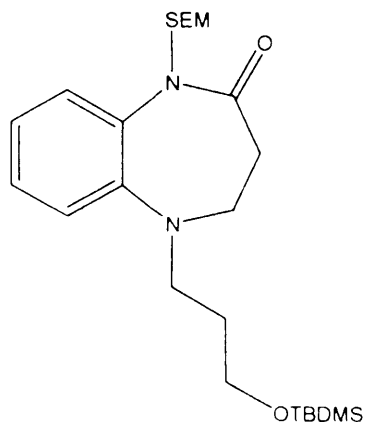
Method C. (58) (0.54 g, 1.19 mmol) and 1 M tetrabutylammonium fluoride/THF solution (5 mL) were refluxed for 18 h. Column chromatography (eluent 9:1 petrol:ethyl acetate) produced the title compound as a yellow oil (0.08 g, 33 %); δ_H 2.38 (2H, t, $J = 6.6$, CH₂), 3.24 (2H, t, $J = 6.3$, CH₂), 3.51 (2H, t, $J = 6.6$, CH₂), 3.61 (2H, q, $J = 6.3$, CH₂OH), 4.65 (1H, t, $J = 5.3$, CH₂), 6.95-7.16 (4H, m, Ar-H), 9.47 (1H, s, NH); δ_C 33.9, 55.0, 55.1, 58.5, 120.5, 121.4, 121.9, 124.9, 132.9, 141.7, 172.4 (C=O); HRMS (ES⁺) m/z 207.1126 [(M+H), 207.1128 calculated for C₁₁H₁₅N₂O₂].

Tert-butyl(3-iodopropoxy)dimethylsilane (60) (Baldwin *et al.*, 2005)



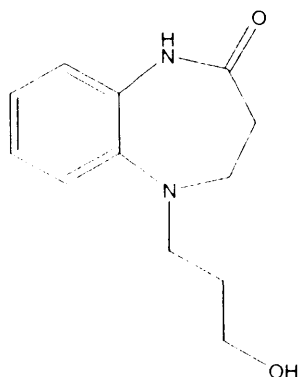
Method F. (59) (2.00 g, 10.75 mmol), imidazole (1.61 g, 23.66 mmol), *tert*-butyldimethylsilyl chloride (TBDMS-Cl) (1.94 g, 12.90 mmol) in DMF (3 mL), produced the product as a yellow oil (2.25 g, 84 %); δ_H 0.00 (6H, s, SiCH₃), 0.81 (9H, s, CCH₃), 1.85 (2H, m, CH₂), 3.23-3.26 (2H, m, CH₂), 3.61 (2H, m, CH₂); δ_C -5.5 (SiCH₃), 17.9 (CCH₃), 25.8, 35.5, 42.0, 59.0 (CH₂O), MS (ES⁺) m/z 299.2 (M-H).

3,4-Dihydro-5-[2(*tert*-butyldimethylsilyloxy)ethyl]-1-(2-trimethylsilyloxy methyl)benzo[2,3-*b*]diazepin-2-one, (61)



Method E. **(38)** (1.90 g, 7.97 mmol), *tert*-butyl(3-iodopropoxy)dimethylsilane (3.93g, 8.45 mmol), potassium carbonate (5.49 g, 39.80 mmol) and DMF (4 mL) were heated at 150 °C for 20 h. Column chromatography (eluent 8.5:1.5 petrol:ethyl acetate) yielded the desired compound as a yellow oil (0.90 g, 30 %); δ_{H} 0.00 (15H, s, SiCH₃), 0.91 (9H, s, CCH₃), 1.64-1.69 (2H, m, CH₂), 2.35 (2H, t, J = 6.7, CH₂), 3.14 (2H, br t, CH₂), 3.49-3.52 (2H, m, CH₂), 3.56 (2H, t, J = 8.1, CH₂), 3.63 (2H, t, J = 6.3, CH₂), 3.70 (2H, t, J = 6.3, CH₂), 5.13 (2H, s, NCH₂O), 7.15 (1H, t, J = 7.9, Ar-H), 7.20 (1H, dd, J = 1.4, 7.9, Ar-H), 7.29 (1H, t, J = 7.9, Ar-H), 7.47 (1H, dd, J = 1.4, 7.9, Ar-H); MS (ES⁺); m/z 464.3 (M⁺), 465.3 (M+H), 487.3 (M+Na).

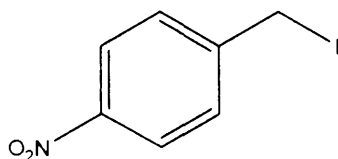
3,4-Dihydro-5-(3-hydroxypropyl)-1H-benzo[2,3-*b*]diazepin-2-one, (63)



Method C. **(61)** (0.83 g, 1.77 mmol) and 1 M tetrabutylammonium fluoride/THF solution (5 mL) were refluxed for 18 h, followed by column chromatography (eluent 1:1 petrol:ethyl acetate) to produce the title compound as a yellow oil (0.10 g, 26 %); δ_{H} 1.58-

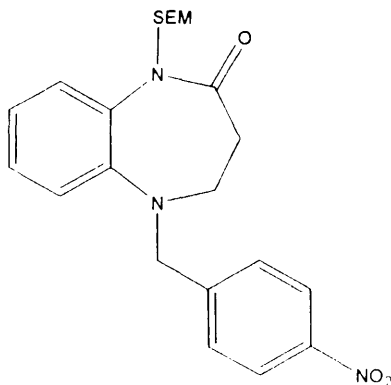
1.63 (2H, m, CH_2), 2.28 (2H, t, $J = 6.7$, CH_2), 3.11 (2H, t, $J = 7.1$, CH_2), 3.37-3.42 (4H, m, CH_2), 4.39 (1H, t, $J = 5.1$, OH), 6.93 (2H, d, $J = 3.3$, Ar-H), 7.05-7.11 (2H, m, Ar-H), 9.40 (1H, s, NH); δ_{C} 29.8, 33.2, 48.7, 55.0, 57.9, 119.7, 121.1, 121.3, 124.4, 133.0, 141.0, 171.9 ($\text{C}=\text{O}$); HRMS (ES^+) m/z 221.1287 [(M+H), 221.1285 calculated for $\text{C}_{12}\text{H}_{17}\text{N}_2\text{O}_2$].

1-Iodomethyl-4-nitrobenzene, (65) (Strazzolini and Runcio, 2003)



Method D. 1-Bromomethyl-4-nitrobenzene (2.50 g, 11.57 mmol), sodium iodide (5.00 g, 33.36 mmol) and acetone (60 mL) were refluxed for 10 h, producing the product as a brown solid (3.16 g, 100 %); m.p. 121-123 °C; δ_{H} 4.73 (2H, s, CH_2), 7.70 (2H, dd, $J = 1.8$, 6.9 Hz, Ar-H), 8.19 (2H, dd, $J = 1.8$, 6.9 Hz, Ar-H); δ_{C} 62.0, 123.3, 124.3, 127.0, 130.6, 131.6, 192.3.

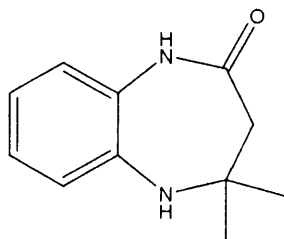
3,4-Dihydro-5-(4-nitrobenzyl)-1-(2-trimethylsilyloxyethyl)benzo[2,3-b]diazepin-2-one, (66)



Method G. (38) (1.43 g, 4.89 mmol), sodium hydride (0.13g, 5.38 mmol), 1-iodomethyl-4-nitrobenzene (2.11 g, 9.78 mmol) in DMF (3.5 mL), followed by column chromatography (eluent 8.25:1.75 petrol:ethyl acetate) produced the title compound as a yellow oil (1.06 g, 51 %); δ_{H} 0.00 (9H, s, SiCH_3), 0.95 (2H, t, $J = 8.2$, CH_2), 2.43 (2H, br t, CH_2), 3.38-3.42 (2H, m, CH_2), 3.64 (2H, t, $J = 8.2$, CH_2), 4.50 (2H, s, CH_2Ph), 5.20 (2H, s, NCH_2O), 7.14-7.17 (1H, m, Ar-H), 7.22-7.24 (2H, m, Ar-H), 7.51 (1H, d, $J = 8.2$, Ar-H), 7.61 (2H, d, $J = 8.8$, Ar-H), 8.18 (2H, d, $J = 8.8$, Ar-H); δ_{C} 0.0, 18.9, 35.3, 56.6,

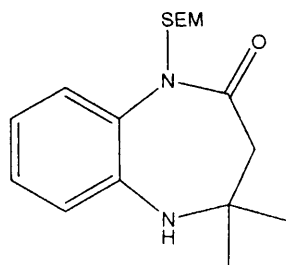
57.9, 66.7, 76.7, 122.4, 124.5, 124.8, 125.1, 128.2, 130.4, 139.1, 143.3, 147.9, 148.1, 173.5 ($\underline{\text{C}}=\text{O}$); MS (ES^+) m/z 450.2 ($\text{M}+\text{Na}$).

3-Hydro-4,4-dimethyl-1*H*-5*H*-benzo[2,3-*b*]diazepin-2-one, (68)



Method A. 1,2-Phenylenediamine (1.00 g, 9.25 mmol), 60% aqueous 3,3-dimethylacrylic acid (1.7 mL) and concentrated hydrochloric acid (0.75 mL) were heated at 100 °C for 8 h, cooled, basified with aqueous ammonia (2 mL), brine (15 mL) was added, followed by column chromatography (eluent 3% MeOH:DCM, increasing to 5% MeOH:DCM) to produce the title compound as a brown oil (0.75 g, 16 %); δ_{H} 1.24 (6H, s, CCH_3), 2.20 (2H, s, CH_2), 4.81 (1H, s, NH), 6.78-6.83 (1H, m, Ar-H), 6.87 (2H, t, $J = 6.66$, Ar-H), 6.91-6.95 (1H, m, Ar-H), 9.43 (1H, s, NH); δ_{C} 30.7, 46.2, 60.4, 120.6, 121.4, 121.7, 124.5, 130.7, 139.2, 167.3 ($\underline{\text{C}}=\text{O}$).

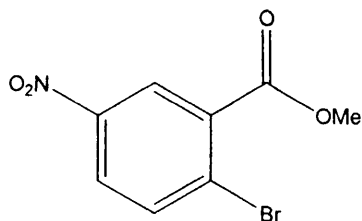
3-Hydro-4,4-dimethyl-1-(2-trimethylsilyloxyethyl)-5*H*-benzo[2,3-*b*]diazepin-2-one, (70)



Method B. (68) (0.26 g, 1.37 mmol), sodium hydride (0.04 g, 1.5 mmol), 2-(trimethylsilyl)ethoxymethyl chloride (0.34 g, 2.05 mmol) in DMF (3 mL), followed by column chromatography (eluent 3:1.5 petrol:ethyl acetate) yielded the title compound as a yellow oil (0.08 g, 18 %); δ_{H} 0.00 (9H, s, SiCH_3), 0.85 (2H, t, $J = 8.2$, CH_2), 1.23 (6H, s, CCH_3), 2.23 (2H, s, CH_2), 3.59 (2H, t, $J = 8.2$, CH_2), 4.72 (1H, s, NH), 5.15 (2H, s, NCH_2O), 7.01-7.06 (2H, m, Ar-H), 7.12 (1H, t, $J = 7.4$, Ar-H), 7.41 (1H, d, $J = 7.4$, Ar-H).

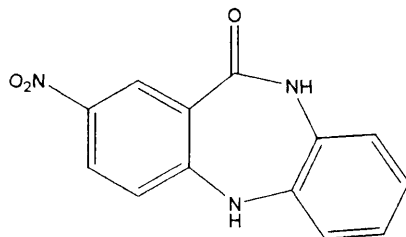
H); δ_C 0.0, 18.6, 29.9, 47.1, 61.1, 66.0, 76.1, 119.9, 123.7, 124.6, 127.4, 136.9, 142.0, 171.7 ($\underline{C=O}$); MS (ES⁺) m/z 343.2 (M+Na), 663.4 (2M+Na).

Methyl 2-bromo-5-nitrobenzoate, (74) (Klein and Boche, 1999)



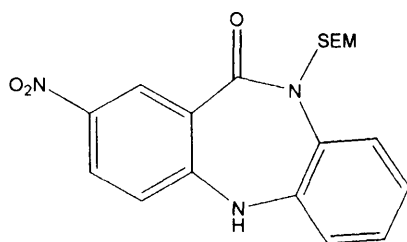
Method H. 2-Bromo-5-nitrobenzoic acid (5.00 g, 20.32 mmol), concentrated sulphuric acid (2.5 mL) and methanol (50 mL) were refluxed for 8 h producing the product as a white solid (5.18 g, 98 %); m.p. 71-74 °C; δ_H 3.92 (3H, s, $\underline{CH_3}$), 8.04 (1H, d, J = 2.8, Ar-H), 8.25 (1H, dd, J = 2.8, 8.8, Ar-H), 8.51 (1H, d, J = 8.8, Ar-H); δ_C 53.5 (OCH₃), 125.9, 127.5, 128.0, 133.8, 136.0, 147.0, 164.8 ($\underline{C=O}$).

4-Nitro-1H-7H-dibenzo[2,3-b][6,7-f]diazepin-2-one, (75) (Giani *et al.*, 1985)



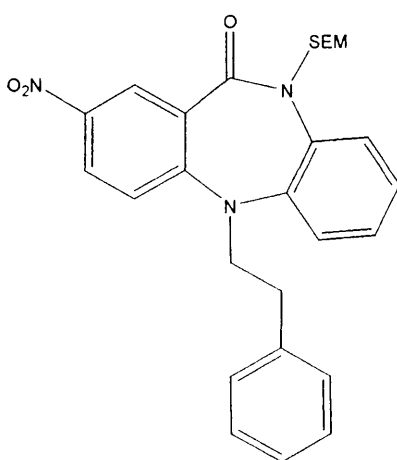
Method I. (74) (0.50 g, 1.92 mmol), 1,2-phenylenediamine (30) (0.62 g, 5.77 mmol) and DMA (4 mL) were heated at 100 °C for 10 h, to produce the product as a brown solid (0.25 g, 51 %); m.p. 338-342 °C; δ_H 6.94-7.02 (4H, m, Ar-H), 7.08 (1H, d, J = 9.0, Ar-H), 8.12 (1H, dd, J = 2.8, 9.0, Ar-H), 8.57 (1H, d, J = 2.8, Ar-H), 9.06 (1H, s, NH), 10.10 (1H, s, CONH); δ_C 119.4, 119.6, 120.3, 121.4, 124.3, 124.8, 128.3, 128.5, 129.3, 135.4, 139.5, 154.4, 165.3 ($\underline{C=O}$); HRMS (ES⁻) m/z 254.0571 [(M-H), 254.0571 calculated for C₁₃H₈N₃O₃].

4-Nitro-1-(2-trimethylsilyloxyethyl)-5H-dibenzo[2,3-b][6,7-f]diazepin-2-one, (82)



Method C. (**75**) (1.55 g, 5.63 mmol), sodium hydride (0.15 g, 6.19 mmol), 2-(trimethylsilyl)ethoxymethyl chloride (**37**) (1.03g, 6.19 mmol) in DMF (6 mL), followed by column chromatography (eluent 3:1 petrol:ethyl acetate) produced the product as a yellow powder (0.65 g, 30 %); m.p. 168-170 °C; δ_{H} 0.00 (9H, s, SiCH₃), 0.89 (2H, t, J = 8.0, CH₂), 3.68 (2H, t, J = 8.0, CH₂), 5.29 (2H, s, NCH₂O), 7.21-7.23 (3H, m, Ar-H), 7.30 (1H, d, J = 9.0, Ar-H), 7.59 (1H, m, Ar-H), 8.26 (1H, dd, J = 2.8, 9.0, Ar-H), 8.54 (1H, d, J = 2.8, Ar-H), 9.11 (1H, s, NH); δ_{C} 0.0 (SiCH₃), 18.8, 66.8, 79.9, 124.5, 125.2, 126.6, 127.6, 127.8, 129.3, 135.3, 137.0, 139.1, 144.5, 145.2, 145.6, 168.2 (C=O); MS (ES⁺) *m/z* 408.2 (M+Na).

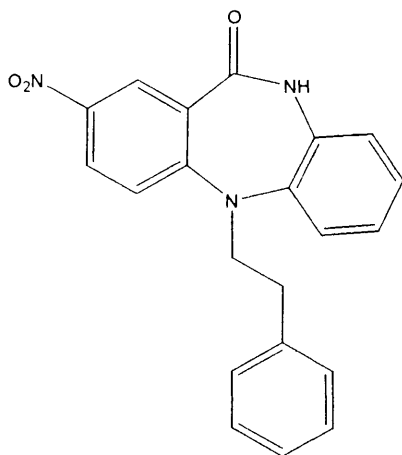
4-Nitro-7-(phenylethyl)-1-(2-trimethylsilyloxyethyl)dibenzo[2,3-b][6,7-f]diazepin-2-one, (91)



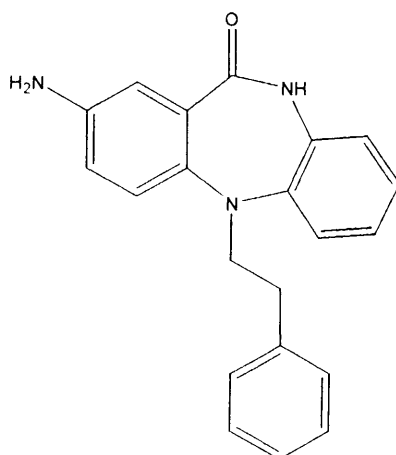
Method E. (**82**) (1.87 g, 4.85 mmol), phenylethyl iodide (3.72 g, 16.01 mmol), potassium carbonate (3.35 g, 24.25 mmol) and DMF (4 mL) were heated at 150 °C for 24 h, followed by column chromatography (eluent 9.5:0.5 petrol:ethyl acetate, increasing to 9:1

petrol:ethyl acetate) to yield the desired compound as a yellow oil (0.50 g, 21 %); δ_{H} 0.00 (9H, s, SiCH₃), 0.92 (2H, t, J = 6.5, CH₂), 2.55 (2H, t, J = 1.6, CH₂), 2.88 (2H, t, J = 2.8, CH₂), 3.63-3.69 (2H, m, CH₂), 4.12-4.16 (2H, m, CH₂), 5.03 (1H, d, J = 10.2, NCHO), 5.38 (1H, d, J = 10.2, NCHO), 7.17-7.33 (5H, m, Ar-H), 7.48 (1H, d, J = 8.0, Ar-H), 7.55 (1H, d, J = 9.0, Ar-H), 7.64 (1H, dd, J = 1.2, 8.0, Ar-H), 8.34 (1H, dd, J = 2.8, 9.0, Ar-H), 8.38 (1H, d, J = 2.8, Ar-H); δ_{C} 0.0 (SiCH₃), 18.8, 34.6, 51.2, 67.1, 78.9, 120.6, 122.8, 125.3, 127.0, 127.6, 128.1, 128.5, 128.7, 129.3, 129.5, 129.7, 130.0, 130.2, 136.8, 140.1, 143.6, 146.0, 159.4, 167.9 (C=O); MS (ES⁺) m/z 512.3 (M+Na).

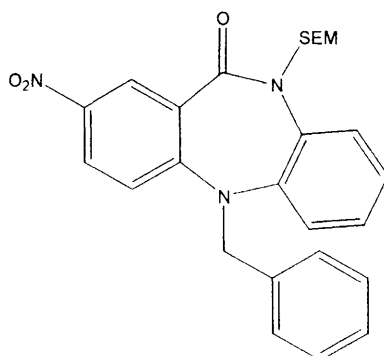
4-Nitro-7-(phenylethyl)-1H-dibenzo[2,3-b][6,7-f]diazepin-2-one, (95)



Method C. (91) (0.25 g, 0.51 mmol) and 1 M tetrabutylammonium fluoride/THF solution (5 mL) were refluxed for 24 h, followed by column chromatography (eluent 3:1 petrol:ethyl acetate) to produce the title compound as a yellow powder (0.04 g, 22 %); m.p. 218-220 °C; δ_{H} 2.86 (2H, t, J = 6.8, CH₂), 4.12 (2H, t, J = 6.8, CH₂), 7.13-7.30 (8H, m, Ar-H), 7.39 (1H, d, J = 9.0, Ar-H), 7.52 (1H, d, J = 9.0, Ar-H), 8.35 (1H, dd, J = 2.8, 9.0, Ar-H), 8.44 (1H, d, J = 2.8, Ar-H), 10.52 (1H, s, NCHO); δ_{C} 33.2, 50.8, 120.2, 121.7, 121.9, 125.1, 125.8, 126.2, 126.9, 127.5, 128.0, 128.2, 128.7, 132.9, 138.8, 141.3, 142.0, 157.6, 166.3 (C=O); MS (ES⁺) m/z 382.1 (M+Na).

4-Amino-7-(phenylethyl)-4-(2-trimethylsilylethoxymethyl)-1H-dibenzo[2,3-b][6,7-f]diazepin-2-one, (99)

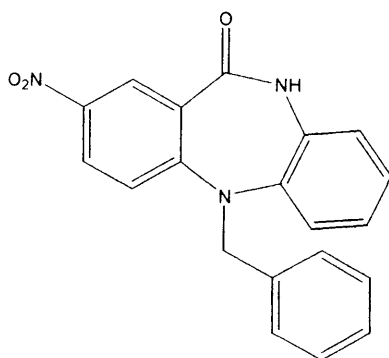
Method J. (**95**) (0.04 g, 0.11 mmol) in dichloromethane (40 mL), produced the product as a yellow powder (0.037 g, 100 %); m.p. 88-92 °C; δ_{H} 2.77 (2H, t, $J = 7.2$, CH_2), 3.75-3.90 (2H, m, CH_2), 5.01 (2H, s, NH_2), 6.74 (1H, dd, $J = 2.7, 8.6$, Ar-H), 6.88 (1H, d, $J = 2.7$, Ar-H), 6.97-7.05 (3H, m, Ar-H), 7.10 (1H, t, $J = 7.3$, Ar-H), 7.19-7.35 (6H, m, Ar-H), 10.02 (1H, s, NHCO); δ_{C} 33.5, 50.1, 114.9, 118.1, 119.4, 121.2, 123.3, 124.4, 125.8, 126.0, 128.1, 128.6, 128.8, 129.0, 133.4, 139.4, 139.6, 140.8, 144.3, 144.5, 168.7 ($\text{C}=\text{O}$); HRMS (ES^+) m/z 330.1607 [(M+H), 330.1601 calculated for $\text{C}_{21}\text{H}_{20}\text{N}_3\text{O}$].

7-(Benzyl)-4-nitro-1-(2-trimethylsilylethoxymethyl)dibenzo[2,3-b][6,7-f]diazepin-2-one, (85)

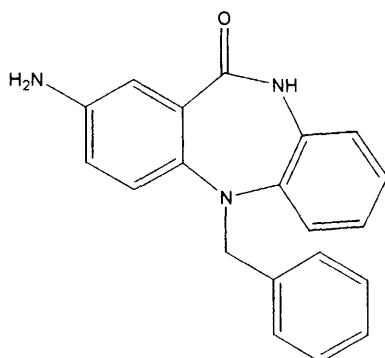
Method E. (**82**) (0.3 g, 0.78 mmol), benzylbromide (0.20 g, 1.17 mmol), potassium carbonate (0.54 g, 3.89 mmol) and DMF (3 mL) were heated at 150 °C for 20 h. The mixture was extracted with dichloromethane, followed by column chromatography (eluent

9.5:0.5 petrol:ethyl acetate) which yielded the desired compound as a yellow dense oil (0.20 g, 54 %); δ_{H} 0.00 (9H, s, SiCH₃), 0.97 (2H, t, J = 8.1, CH₂), 3.75 (2H, t, J = 8.1, CH₂), 4.56 (2H, s, CH₂Ph), 5.41 (1H, d, J = 10.3, NCH₂O), 5.54 (1H, d, J = 10.3, NCH₂O), 7.25-7.29 (4H, m, Ar-H), 7.33 (1H, t, J = 7.6, Ar-H), 7.37-7.52 (5H, m, Ar-H), 8.27 (1H, dd, J = 2.8, 9.0, Ar-H), 8.40 (1H, d, J = 2.8, Ar-H); δ_{C} 0.5, 19.4, 54.1, 67.9, 79.3, 121.4, 123.3, 125.9, 127.6, 128.3, 128.6, 128.9, 129.2, 129.8, 130.1, 130.4, 137.1, 138.6, 144.3, 147.5, 159.6, 168.6 (C=O); MS (ES⁺) m/z 450.2 (M+Na).

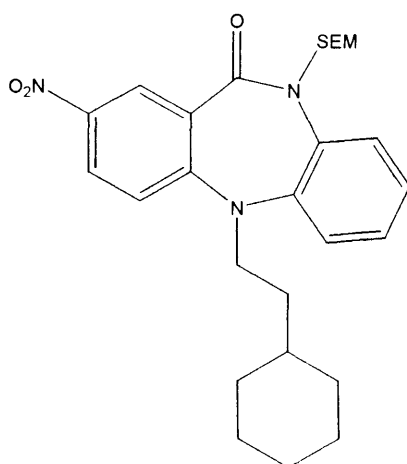
7-(Benzyl)-4-nitro-1H-dibenzo[2,3-b][6,7-f]diazepin-2-one, (93)



Method C. (**85**) (0.15 g, 0.31 mmol) and 1 M tetrabutylammonium fluoride/THF solution (5 mL) were refluxed for 20 h, followed by column chromatography (eluent 4:1 petrol:ethyl acetate) to produce the title compound as an orange powder (0.04 g, 37 %); m.p. 258-261 °C; δ_{H} 5.14 (2H, s, CH₂Ph), 7.11-7.15 (3H, m, Ar-H), 7.20 (1H, t, J = 7.5, Ar-H), 7.30 (2H, t, J = 7.5, Ar-H), 7.38 (1H, d, J = 7.5, Ar-H), 7.45 (2H, d, J = 7.5, Ar-H), 7.48 (1H, d, J = 9.1, Ar-H), 8.27 (1H, dd, J = 2.8, 9.1, Ar-H), 8.42 (1H, d, J = 2.8, Ar-H), 10.66 (1H, s, NH); δ_{C} 53.0, 120.4, 121.7, 121.9, 125.0, 125.2, 126.8, 127.2, 127.9, 128.0, 128.4, 130.3, 132.8, 136.9, 141.7, 142.2, 157.5, 166.5 (C=O); MS (ES⁺) m/z 368.1 (M+Na).

4-Amino-7-(benzyl)-1*H*-dibenzo[2,3-*b*][6,7-*f*]diazepin-2-one, (97)

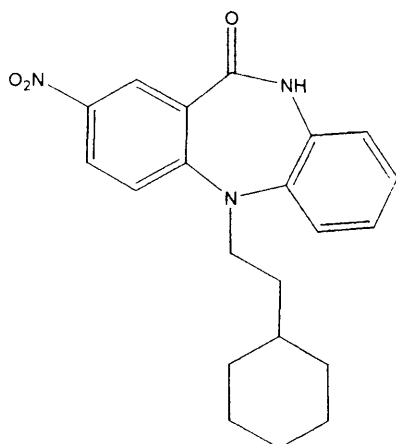
Method J. (**93**) (0.17 g, 0.49 mmol) in dichloromethane (50 mL) produced the product as a brown oil (0.13 g, 84 %); δ_{H} 4.87 (2H, d, $J = 6.3$ Hz, CH_2), 4.96 (2H, s, NH_2), 6.63 (1H, dd, $J = 2.8, 8.6$, Ar-H), 6.85 (1H, d, $J = 2.8$, Ar-H), 6.95-7.20 (8H, m, Ar-H), 7.26 (1H, t, $J = 7.5$, Ar-H), 7.41 (1H, d, $J = 7.5$, Ar-H), 10.10 (1H, s, NHCO); δ_{C} 54.2, 116.7, 119.8, 121.5, 123.1, 125.3, 126.2, 128.3, 128.7, 129.7, 130.1, 130.7, 135.3, 140.1, 143.0, 146.3, 146.6, 170.7 (C=O); HRMS (ES^+) m/z 316.1443 [(M+H), 316.1444 calculated for $\text{C}_{20}\text{H}_{18}\text{N}_3\text{O}$].

7-(Cyclohexylethyl)-4-nitro-1-(2-trimethylsilyloxyethyl)dibenzo[2,3-*b*][6,7-*f*]diazepin-2-one, (92)

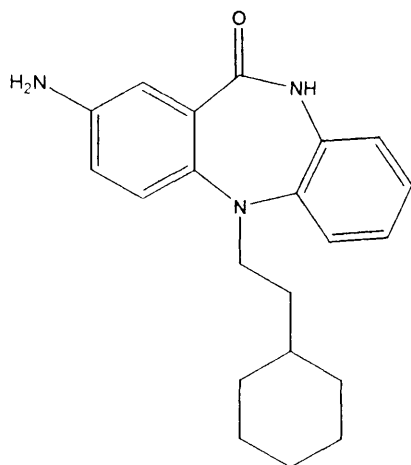
Method E. (**82**) (0.3 g, 0.78 mmol), cyclohexylethyl iodide (0.37g, 1.66 mmol), potassium carbonate (0.54 g, 3.89 mmol) and DMF (3 mL) were heated at 150 °C for 22 h, followed by column chromatography (eluent 9.5:0.5 petrol:ethyl acetate) to yield the desired compound as a yellow dense oil (0.20 g, 54 %); δ_{H} 0.00 (9H, s, SiCH_3), 0.87-1.68 (15H, m, Alkyl-H), 3.68 (2H, t, $J = 8.1$, CH_2O), 3.88 (2H, t, $J = 6.2$, NCH_2CH_2), 5.36 (1H, d, $J =$

10.3, NCHO), 5.45 (1H, d, $J = 10.3$, NCHO), 7.26-7.30 (2H, m, Ar-H), 7.38-7.41 (1H, dd, $J = 1.8, 7.8$, Ar-H), 7.48 (1H, d, $J = 9.0$, Ar-H), 7.64 (1H, dd, $J = 1.8, 7.8$, Ar-H). 8.33 (1H, dd, $J = 2.8, 9.0$, Ar-H), 8.38 (1H, d, $J = 2.8$, Ar-H); δ_C 0.0 (SiCH₃), 18.7, 27.1, 27.4, 33.9, 35.9, 36.4, 47.7, 67.0, 78.4, 120.4, 122.6, 125.5, 126.9, 128.1, 128.5, 128.7, 129.2, 136.5, 143.5, 146.7, 159.7, 168.1 (C=O); MS (ES⁺) m/z 518.3 (M+Na).

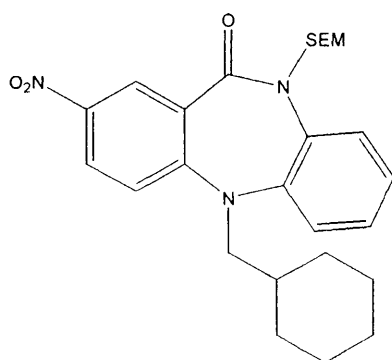
7-(Cyclohexylethyl)-4-nitro-1H-dibenzo[2,3-b][6,7-f]diazepin-2-one, (96)



Method C. (92) (0.16 g, 0.32 mmol) and 1 M tetrabutylammonium fluoride/THF solution (5 mL) were refluxed for 20 h. Column chromatography (eluent 8.5:1.5 petrol:ethyl acetate) produced the title compound as a yellow powder (0.07 g, 60 %); m.p. 240-243 °C; δ_H 0.88-1.67 (13 H, m, Alkyl-H), 3.90 (2H, t, $J = 6.5$, CH₂), 7.14-7.20 (3H, m, Ar-H), 7.31 (1H, d, $J = 6.9$, Ar-H), 7.45 (1H, d, $J = 9.0$, Ar-H), 8.34 (1H, dd, $J = 2.8, 9.0$, Ar-H), 8.43 (1H, d, $J = 2.8$, Ar-H), 10.58 (1H, s, NH); δ_C 26.0, 30.7, 32.5, 34.2, 34.8, 47.1, 120.0, 121.7, 121.9, 125.0, 125.2, 126.9, 127.4, 127.8, 132.9, 141.6, 141.9, 157.9, 166.6 (C=O); MS (ES⁺) m/z 388.2 (M+Na).

4-Amino-7-(cyclohexylethyl)-1*H*-dibenzo[2,3-*b*] [6,7-*f*]diazepin-2-one, (100)

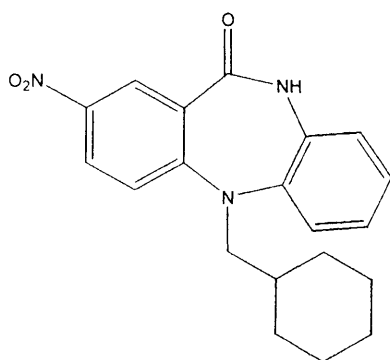
Method J. (**96**) (0.05 g, 0.14 mmol) in dichloromethane (30 mL) produced the compound as a yellow solid (0.046 g, 100 %); m.p. 186-189 °C; δ_{H} 1.10-1.63 (13H, m, Alkyl-H), 3.61 (2H, t, $J = 6.4$, CH_2), 5.00 (2H, s, NH_2), 6.69 (1H, dd, $J = 2.6, 8.5$, Ar-H), 6.84 (1H, d, $J = 2.6$, Ar-H), 6.90 (1H, d, $J = 8.5$, Ar-H), 7.00-7.14 (4H, m, Ar-H), 10.02 (1H, s, NH); δ_{C} 25.8, 26.1, 32.6, 34.6, 34.9, 40.0, 114.8, 117.2, 118.0, 119.3, 121.1, 123.1, 124.3, 128.9, 133.4, 141.2, 144.4, 144.7, 168.8 ($\text{C}=\text{O}$); HRMS (ES^+) m/z 336.2070 (M^+H), 336.2070 calculated for $\text{C}_{21}\text{H}_{26}\text{N}_3\text{O}$.

7-(Cyclohexylmethyl)-4-nitro-1-(2-trimethylsilylethoxymethyl)dibenzo[2,3-*b*] [6,7-*f*]diazepin-2-one, (88)

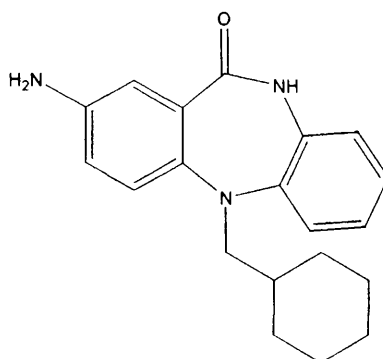
Method E. (**82**) (0.95 g, 2.45 mmol), cyclohexylmethyl iodide (1.66 g, 7.30 mmol), potassium carbonate (1.69 g, 12.26 mmol) and DMF (3 mL) were heated at 150 °C for 22 h. Column chromatography (eluent 4 % ethyl acetate:petrol) yielded the desired compound as a dense oil (0.57 g, 31 %); δ_{H} 0.00 (9H, s, SiCH_3), 0.87-1.83 (13H, m, Alkyl-H), 3.22 (2H, t, $J = 5.7$, CH_2), 3.64-3.67 (2H, m, CH_2), 5.34 (1H, d, $J = 10.3$,

NCHO), 5.45 (1H, d, $J = 10.3$, NCHO), 7.23-7.30 (2H, m, Ar-H), 7.39 (1H, d, $J = 7.8$, Ar-H), 7.48 (1H, d, $J = 9.1$, Ar-H), 7.62 (1H, dd, $J = 1.4, 7.8$, Ar-H), 8.30 (1H, dd, $J = 2.8, 9.1$, Ar-H), 8.37 (1H, d, $J = 2.8$, Ar-H); δ_c 0.0 (SiCH₃), 18.8, 26.6, 27.7, 30.5, 32.6, 36.2, 68.1, 78.5, 120.6, 122.8, 125.4, 126.8, 128.0, 128.5, 128.7, 129.3, 136.6, 143.5, 147.0, 159.6, 168.2 (C=O); MS (ES⁺) m/z 504.3 (M+Na).

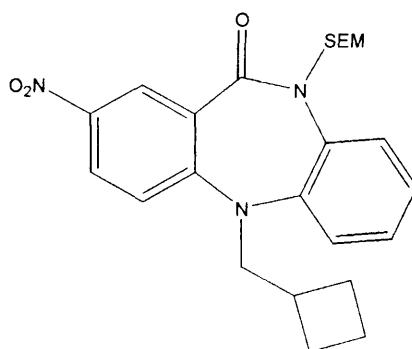
7-(Cyclohexylmethyl)-4-nitro-1H-dibenzo[2,3-*b*][6,7-*f*]diazepin-2-one, (94)



Method C. (**88**) (0.53 g, 1.09 mmol) and 1 M tetrabutylammonium fluoride/THF solution (5 mL) were refluxed for 24 h. Column chromatography (eluent 9:1 petrol:ethyl acetate) produced the title compound as a yellow powder (0.18 g, 47 %); m.p. 256-258 °C; δ_H 0.95-1.83 (11H, m, Alkyl-H), 3.72 (2H, t, $J = 9.3$, CH₂), 7.13-7.21 (3H, m, Ar-H), 7.32 (1H, d, $J = 7.6$, Ar-H), 7.45 (1H, d, $J = 9.3$, Ar-H), 8.32 (1H, dd, $J = 2.9, 9.3$, Ar-H), 8.43 (1H, d, $J = 2.9$, Ar-H); δ_c 25.2, 26.0, 30.2, 34.7, 55.8, 120.2, 121.9, 122.0, 125.0, 125.1, 127.0, 127.4, 127.7, 132.9, 141.7, 141.9, 158.0, 166.6 (C=O); MS (ES⁺) m/z 374.2 (M+Na).

4-Amino-7-(cyclohexylmethyl)-1*H*-dibenzo[2,3-*b*][6,7-*f*]diazepin-2-one, (98)

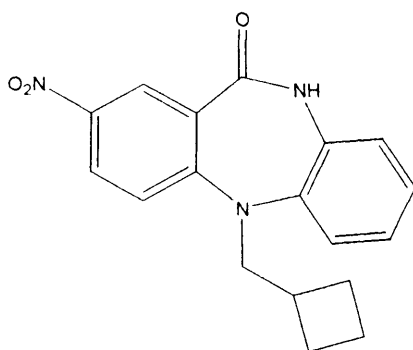
Method J. (94) (0.16 g, 0.46 mmol) in dichloromethane (30 mL), followed by column chromatography (eluent 1:1 petrol:ethyl acetate) produced the title compound as a yellow solid (0.094 g, 64 %); m.p. 254-257 °C; δ_{H} 0.88-1.85 (13H, m, Alkyl-H), 5.00 (2H, s, NH₂), 6.70 (1H, dd, *J* = 2.6, 8.6 Hz, Ar-H), 6.84 (1H, d, *J* = 2.6 Hz, Ar-H), 6.91 (1H, d, *J* = 8.6 Hz, Ar-H), 6.98-7.13 (4H, m, Ar-H), 10.00 (1H, s, NHCO); δ_{C} 25.4, 26.2, 30.5, 34.5, 55.0, 115.9, 118.0, 118.4, 119.3, 121.2, 122.9, 128.9, 133.5, 141.4, 144.4, 144.9, 168.8 (C=O); HRMS (ES⁺) *m/z* 322.1913 [(M+H), 322.1914 calculated for C₂₀H₂₅N₃O].

7-(Cyclobutylmethyl)-4-nitro-1-(2-trimethylsilyloxyethyl)dibenzo[2,3-*b*][6,7-*f*]diazepin-2-one, (101)

Method E. (82) (0.94 g, 2.45 mmol), cyclobutylmethyl bromide (1.46 g, 9.80 mmol), potassium carbonate (1.68 g, 12.19 mmol) and DMF (3 mL) were heated at 150 °C for 22 h, followed by column chromatography (eluent 9:1 petrol:ethyl acetate) yielding the desired compound as a yellow oil (0.28 g, 25 %); δ_{H} 0.00 (9H, s, SiCH₃), 0.87-0.92 (3H, m, Alkyl-H), 1.27 (1H, s, Alkyl-H), 1.71-1.96 (5H, m, Alkyl-H), 3.67 (2H, t, *J* = 8.1, CH₂), 3.86-3.98 (2H, m, CH₂), 5.34 (1H, d, *J* = 10.3, NCHO), 5.45 (1H, d, *J* = 10.3, NCHO), 7.10-7.40 (3H, m, Ar-H), 7.46 (1H, d, *J* = 9.0, Ar-H), 7.62 (1H, dd, *J* = 1.8, 7.0,

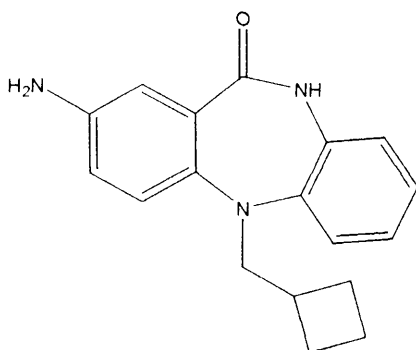
Ar-H), 8.29 (1H, dd, $J = 2.8, 9.0$, Ar-H), 8.37 (1H, d, $J = 2.8$, Ar-H); δ_C 0.0 (SiCH₃), 18.8, 19.3, 27.1, 34.2, 55.4, 69.5, 78.5, 120.6, 122.8, 125.4, 126.9, 127.9, 128.5, 128.7, 129.2, 136.5, 143.5, 146.7, 159.7, 168.1 (C=O); MS (ES⁺) m/z 476.2 (M+Na).

7-(Cyclobutylmethyl)-4-nitro-1H-dibenzo[2,3-b][6,7-f]diazepin-2-one, (102)



Method C. (101) (0.26 g, 0.57 mmol) and 1 M tetrabutylammonium fluoride/THF solution (5 mL) were refluxed for 24 h, followed by column chromatography (eluent 3:2 petrol:ethyl acetate) to produce the title compound as a yellow powder (0.08 g, 44 %); m.p. 270-272 °C; δ_H 1.62-1.87 (7H, m, Alkyl-H), 3.85 (2H, d, $J = 4.8$, NCH₂), 7.03-7.29 (4H, m, Ar-H), 7.36 (1H, d, $J = 9.0$, Ar-H), 8.31 (1H, dd, $J = 2.9, 9.0$, Ar-H), 8.35 (1H, d, $J = 2.9$, Ar-H), 10.47 (1H, s, NH); δ_C 17.9, 25.6, 32.7, 54.9, 120.2, 121.7, 121.9, 124.9, 125.1, 126.9, 127.4, 127.7, 132.9, 141.6, 141.8, 158.0, 166.6 (C=O); MS (ES⁺) m/z 346.1 (M+Na).

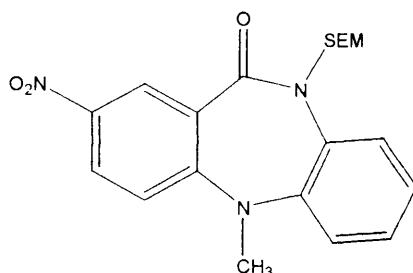
4-Amino-7-(cyclobutylmethyl)-1H-dibenzo[2,3-b][6,7-f]diazepin-2-one, (103)



Method J. (102) (0.07 g, 2.16 mmol) in dichloromethane (30 mL) produced the product as a yellow solid (0.064 g, 100 %); m.p. 224-227 °C; δ_H 1.65-1.93 (6H, m, Alkyl-H), 2.46-

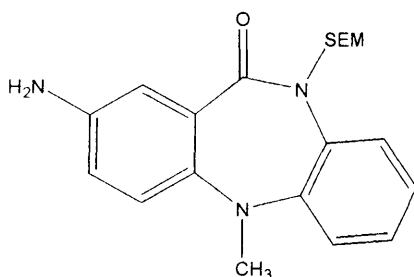
2.49 (1H, m, CH), 3.54-3.71 (1H, m, CH), 5.00 (2H, s, NH₂), 6.69 (1H, dd, J = 2.8, 8.5, Ar-H), 6.89 (1H, d, J = 8.5, Ar-H), 6.98-7.10 (5H, m, Ar-H), 10.00 (1H, s, CONH); δ_C 18.0, 25.8, 32.9, 54.2, 114.7, 117.9, 119.6, 119.8, 121.1, 123.2, 124.2, 129.0, 133.6, 141.3, 144.4, 144.7, 168.7 (C=O); HRMS (ES⁺) m/z 294.1599 [(M+H), 294.1601 calculated for C₁₈H₂₀N₃O].

7-(Methyl)-4-nitro-1-(2-trimethylsilyloxyethyl)dibenzo[2,3-b][6,7-f]diazepin-2-one, (105)



Method G. (**82**) (1.09 g, 2.83 mmol), sodium hydride (0.07 g, 3.11 mmol), methyl iodide (0.48 g, 3.39 mmol) in DMA (3.5 mL) produced the title compound as a yellow solid (2.10 g, 83 %); m.p. 78-80 °C; δ_H 0.00 (9H, s, SiCH₃), 0.90 (2H, t, J = 8.0, CH₂), 3.45 (3H, s, CH₃), 3.66-3.70 (2H, m, CH₂), 5.32 (1H, d, J = 10.3, NCHO), 5.42 (1H, d, J = 10.3, NCHO), 7.28-7.32 (2H, m, Ar-H), 7.41-7.46 (2H, m, Ar-H), 7.64 (1H, dd, J = 1.8, 7.7, Ar-H), 8.34 (1H, dd, J = 2.8, 9.1, Ar-H), 8.44 (1H, d, J = 2.8, Ar-H); δ_C 0.0 (SiCH₃), 18.8, 39.1, 66.9, 79.1, 119.3, 121.5, 125.5, 126.9, 127.9, 128.1, 128.7, 128.9, 135.6, 143.3, 147.6, 160.0, 168.1 (C=O); MS (ES⁺) m/z 422.2 (M+Na).

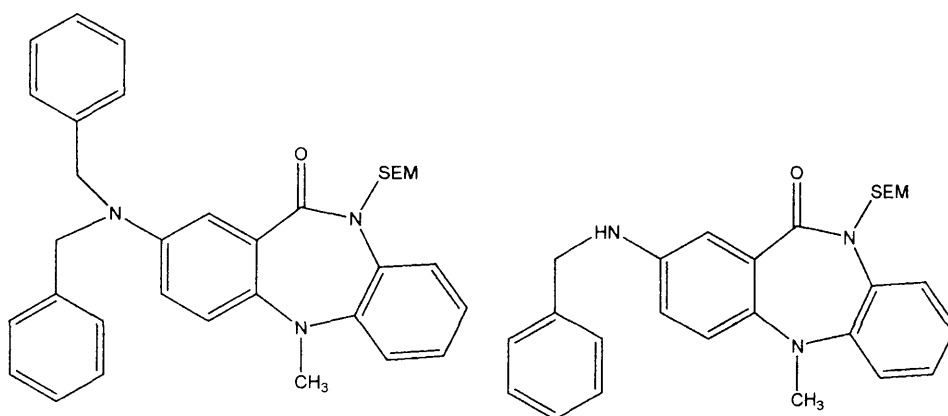
4-Amino-7-(methyl)-1-(2-trimethylsilyloxyethyl)dibenzo[2,3-b][6,7-f]diazepin-2-one, (106)



Method J. (**105**) (2.09 g, 5.23 mmol) in dichloromethane (70 mL) produced the product as a brown oil (1.43 g, 73 %); δ_H 0.00 (9H, s, SiCH₃), 0.89 (2H, t, J = 8.0 Hz, CH₂), 3.21

(3H, s, CH_3), 3.65 (2H, t, $J = 2.0$, CH_2), 5.16 (1H, d, $J = 10.1$, NCHO), 5.23 (2H, br s, NH_2), 5.41 (1H, d, $J = 10.1$, NCHO), 6.72 (1H, dd, $J = 2.8$, 8.6, Ar-H), 6.87 (1H, d, $J = 2.8$, Ar-H), 6.94 (1H, d, $J = 8.6$, Ar-H), 7.12 (1H, t, $J = 6.6$, Ar-H), 7.19-7.25 (2H, m, Ar-H), 7.53 (1H, dd, $J = 0.8$, 7.9, Ar-H); δ_{C} 0.0 (SiCH_3), 18.9, 37.9, 66.6, 79.0, 116.8, 118.3, 119.2, 119.4, 124.8, 125.1, 127.4, 128.9, 136.5, 144.9, 145.8, 150.5, 170.2 ($\text{C}=\text{O}$); MS (ES^+) m/z 392.2 ($\text{M}+\text{Na}$).

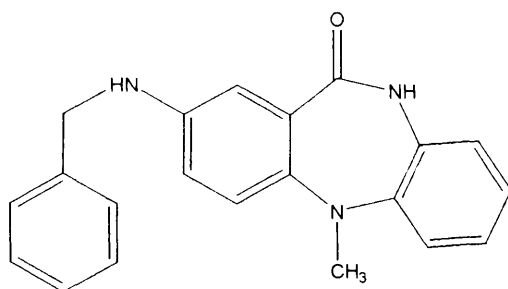
4,4-Dibenzylamino-7-(methyl)-1-(2-trimethylsilylethoxymethyl)dibenzo[2,3-*b*] [6,7-*f*] diazepin-2-one, (107), 4-benzylamino-7-(methyl)-1-(2-trimethylsilylethoxymethyl) dibenzo[2,3-*b*] d[6,7-*f*]iazepin-2-one, (108)



Method K. (106) (0.61 g, 1.66 mmol), benzyl bromide (0.31, 1.82 mmol), potassium carbonate (0.25 g, 1.82 mmol) and DMF (3 mL) were heated at 150 °C for 24 h, followed by column chromatography (eluent 9.5:1.5 petrol:ethyl acetate) yielded the dibenzylated compound (107) as a yellow powder (0.43 g, 56 %), then increasing to 9:1 petrol:ethyl acetate yielded the desired compound (108) as a yellow oil (0.09 g, 12 %), data for compound 107: m.p. 125-127 °C; δ_{H} 0.00 (9H, s, SiCH_3), 0.83 (2H, t, $J = 8.0$, CH_2), 3.14 (3H, s, CH_3), 3.57 (2H, t, $J = 8.0$, CH_2), 4.65 (4H, s, $2 \times \text{PhCH}_2$), 5.12 (1H, d, $J = 10.1$, NCHO), 5.32 (1H, d, $J = 10.1$, NCHO), 6.76 (1H, dd, $J = 3.1$, 9.0, Ar-H), 6.90 (1H, d, $J = 3.1$, Ar-H), 6.96 (1H, d, $J = 9.0$, Ar-H), 7.08 (1H, t, $J = 7.8$, Ar-H), 7.17-7.33 (12H, m, Ar-H), 7.47 (1H, d, $J = 7.8$, Ar-H); δ_{C} 0.0 (SiCH_3), 18.9, 32.1, 37.9, 55.8, 66.6, 79.0, 115.5, 117.7, 118.6, 119.4, 124.9, 125.2, 127.5, 127.9, 128.0, 128.2, 128.9, 129.9, 130.6, 130.9, 136.3, 140.2, 145.2, 145.6, 150.3, 170.1 ($\text{C}=\text{O}$), MS (ES^+) m/z 549.3551 (M); data for compound 108: δ_{H} 0.00 (9H, s, SiCH_3), 0.89 (2H, t, $J = 8.0$, CH_2), 3.18 (3H, s, CH_3), 3.64 (2H, t, $J = 8.0$, CH_2), 4.26 (2H, d, $J = 6.0$, PhCH_2), 5.16 (1H, d, $J = 10.1$, NCHO), 5.40

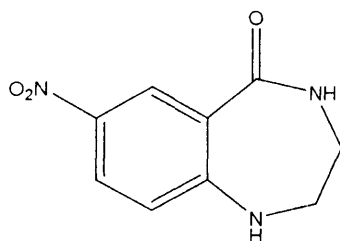
(1H, d, $J = 10.1$, NCH_O), 6.26 (1H, t, $J = 6.0$, Ar-H), 6.71 (1H, dd, $J = 2.8, 8.8$, Ar-H), 6.85 (1H, d, $J = 2.8$, Ar-H), 6.97 (1H, d, $J = 8.8$, Ar-H), 7.12 (1H, d, $J = 7.3$, Ar-H), 7.21-7.36 (7H, m, Ar-H), 7.53 (1H, d, $J = 7.3$, Ar-H); δ_C 0.0 (SiCH₃), 15.1, 37.9, 48.0, 66.6, 79.0, 115.3, 117.4, 118.4, 119.3, 124.8, 125.1, 127.4, 128.0, 128.4, 129.0, 129.7, 131.3, 136.4, 141.4, 145.0, 145.9, 150.4, 170.2 (C=O); MS (EI⁺) m/z 459.3 (M).

4-Benzylamino-7-(methyl)-1H-dibenzo[2,3-b][6,7-f]diazepin-2-one, (104)



Method C. (108) (0.17 g, 0.37 mmol) and 1 M tetrabutylammonium fluoride/THF solution (5 mL) were refluxed for 19 h, producing the title compound as a yellow powder (0.05 g, 41 %); m.p. 198-201 °C; δ_H 3.17 (3H, s, CH₃), 4.28 (2H, d, $J = 5.2$ Hz, CH₂Ph), 6.25 (1H, br t, NH), 6.74 (1H, d, $J = 7.6$ Hz, Ar-H), 6.91 (1H, s, Ar-H), 6.96 (1H, d, $J = 8.6$ Hz, Ar-H), 6.99-7.02 (2H, m, Ar-H), 7.08-7.14 (2H, m, Ar-H), 7.24-7.25 (1H, m, Ar-H), 7.32-7.35 (4H, m, Ar-H), 10.09 (1H, s, NH); δ_C 37.4, 46.6, 113.6, 116.4, 118.0, 118.2, 121.1, 123.1, 124.4, 126.6, 127.0, 127.7, 128.3, 132.3, 141.1, 142.4, 144.4, 145.4, 168.7 (C=O); HRMS (ES⁺) m/z 330.1598 [(M+H), 330.1601 calculated for C₂₁H₂₀N₃O₃].

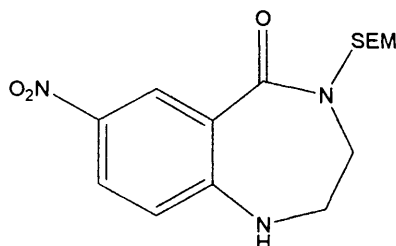
2,3-Dihydro-7-nitro-1H-4H-benzo[6,7-f]diazepin-5-one, (112)



Method I. (73) (8 g, 30.76 mmol), ethylenediamine, (111) (2.77 g, 46.15 mmol) and DMA (3 mL) were heated at 100 °C for 3 h, produced the product as an orange powder (3.74 g, 59 %); m.p. decomposed at 202 °C; δ_H 3.34 (2H, q, CH₂), 3.49 (2H, q, CH₂), 6.80 (1H, d, $J = 9.2$, Ar-H), 7.94 (1H, d, $J = 2.9, 9.2$, Ar-H), 8.13 (1H, t, NH), 8.36 (1H, t, NH), 8.73

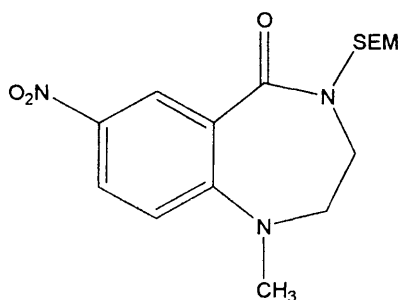
(1H, d, $J = 2.9$, Ar-H); δ_c 41.1 ($\underline{\text{CH}_2}$), 47.6 ($\underline{\text{CH}_2}$), 114.8, 118.7, 126.9, 131.6, 136.0, 152.1, 168.0 ($\underline{\text{C=O}}$); HRMS (ES⁺) m/z 209.2 [(M+H), 207.19 calculated for C₉H₁₀N₃O₃].

2,3-Dihydro-7-nitro-4-(2-trimethylsilyloxyethyl)-1H-benzo[6,7-f]diazepin-5-one, (113)



Method B. (**112**) (1.00 g, 4.83 mmol), sodium hydride (0.13 g, 5.31 mmol), SEM-Cl (1.21 g, 7.24 mmol) in DMF (3.5 mL), followed by column chromatography (eluent 3:2 petrol:ethyl acetate) yielded a yellow powder (0.45 g, 27 %); m.p. 157-160 °C; δ_H 0.00 (9H, s, SiCH₃), 0.90 (2H, t, $J = 8.1$, CH₂), 3.52-3.55 (4H, m, CH₂), 3.59-3.61 (2H, m, CH₂), 4.91 (2H, s, NCH₂O), 6.81 (1H, d, $J = 9.3$, Ar-H), 7.98 (1H, dd, $J = 2.9, 9.3$, Ar-H), 8.07 (1H, br t, NH), 8.64 (1H, d, $J = 2.9$, Ar-H); δ_c 0.0, 18.7, 46.5, 48.3, 66.1, 78.1, 116.4, 119.8, 128.0, 132.6, 137.2, 152.6, 168.8 ($\underline{\text{C=O}}$); MS (ES⁺) m/z 359.8 (M+Na).

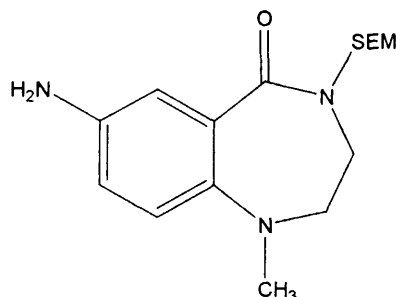
2,3-Dihydro-1-(methyl)-7-nitro-4-(2-trimethylsilyloxyethyl)benzo[6,7-f]diazepin-5-one, (121)



Method G. (**113**) (0.41 g, 1.20 mmol), sodium hydride (0.03 g, 1.32 mmol), methyl iodide (0.31 g, 2.19 mmol) in DMF (3.5 mL), produced the desired product as a yellow oil (0.38 g, 88 %); δ_H 0.00 (9H, s, SiCH₃), 0.91 (2H, t, $J = 8.1$, CH₂), 3.00 (3H, s, CH₃), 3.54 (2H, t, $J = 8.1$, CH₂), 3.56 (2H, t, $J = 5.8$, CH₂), 4.89 (2H, s, NCH₂O), 6.66-6.67 (1H, m, Ar-H),

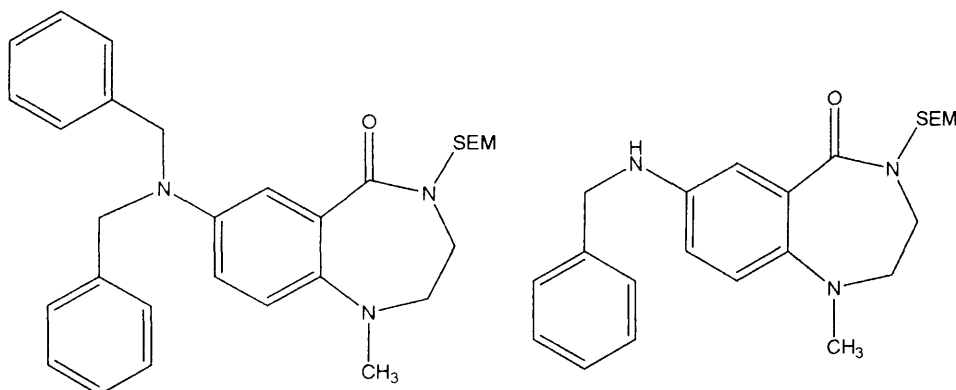
6.70-6.72 (2H, m, Ar-H); δ_c 0.0, 18.8, 32.1, 56.2, 59.6, 66.2, 76.7, 118.5, 124.6, 128.5, 129.5, 139.0, 152.9, 169.6 ($\underline{C=O}$); MS (ES⁺) m/z 352.2 (M+H).

7-Amino-2,3-dihydro-1-(methyl)-4-(2-trimethylsilylethoxymethyl)benzo[6,7-f]diazepin-5-one, (122)



Method J. (121) (0.33 g, 0.93 mmol) in dichloromethane (150 mL), produced the product as a yellow oil (0.31 g, 100 %); δ_H 0.00 (9H, s, SiCH₃), 0.90 (2H, t, J = 8.1, CH₂), 2.65 (3H, s, CH₃), 3.00 (2H, t, J = 5.8, CH₂), 3.25-3.29 (2H, m, CH₂), 3.54 (2H, t, J = 8.1, CH₂), 4.85 (2H, s, NH₂), 4.89 (2H, s, NCH₂O), 6.66-6.67 (1H, m, Ar-H), 6.70-6.72 (2H, m, Ar-H); δ_c 0.0, 18.9, 32.0, 56.2, 60.3, 65.6, 75.7, 116.1, 118.7, 119.7, 132.0, 138.2, 144.7, 172.1 ($\underline{C=O}$); MS (ES⁺) m/z 344.2 (M+Na).

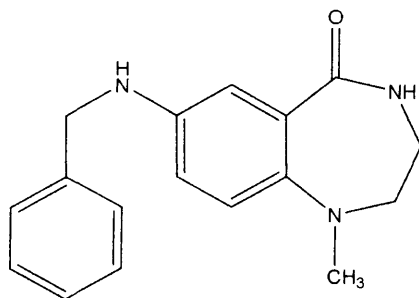
7,7-Dibenzylamino-2,3-dihydro-1-(methyl)-4-(2-trimethylsilylethoxymethyl)benzo[6,7-f]diazepin-5-one (123), 7-Benzylamino-2,3-dihydro-1-(methyl)-4-(2-trimethylsilylethoxymethyl)benzo[6,7-f]diazepin-5-one, (124)



Method K. (122) (0.50 g, 1.57 mmol), potassium carbonate (0.24 g, 1.72 mmol), benzyl bromide (0.27 g, 1.57 mmol) in DMF (3 mL), followed by column chromatography using 4:1 petrol:ethyl acetate as eluent produced the dibenzylated compound (123) as a brown

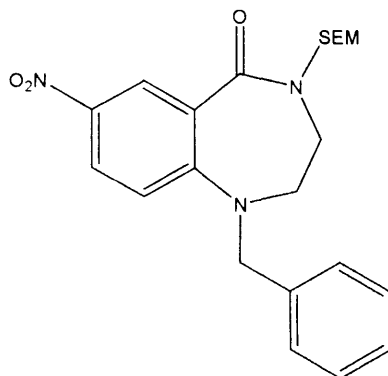
oil (0.25 g, 32 %), then increasing to 3.5:1.5 petrol:ethyl acetate yielded the desired compound (**124**) as a yellow oil (0.11 g, 17 %); data for compound **123**: δ_{H} 0.00 (9H, s, SiCH₃), 0.90 (2H, t, J = 10.0, CH₂), 2.68 (3H, s, CH₃), 3.06 (2H, t, J = 5.0, CH₂), 3.31-3.34 (2H, m, CH₂), 3.53 (2H, t, J = 7.5, CH₂), 4.66 (2×2H, s, CH₂Ph), 4.89 (2H, s, NCH₂O), 6.80 (2H, s, Ar-H), 6.85 (1H, s, Ar-H), 7.25-7.30 (6H, m, Ar-H), 7.34-7.37 (4H, m, Ar-H); δ_{C} 0.0, 18.8, 22.5, 51.5, 55.8, 59.0, 60.1, 65.6, 75.7, 127.8, 128.0, 128.1, 129.8, 130.1, 130.5, 130.8, 131.2, 132.9, 136.0, 137.4, 138.7, 140.2, 144.6, 164.5; MS (ES⁺) m/z 500.3286 (M-H); data for compound **124**: δ_{H} 0.00 (9H, s, SiCH₃), 0.90 (2H, t, J = 8.2, CH₂), 2.65 (3H, s, CH₃), 3.01 (2H, t, J = 5.9, CH₂), 3.29 (2H, m, CH₂), 3.53 (2H, t, J = 8.2, CH₂), 4.24 (2H, d, J = 6.1, CH₂-Ph), 4.89 (2H, s, CH₂), 6.09 (1H, t, J = 6.1, NH), 6.67 (1H, dd, J = 2.8, 8.7, Ar-H), 6.73-6.75 (2H, m, Ar-H), 7.23 (1H, t, J = 7.1, Ar-H), 7.31-7.37 (4H, m, Ar-H); δ_{C} 0.0, 18.9, 32.0, 46.3, 48.3, 60.3, 65.7, 75.7, 114.8, 116.7, 119.7, 128.0, 128.5, 129.6, 130.5, 132.7, 136.1, 138.3, 141.7, 145.0, 172.1 (C=O); MS (EI⁺) m/z 411.2 (M⁺).

7-Benzylamino-2,3-dihydro-1-(methyl)-4H-benzo[6,7-f]diazepin-5-one, (**120**)



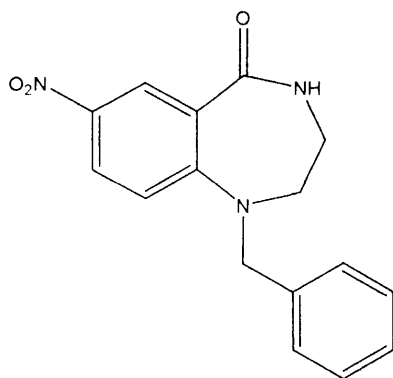
Method C. (**124**) (0.11 g, 0.27 mmol) and 1 M tetrabutylammonium fluoride/THF solution (5 mL) were refluxed for 18 h. Column chromatography (eluent 4:1 ethyl acetate:petrol) produced the title compound as a yellow oil (0.03 g, 40 %); δ_{H} 2.68 (3H, s, CH₃), 2.95 (2H, t, J = 5.8, CH₂), 3.05 (2H, q, J = 5.8, CH₂), 4.23 (2H, d, J = 5.8, CH₂Ph), 6.02 (1H, t, J = 5.8, NH), 6.64 (1H, dd, J = 2.9, 8.7, Ar-H), 6.71 (1H, s, Ar-H), 6.74 (1H, d, J = 2.9, Ar-H), 7.23 (1H, t, J = 7.2, Ar-H), 7.99 (1H, t, J = 5.8, CONH), 7.31-7.37 (4H, m, Ar-H); δ_{C} 46.9, 48.6, 59.7, 113.3, 115.1, 118.5, 126.5, 127.1, 128.2, 128.7, 130.7, 137.4, 142.4, 142.6, 171.6 (C=O); HRMS (EI⁺) m/z 282.1599 [(M+H), 282.1601 calculated for C₁₇H₂₀N₃O].

1-(Benzyl)-2,3-dihydro-7-nitro-4-(2-trimethylsilylethoxymethyl)benzo[6,7-f]diazepin-5-one, (114)



Method E. (113) (0.27 g, 0.80 mmol), benzylbromide (0.41 g, 2.40 mmol), potassium carbonate (0.55 g, 4.00 mmol) and DMF (3 mL) were heated at 150 °C for 20 h, followed by column chromatography (eluent 7:3 petrol:ethyl acetate) to yield the desired compound as a yellow oil (0.11 g, 32 %); δ_{H} 0.00 (9H, s, SiCH₃), 0.89 (2H, t, J = 8.0, CH₂), 3.54 (2H, t, J = 8.0, CH₂), 3.65 (2H, br t, CH₂), 3.70 (2H, br t, CH₂), 4.69 (2H, s, Ph-CH₂), 4.93 (2H, s, NCH₂O), 6.95 (1H, d, J = 9.3, Ar-H), 7.24-7.28 (3H, m, Ar-H), 7.34-7.37 (2H, m, Ar-H), 8.07 (1H, d, J = 9.3, Ar-H), 8.45 (1H, s, Ar-H), δ_{C} 0.0, 18.7, 45.6, 57.3, 58.1, 66.1, 77.0, 119.0, 124.1, 128.2, 128.6, 129.2, 130.1, 130.3, 137.7, 139.0, 152.2, 169.4 (C=O); MS MS (ES⁺) m/z 378.2 [(M-Si(CH₃)₃+Na)].

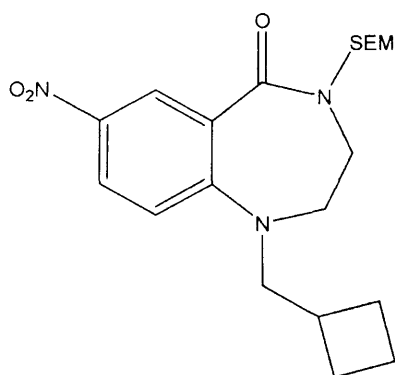
1-(Benzyl)-2,3-dihydro-7-nitro-1H-benzo[6,7-f]diazepin-5-one, (116)



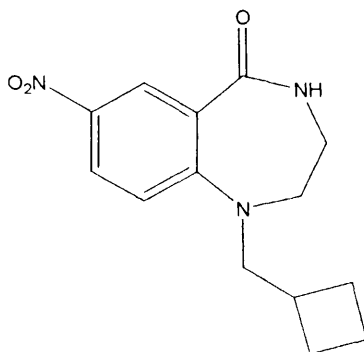
Method C. (114) (0.31 g, 0.73 mmol) and 1 M tetrabutylammonium fluoride/THF solution (5 mL) were refluxed for 20 h, followed by column chromatography (eluent 1:1 petrol:ethyl acetate) to produce the title compound as a yellow powder (0.06 g, 28 %); m.p. 199-201 °C; δ_{H} 2.94-2.96 (2H, m, CH₂), 3.42 (2H, br t, CH₂), 4.50 (2H, s, CH₂Ph),

6.64 (1H, d, $J = 9.4$, Ar-H), 7.00-7.06 (2H, m, Ar-H), 7.12-7.15 (3H, m, Ar-H), 7.79 (1H, dd, $J = 2.8, 9.4$, Ar-H), 8.27 (1H, br t, NH), 8.39 (1H, d, $J = 2.8$, Ar-H); δ_c 18.1, 56.6, 57.2, 117.0, 120.9, 126.6, 126.8, 127.2, 128.8, 129.4, 136.4, 137.1, 151.4, 168.3 ($\underline{C=O}$); MS (ES^+) m/z 320.1 (M+Na).

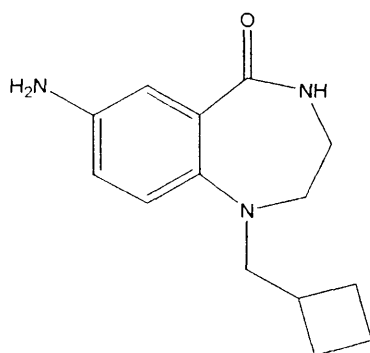
1-(Cyclobutylmethyl)-2,3-dihydro-7-nitro-4-(2-trimethylsilylethoxymethyl)benzo [6,7-f]diazepin-5-one, (115)



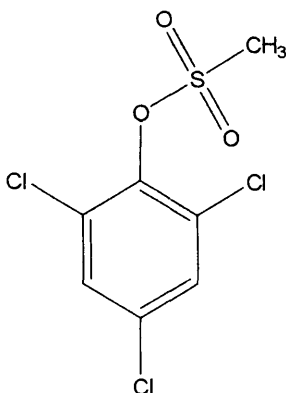
Method E. (113) (0.20 g, 0.59 mmol), cyclobutylmethyl bromide (0.53 g, 3.56 mmol), potassium carbonate (0.41 g, 2.96 mmol) and DMF (3 mL) were heated at 150 °C for 22 h, followed by column chromatography (eluent 9:1 petrol:ethyl acetate) to yield the desired compound as a yellow oil (0.10 g, 41 %); δ_H 0.00 (9H, s, SiCH₃), 0.91 (2H, t, $J = 7.5$, CH₂), 1.71-1.79 (2H, m, Alkyl-H), 1.81-1.87 (2H, m, Alkyl-H), 2.01-2.03 (2H, m, Alkyl-H), 2.65 (1H, t, $J = 7.5$, CH₂), 3.46 (2H, d, $J = 6.8$, CH₂), 3.54 (2H, t, $J = 7.5$, CH₂), 3.58-3.61 (4H, m, CH₂), 4.91 (2H, s, NCH₂O), 7.06 (1H, d, $J = 9.0$, Ar-H), 8.12 (1H, d, $J = 9.0$, Ar-H), 8.41 (1H, s, Ar-H); δ_c 0.0, 18.8, 19.4, 27.6, 32.01, 34.5, 45.8, 59.2, 66.2, 77.0, 118.9, 124.4, 128.2, 130.1, 138.7, 152.3, 169.4 ($\underline{C=O}$); MS (ES^+) m/z 428.2 (M+Na).

1-(Cyclobutylmethyl)-2,3-dihydro-7-nitro-4H-benzo[6,7-f]diazepin-5-one, (117)

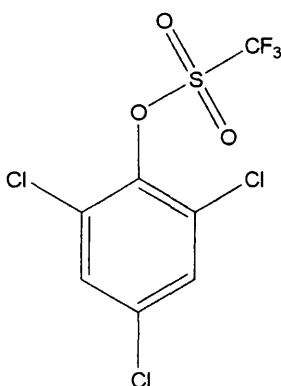
Method C. (115) (0.90 g, 2.20 mmol) and 1 M tetrabutylammonium fluoride/THF solution (4 mL) were refluxed for 24 h, followed by column chromatography (eluent 2:3 petrol:ethyl acetate) to produce the title compound as a yellow oil (0.1 g, 17 %); δ_{H} 1.71-1.90 (6H, m, Alkyl-H), 1.97-2.02 (2H, m, Alkyl-H), 2.65-2.70 (1H, m, Alkyl-H), 3.52 (2H, d, $J = 7.0$, CH_2), 3.60 (2H, br t, CH_2), 7.02 (1H, d, $J = 9.5$, Ar-H), 8.07 (1H, d, $J = 9.5$, Ar-H), 8.41 (1H, br t, NH), 8.64 (1H, s, Ar-H); δ_{C} 18.1, 20.4, 26.2, 33.3, 57.3, 58.4, 116.7, 120.6, 126.6, 129.7, 136.6, 151.3, 168.1 ($\text{C}=\text{O}$); MS (ES^+) m/z 298.1 [(M+Na)].

7-Amino-1-(cyclobutylmethyl)-2,3-dihydro-4H-benzo[6,7-f]diazepin-5-one, (119)

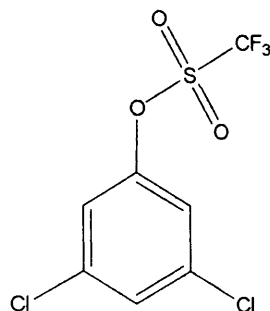
Method J. (117) (0.026 g, 0.094 mmol) in methanol (5 mL) produced the product as a brown oil (0.023 g, 99 %); δ_{H} 1.60-1.67 (2H, m, Alkyl-H), 1.77-1.84 (2H, m, Alkyl-H), 1.95-1.97 (2H, m, Alkyl-H), 2.46-2.49 (1H, m, Alkyl-H), 2.90-2.92 (2H, m, CH_2), 2.98-3.02 (4H, m, CH_2), 4.80 (2H, s, NH_2), 6.62 (1H, d, $J = 8.6$, Ar-H), 6.67-6.70 (2H, m, Ar-H), 7.90 (1H, br t, NH); δ_{C} 18.1, 22.6, 26.4, 33.5, 57.9, 58.3, 114.4, 116.8, 119.8, 131.6, 136.7, 143.3, 171.7 ($\text{C}=\text{O}$); HRMS (ES^+) m/z 268.1417 [(M+Na), 268.1420 calculated for $\text{C}_{14}\text{H}_{19}\text{ON}_3\text{Na}$].

Methanesulfonic acid 2,4,6-trichlorophenolate (136)

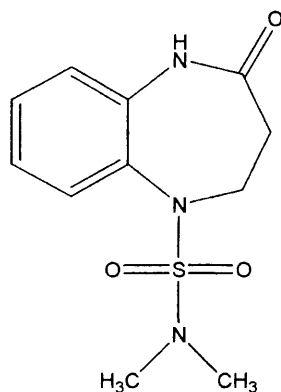
Method L. 2,4,6-Trichlorophenol (2.00 g, 10.13 mmol) and methanesulfonyl chloride (2.32 g, 20.26 mmol) in tetrahydrofuran (45 mL), followed by the addition of triethylamine (TEA) (3.07 g, 30.39 mmol) produced the desired product as a brown solid (2.78 g, 100 %); δ_{H} 3.71 (3H, s, CH_3), 7.90 (2H, s, Ar-H); δ_{C} 40.9, 129.4, 130.1, 132.3, 141.6 (C-O).

Trifluoromethanesulfonic acid 2,4,6-trichlorophenolate (139)

Method L. 2,4,6-Trichlorophenol (1.50 g, 7.60 mmol) and trifluoromethanesulfonyl chloride (1.92 g, 11.40 mmol) in tetrahydrofuran (20 mL), followed by the addition of triethylamine (TEA) (2.31 g, 22.79 mmol) produced the desired product as a clear oil (2.50 g, 100 %); δ_{H} 8.10 (2H, Ar-H); δ_{C} 119.1, 128.8, 130.2, 134.4, 140.6.

Trifluoromethanesulfonic acid 3,5-dichlorophenolate (143)

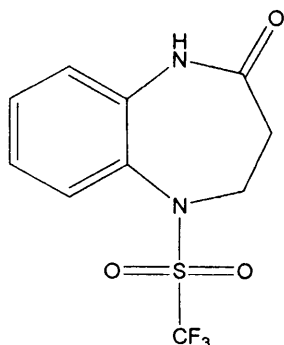
Method L. 3,5-Dichlorophenol (1.50 g, 9.20 mmol) and trifluoromethanesulfonyl chloride (3.10 g, 18.40 mmol) in tetrahydrofuran (20 mL), followed by the addition of triethylamine (TEA) (2.79 g, 27.60 mmol). The required product was obtained using a column chromatography (eluent 100% petrol) as a clear oil (1.63 g, 60 %); δ_{H} 7.83 (2H, s, Ar-H), 7.86 (1H, s, Ar-H); δ_{C} 30.63, 116.85, 119.40, 121.28, 129.31, 135.22, 149.15.

3,4-Dihydro-5-(sulfonic acid dimethylamide)-1H-benzo[2,3-b]diazepin-2-one, (129)

To a solution of 3,4-dihydro-1H-5H-benzo[2,3-b]diazepin-2-one, (26) (0.50 g, 3.08 mmol) and *N,N*-dimethylsulfamoyl chloride (0.49 g, 3.39 mmol) in DMF (4 mL) under nitrogen was added aluminium chloride (AlCl_3) (0.41 g, 3.08 mmol). The resultant solution was stirred overnight at room temperature. Water (50 mL) was added and the organic phase was extracted with ethyl acetate (3×50 mL), dried (MgSO_4), filtered and evaporated to leave the title compound as an off-white solid (0.1 g, 12 %); m.p. 142-145 °C; δ_{H} 2.40 (2H, t, $J = 6.9$, CH_2), 2.69 (6H, s, N- CH_3), 3.96 (2H, t, $J = 6.9$, CH_2), 7.10 (1H, d, $J = 7.9$, Ar-H), 7.20 (1H, t, $J = 6.9$, Ar-H), 7.34 (1H, t, $J = 6.9$, Ar-H), 7.47 (1H, d, $J = 6.9$, Ar-H), 9.85 (1H, s, NH); δ_{C} 33.3, 37.6 (N- CH_3), 51.0, 122.5, 125.0, 128.5, 130.1,

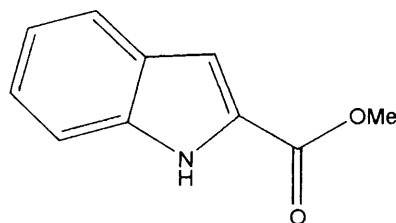
131.5, 137.7, 171.7 ($\underline{\text{C}}=\text{O}$); HRMS (ES^+) m/z 287.1169 [($\text{M}+\text{NH}_4$)], 287.1172 calculated for $\text{C}_{11}\text{H}_{19}\text{O}_3\text{N}_4\text{S}$].

3,4-Dihydro-5-(trifluoromethanesulfonyl)-1H-benzo[2,3-b]diazepin-2-one, (132)



To a solution of 3,4-dihydro-1H-5H-benzo[2,3-b]diazepin-2-one (**26**) (0.50 g, 3.08 mmol) and methanesulfonyl chloride (0.35 g, 3.08 mmol) in THF (20 mL) under nitrogen was added trifluoroacetic anhydride (0.65 g, 0.44 mmol). The resultant solution was stirred overnight at room temperature. Water (50 mL) was added and the organic phase was extracted with ethyl acetate (3 × 50 mL), dried (MgSO_4), filtered and evaporated to leave the title compound as an off-white solid (0.49 g, 54 %); m.p. 138-140 °C; δ_{H} 2.35 (1H, dd, $J = 5.1, 13.8$, $\underline{\text{CH}}$), 2.56-2.63 (1H, m, $\underline{\text{CH}}$), 3.72 (1H, q, $J = 7.4$, $\underline{\text{CH}}$), 4.64 (1H, dt, $J = 5.5$, $\underline{\text{CH}}$), 7.17 (1H, d, $J = 7.9$, $\underline{\text{Ar-H}}$), 7.27 (1H, t, $J = 7.9$, $\underline{\text{Ar-H}}$), 7.41 (1H, d, $J = 7.9$, $\underline{\text{Ar-H}}$), 7.47 (1H, t, $J = 7.9$, $\underline{\text{Ar-H}}$); δ_{C} 32.0, 49.3, 114.7, 122.5, 125.1, 129.2, 129.7, 130.4, 137.3, 171.0 ($\underline{\text{C}}=\text{O}$); MS (ES^+) m/z 294.1 (M).

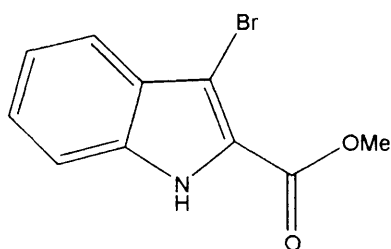
Methyl-1H-indole-2-carboxylate (147) (Jorgensen *et al.*, 2005)



Method H. Indole-2-carboxylic acid (2.00 g, 12.41 mmol), methanol (50 mL) and concentrated sulphuric acid (2 mL), produced the product as a yellow powder (2.08 g, 95 %); m.p. 150-152 °C; δ_{H} 3.89 (3H, s, $\underline{\text{CH}_3}$), 7.09 (1H, t, $J = 7.6$, $\underline{\text{Ar-H}}$), 7.17 (2H, s, $\underline{\text{Ar-H}}$),

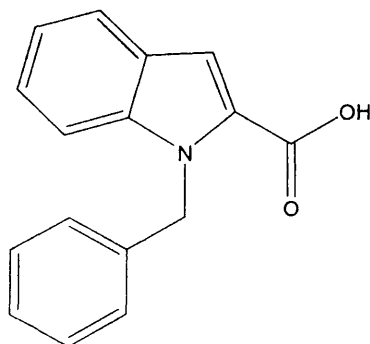
7.28 (1H, t, $J = 7.6$, Ar-H), 7.47 (1H, dd, $J = 0.6, 8.3$, Ar-H), 11.95 (1H, br s, NH); δ_C 52.1, 108.1, 112.9, 120.5, 122.4, 125.0, 127.1, 127.4, 137.7, 162.1 (C=O); MS (ES⁻) 173.9 m/z (M-H).

Methyl 3-bromo-1H-indole-2-carboxylate (148) (Barker *et al.*, 1999)



To a suspension of methyl-1H-indole-2-carboxylate (**147**) (2.00 g, 11.46 mmol) in DMF (8 mL) under nitrogen, a solution of N-bromosuccinamide (NBS) (2.24 g, 12.58 mmol) in DMF (2 mL) was added dropwise and the reaction was left stirring overnight. Ice was added, and the resulting precipitate was filtered and washed with water to produce the title compound as an off-white solid (2.76 g, 95 %); m.p. 148-150 °C; δ_H 3.92 (3H, s, CH₃), 7.21 (1H, t, Ar-H), 7.37 (1H, t, $J = 7.5$, Ar-H), 7.51 (1H, d, $J = 8.3$, Ar-H), 7.56 (1H, d, $J = 8.3$, Ar-H), 12.31 (1H, s, NH); δ_C 52.4, 96.4, 113.4, 120.5, 121.6, 124.1, 126.4, 127.1, 136.2, 160.9 (C=O); MS (ES⁻) m/z 251.9 (M-H).

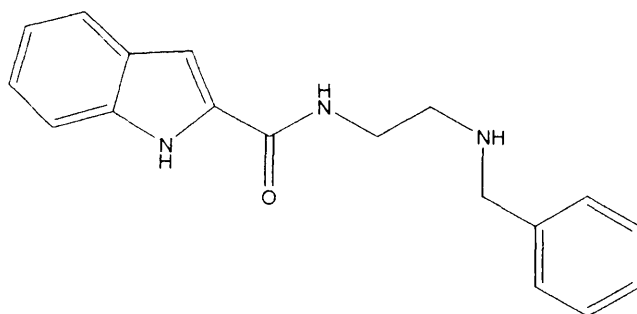
1-Benzyl indole-2-carboxylic acid (152) (Olgen *et al.*, 2001)



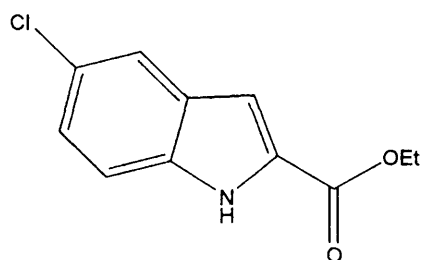
Methyl-1H-indole-2-carboxylate (**147**) (3.09 g, 17.40 mmol) was dissolved in THF (40 mL) under nitrogen and cooled to 0 °C. Sodium hydride (1.4 g, 58.33 mmol) was added slowly over a period of 10 min and stirred for 1 h. Benzyl bromide (4.54 g, 26.54 mmol) was added dropwise to the mixture, which was then left to stir for a further 3h. Distilled

water was added to destroy the sodium hydride and the solvents were evaporated. The residue was dissolved in MeOH (30 mL) and NaOH (4 M, 30 mL). The mixture was stirred at 80 °C for 6h. After the mixture had cooled to room temperature the solvents were evaporated and water was added to dissolve the remaining mixture. This was followed by dropwise addition of concentrated HCl to pH2, and the resultant solution was extracted with ethyl acetate, and dried over MgSO₄. The solvent was evaporated under the reduced pressure, producing the desired product as a pale yellow solid (4.74 g, 81 %); m.p. 125-148 °C; δ_{H} 5.89 (2H, s, CH₂), 7.03 (1H, d, J = 7.7, Ar-H), 7.07-7.31 (4H, m, Ar-H), 7.34 (1H, s, Ar-H), 7.45 (1H, d, J = 8.2, Ar-H), 7.54 (1H, d, J = 8.2, Ar-H), 7.65 (1H, d, J = 8.2, Ar-H), 7.72 (1H, d, J = 8.2, Ar-H), 12.98 (1H, br s, COOH); δ_{C} 47.2, 110.8, 111.6, 121.0, 122.7, 125.3, 125.9, 126.6, 127.3, 128.5, 128.8, 139.0, 139.3, 163.3 (C=O); MS (ES⁻) *m/z* 249.8 (M-1).

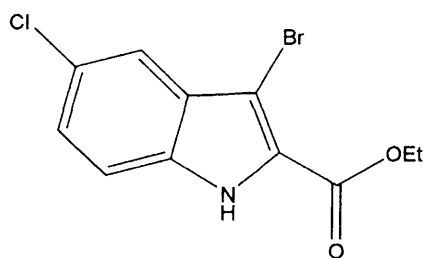
(2-Benzylamine)-(1H-indolo-2-carboxamido)ethyl amine (156)



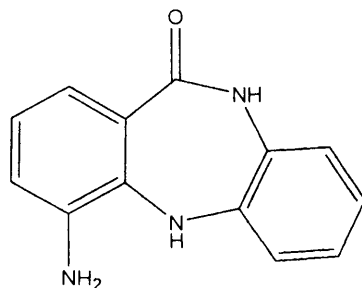
N-Benzylethylenediamine (155) (0.20 g, 1.33 mmol) and 4-dimethylaminopyridine (DMAP) (0.12 g, 0.98 mmol) were dissolved in dichloromethane (20 mL) at 0 °C. To this was added indole-2-carboxylic acid (0.2 g, 1.24 mmol) in DCM (2 mL), then 1-(3-dimethylaminopropyl)-3-ethyl carbodiimide.HCl (EDCI) (0.26 g, 1.36 mmol) in DCM (2 mL) was added. The mixture was stirred for 4 h at 0 °C, then allowed to reach to room temperature, and stirred for a further 24 h. The solvent was evaporated and water was added. The precipitate was filtered and washed with water, producing the title compound as a white solid (0.064 g, 18 %); m.p. 250-253 °C; δ_{H} 3.66 (4H, s, 2 × CH₂), 4.99 (2H, br s, CH₂-Ph), 7.08 (1H, t, J = 7.4, Ar-H), 7.13 (1H, s, Ar-H), 7.22 (1H, t, J = 7.4, Ar-H), 7.34-7.51 (6H, m, Ar-H), 7.66 (1H, d, J = 8.1, Ar-H), 8.73 (1H, s, NH), 11.48 (1H, s, NH); δ_{C} 14.1, 20.2, 59.7, 102.5, 112.1, 112.3, 119.7, 121.5, 123.3, 123.4, 127.1, 127.3, 128.7, 129.6, 131.5, 135.9, 136.4, 161.4; MS (ES⁺) *m/z* 294.2 (M+H).

Ethyl 5-chloro-1H-indole-2-carboxylate (160) (Rydon and Tweddle, 1955)

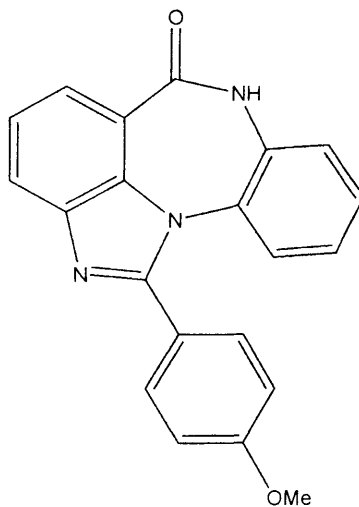
Method H. 5-Chloroindole-2-carboxylic acid (1.00 g, 5.11 mmol), ethanol (30 mL) and concentrated sulphuric acid (2 mL), produced the product as a brown powder (1.13 g, 99 %); m.p. 167-170 °C; δ_{H} 1.37 (3H, t, $J = 7.1$, CH_3), 4.38 (2H, q, $J = 7.1$, CH_2), 7.15 (1H, s, Ar-H), 7.29 (1H, dd, $J = 2.0, 8.8$ Hz, Ar-H), 7.50 (1H, d, $J = 8.8$, Ar-H), 7.76 (1H, d, $J = 2.0$, Ar-H), 12.12 (1H, s, NH); δ_{C} 14.6, 61.0, 107.5, 114.6, 121.4, 125.0, 125.2, 128.1, 129.2, 136.1, 161.4.

Ethyl 3-bromo-5-chloro-1H-indole-2-carboxylate (161) (Hiremath *et al.*, 1984)

To a suspension of ethyl-1H-5-chloroindole-2-carboxylate (**160**) (1.00 g, 4.80 mmol) in DMF (18 mL) under nitrogen, a solution of *N*-bromosuccinamide (NBS) (0.94 g, 5.28 mmol) in DMF (2 mL) was added dropwise to the reaction and the reaction was left stirring overnight. Ice was added, and the resulting precipitate was filtered and washed with water to produce the title compound as an off white powder (1.40 g, 100 %); m.p. 190-194 °C; δ_{H} 1.38 (3H, t, $J = 7.1$, CH_3), 4.40 (2H, q, $J = 7.1$, CH_2), 7.38 (1H, dd, $J = 2.0, 8.8$, Ar-H), 7.53 (1H, d, $J = 8.8$, Ar-H), 7.56 (1H, d, $J = 2.0$, Ar-H), 12.46 (1H, s, NH); δ_{C} 14.5, 61.4, 95.3, 115.4, 119.4, 125.8, 126.2, 126.6, 128.1, 134.6, 160.2.

6-Amino-1*H*-7*H*-dibenzo[2,3-*b*][6,7-*f*]diazepin-2-one, (168) (Lubisch *et al.*, 2003)

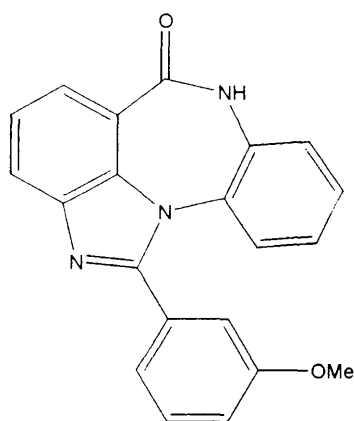
Method J. (**167**) (0.30 g, 1.18 mmol) in methanol (120 mL) produced the product as a white solid (0.27 g, 100 %); m.p. 206-208 °C; δ_{H} 5.23 (2H, s, NH_2), 6.66 (1H, s, NH), 6.71 (1H, t, $J = 7.5$, Ar-H), 6.78 (1H, d, $J = 7.5$, Ar-H), 6.89-6.98 (5H, m, Ar-H), 9.85 (1H, s, CONH); δ_{C} 118.2, 119.4, 121.0, 121.4, 121.9, 124.0, 124.2, 125.9, 131.2, 135.8, 138.4, 140.9, 168.9 (C=O); MS (ES⁺) m/z 248.1 (M+Na).

1-(4'-Methoxyphenyl)benzo[*b*]imidazo[4,5,1-*j,k*] [1,4]benzodiazepin-6(7*H*)-one (172)
(Lubisch *et al.*, 2003)

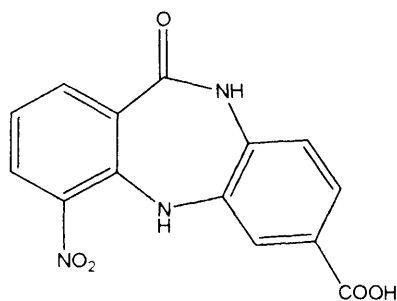
Method M. (**168**) (0.25 g, 1.13 mmol), sodium hydrogen sulfite (0.17 g, 1.66 mmol), 4-methoxybenzaldehyde (**170**) (0.15 g, 1.13 mmol) and DMA (5 mL), were heated at 140 °C for 20 h producing the product as a yellow solid (0.19 g, 50 %); m.p. 199-201 °C; δ_{H} 3.82 (3H, s, CH_3), 6.68 (1H, d, $J = 8.6$, Ar-H), 6.88 (1H, t, $J = 7.8$, Ar-H), 7.06 (2H, d, $J = 8.6$, Ar-H), 7.21 (1H, t, $J = 7.8$, Ar-H), 7.36 (1H, d, $J = 7.8$, Ar-H), 7.41 (1H, t, $J = 7.8$, Ar-H), 7.74 (2H, d, $J = 8.6$, Ar-H), 7.88 (1H, d, $J = 7.00$, Ar-H), 7.93 (1H, d, $J = 7.8$, Ar-H), 10.25 (1H, s, NH), δ_{C} 55.3 (OCH_3), 114.4, 117.9, 122.4, 123.5, 123.8, 124.4, 125.2,

125.7, 127.1, 128.6, 130.5, 130.6, 130.7, 139.7, 142.9, 154.3, 161.0, 165.5 ($\underline{\text{C}}=\text{O}$); HRMS (ES^+) m/z 342.1240 [(M+H), 342.1237 calculated for $\text{C}_{21}\text{H}_{16}\text{O}_2\text{N}_3$]; CHN for $\text{C}_{21}\text{H}_{15}\text{N}_3\text{O}_2 \cdot 0.4 \text{ H}_2\text{O}$ found C 72.31 %, H 4.53 %, N 11.70 %, calculated C 72.38 %, H 4.70 %, N 11.95 %.

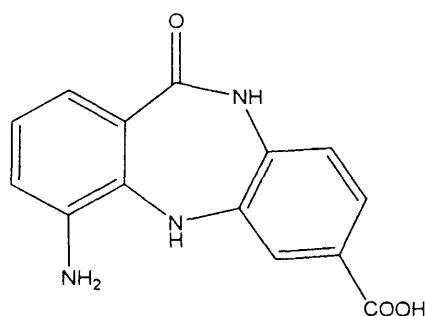
1-(3'-Methoxyphenyl)benzo[*b*]imidazo[4,5,1-*j,k*] [1,4]benzodiazepin-6(7*H*)-one (171)
(Lubisch *et al.*, 2003)



Method M. (**168**) (0.44 g, 1.96 mmol), sodium hydrogen sulfite (0.30 g, 2.89 mmol), 3-methoxybenzaldehyde (**169**) (0.24 g, 1.96 mmol) and DMA (6 mL), were heated at 140 °C for 20 h producing the product as an orange/yellow solid (0.19 g, 50 %); m.p. 188-194 °C; δ_{H} 3.81 (3H, s, $\underline{\text{C}}\text{H}_3$), 6.69 (1H, d, $J = 8.2$, Ar- $\underline{\text{H}}$), 6.91 (1H, t, $J = 7.7$, Ar- $\underline{\text{H}}$), 7.13 (1H, dd, $J = 1.78, 8.2$, Ar- $\underline{\text{H}}$), 7.22 (1H, t, $J = 7.7$, Ar- $\underline{\text{H}}$), 7.30 (1H, d, $J = 7.7$, Ar- $\underline{\text{H}}$), 7.38 (1H, d, $J = 8.2$, Ar- $\underline{\text{H}}$), 7.41 (1H, d, $J = 2.0$, Ar- $\underline{\text{H}}$), 7.42 (1H, s, Ar- $\underline{\text{H}}$), 7.46 (1H, t, $J = 7.7$, Ar- $\underline{\text{H}}$), 7.93 (1H, d, Ar- $\underline{\text{H}}$), 7.99 (1H, d, Ar- $\underline{\text{H}}$), 10.24 (1H, s, $\underline{\text{N}}\text{H}$); δ_{C} 55.3 ($\underline{\text{O}}\underline{\text{C}}\underline{\text{H}}_3$), 114.1, 116.4, 118.0, 121.5, 123.7, 124.0, 124.3, 125.5, 126.2, 127.2, 130.0, 130.1, 130.5, 131.6, 139.5, 142.8, 154.1, 159.4, 165.3 ($\underline{\text{C}}=\text{O}$); HRMS (ES^+) m/z 342.1233 [(M+H), 342.1237 calculated for $\text{C}_{21}\text{H}_{16}\text{O}_2\text{N}_3$].

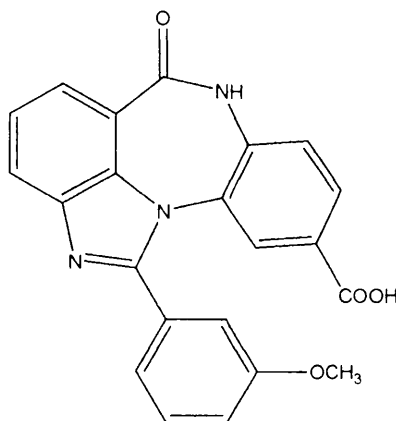
6-Nitro-9-carboxy-1*H*-7*H*-dibenzo[2,3-*b*][6,7-*f*]diazepin-2-one (184)

Method I. (**166**) (0.50 g, 1.92 mmol), 3,4-diaminobenzoic acid (0.56 g, 3.84 mmol) and DMA (3 mL), were heated at 100 °C for 13 h followed by recrystallization from hot methanol, produced the product as a dark brown solid (0.15 g, 26 %); m.p. > 360 °C; δ_{H} 7.15 (2H, m, Ar-H), 7.60 (1H, d, $J = 1.5$, Ar-H), 7.64 (1H, dd, $J = 1.7, 8.2$, Ar-H), 8.06 (1H, dd, $J = 1.4, 7.7$, Ar-H), 8.21 (1H, dd, $J = 1.6, 8.0$, Ar-H), 8.84 (1H, s, NH), 10.65 (1H, s, NH), 12.94 (1H, s, COOH); δ_{C} 121.0, 121.2, 123.9, 126.1, 126.9, 127.4, 129.9, 134.9, 135.3, 136.8, 138.7, 144.2, 166.2 (C=O), 166.5 (C=O); MS (CI) m/z (299.2) (M).

6-Amino-9-carboxy-1*H*-7*H*-dibenzo[2,3-*b*][6,7-*f*]diazepin-2-one (185)

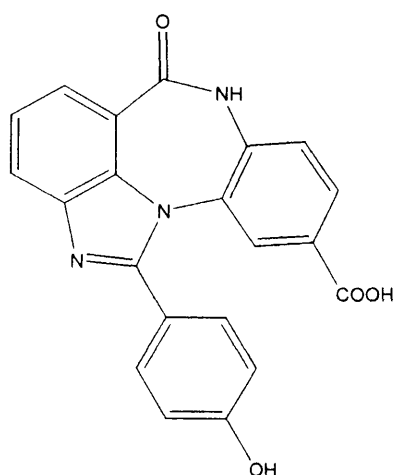
Method J. (**184**) (1.70 g, 5.68 mmol) in methanol (150 mL) produced the product as a dark brown solid (1.08 g, 71 %); m.p. > 360 °C; δ_{H} 5.34 (2H, br s, NH₂), 6.73 (1H, t, $J = 7.7$ Hz, Ar-H), 6.60 (1H, dd, $J = 1.2, 7.7$, Ar-H), 6.85 (1H, s, Ar-H), 6.90 (1H, dd, $J = 1.2, 7.7$, Ar-H), 7.04 (1H, d, $J = 8.2$, Ar-H), 7.51 (1H, dd, $J = 1.6, 8.2$, Ar-H), 7.77 (1H, s, NH), 10.14 (1H, s, CONH), 12.73 (1H, br s, COOH); δ_{C} 118.5, 119.4, 120.6, 122.2, 122.5, 124.5, 125.7, 126.4, 135.0, 135.5, 138.5, 140.2, 166.9 (C=O), 168.8 (C=O).

1-(3'-Methoxyphenyl)benzo[*b*]imidazo[4,5,1-*jk*]-10-carboxy[1,4]benzodiazepin-6(7*H*)-one (186)



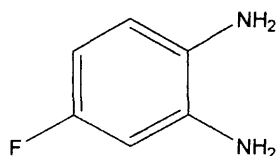
Method M. (**185**) (0.78 g, 2.99 mmol), sodium hydrogen sulfite (0.45 g, 4.35 mmol), 3-methoxybenzaldehyde (0.35 g, 2.90 mmol) and DMA (6 mL) were heated at 140 °C for 8 h. The precipitate produced was recovered by filtration and dried under vacuum, forming a pale brown solid (1.11 g), which was recrystallized from methanol. This was left for 2 h at which time the precipitate formed was recovered by filtration. This was again dissolved using ethanol and left to cool, yielding a white, papery, translucent solid; m.p. 330-334 °C; δ_{H} 3.78 (3H, s, CH₃), 7.12 (1H, dd, J = 2.8, 8.3, Ar-H), 7.29 (1H, s, Ar-H), 7.31 (1H, d, J = 1.9, Ar-H), 7.41 (1H, d, J = 8.3, Ar-H), 7.44 (1H, t, J = 1.9, Ar-H), 7.46 (1H, s, Ar-H), 7.48 (1H, s, Ar-H), 7.73 (1H, dd, J = 2.1, 8.3, Ar-H), 7.94 (1H, d, J = 7.0, Ar-H), 8.00 (1H, d, J = 7.7, Ar-H), 10.52 (1H, s, NH), 12.68 (1H, s, COOH); δ_{C} 55.3 (OCH₃), 113.9, 116.6, 117.6, 121.5, 123.4, 123.8, 124.3, 126.2, 126.4, 126.8, 128.0, 129.4, 130.3, 131.3, 134.6, 139.0, 142.8, 154.0, 159.5, 164.8 (C=O), 165.6 (C=O); HRMS (ES⁺) *m/z* 386.1141 [(M+H), 386.1135 calculated for C₂₂H₁₆N₃O₄].

1-(4'-Hydroxyphenyl)benzo[*b*]imidazo[4,5,1-*jk*]-10-carboxy[1,4]benzodiazepin-6(7*H*)-one (188)

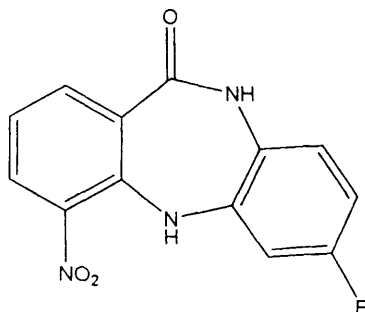


Method M. (**185**) (0.24 g, 0.88 mmol), sodium hydrogen sulfite (0.14 g, 0.88 mmol), 4-hydroxybenzaldehyde (0.12 g, 2.90 mmol) and DMA (5 mL) were heated at 140 °C for 13 h. Recrystallization (hot methanol) formed the product as a beige amorphous solid (0.015 g, 9 %); m.p. > 360 °C; δ_{H} 6.88 (2H, m, $J = 8.4$, Ar-H), 7.37 (1H, s, Ar-H), 7.43 (2H, dd, $J = 5.4, 8.0$, Ar-H), 7.64 (2H, m, $J = 8.4$, Ar-H), 7.73 (1H, dd, $J = 1.20, 8.4$, Ar-H), 7.88 (1H, d, $J = 7.7$, Ar-H), 7.94 (1H, d, $J = 7.7$, Ar-H), 10.15 (1H, br s, OH), 10.51 (1H, s, NH). 12.81 (1H, s, COOH); δ_{C} 115.9, 117.5, 120.5, 123.6, 123.7, 123.9, 125.6, 126.5, 126.7, 127.9, 130.2, 130.8, 134.6, 139.3, 143.0, 154.8, 159.6, 165.1, 165.7, HRMS (ES⁺) m/z 372.0979 [(M+H), 372.0977 calculated for C₂₁H₁₄N₃O₄].

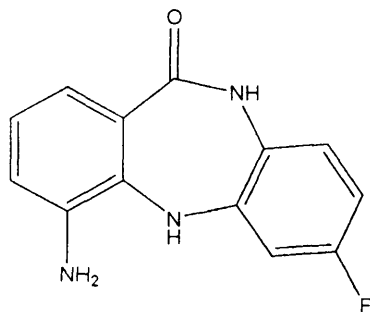
4-Fluoro-1,2-phenylenediamine (178) (Grivas and Olsson, 1985)



Method J. 4-Fluoro-2-nitrophenyl amine (1.00 g, 6.41 mmol), Raney Nickel (catalytic amount which replaced 10 % Pd/C (100 mL)) produced the product as a brown solid (0.71 g, 88 %); m.p. 81-83 °C; δ_{H} 4.25 (2H, br s, NH₂), 4.73 (2H, br s, NH₂), 6.13 (1H, d t, $J = 2.9, 8.6$ Ar-H), 6.32 (1H, dd, $J = 2.9, 11.0$, Ar-H), 6.45 (1H, dd, $J = 7.2$, Ar-H); δ_{C} 101.2 (dd, $J = 23.3, 142.8$, C-F), 114.4, 130.9, 136.8, 154.7, 156.5.

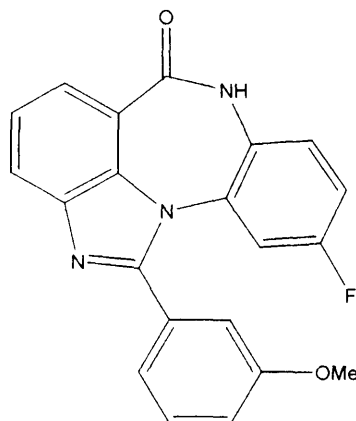
6-Nitro-9-fluoro-1*H*-7*H*-dibenzo[2,3-*b*][6,7-*f*]diazepin-2-one (179)

Method I. Methyl 2-bromo-3-nitrobenzoate (**166**) (2.20 g, 8.46 mmol), 4-fluoro-1,2-phenylenediamine (2.00 g, 15.86 mmol) and DMA (5 mL) were heated at 100 °C for 12 h. Recrystallization from hot methanol yielded a dark brown solid (2.32 g, 100 %); m.p. decomposed at 320 °C; δ_{H} 6.87-6.93 (2H, ddd, $J = 2.9, 8.2, 11.1$, Ar-H), 7.06 (1H, dd, $J = 7.6$, Ar-H), 7.15 (1H, t, $J = 8.2$, Ar-H), 8.06 (1H, dd, $J = 1.6, 7.6$, Ar-H), 8.21 (1H, dd, $J = 1.6, 8.2$, Ar-H), 8.71 (1H, s, NH), 10.47 (1H, s, CONH); δ_{C} 109.4 (dd, $J = 23.9, 422.6$, C-F), 121.1, 124.1, 127.4, 129.9, 132.0, 132.2, 133.5, 138.4, 138.7, 144.8, 158.1, 160.0, 166.3 (C=O); MS (CI) m/z 273.2 (M).

6-Amino-9-fluoro-1*H*-7*H*-dibenzo[2,3-*b*][6,7-*f*]diazepin-2-one (181)

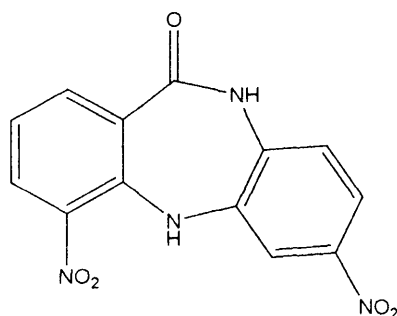
Method J. (**179**) (2.00 g, 7.32 mmol) in methanol (170 mL) produced the product as a light brown solid (1.00 g, 56 %); m.p. 232-235 °C; δ_{H} 5.26 (2H, br s, NH₂), 6.65 (1H, s, NH), 6.72 (1H, dd, $J = 7.7$, Ar-H), 6.78-6.83 (3H, m, Ar-H), 6.90 (1H, dd, $J = 1.5, 7.6$, Ar-H), 7.12-7.15 (1H, m, Ar-H), 9.97 (1H, s, CONH); δ_{C} 108.8 (dd, $J = 23.8, 356.7$, C-F), 118.4, 119.4, 122.1, 122.4, 125.9, 132.6, 135.7, 137.1, 138.6, 157.1, 159.0, 168.8 (C=O); MS (ES⁺) m/z 242.1 (M-H).

1-(3'-Methoxyphenyl)benzo[*b*]imidazo[4,5,1-*jk*]-10-fluorodibenzodiazepin-6(7*H*)-one (182)



Method M. (**181**) (0.60 g, 2.47 mmol), sodium hydrogen sulfite (0.39 g, 2.47 mmol), 3-methoxybenzaldehyde (0.34 g, 2.47 mmol) and DMA (4 mL) were heated at 140 °C for 11 h produced the product as a light brown solid (0.89 g, 100 %); m.p. 239-242 °C; δ_{H} 3.81 (3H, s, OCH₃), 6.70 (1H, dd, *J* = 5.6, 9.2, Ar-H), 6.81 (1H, t, *J* = 7.6, Ar-H), 7.13 (1H, dd, *J* = 2.6, 8.1, Ar-H), 7.20 (1H, dd, *J* = 2.9, 9.9, Ar-H), 7.29 (1H, dd, *J* = 0.9, 7.6, Ar-H), 7.41-7.47 (3H, m, Ar-H), 7.94 (1H, dd, *J* = 0.9, 7.6, Ar-H), 8.00 (1H, dd, *J* = 0.9, 7.6, Ar-H), 10.31 (1H, s, NH); δ_{C} 55.3, 110.6 (dd, *J* 24.5, 147.8, C-F), 114.1, 116.5, 117.6, 121.5, 123.9, 124.2, 126.2, 126.5, 127.2, 130.3, 131.3, 132.4, 139.1, 142.7, 154.0, 159.1, 159.4, 161.0, 165.1 (C=O); HRMS (ES⁺) *m/z* 360.1144 [(M+H), 360.1143 calculated for C₂₁H₁₅FN₃O₂]; CHN for C₂₁H₁₄FN₃O₂·0.4 H₂O found C 68.58 %, H 3.86 %, N 11.31 %, calculated C 68.86 %, H 4.25 %, N 11.36 %.

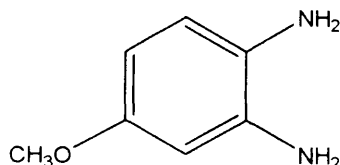
6,9-Dinitro-1*H*-7*H*-dibenzo[2,3-*b*][6,7-*f*]diazepin-2-one (191)



Method I. Methyl 2-bromo-3-nitrobenzoate (**166**) (1.00 g, 3.85 mmol), 4-nitro-1,2-phenylenediamine (1.18 g, 7.69 mmol) and DMA (3 mL) were heated at 100 °C for 14 h, followed by recrystallization from hot methanol yielding a dark brown solid (0.58 g, 50

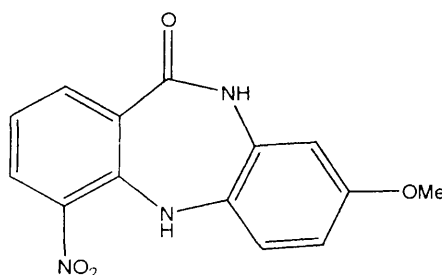
%); m.p. decomposed at 190 °C; δ_{H} 7.18-7.25 (2H, m, Ar-H), 7.93 (1H, s, Ar-H), 7.97 (1H, d, $J = 8.3$, Ar-H), 8.05 (1H, d, $J = 7.5$, Ar-H), 8.21 (1H, d, $J = 8.3$, Ar-H), 8.91 (1H, s, NH), 10.89 (1H, s, CONH); δ_{C} 118.27, 120.32, 121.21, 121.66, 127.08, 130.06, 137.00, 137.33, 138.43, 139.03, 143.21, 143.34, 165.99 (C=O); MS (ES⁻) m/z 323.7 (M+Na).

4-Methoxy-1,2-phenylenediamine (**193**) (Vass *et al.*, 2001)

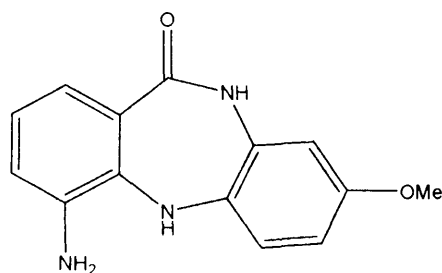


Method J. 4-Methyl-2-nitrophenylamine (1.50 g, 9.86 mmol) in methanol (100 mL) produced the product as a purple solid (1.21 g, 100 %); m.p 84-86 °C; δ_{H} 3.40 (3H, s, CH₃), 4.17 (2H, s, NH₂), 4.32 (2H, s, NH₂), 6.20 (1H, dd, $J = 1.8, 7.7$, Ar-H), 6.34 (1H, s, Ar-H), 6.40 (1H, d, $J = 7.7$, Ar-H); δ_{C} 20.5, 114.7, 115.3, 117.6, 125.6, 132.3, 135.0.

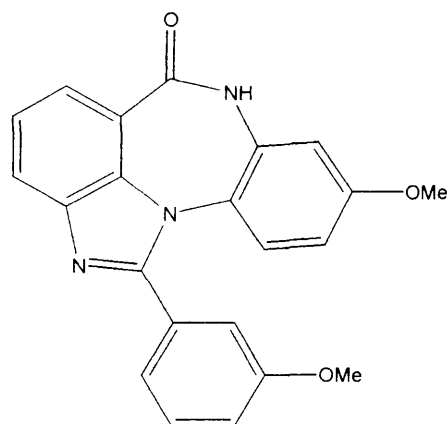
6-Nitro-10-methoxy-1*H*-7*H*-dibenzo[2,3-*b*][6,7-*f*]diazepin-2-one (**194**)



Method I. Methyl 2-bromo-3-nitrobenzene (**166**) (1.25 g, 4.81 mmol), 4-methoxy-1,2-phenylenediamine. 2HCl (**193**) (2.03 g, 9.61 mmol), triethylamine (1.46 g, 14.42 mmol) and DMA (4 mL) were heated at 100 °C for 18 h. The solution was cooled, washed with hydrochloric acid (15 mL, 1 M) and recrystallized from hot methanol to produce the product as a dark brown solid (1.20 g, 88 %); m.p. 249-252 °C; δ_{H} 3.70 (3H, s, CH₃), 6.64-6.66 (2H, m, Ar-H), 6.95 (1H, dd, $J = 1.6, 7.6$, Ar-H), 7.11 (1H, t, $J = 8.1$, Ar-H), 8.06 (1H, dd, $J = 1.6, 7.6$, Ar-H), 8.21 (1H, dd, $J = 1.7, 8.1$, Ar-H), 8.71 (1H, s, NH), 10.33 (1H, s, CONH); δ_{C} 55.4, 106.6, 109.9, 120.5, 122.4, 127.3, 129.8, 130.1, 131.5, 137.9, 141.1, 145.6, 156.6, 166.4 (C=O); MS (CI⁺) 286.1 (M+H).

6-Amino-10-methoxy-1*H*-7*H*-dibenzo[2,3-*b*][6,7-*f*]diazepin-2-one (195)

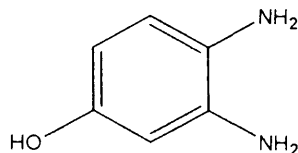
Method J. (194) (1.20 g, 4.21 mmol) in methanol (200 mL) produced the product as a brown powder (0.87 g, 81 %); m.p 206-209 °C; δ_{H} 3.76 (3H, s, CH_3), 5.20 (2H, s, NH_2), 6.46 (1H, s, NH), 6.55-6.58 (2H, m, Ar-H), 6.68 (1H, t, $J = 7.7$, Ar-H), 6.76 (1H, dd, $J = 1.6, 7.7$, Ar-H), 6.88 (1H, dd, $J = 1.6, 7.7$, Ar-H), 7.03 (1H, d, $J = 8.3$, Ar-H), 9.80 (1H, s, CONH); δ_{C} 55.2, 106.5, 109.1, 118.0, 119.4, 121.6, 122.0, 125.8, 132.2, 134.0, 136.5, 138.3, 155.4, 169.0 ($\text{C}=\text{O}$); MS (ES^+) m/z 533.2 (2M+Na).

1-(3'-Methoxyphenyl)benzo[*b*]imidazo[4,5-*jk*]-9-methoxy[1,4]benzodiazepin-6(7*H*)7-one (196)

Method M. (195) (0.85 g, 3.33 mmol), sodium hydrogen sulfite (0.52 g, 4.99 mmol), 3-methoxybenzaldehyde (0.45 g, 3.33 mmol) and DMA (4 mL) were heated at 140 °C for 24 h. Recrystallization from hot methanol, formed the product as a light brown solid (0.55 g, 39 %); m.p. 276-278 °C; δ_{H} 3.72 (3H, s, CH_3), 3.81 (3H, s, CH_3), 6.53 (1H, dd, $J = 2.8, 9.1$ Hz, Ar-H), 6.60 (1H, d, $J = 9.1$ Hz, Ar-H), 6.96 (1H, s, Ar-H), 7.11 (1H, dd, $J = 2.6, 8.3$, Ar-H), 7.29 (1H, d, $J = 7.6$ Hz, Ar-H), 7.40-7.45 (3H, m, Ar-H), 7.93 (1H, dd, $J = 0.9, 7.6$ Hz, Ar-H), 10.13 (1H, s, NH); δ_{C} 55.2, 55.4, 108.3, 109.9, 114.1, 116.2, 117.7, 121.5, 123.0, 123.6, 124.0, 126.1, 126.3, 130.1, 131.6, 133.2, 139.1, 142.7, 153.6, 157.9, 159.4,

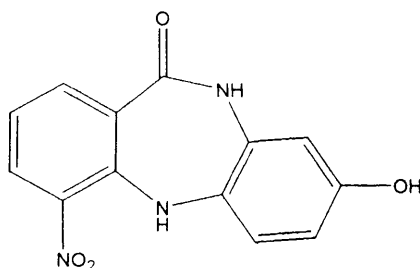
165.3 ($\text{C}=\text{O}$); HRMS (ES^+) m/z 372.1340 [(M+H), 372.1343 calculated for $\text{C}_{22}\text{H}_{18}\text{N}_3\text{O}_3$]; CHN for $\text{C}_{22}\text{H}_{17}\text{N}_3\text{O}_3 \cdot 0.4 \text{ H}_2\text{O}$ found C 69.84 %, H 4.91 %, N 11.01 %, calculated C 69.79 %, H 4.74 %, N 11.10 %.

4-Hydroxy-1,2-phenylenediamine (197) (Sasaki *et al.*, 2005)

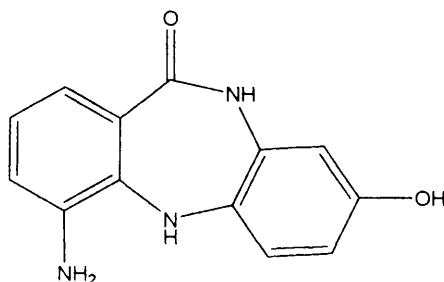


Method J. 4-Amino-3-nitrophenol (2.00 g, 12.98 mmol) in methanol (150 mL) produced the product as a black powder (1.62 g, 100 %); m.p 178-180 °C; δ_{H} 3.81 (2H, br s, NH_2), 4.32 (2H, br s, NH_2), 5.81 (1H, dd, $J = 2.7, 8.2$, Ar-H), 6.03 (1H, d, $J = 2.7$, Ar-H), 6.32 (1H, d, $J = 8.2$, Ar-H); δ_{C} 102.3, 103.3, 115.9, 126.6, 136.7, 149.8.

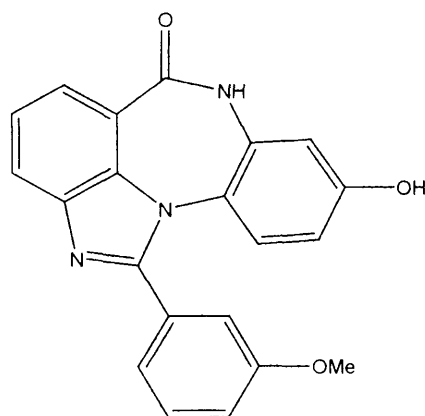
6-Nitro-10-hydroxy-1*H*-7*H*-dibenzo[2,3-*b*][6,7-*f*]diazepin-2-one (198)



Method I. Methyl 2-bromo-3-nitrobenzene (**166**) (1.5g, 5.77 mmol), 4-hydroxy-1,2-phenylenediamine (1.43 g, 11.54 mmol) and DMA (4 mL) were heated at 100 °C for 16 h. Recrystallization from hot methanol produced the product as a black powder (0.95 g, 61 %); m.p > 360 °C; δ_{H} 6.45 (1H, dd, $J = 2.6, 8.3$, Ar-H), 6.82 (1H, d, $J = 2.6$, Ar-H), 7.09 (1H, t, $J = 8.3$, Ar-H), 8.05 (1H, dd, $J = 1.6, 7.7$, Ar-H), 8.20 (1H, dd, $J = 1.6, 8.3$, Ar-H), 8.66 (1H, s, NH), 9.42 (1H, s, OH), 10.30 (1H, s, CONH); δ_{C} 107.6, 110.6, 120.4, 123.5, 127.4, 128.6, 129.7, 131.4, 137.7, 139.1, 145.9, 154.8, 166.5 ($\text{C}=\text{O}$); MS (ES^+) m/z 269.8 (M-H).

6-Amino-10-hydroxy-1*H*-7*H*-dibenzo[2,3-*b*][6,7-*f*]diazepin-2-one (199)

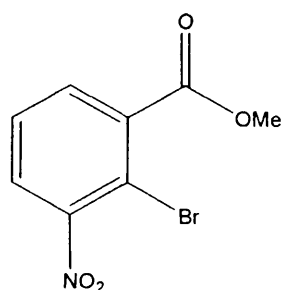
Method J. (198) (0.92 g, 3.39 mmol) in methanol (180 mL) produced the product as a black powder (0.65 g, 79 %); m.p 242-245 °C; δ_{H} 6.19 (2H, br s, NH_2), 6.35 (1H, s, NH), 6.37 (1H, dd, $J = 2.7, 8.5$, Ar-H), 6.44 (1H, d, $J = 2.7$, Ar-H), 6.67 (1H, t, $J = 7.7$, Ar-H), 6.75 (1H, dd, $J = 1.6, 7.7$, Ar-H), 6.87 (1H, dd, $J = 1.6, 7.7$, Ar-H), 6.91 (1H, d, $J = 8.5$, Ar-H), 9.08 (1H, s, OH), 9.77 (1H, s, CONH); δ_{C} 107.6, 110.7, 117.9, 119.4, 121.5, 122.1, 125.9, 132.1, 132.6, 136.9, 138.2, 153.3, 169.2 (C=O); MS (ES^+) m/z 264.1 (M+Na).

1-(3'-Methoxyphenyl)benzo[*b*]imidazo[4,5,1-*j,k*]-9-hydroxybenzodiazepin-6(7*H*)-one (200)

Method M. (199) (0.27 g, 1.12 mmol), sodium hydrogen sulfite (0.17 g, 1.68 mmol), 3-methoxybenzaldehyde (0.15 g, 1.12 mmol) and DMA (3 mL) were heated at 140 °C for 13 h, forming the product as a black powder (0.08 g, 20 %); m.p. decomposed at 338 °C; δ_{H} 3.80 (3H, s, CH_3), 6.31 (1H, dd, $J = 2.7, 8.9$, Ar-H), 6.48 (1H, d, $J = 8.9$, Ar-H), 6.79 (1H, d, $J = 2.7$, Ar-H), 7.12 (1H, dd, $J = 2.7, 8.9$, Ar-H), 7.30 (1H, d, $J = 7.6$, Ar-H), 7.40-7.44 (3H, m, Ar-H), 7.92 (1H, dd, $J = 0.9, 7.6$, Ar-H), 7.97 (1H, dd, $J = 0.9, 7.6$, Ar-H), 9.78 (1H, s, OH), 10.12 (1H, s, NH); δ_{C} 55.3, 109.5, 111.5, 114.1, 116.2, 117.8, 121.5, 121.7,

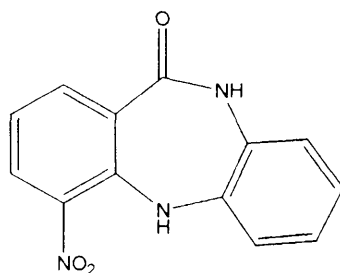
123.5, 123.7, 123.9, 126.0, 126.4, 130.1, 131.6, 139.2, 142.7, 153.6, 156.3, 159.4, 165.5 ($\underline{\text{C}}=\text{O}$); HRMS (ES⁺) m/z 358.1180 [(M+H), 358.1186 calculated for C₂₁H₁₆N₃O₃].

Methyl 2-bromo-3-nitrobenzoate, (166) (Krolski *et al.*, 1988)



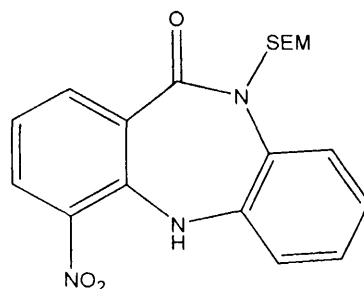
Method H. 2-Bromo-3-nitrobenzoic acid (0.50 g, 2.03 mmol), methanol (20 mL) and concentrated sulphuric acid (1 mL) were refluxed for 5 h, producing the product as a white solid (0.52 g, 98 %); m.p. 77-80 °C [lit (Harris *et al.*, 1990) 76-77 °C]; δ_{H} 3.92 (3H, s, OCH₃), 8.04 (1H, d, J = 8.8 Ar-H), 8.25 (1H, dd, J = 2.8, 8.8, A-H), 8.51 (1H, d, J = 2.8, Ar-H); δ_{C} 53.5 ($\underline{\text{C}}\text{H}_2$), 111.4, 127.3, 129.9, 133.3, 135.8, 151.9, 165.7 ($\underline{\text{C}}=\text{O}$).

6-Nitro-1H-7H-dibenzo[2,3-b]d[6,7-f]iazepin-2-one, (167) (Lubisch *et al.*, 2003)



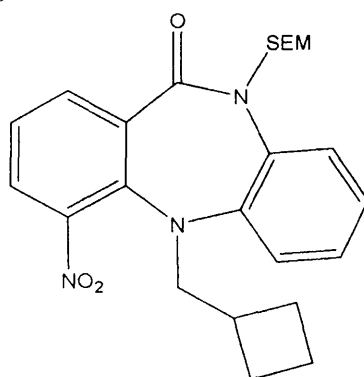
Method I. (166) (1.01 g, 3.88 mmol), 1,2-phenylenediamine, (30) (0.63 g, 5.83 mmol) and DMA (3 mL) were heated at 100 °C for 10 h, producing the title compound as a brown solid (0.53 g, 48 %); m.p. 304-306 °C; δ_{H} 7.03-7.09 (4H, m, Ar-H), 7.14 (1H, t, J = 7.5, Ar-H), 8.07 (1H, dd, J = 1.5, 7.5, Ar-H), 8.23 (1H, dd, J = 1.5, 7.5, Ar-H), 8.80 (1H, s, NH), 10.41 (1H, s, CONH); δ_{C} 121.3, 121.7, 123.1, 125.1, 125.3, 128.0, 130.2, 130.9, 137.6, 138.6, 139.2, 145.4, 166.7 ($\underline{\text{C}}=\text{O}$); HRMS (ES⁻) m/z 254.0571 [(M-H), 254.0571 calculated for C₁₃H₈N₃O₃].

6-Nitro-1-(2-trimethylsilyloxyethyl)-7H-dibenzo[2,3-b][6,7-f]diazepin-2-one, (202)



Method B. (**167**) (1.58 g, 5.74 mmol), sodium hydride (0.15 g, 6.31 mmol), 2-(trimethylsilyloxyethyl) chloride (1.05 g, 6.31 mmol) in DMF (5 mL). Column chromatography (using 9:1 petrol:ethyl acetate) produced the product as an orange dense oil (1.27 g, 57 %); δ_{H} 0.00 (9H, s, SiCH₃), 0.91 (2H, t, J = 8.0, CH₂), 3.69 (2H, t, J = 8.0, CH₂), 5.32 (2H, s, NCH₂O), 7.19-7.25 (4H, m, Ar-H), 7.61 (1H, d, J = 8.0, Ar-H), 8.04 (1H, d, J = 8.0, Ar-H), 8.24 (1H, dd, J = 1.0, 8.0, Ar-H), 8.76 (1H, s, NH); δ_{C} 0.0 (SiCH₃), 18.8, 66.9, 79.3, 123.1, 124.7, 125.0, 126.8, 127.7, 129.8, 130.3, 135.2, 139.6, 140.3, 144.0, 147.4, 168.4 (C=O); MS (ES⁺) m/z 408.2 (M+Na).

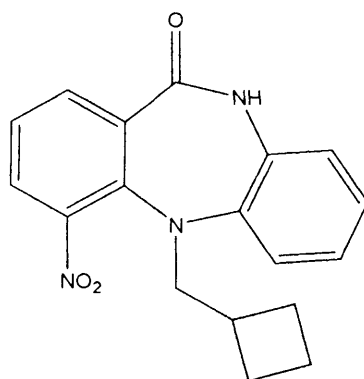
7-Cyclobutylmethyl-6-nitro-1-(2-trimethylsilyloxyethyl)dibenzo[2,3-b][6,7-f]diazepin-2-one, (203)



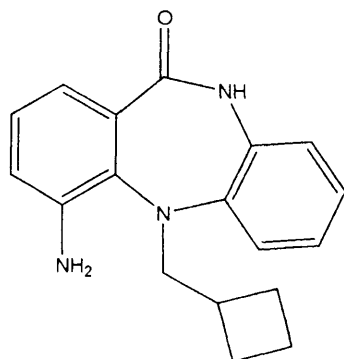
Method E. (**202**) (0.64 g, 0.95 mmol), cyclobutylmethyl bromide (0.99 g, 6.64 mmol), potassium carbonate (1.14 g, 8.24 mmol) and DMF (3 mL) were heated at 150 °C for 24 h, followed by column chromatography (eluent 10 % ethyl acetate:petrol) to yield the desired compound as a dense yellow oil (0.27 g, 36 %); δ_{H} 0.00 (9H, s, SiCH₃), 0.92-0.94 (2H, m, Alkyl-H), 0.91-0.96 (2H, m, Alkyl-H), 1.68-1.79 (4H, m, Alkyl-H), 2.26-2.29 (1H, m, Alkyl-H), 3.13-3.17 (1H, m, Alkyl-H), 3.65-3.70 (3H, m, Alkyl-H), 5.02 (1H, d, J

= 10.0, NCHO), 5.57 (1H, d, $J = 10.0$, NCHO), 7.25-7.29 (2H, m, Ar-H), 7.37-7.41 (2H, m, Ar-H), 7.60 (1H, dd, $J = 1.4, 7.8$, Ar-H), 7.89 (1H, dd, $J = 1.4, 7.8$, Ar-H), 7.95 (1H, dd, $J = 1.4, 7.8$, Ar-H); δ_C 0.0 (SiCH₃), 18.9, 19.1, 26.6, 35.8, 56.8, 67.6, 79.3, 124.5, 125.2, 126.6, 127.7, 127.9, 129.3, 135.3, 137.0, 139.1, 144.5, 145.2, 145.6, 168.2 (C=O); MS (ES⁺) m/z 476.2 (M+Na).

7-(Cyclobutylmethyl)-6-nitro-1H-dibenzo[2,3-b][6,7-f]diazepin-2-one, (204)



Method C. (**203**) (0.27 g, 0.60 mmol) and 1 M tetrabutylammonium fluoride/THF solution (5 mL), were refluxed for 19 h. Column chromatography (eluent 8.5:1.5 petrol:ethyl acetate) produced the title compound as a yellow powder (0.11 g, 57 %); m.p. 196-199 °C; δ_H 1.53-1.82 (6H, m, Alkyl-H), 2.21-2.23 (1H, m, CH), 3.09-3.16 (1H, m, CH), 4.09-4.12 (1H, m, CH), 7.10-7.29 (3H, m, Ar-H), 7.42 (1H, t, $J = 7.8$, Ar-H), 7.96 (1H, dd, $J = 1.5, 7.8$, Ar-H), 8.00 (2H, dd, $J = 1.5, 7.8$, Ar-H), 10.60 (1H, s, NH); δ_C 17.7, 25.4, 34.2, 56.7, 121.4, 124.7, 125.0, 125.4, 126.0, 128.0, 134.0, 134.9, 135.0, 140.1, 143.0, 145.5, 166.1 (C=O); MS (ES⁺) m/z 346.1 (M+Na).

6-Amino-7-(cyclobutylmethyl)-1*H*-dibenzo[2,3-*b*][6,7-*f*]diazepin-2-one, (201)

Method J. (**204**) (0.093 g, 0.28 mmol) in dichloromethane (30 mL) produced the product as a white solid (0.085 g, 100 %); m.p. 172-174 °C; δ_{H} 1.50-1.82 (6H, m, Alkyl-H), 2.27-2.30 (1H, m, CH), 3.19-3.32 (2H, m, CH₂), 5.34 (2H, s, NH₂), 6.87 (2H, d, J = 7.8, Ar-H), 6.94-7.16 (4H, m, Ar-H), 7.45 (1H, d, J = 7.8, Ar-H), 10.24 (1H, s, NH); δ_{C} 13.8, 25.7, 34.6, 58.7, 117.8, 117.9, 121.1, 124.6, 126.5, 126.7, 129.2, 132.2, 134.9, 137.1, 141.0, 145.1, 168.5 (C=O); HRMS (ES⁺) m/z 294.1602 [(M+H), 294.1601 calculated for C₁₈H₂₀N₃O].

REFERENCES

- Abell, A. D., Nabbs, B. K., and Battersby, A. R. **1998**. The reaction of N-magnesium derivatives of pyrroles with N-mesylchloromethylpyrroles: a synthesis of dipyrrolymethanes. *J.Org.Chem.* **6**, 8163-8169.
- Akinago, S., Sugiyama, K., and Akiyama, T. **2000**. UCN-01 (7-hydroxystaurosporine) and other indolocarbazole compounds: a new generation of anti-cancer agents for the new century? *Anti-Cancer Drug Des.* **15**, 43-52.
- Alberts, B., Bray, D., Lewis, J., Raff, M., Roberts, K., and Walter, P. **1998**. "Essential cell biology: an introduction to the molecular biology of the cell," Garland Publishing, New York & London.
- Alberts, B., Bray, D., Lewis, J., Raff, M., Roberts, K., and Watson, J. D. **1994**. "Molecular biology of the cell," 3rd Ed. Garland Publishing Inc.
- Albuschat, R., Lowe, W., Weber, M., Luger, P., and Jendrossek, V. **2004**. 4-Anilinoquinazolines with lavendustin a subunit as inhibitors of epidermal growth factor receptor tyrosine kinase: syntheses, chemical and pharmacological properties. *Eur. J. Med.Chem.* **39**, 1001-1011.
- Althaus, F., and Richter, C. **1987**. ADP-ribosylation of proteins. Enzymology and biological significance. *Mol. Biol. Biochem. Biophys.* **37**, 1-237.
- Ame, J. C., Rolli, V., Schreiber, V., Niedergang, C., Apiou, F., Decker, P., Muller, S., Hoger, T., Murcia, J. M. D., and de Murcia, G. **1999**. PARP-2, a novel mammalian DNA damage-dependent poly(ADP-ribose) polymerase. *J. Biol. Chem.* **274**, 17860-17868.
- Anderson, C. W., and LeesMiller, S. P. **1992**. The nuclear serine/threonine protein kinase DNA-PK. *Crit. Rev. Eukaryot. Gene. Expr.* **2**, 283-314.

- Annoura, H., and Tatsuoka, T. **1995**. Total syntheses of hymenialdisine and debromohymenialdisine: stereospecific construction of the 2-amino-4-oxo-2-imidazolin-5 (Z)-disubstituted ylidene ring system. *Tetrahedron Lett.* **36**, 413-416.
- Arienti, K. L., Brunmark, A., Axe, F. U., McClure, K., Lee, A., Blevitt, J., Neff, D. K., Huang, L. M., Crawford, S., Pandit, C. R., Karlsson, L., and Breitenbucher, J. G. **2005**. Checkpoint kinase inhibitors: SAR and radioprotective properties of a series of 2-arylbenzimidazoles. *J. Med. Chem* **48**, 1873-1885.
- Arris, C. E., Boyle, F. T., Calvert, A. H., Curtin, N. J., Endicott, J. A., Garman, E. F., Gibson, A. E., Golding, B. T., Grant, S., Griffin, R. J., Jewsbury, P., Johnson, L. N., Lawrie, A. M., Newell, D. R., Nobbel, M. E. M., Sausville, E. A., Schultz, R., and Yu, W. **2000**. Identification of novel purine and pyrimidine CDKIs with distinct molecular interactions and tumour cell growth inhibition profiles. *J. Med. Chem* **43**, 2797-2804.
- Atkinson, G. E., Cowan, A., McInnes, C., Zheleva, D. I., Fischer, P. M., and Chan, W. C. **2002**. Peptide inhibitors of CDK2-cyclin A that target the cyclin recruitment-site: Structural variants of the C-terminal Phe. *Bioorg. Med.Chem. Lett.* **12**, 2501-2505.
- Bachman, G. B., and Helsey, L. V. **1949**. The preparation of vinyl derivatives of five-atom heterocyclic rings. *Angew. Chem.* **71**, 1985-1988.
- Baldwin, J. E., Adlington, R. M., Sham, V. W., Marquez, R., and Bugler, P. G. **2005**. Biomimetic synthesis of (+/-)-aculeatin D. *Tetrahedron* **6**, 2353-2363.
- Barker, A. J., Kettle, J. G., and Faull, A. W. **1999**. Preparation of indoles as MCP-1 receptor antagonists. In "WO 9907678".
- Barraja, P., Diana, P., Lauria, A., Passannanti, A., Almerico, A., Minnei, C., Longu, S., Congiu, D., Muisu, C., and LaColla, P. **1999**. Indolo[3,2-c]cinnolines with antiproliferative, antifungal, and antibacterial activity. *Bioorg. Med. Chem.* **7**, 1591-1596.
- Bartek, J., Bartkova, J., and Lukas, J. **1996**. The retinoblastoma protein pathway and the restriction point. *Curr. Opin. Cell. Biol* **8**, 805-814.

- Bartek, J., Falck, J., and Lukas, J. **2001**. CHK2 kinase-a busy messenger. *Nat. Rev. Mol. Cell Biol.* **2**, 877-886.
- Bartek, J., and Lukas, J. **2001**. Mammalian G1- and S-phase checkpoints in response to DNA damage. *Curr. Opin. Cell Biol.* **13**, 738-747.
- Bartek, J., and Lukas, J. **2003**. Chk1 and Chk2 kinases in checkpoint control and cancer. *Cancer Cell* **3**, 421-429.
- Bell, D. W., Varley, J. M., Szydlo, T. E., Kang, D. H., Wahrer, D. C. R., Shannon, K. E., Lubratovich, M., Verselis, S. J., Isselbacher, K. J., Fraumeni, J. F., Birch, J. M., Li, F. P., Garber, J. E., and Haber, D. A. **1999**. Heterozygous germ line hCHK2 mutations in Li-Fraumeni syndrome. *Science* **286**, 2528-2531.
- Benjamin, R. C., and Gill, D. M. **1981**. Poly(ADP-ribose) synthesis in vitro programmed by damaged DNA. *J. Biol. Chem.* **255**, 10502-10508.
- Bhattacharyya, A., Ear, U. S., Koller, B. H., Weichselbaum, R. R., and Bishop, D. K. **2000**. The breast cancer susceptibility gene BRCA1 is required for subnuclear assembly of Rad51 and survival following treatment with the DNA cross-linking agent cisplatin. *J. Biol. Chem.* **275**, 23899-23903.
- Blackburn, E. H. **1991**. Structure and function of telomeres. *Nature* **350**, 569-573.
- Boulton, S., Kyle, S., and Durkacz, B. W. **1999**. Interactive effects of inhibitors of poly(ADP-ribose) polymerase and DNA-dependent protein kinase on cellular responses to DNA damage. *Carcinogenesis* **20**, 199-203.
- Bowman, K. J., Newell, D. R., Calvert, A. H., and Curtin, N. J. **2001**. Differential effects of the poly (ADP-ribose) polymerase (PARP) inhibitor NU1025 on topoisomerase I and II inhibitor cytotoxicity in L1210 cells in vitro. *Br. J. Cancer* **84**, 106-112.
- Bramson, H. N., Corona, J., Davis, S. T., Dickerson, S. H., Edelstein, M., Frye, S. V., Gampe, R. T., Harris, P. A., Hassell, A., Holmes, W. D., Hunter, R. N., Lackey, K. E., Lovejoy, B., Luzzio, M. J., Montana, V., Rocque, W. J., Rusnak, D., Shewchuk, L., Veal, J. M., Walker, D. H., and Kuyper, L. F. **2001**. Oxindole-based inhibitors of cyclin-dependent kinase 2 (CDK2): Design, synthesis,

- enzymatic activities, and X-ray crystallographic analysis. *J. Med. Chem.* **44**, 4339-4358.
- Brown, N. R., Noble, M. E. M., Lawrie, A. M., Morris, M. C., Tunnah, P., Divita, G., Johnson, L. N., and Endicott, J. A. **1999a**. Effects of phosphorylation of threonine 160 on cyclin-dependent kinase 2 structure and activity. *J. Biol. Chem.* **274**, 8746-8756.
- Brown, V. D., Phillips, R. A., and Gallie, B. L. **1999b**. Cumulative effect of phosphorylation of pRB on regulation of E2F activity. *Mol. Cell. Biol.* **19**, 3246-3256.
- Buolamwini, J. K. **2001**. Cell cycle molecular targets and drug discovery., Vol. 2001. [WWW]<URL: <http://www.eurekah.com/reports/cellcycle/buolamwini/index.html>>.
- Calabrese, C. R., Almassy, R., Barton, S., Batey, M. A., Calvet, A. H., CananKokh, S., Durkacz, B. W., Hostomsky, Z., Kumpf, R. A., Kyle, S., Li, J., Maegley, K., Newell, D. R., Notarianni, E., Stratford, I. J., Skalitzky, D. J., Thomas, H. D., Wang, L. Z., Webber, S. E., Williams, K. J., and Curtin, N. J. **2004**. Anticancer chemosensitization and radiosensitization by the novel poly (ADP-ribose) polymerase-1 inhibitor AG14361. *J. Nat. Cancer Instit.* **96**, 56-67.
- Chaturvedi, P., Eng, W. K., Zhu, Y., Mattern, M. R., Mishra, R., Hurle, M. R., Zhang, X. L., Annan, R. S., Lu, Q., Faucette, L. F., Scott, G. F., Li, X. T., Carr, S. A., Johnson, R. K., Winkler, J. D., and Zhou, B. B. S. **1999**. Mammalian Chk2 is a downstream effector of the ATM-dependent DNA damage checkpoint pathway. *Oncogene* **18**, 4047-4054.
- Chehab, N. H., Malikzay, A., Appel, M., and Halazonetis, T. D. **2000**. Chk2/hCds1 functions as a DNA damage checkpoint in G(1) by stabilizing p53. *Genes Dev.* **14**, 278-288.
- Cohen, P. **1999**. The development and therapeutic potential of protein kinase inhibitors. *Curr. Opin. Chem. Biol.* **3**, 459-465.

- Coleman, K. G., Lysikatos, J. P., and Yang, B. V. **1997**. Chemical inhibitors of cyclin dependent kinases. *Annu. Rep. Med. Chem* **32**, 171-179.
- Cooper, G. M. **2000**. "The cell: A Molecular Approach," 2nd Ed. ASM press, U.S.A.
- Crews, C. M., and Mohan, R. **2000**. Small-molecule inhibitors of the cell cycle. *Curr. Opin. Chem. Biol.* **4**, 47-53.
- Curman, D., Cinel, B., Williams, D. E., Rundle, N., Block, W. D., Goodarzi, A. A., Hutchins, J. R., Clarke, P. R., Zhou, B. B., Lees-Miller, S. P., Andersen, R. J., and Roberge, M. **2001**. Inhibition of the G(2) DNA damage checkpoint and of protein kinases Chk1 and Chk2 by the marine sponge alkaloid debromohymenialdisine. *J. Biol. Chem.* **276**, 17914-17919.
- D'Amours, D., Desnoyers, S., D'Silva, I., and Poirier, G. G. **1999**. Poly(ADP-ribosylation) reactions in the regulation of nuclear functions. *Biochem. J.* **342**, 249-268.
- D'Silva, I., Pelletier, J. D., Lagueux, J., D'Amours, D., Chaudhry, M. A., Weinfeld, M., Lees-Miller, S. P., and Poirier, G. G. **1999**. Relative affinities of poly(ADP-ribose) polymerase and DNA-dependent protein kinase for DNA strand interruptions. *BBA-Protein Struct. M.* **1430**, 119-126.
- Davidovic, L., Vodenicharov, M., Affar, E. B., and Poirier, G. G. **2001**. Importance of poly(ADP-ribose) glycohydrolase in the control of poly(ADP-ribose) metabolism. *Exp. Cell Res.* **268**, 7-13.
- Davies, T. G., Bentley, J., Arris, C. E., Boyle, F. T., Curtin, N. J., Endicott, J. A., Gibson, A. E., Golding, B. T., Griffin, R. J., Hardcastle, I. R., Jewsbury, P., Johnson, L. N., Mesguiche, V., Newell, D. R., Noble, M. E. M., Tucker, J. A., Wang, L., and Whitfield, H. J. **2002**. Structure-based design of a potent purine-based cyclin-dependent kinase inhibitor. *Nat. Struct. Biol.* **9**, 745-749.
- De Azvedo, W. F., Leclerc, S., Meijer, L., Havilcek, L., Strand, M., and Kim, S. H. **1997**. Inhibition of cyclin-dependent kinases by purine analogues crystal structure of human cdk2 complexed with Roscovitine. *Eur. J. Biochem* **243**, 518-526.

- Desroches, C., Lopes, C., Kessler, V., and parola, S. **2003**. Design and synthesis of multifunctional thiacalixarenes and related metal derivatives for the preparation of sol-gel hybrid materials with non-linear optical properties. *Dalton transactions* **10**, 2085-2092.
- Draetta, G., and Eckstein, J. **1997**. Cdc25 protein phosphatases in cell proliferation. *Biochim. Biophys. Acta-Rev. Cancer* **1332**, M53-M63.
- Dreyer, M. K., Borchering, D. R., Dumont, J. A., Peet, N. P., Tsay, J. T., Wright, P. S., Bitonti, A. J., Shen, J., and Kim, S. H. **2001**. Crystal structure of human cyclin-dependent kinase 2 in complex with the adenine-derived inhibitor H717. *J. Med. Chem* **44**, 524-530.
- Eldeiry, W. S., Tokino, T., Velculescu, V. E., Levy, D. B., Parsons, R., Trent, J. M., Lin, D., Mercer, W. E., Kinzler, K. W., and Vogelstein, B. **1993**. Waf1, a Potential Mediator of P53 Tumor Suppression. *Cell* **75**, 817-825.
- Elledge, S. J. **1996**. Cell cycle checkpoints: Preventing an identity crisis. *Science* **274**, 1664-1672.
- Evans, T., Rosenthal, E. T., Youngblom, J., Distel, D., and Hunt, T. **1983**. Cyclin: a protein specified by maternal mRNA in sea urchin eggs that is destroyed at each cleavage division. *Cell* **33**, 389-396.
- Fabbro, D., Ruetz, S., Buchdunger, E., Cowan-Jacob, S. W., Fendrich, G., Liebetanz, J., Mestan, J., O'Reilly, T., Traxler, P., Chaudhuri, B., Fretz, H., Zimmermann, J., Meyer, T., Caravatti, G., Furet, P., and Manley, P. W. **2002**. Protein kinases as targets for anticancer agents: from inhibitors to useful drugs. *Pharmacol. Ther.* **93**, 79-98.
- Falck, J., Mailand, N., Syljuasen, R. G., Bartek, J., and Lukas, J. **2001**. The ATM-Chk2-Cdc25A checkpoint pathway guards against radioresistant DNA synthesis. *Nature* **410**, 842-847.
- Ferraris, D. V., Li, J.-H., Kalish, V. J., and Zhang, J. **2002**. Preparation of benzazepinones, isoquinolinones and related compounds as inhibitors of poly(ADP-ribose) polymerase (PARP) for the prevention and/or treatment of

- tissue damage from cell trauma or cell death due to necrosis or apoptosis. In "WO 2002044183".
- Fischer, P. M., and Lane, D. P. **2000**. Inhibitors of cyclin-dependent kinases as anti-cancer therapeutics. *Curr. Med. Chem.* **7**, 1213-1245.
- Fisher, R. P., and Morgan, D. O. **1994**. A Novel Cyclin Associates with Mo15/Cdk7 to Form the Cdk- Activating Kinase. *Cell* **78**, 713-724.
- Fry, D. W. **1999**. Inhibition of the epidermal growth factor receptor family of tyrosine kinases as an approach to cancer chemotherapy: Progression from reversible to irreversible inhibitors. *Pharmacol. Ther.* **82**, 207-218.
- Gaken, J. A., Tavassoli, M., Gan, S. U., Vallian, S., Giddings, I., Darling, D. C., GaleaLauri, J., Thomas, M. G., Abedi, H., Schreiber, V., MenissierdeMurcia, J., Collins, M. K. L., Shall, S., and Farzaneh, F. **1996**. Efficient retroviral infection of mammalian cells is blocked by inhibition of poly(ADP-ribose) polymerase activity. *J. Virol.* **70**, 3992-4000.
- Garin, J., Melendez, E., Merchan, F. L., and Tejero, T. **1987**. Pyrido [2,3-*b*] [1,5] Benzodiazepines - Synthesis and Reactivity Towards (Hetero) Aromatic Acid Halides. *An. Quim. C-Org. Bioquim.* **83**, 52-54.
- Garrett, M. D., and Fattaey, A. **1999**. CDK inhibition and cancer therapy. *Curr. Opin. Genet. Dev.* **9**, 104-111.
- Gartel, A. L., Serfas, M. S., and Tyner, A. L. **1996**. p21-Negative regulator of the cell cycle. *Proc. Soc. Exp. Biol. Med.* **213**, 138-146.
- Giani, R. P., Borsa, M., Parini, E., and Tonon, G. C. **1985**. A new facile synthesis of 11-oxo-10,11-dihydro-5*H*- dibenzo [b,e][1,4] diazepines. *Synthesis*, 550-552.
- Gibson, A. E., Arris, C. E., Bentley, J., Boyle, F. T., Curtin, N. J., Davies, T. G., Endicott, J. A., Golding, B. T., Grant, S., Griffin, R. J., Jewsbury, P., Johnson, L. N., Mesguiche, V., Newell, D. R., Noble, M. E. M., Tucker, J. A., and Whitfield, H. J. **2002**. Probing the ATP ribose-binding domain of cyclin-dependent kinases 1 and 2 with O6-substituted guanine derivatives. *J. Med. Chem.* **45**, 3381-3393.

- Gill, G. N., and Lazar, C. S. **1981**. Increased Phosphotyrosine Content and Inhibition of Proliferation in Egf-Treated A431 Cells. *Nature* **293**, 305-307.
- Graves, P. R., Yu, L., Schwarz, J. K., Gales, J., Sausville, E. A., O'Connor, P. M., and Piwnica-Worms, H. **2000**. The Chk1 protein kinase and the Cdc25C regulatory pathways are targets of the anticancer agent UCN-01. *J. Biol. Chem.* **275**, 5600-5605.
- Gray, N., Detivaud, L., Doerig, C., and Meijer, L. **1999**. ATP-site directed inhibitors of cyclin-dependent kinases. *Curr. Med. Chem.* **6**, 859-875.
- Greenblatt, M. S., Bennett, W. P., Hollstein, M., and Harris, C. C. **1994**. Mutations in the P53 Tumor-Suppressor Gene - Clues to Cancer Etiology and Molecular Pathogenesis. *Cancer Res.* **54**, 4855-4878.
- Greene, T. W., and Wuts, P. G. M. **1999**. "Protective groups in organic synthesis," 3rd Ed. Wiley-Interscience.
- Griffin, R. J., Pemberton, L. C., Rhodes, D., Bleasdale, C., Bowman, K., Calvert, A. H., Curtin, N. J., Durkacz, B. W., Newell, D. R., and Porteous, J. K. **1995**. Novel potent inhibitors of the DNA repair enzyme poly (ADP-ribose) polymerase (PARP). *AntiCancer Drug Des.* **10**, 507-514.
- Griffin, R. J., Srinivasan, S., Bowman, K. J., Calvet, A. H., Curtin, N. J., Newell, D. R., Pemberton, L. C., and Golding, B. T. **1998**. Resistance-modifying agents. Synthesis and biological properties of quinazolinone inhibitors of the DNA repair enzyme poly (ADP-ribose) polymerase (PARP). *J. Med. Chem.* **41**, 5247-5256.
- Grivas, S., and Olsson, K. **1985**. An improved synthesis of 3,8-dimethyl-3*H*-imidazo[4,5-*f*]quinoxalin-2-amine("MeIQx") and its 2-¹⁴C-labelled analogue. *Acta Chemica Scandinavica B* **39**, 31-34.
- Gross, M. E., Zorbas, M. A., Danels, Y. J., Garcia, R., Gallick, G. E., Olive, M., Brattain, M. G., Boman, B. M., and Yeoman, L. C. **1991**. Cellular Growth-Response to Epidermal Growth-Factor in Colon- Carcinoma Cells with an Amplified Epidermal Growth-Factor Receptor Derived from a Familial Adenomatous Polyposis Patient. *Cancer Res.* **51**, 1452-1459.

- Guo, M., and Hay, B. H. **1999**. Cell proliferation and apoptosis. *Curr. Opin. Cell. Biol* **11**, 754-752.
- Hardcastle, I. R., Arris, C. E., Bentley, J., Boyle, F. T., Chen, Y. H., Curtin, N. J., Endicott, J. A., Gibson, A. E., Golding, B. T., Griffin, R. J., Jewsbury, P., Menyerol, J., Mesguiche, V., Newell, D. R., Noble, M. E. M., Pratt, D. J., Wang, L. Z., and Whitfield, H. J. **2004**. N-2-substituted O-6-cyclohexylmethylguanine derivatives: Potent inhibitors of cyclin-dependent kinases 1 and 2. *J. Med. Chem* **47**, 3710-3722.
- Harley, C. B. **1991**. Telomere loss: mitotic clock or genetic time bomb? *Mutat. Res.* **256**, 271-282.
- Harley, C. B., Futcher, A. B., and Greider, C. W. **1990**. Telomeres shorten during ageing of human fibroblasts. *Nature* **345**, 458-460.
- Harper, J. W. **1997**. Cyclin dependent kinase inhibitors. *Cancer Surv.* **29**, 91-107.
- Harper, J. W., Adami, G. R., Wei, N., Keyomarsi, K., and Elledge, S. J. **1993**. The p21 CDK-interacting protein CIP1 is a potent inhibitor of G1 cyclin-dependent kinases. *Cell* **75**, 805-816.
- Harris, N. V., Smith, C., and Bowden, K. **1990**. Antifolate and antibacterial activities of 5-substituted 2, 4-diaminoquinazolines. *J. Med. Chem.* **33**, 434-444.
- Hartwell, L. **1992**. Defects in a cell cycle checkpoint may be responsible for the genomic instability of cancer cells. *Cell* **71**, 543-546.
- Hartwell, L. H., and Kastan, M. B. **1994**. Cell-Cycle Control and Cancer. *Science* **266**, 1821-1828.
- Hatakeyama, K., Nemoto, Y., Ueda, K., and Hayaishi, O. **1986**. Purification and Characterization of Poly(Adp-Ribose) Glycohydrolase - Different Modes of Action on Large and Small Poly(Adp-Ribose). *J. Biol. Chem.* **261**, 4902-4911.
- Hengst, L., and Reed, S. I. **1996**. Translational control of p27(kip1) accumulation during the cell cycle. *Science* **271**, 1861-1864.

- Hinterding, K., AlonsoDiaz, D., and Waldmann, H. **1998**. Organic synthesis and biological signal transduction. *Angew. Chem. Int. Ed* **37**, 688-749.
- Hiremath, S. P., Badami, P. S., and Purohoit, M. G. **1984**. Synthesis of substituted 7,12-dihydroindolo[3,2-*b*][1,4]benzodiazepin-5-(6*H*)-ones and 1,2,3,4,5,6-hexahydro[1,3]diazepino[5,6-*b*]indole-1,5-diones. *Indian J. Chem, Section B: Organic Chemistry including Medicinal Chemistry* **23B**, 1058-1063.
- Ho, A., and Dowdy, S. F. **2002**. Regulation of G(1) cell-cycle progression by oncogenes and tumor suppressor genes. *Curr. Opin. Genet. Dev.* **12**, 47-52.
- Hoessel, R., Leclerc, S., Endicott, J. A., Nobel, M. E. M., Lawrie, A., Tunnah, P., Leost, M., Damiens, E., Marie, D., Marko, D., Niederberger, E., Tang, W. C., Eisenbrand, G., and Meijer, L. **1999**. Indirubin, the active constituent of a Chinese antileukaemia medicine, inhibits cyclin-dependent kinases. *Nat. Cell Biol.* **1**, 60-67.
- Hossel, R., nLecrec, S., Endicott, J. A., Nobbel, M. E. M., Lawrie, A., Tunnah, P., Leost, M., Damiens, E., Marie, D., Marko, D., Niederberger, E., Tang, W., Eisenbrand, G., and Meijer, L. **1999**. Indirubin, the active constituent of a Chinese antileukemia medicine, inhibits cyclin-dependent kinases. *Nat. Cell. Biol.* **1**, 60-67.
- Hunter, T. **1987**. A 1001 Protein-Kinases. *Cell* **50**, 823-829.
- Jagtap, P., and Szabo, C. **2005**. Poly(ADP-ribose) polymerase and the therapeutic effects of its inhibitors. *Nat. Rev. Drug Discov.* **4**, 421-440.
- Jeffery, D. A., Springer, M., King, D. S., and O'Shea, E. K. **2001**. Multisite phosphorylation of Pho4 by the cyclin-CDK Pho80-Pho85 is semi-processive with site preference. *J. Mol. Biol* **306**, 997-1010.
- Jeffrey, P. D., Ruso, A. A., Polyak, K., Gibbs, E., Hurwitz, J., Massague, J., and Pavletich, N. P. **1995**. Mechanism of Cdk Activation Revealed by the Structure of a Cyclina-Cdk2 Complex. *Nature* **376**, 313-320.

- Johnson, D. G., and Walker, C. L. **1999**. Cyclins and cell cycle checkpoints. *Annu. Rev. Pharmacol. Toxicol.* **39**, 295-312.
- Jorgensen, M. R., Olsen, C. A., Mellor, I. R., Usherwood, P. N. R., Witt, M., Franzyk, H., and Jaroszewski, J. W. **2005**. The effects of conformational constraints and steric bulk in the amino acid moiety of philanthotoxins on AMPAR antagonism. *J. Med. Chem* **48**, 56-70.
- Kaldis, P., Sutton, A., and Solomon, M. J. **1996**. The Cdk-activating kinase (CAK) from budding yeast. *Cell* **86**, 553-564.
- Kaneko, Y., Watanabe, N., Morisaki, H., Akita, H., Fujimoto, A., Tominaga, K., Terasawa, M., Tachibana, A., Ikeda, K., and Nakanishi, M. **1999**. Cell cycle-dependent and ATM-independent expression of human Chk1 kinase. *Oncogene* **18**, 3673-3681.
- Kastan, M. B., and Bartek, J. **2004**. Cell-cycle checkpoints and cancer. *Nature* **432**, 316-323.
- Kastan, M. B., and Lim, D. S. **2000**. The many substrates and functions of ATM. *Nat. Rev. Mol. Cell Biol.* **1**, 179-186.
- Kastan, M. B., Zhan, Q. M., Eldeiry, W. S., Carrier, F., Jacks, T., Walsh, W. V., Plunkett, B. S., Vogelstein, B., and Fornace, A. J. **1992**. A Mammalian-Cell Cycle Checkpoint Pathway Utilizing P53 and Gadd45 Is Defective in Ataxia-Telangiectasia. *Cell* **71**, 587-597.
- Kavanaugh, W. M., and Williams, L. T. **1996**. "Signalling through receptor Tyrosine kinases: In Signal Transduction," Chapman & Hall.
- Kawabe, T., Muslin, A. J., and Korsmeyer, S. J. **1997**. HOX11 interacts with protein phosphatases PP2A and PP1 and disrupts a G2/M cell-cycle checkpoint. *Nature* **385**, 454-458.
- Kickhoefer, V. A., Siva, A. C., Kedersha, N. L., Inman, E. M., Ruland, C., Streuli, M., and Rome, L. H. **1999**. The 193-kD vault protein, VPARP, is a novel Poly(ADP-ribose) polymerase. *J. Cell Biol.* **146**, 917-928.

- Klein, M., and Boche, G. **1999**. Regiospecific synthesis of substituted nitrofluorenes with the Negishi coupling reaction as key step. *Synthesis* **7**, 1246-1250.
- Knockaert, M., Greengard, P., and Meijer, L. **2002**. Pharmacological inhibitors of cyclin-dependent kinases. *Trends Pharmacol. Sci.* **23**, 417-425.
- Koh, J., Enders, G. H., B.D., D., and Harlow, E. **1995**. Tumor-derived p16 alleles encoding proteins defective in cell-cycle inhibition. *Nature* **375**, 506-510.
- Krolski, M. E., Renaldo, A. F., Rudisill, D. E., and Stille, J. K. **1988**. Palladium-catalyzed coupling of 2-bromoanilines with vinylannanes. A regiocontrolled synthesis of substituted indoles. *J. Org. Chem.* **53**, 1170-1176.
- Kropp, P. J., and Pienta, N. J. **1983**. Photochemistry of Alkyl-Halides .9. Geminal Dihalides. *J. Org. Chem.* **48**, 2084-2090.
- Kunick, C., Schultz, C., Lemcke, T., Zaharevitz, D. W., Gussio, R., Jaluri, R. K., Sausville, E. A., Leost, M., and Meijer, L. **2000**. 2-Substituted Paullones: CDK1/cyclin C inhibiting property and in vitro antiproliferative activity. *Bioorg. Med. Chem. Lett* **10**, 567-569.
- LaBaer, J., Garrett, M. D., Stevenson, L. F., Slingerland, J. M., Sandhu, C., Chou, H. S., Fattaey, A., and Harlow, E. **1997**. New functional activities for the p21 family of CDK inhibitors. *Genes Dev.* **11**, 847-862.
- Lee, J. S., Collins, K. M., Brown, A. L., Lee, C. H., and Chung, J. H. **2000**. hCds1-mediated phosphorylation of BRCA1 regulates the DNA damage response. *Nature* **404**, 201-204.
- Lee, S. E., Mitchell, R. A., Cheng, A., and Hendrickson, E. A. **1997**. Evidence for DNA-PK-dependent and independent DNA double-strand break repair pathways in mammalian cells as a function of the cell cycle. *Mol. Cell. Biol.* **17**, 1425-1433.
- Lieber, M., Smith, B., Szakal, A., Nelson-Rees, W., and Todaro, G. **1976**. A continuous tumour-cell line from a human lung carcinoma with properties of type II alveolar epithelial cells. *Int. J. Cancer.* **17**, 62-70.

- Liu, Q., Guntuku, S., Cui, X., Matsuoka, S., Cortez, D., Tamai, K., Luo, G., Carattini-Rivera, S., DeMayo, F., Bradley, A., Donehower, L., and Elledge, S. **2000**. Chk1 is an essential kinase that is regulated by Atr and required for the G(2)/M DNA damage checkpoint. *Genes. Dev.* **14**, 1448-1459.
- Lubisch, W., Grandel, R., Braje, W., Subkowski, T., Mueller, R., Wernet, W., and Drescher, K. **2003**. Preparation of dibenzodiazepine derivatives and use as inhibitors of poly (ADP-ribose) polymerase. *In* "WO 2003-EP192 20030110".
- Lukas, C., Bartkova, J., Latella, L., Falck, J., Mailand, N., Schroeder, T., Sehested, M., Lukas, J., and Bartek, J. **2001**. DNA damage-activated kinase Chk2 is independent of proliferation or differentiation yet correlates with tissue biology. *Cancer Res.* **61**, 4990-4993.
- Madani, H., Thompson, A. S., and Threadgill, M. D. **2002**. An expedient synthesis of 7-O-functionalised pyrrolo [2,1- c][1,4] benzodiazepine-5,11-diones. *Tetrahedron* **58**, 8107-8111.
- Makosza, M., and Kwast, E. **1995**. Vicarious nucleophilic substitution of hydrogen in nitroderivatives of five-membered heteromatic compounds. *Tetrahedron* **51**, 8339-8354.
- Malanga, M., and Althaus, F. R. **1994**. Poly(Adp-Ribose) Molecules Formed During DNA-Repair in-Vivo. *J. Biol. Chem.* **269**, 17691-17696.
- Markwalder, J. A., Arnone, M. R., Benfield, P. A., Boisclair, M., Burton, C. R., Chang, C. H., Cox, S. S., Czerniak, P. M., Dean, C. L., Doleniak, D., Grafstrom, R., Harrison, B. A., Kaltenbach, R. F., Nugiel, D. A., Rossi, K. A., Sherk, S. R., Sisk, L. M., Stouten, P., Trainor, G. L., Worland, P., and Seitz, S. P. **2004**. Synthesis and biological evaluation of 1-aryl-4,5-dihydro-1H-pyrazolo 3,4-d pyrimidin-4-one inhibitors of cyclin-dependent kinases. *J. Med. Chem* **47**, 5894-5911.
- Meijer, L. **1995**. Chemical inhibitors of cyclin dependent kinases. *Prog. Cell Cycle Res.* **1**, 351-363.
- Meijer, L. **1996**. Chemical inhibitors of cyclin dependent kinases. *Trends. Cell Biol.* **6**, 393-397.

- Meijer, L., Borgne, A., Mulner, O., Chong, J. P. J., Blow, J. J., Inagaki, N., Inagaki, M., Delcros, J. G., and Moulinoux, J. P. **1997**. Biochemical and cellular effects of roscovitine, a potent and selective inhibitor of the cyclin-dependent kinases cdc2, cdk2 and cdk5. *Eur. J. Biochem.* **243**, 527-536.
- Meijer, L., Leclerc, S., and Leost, M. **1999**. Properties and potential applications of chemical inhibitors of cyclin-dependent kinases. *Pharmacol. Ther.* **82**, 279-284.
- Meijer, L., Thunnissen, A., White, A. W., Garnier, M., Nikolic, M., Tsai, L. H., Walter, J., Cleverley, K. E., Salinas, P. C., Wu, Y. Z., Biernat, J., Mandelkow, E. M., Kim, S. H., and Pettit, G. R. **2000**. Inhibition of cyclin-dependent kinases, GSK-3 β and CK1 by hymenialdisine, a marine sponge constituent. *Chem. Biol.* **7**, 51-63.
- Morgan, D. O. **1995**. Principles of Cdk Regulation. *Nature* **374**, 131-134.
- Morgan, D. O., and Debonadt, H. L. **1994**. Protein-Kinase Regulation - Insights from Crystal-Structure Analysis. *Curr. Opin. Cell Biol.* **6**, 239-246.
- Moynahan, M. E., Chiu, J. W., Koller, B. H., and Jasin, M. **1999**. Brcal controls homology-directed DNA repair. *Mol. Cell.* **4**, 511-518.
- Murray, A., and Hunt, T. **1993**. "The Cell Cycle: an introduction," Freeman, W. H. and Company.
- Murray, A. W. **2004**. Recycling the cell cycle: cyclins revisited. *Cell* **116**, 221-234.
- Neidle, S., and Parkinson, G. **2002**. Telomere maintenance as a target for anticancer drug discovery. *Nature Rev. Drug. Dis.* **1**, 383-393.
- Newcomb, M., and Courtney, A. R. **1980**. Reactions of lithiostannanes with 6-halo-1-hexenes. *J.Org.Chem.* **45**, 1707-1708.
- Noble, M. E. M., and Endicott, J. A. **1999**. Chemical inhibitors of cyclin-dependent kinases: Insights into design from X-ray crystallographic studies. *Pharmacol. Ther.* **82**, 269-278.

- Noble, M. E. M., Endicott, J. A., Brown, N. R., and Johnson, L. N. **1997**. The cyclin box fold: protein recognition in cell-cycle and transcription control. *Trends Biochem. Sci.* **22**, 482-487.
- Noonberg, S. B., and Benz, C. C. **2000**. Tyrosine kinase inhibitors targeted to the epidermal growth factor receptor subfamily - Role as anticancer agents. *Drugs* **59**, 753-767.
- Nugiel, D. A., Etkorn, A. M., Vidwans, A., Benfield, P. A., Boisclair, M., Burton, C. R., Cox, S., Czerniak, P. M., Doleniak, D., and Seitz, S. P. **2001**. Indonopyrazoles as novel cyclin dependent kinase (CDK) inhibitors. *J. Med. Chem.* **44**, 1334-1336.
- Nurse, P. **1998**. Yoshio Masui and cell cycle control, past, present and future. *Biol. Cell.* **90**, 447-452.
- Nurse, P., Masui, Y., and Hartwell, L. **1998**. Understanding the cell cycle. *Nat. Med.* **4**, 1103-1106.
- Nyberg, K. A., Michelson, R. J., Putnam, C. W., and Weinert, T. A. **2002**. Toward maintaining the genome: DNA damage and replication checkpoints. *Annu. Rev. Genet.* **36**, 617-656.
- O'Neill, T., Giarratani, L., Chen, P., Iyer, L., Lee, C. H., Bobiak, M., Kanai, F., Zhou, B. B., Chung, J. H., and Rathbun, G. A. **2002**. Determination of substrate motifs for human Chk1 and hCds1/Chk2 by the oriented peptide library approach. *J. Biol. Chem.* **277**, 16102-16115.
- Obaya, A. J., and Sedivy, J. M. **2002**. Regulation of cyclin-Cdk activity in mammalian cells. *Cell. Mol. Life Sci.* **59**, 126-142.
- Ogle, C. A., Martin, S. W., Dziobak, M. P., Urban, M. W., and Mendenhall, G. D. **1983**. Decomposition rates, synthesis, and spectral properties of a series of alkyl hyponitrites. *J. Med. Chem.* **48**, 3728-3733.
- Okamoto, A., Demetrick, D. J., Spillare, E. A., Hagiwara, K., Hussain, S. P., Bennett, W. P., Forrester, K., Gerwin, B., Serrano, M., Beach, D. H., and Harris, C. C. **1994**.

- Mutations and Altered Expression of P16(Ink4) in Human Cancer. *Proc. Natl. Acad. Sci. USA* **91**, 11045-11049.
- Olgen, S., Akaho, E., and Nebioglu, D. **2001**. Synthesis and receptor docking studies of N-substituted indole-2-carboxylic acid esters as a search for COX-2 selective enzyme inhibitors. *Europ. J. Med. Chem.* **36**, 747-770.
- Oliver, A. W., Ame, J. C., Roe, S. M., Good, V., de Murcia, G., and Pearl, L. H. **2004**. Crystal structure of the catalytic fragment of murine poly (ADP-ribose) polymerase-2. *Nucleic Acids Res.* **32**, 456-464.
- Osada, S., and Saji, S. **2003**. New approach to cancer therapy: The application of signal transduction to anti-cancer drug. *Curr. Med. Chem. - Anti Cancer Agents* **3**, 119-131.
- Pavletich, N. P. **1999**. Mechanism of Cyclin-dependent kinase regulation: Structures of Cdk, their Cyclin Activators, and Cip and INK4 inhibitors. *J. Mol. Biol.* **287**, 821-828.
- Pecorino, L. **2005**. "Molecular biology of cancer: Mechanisms, Targets, and Therapeutics," Oxford University Press, New York.
- Peukert, S., and Schwahn, U. **2004**. New inhibitors of poly(ADP-ribose) polymerase (PARP). *Expert Opin. Ther. Patents* **14**, 1531-1551.
- Peyronneau, M., Boisdon, M. T., Roques, N., Mazieres, S., and Le Roux, C. **2004**. Total synergistic effect between triflic acid and bismuth (III) or antimony (III) chlorides in catalysis of the methanesulfonylation of arenes. *Eur. J. Org. Chem.*, 4636-4640.
- PezerRoger, I., Ivorra, C., Diez, A., Cortes, M. J., Poch, E., SanzGonzalez, S. M., and Andres, V. **2002**. Inhibition of cellular proliferation by drug targeting of cyclin-dependent kinases. [WWW] <http://www.bentham.org/cpb1-1/Vincente%20Andres/V%20andres.htm>.
- Piret, B., Legrandpoels, S., Sappey, C., and Piette, J. **1995**. Nf-Kappa-B Transcription Factor and Human-Immunodeficiency-Virus Type-1 (Hiv-1) Activation by Methylene-Blue Photosensitization. *Eur. J. Biochem.* **228**, 447-455.

- PlanasSilva, M. D., and Weinberg, R. A. **1997**. The restriction point and control of cell proliferation. *Curr. Opin. Cell Biol.* **9**, 768-772.
- Pommier, Y., Sordet, O., Rao, V. A., Zhang, H. L., and Kohn, K. W. **2005**. Targeting Chk2 kinase: Molecular interaction maps and therapeutic rationale. *Curr. Pharm. Design* **11**, 2855-2872.
- Puodziunaite, B., Kosychova, L., Janciene, R., and Stumbreviciute, Z. **1997**. 2,3-Dihydro-1H-1,5-benzodiazepines: A conversion of thiolactams to amidines. *Mon. Chem.* **128**, 1275-1281.
- Rahman, N., and Stratton, M. R. **1998**. The genetics of breast cancer susceptibility. *Annu. Rev. Genet.* **32**, 95-121.
- Raymond, E., Faivre, S., and Armand, J. P. **2000**. Epidermal growth factor receptor tyrosine kinase as a target for anticancer therapy. *Drugs* **60**, 15-23.
- Rialet, V., and Meijer, L. **1991**. A New Screening-Test for Antimitotic Compounds Using the Universal M Phase-Specific Protein-Kinase, P34cdc2 Cyclin Bcdc13, Affinity-Immobilized on P13suc1-Coated Microtitration Plates. *Anti-cancer Res.* **11**, 1581-1590.
- Ringo, J. **2004**. "Fundamental Genetics," 1st Ed. Cambridge University Press.
- Roberts, J. M., and Heichman, K. A. **1994**. Rules to replicate by. *Cell* **79**, 557-562.
- Russo, A. A., Jeffrey, P. D., Patten, A. K., Massague, J., and Pavletich, N. P. **1996**. Crystal structure of the p27(Kip1) cyclin-dependent-kinase inhibitor bound to the cyclin A Cdk2 complex. *Nature* **382**, 325-331.
- Rydon, H. N., and Tweddle, J. C. **1955**. Experiments on the synthesis of bz-substituted indoles and tryptophans. III. The synthesis of four bz-chloroindoles and -tryptophans. *J. Chem. Soc.*, 3499-3503.
- Sasaki, E., Kojima, H., Nishimatsu, H., Urano, Y., Kikuchi, K., Hirata, Y., and Nagano, T. **2005**. Highly sensitive near-infrared fluorescent probes for nitric oxide and their application to isolated organs. *J. Am. Chem.Soc.* **127**, 3684-3685.

- Sausville, E. A. **2003**. Cyclin-dependent kinase modulators studied at the NCI: pre-clinical and clinical studies. *Curr. Med. Chem. - Anti Cancer Agents* **3**, 47-56.
- Schultz, C., Link, A., Leost, M., Zaharevitz, D. W., Gussio, R., Sausville, E. A., Meijer, L., and Kunick, C. **1999**. Paullones, a series of cyclin-dependent kinase inhibitors: Synthesis, evaluation of CDK1/cyclin B inhibition, and in vitro antitumor activity. *J. Med. Chem.* **42**, 2909-2919.
- Schulze-Gahmen, U., Brandsen, J., Jones, H. D., Morgan, D. O., Meijer, L., Vesely, J., and Kim, S. H. **1995**. Multiple-Modes of Ligand Recognition - Crystal-Structures of Cyclin-Dependent Protein-Kinase-2 in Complex with Atp and two Inhibitors, Olomoucine and Isopentenyladenine. *Protein-Struct. Funct. Genet.* **22**, 378-391.
- Schulze-Gahmen, U., DeBondt, H. L., and Kim, S. H. **1996**. High-resolution crystal structures of human cyclin-dependent kinase 2 with and without ATP: Bound waters and natural ligand as guides for inhibitor design. *J. Med. Chem.* **39**, 4540-4546.
- Schulze-Osthoff, K., Los, M., and Baeuerle, P. A. **1995**. Redox signalling by transcription factors NF-kappa B and AP-1 in lymphocytes. *Biochem. Pharmacol.* **50**, 735.
- Serrano, M. **1997**. The tumor suppressor protein p16INK4a. *Exp. Cell Res.* **237**, 7-13.
- Serrano, M., Hannon, G. J., and Beach, D. **1993**. A New Regulatory Motif in Cell-Cycle Control Causing Specific Inhibition of Cyclin-D/Cdk4. *Nature* **366**, 704-707.
- Sharma, V., and Tepe, J. J. **2004**. Potent inhibition of checkpoint kinase activity by a hymenialdisine-derived indoloazepine. *Bioorg. Med. Chem. Lett.* **14**, 4319-4321.
- Sherr, C. J. **1993**. Mammalian G1 cyclins. *Cell* **73**, 1059-1065.
- Sherr, C. J. **1994**. G1 Phase Progression - Cycling on Cue. *Cell* **79**, 551-555.
- Sherr, C. J. **1996**. Cancer cell cycles. *Science* **274**, 1672-1677.
- Sherr, C. J., and Roberts, J. M. **1995**. Inhibitors of Mammalian G(1) Cyclin-Dependent Kinases. *Genes. Dev.* **9**, 1149-1163.

- Shieh, W. M., Ame, J. C., Wilson, M. V., Wang, Z. Q., Koh, D. W., Jacobson, M. K., and Jacobson, E. L. **1998**. Poly(ADP-ribose) polymerase null mouse cells synthesize ADP-ribose polymers. *J. Biol. Chem.* **273**, 30069-30072.
- Shiloh, Y., and Kastan, M. B. **2001**. ATM: Genome stability, neuronal development, and cancer cross paths. *In "Advances in Cancer Research, Vol 83"*, Vol. 83, pp. 209-254.
- Sielecki, T. M., Boylan, J. F., Benfield, P. A., and Trainor, G. L. **2000**. Cyclin-dependent kinase inhibitors: Useful targets in cell cycle regulation. *Journal of Medicinal Chemistry* **43**, 1-18.
- Skalitzky, D. J., Marakovits, J. T., Maegley, K. A., Ekker, A., Yu, X. H., Hostomsky, Z., Webber, S. E., Eastman, B. W., Almassy, R., Li, J., Curtin, N. J., Newell, D. R., Calvert, A. H., Griffin, R. J., and Golding, B. T. **2003**. Tricyclic benzimidazoles as potent poly (ADP-ribose) polymerase-1 inhibitors. *J. Med. Chem.* **46**, 210-213.
- Smith, S. **2001**. The world according to PARP. *Trends Biochem.Sci.* **26**, 174-179.
- Smith, S., and de Lange, T. **2000**. Tankyrase promotes telomere elongation in human cells. *Curr. Biol.* **10**, 1299-1302.
- Smith, S., Giriat, I., Schmitt, A., and de Lange, T. **1998**. Tankyrase, a poly(ADP-ribose) polymerase at human telomeres. *Science* **282**, 1484-1487.
- Solomon, M. J., Glotzer, M., Lee, T. H., Philippe, M., and Kirschner, M. W. **1990**. Cyclin Activation of P34cdc2. *Cell* **63**, 1013-1024.
- Solute, H. D., Vasquez, J., Long, A., Albert, S., and Brennan, M. **1973**. A human cell line from a pleural effusion derived from a breast carcinoma. *J.Nat. Can.* **51**, 1409-1416.
- Sordet, O., Khan, Q., Kohn, K., and Pommier, Y. **2003**. Apoptosis induced by topoisomerase inhibitors. *Curr. Med. Chem. Anti-Canc. Agents* **3**, 271-290.
- Southan, G. J., and Szabo, C. **2003**. Poly(ADP-ribose) polymerase inhibitors. *Curr. Med. Chem.* **10**, 321-340.

- Strazzolini, P., and Runcio, A. **2003**. Oxidation of benzylic alcohols and ethers to carbonyl derivatives by nitric acid in dichloromethane. *Europ. J. Org. Chem.* **3**, 526-536.
- Suganuma, M., Kawabe, T., Hori, H., Funabiki, T., and Okamoto, T. **1999**. Sensitization of cancer cells to DNA damage-induced cell death by specific cell cycle G2 checkpoint abrogation. *Cancer Res.* **59**, 5887-5891.
- Suto, M. J., Turner, W. R., Arundelsuto, C. M., Werbel, L. M., and Seboltleopold, J. S. **1991**. Dihydroisoquinolinones - the Design and Synthesis of a New Series of Potent Inhibitors of Poly(ADP-Ribose) Polymerase. *Anti-Cancer Drug Design.* **6**, 107-117.
- Swanton, C. **2004**. Cell cycle targeted therapies. *lancet. oncol.* **5**, 27-36.
- Taylor, S. S., and Radzioandzelm, E. **1994**. Three Protein-Kinase Structures Define a Common Motif. *Structure* **2**, 345-355.
- Tenzer, A., and Pruschy, M. **2003**. Potentiation of DNA-damage-induced cytotoxicity by G₂ checkpoint abrogators. *Curr. Med. Chem. - Anti Cancer Agents* **3**, 35-46.
- Toledo, L. M., Lydon, N. B., and Elbaum, D. **1999**. <http://www.chemsoc.org/exemplarchem/entries/jagfin/jagfin/contents/therap.htm>.
- Tominaga, K., Morisaki, H., Kanako, Y., Fujimoto, A., Tanaka, T., Ohtsubo, M., Hirai, M., Okayama, H., Ikeda, K., and Nakanishi, M. **1999**. Role of human Cds1 (Chk2) kinase in DNA damage checkpoint and its regulation by p53. *J. Biol. Chem.* **274**, 31463-31467.
- Traxler, P., and Furet, P. **1999**. Strategies toward the design of novel and selective protein tyrosine kinase inhibitors. *Pharmacol. Ther.* **82**, 195-206.
- Vass, A., Dudas, J., Toth, J., and Varma, R. S. **2001**. Solvent-free reduction of aromatic nitro compounds with alumina-supported hydrazine under microwave irradiation. *Tet. Lett.* **42**, 5347-5349.

- Veeranna, G. J., Shetty, K. T., Amin, N., Grant, P., Albers, R. W., and Pant, H. C. **1996**. Inhibition of neuronal cyclin-dependent kinase-5 by staurosporine and purine analogs is independent of activation by munc-18. *Neurochem. Res.* **21**, 629-636.
- Velu, T. J. **1990**. Structure, function and transforming potential of the epidermal growth factor receptor. *Mol. Cell. Endocrinol.* **70**, 205-216.
- Vesely, J., Havlicek, L., Strnad, M., Blow, J. J., Donelladeana, A., Pinna, L., Letham, D. S., Kato, J., Detivaud, L., Leclerc, S., and Meijer, L. **1994**. Inhibition of Cyclin-Dependent Kinases by Purine Analogs. *Eur. J. Biochem.* **224**, 771-786.
- Vidal, A., and Koff, A. **2000**. Cell-cycle inhibitors: three families united by a common cause. *Gene* **247**, 1-15.
- Virag, L., and Szabo, C. **2002**. The therapeutic potential of poly(ADP-ribose) polymerase inhibitors. *Pharmacol. Rev.* **54**, 375-429.
- Walker, D. H. **1998**. Small-molecule inhibitors of cyclin-dependent kinases: Molecular tools and potential therapeutics. *Curr. Top. Microbiol. Immunol.* **227**, 149-165.
- Wan, Y., Hur, W., Cho, C., Liu, Y., Adrian, F., Lozach, O., Bach, S., Mayer, T., Fabbro, D., Meijer, L., and Gray, N. **2004**. Synthesis and target identification of hymenialdisine analogs. *Chem. Biol.* **11**, 247-259.
- Wang, H., Zeng, Z., Bui, T., DiBiase, S., Qin W, X. F., Powell, S., and Iliakis, G. **2001**. Nonhomologous end-joining of ionizing radiation-induced DNA double-stranded breaks in human tumor cells deficient in BRCA1 or BRCA2. *Cancer Res.* **61**, 270-277.
- Wang, Z. Q., Auer, B., Stingl, L., Berghammer, H., Haidacher, D., Schweiger, M., and Wagner, E. F. **1995**. Mice Lacking Adprt and Poly(Adp-Ribosyl)Ation Develop Normally but Are Susceptible to Skin-Disease. *Genes Dev.* **9**, 509-520.
- Ward, I. M., Wu, X. L., and Chen, J. J. **2001**. Threonine 68 of Chk2 is phosphorylated at sites of DNA strand breaks. *J. Biol. Chem.* **276**, 47755-47758.
- Webb II, R. R., Venuti, M. C., and Eigenbrot, C. **1991**. Synthesis of a tetramethyl analogue of teleocidin. *J.Org.Chem.* **56**, 4706-4713.

- Webber, S. E., Canan-Koch, S. S., Tikhe, J., and Thoresen, L. H. **2000**. Preparation of 3,4-dihydropyrrolo[4,3,2-de]isoquinolin-5(1H)-ones and analogs as poly(ADP-ribose)polymerase inhibitors. *In* "200004204".
- Weinfeld, M., Chaudhry, M. A., Damours, D., Pelletier, J. D., Poirier, G. G., Povirk, L. F., and LeesMiller, S. P. **1997**. Interaction of DNA-dependent protein kinase and poly(ADP-ribose) polymerase with radiation-induced DNA strand breaks. *Radiat. Res.* **148**, 22-28.
- Whitacre, C. M., Hashimoto, H., Tsai, M. L., Chatterjee, S., Berger, S. J., and Berger, N. A. **1995**. Involvement of Nad-Poly(Adp-Ribose) Metabolism in P53 Regulation and Its Consequences. *Cancer Res.* **55**, 3697-3701.
- White, A. W., Almassy, R., Calvert, A. H., Curtin, N. J., Griffin, R. J., Hostomsky, Z., Maegley, K., Newell, D. R., Srinivasan, S., and Golding, B. T. **2000**. Resistance-modifying agents. 9. Synthesis and biological properties of benzimidazole inhibitors of the DNA repair enzyme poly(ADP-ribose) polymerase. *J. Med. Chem.* **43**, 4084-4097.
- Whitten, J. P., Matthews, D. P., and McCarthy, J. R. **1986**. [2-(Trimethylsilyl)ethoxy]methyl (SEM) as a novel and effective imidazole and fused aromatic imidazole protecting group. *J.Org.Chem.* **51**, 1891-1894.
- Wirger, A., Perabo, F. G. E., Burgemeister, S., Haase, L., Schmidt, D. H., Doehn, C., Mueller, S. C., and Jocham, D. **2005**. Flavopiridol, an inhibitor of cyclin-dependent kinases, induces growth inhibition and apoptosis in bladder cancer cells in vitro and in vivo. *Anti-Cancer Research.* **25**, 4341-4347.
- Xiao, Z., Chen, Z. H., Gunasekera, A. H., Sowin, T. J., Rosenberg, S. H., Fesik, S., and Zhang, H. Y. **2003**. Chk1 mediates S and G(2) arrests through Cdc25A degradation in response to DNA-damaging agents. *J. Biol. Chem.* **278**, 21767-21773.
- Yanlui, V. W., and Grandis, J. R. **2002**. EGFR-Mediated cell cycle regulation. *Anti-Cancer Res.* **22**, 1-11.

- Yao, S. L., Akhtar, A. J., McKenna, K. A., Bedi, G. C., Sidransky, D., Mabry, M., Ravi, R., Collector, M. I., Jones, R. J., Sharkis, S. J., Fuchs, E. J., and Bedi, A. **1996**. Selective radiosensitization of p53-deficient cells by caffeine-mediated activation of p34(cdc2) kinase. *Nat. Med.* **2**, 1140-1143.
- Yu, Q., La Rose, J., Zhang, H. L., Takemura, H., Kohn, K. W., and Pommier, Y. **2002**. UCN-01 inhibits p53 up-regulation and abrogates gamma- radiation-induced G(2)-M checkpoint independently of p53 by targeting both of the checkpoint kinases, Chk2 and Chk1. *Cancer Res.* **62**, 5743-5748.
- Zaharevitz, D. W., Gussio, R., Leost, M., Senderowicz, A. M., Lahusen, T., Kunick, C., Meijer, L., and Sausville, E. A. **1999a**. Discovery and initial characterization of the paullones, a novel class of small-molecule inhibitors of cyclin-dependent kinases. *Cancer Res.* **59**, 2566-2569.
- Zaharevitz, D. W., Gussio, R., Wiegand, A., Jalluri, R., Pattabiraman, N., Kellogg, G. E., Pallansch, L. A., Yang, S. S., and Buckheit, R. W. **1999b**. Discovery of novel HIV-1 reverse transcriptase inhibitors using a combination of 3D database searching and 3D QSAR. *Med. Chem. Res.* **9**, 551-564.
- Zetterberg, A., Larsson, O., and Wiman, K. G. **1995**. What Is the Restriction Point. *Curr. Opin. Cell Biol.* **7**, 835-842.
- Zhang, X., Mar, V., Zhou, W., Harrington, L., and Robinson, M. **1999**. Telomere shortening and apoptosis in telomerase-inhibited human tumor cells. *Genes Dev* **13**, 2388-2399.
- Zhou, B., and Sausville, E. **2003**. Drug discovery targeting Chk1 and Chk2 kinases. *Prog. Cell Cycle Res.* **5**, 413-421.
- Zhou, B. B. S., Anderson, H. J., and Roberge, M. **2003**. Targeting DNA checkpoint kinases in cancer therapy. *Cancer Biol. Ther.* **2**, S16-S22.
- Zhou, B. B. S., and Bartek, J. **2004**. Targeting the checkpoint kinases: chemosensitization versus chemoprotection. *Nat. Rev. Cancer* **4**, 216-225.

Zhou, B. B. S., and Elledge, S. J. **2000**. The DNA damage response: putting checkpoints in perspective. *Nature* **408**, 433-439.

APPENDIX A

PROCEDURE USED WITHIN THE RESEARCH GROUP TO GENERATE THE CHK2 HOMOLOGY MODEL

A homology model was obtained using Modeller with 2Cpk and 2Phk pdb files as templates. The final model was refined by correcting amino acid outsiders. The supposed active site is located in a conserved region between a set of beta sheets and alpha helices, a hinge-like region of the protein. The active site was too cluttered with side-chains to generate any docking results. In order to accommodate a ligand inside the active site, “infinite dynamics” were applied to the protein, until a high-energy state was reached. This open state of the protein was then suitable to accommodate the ligand, the latter was positioned in the active site where the docking box (MOE default setting) incorporated the residues suspected to interact with our inhibitor. The backbone of the enzyme was then fixed, and a first docking was then achieved by simulating annealing (one input and high number of cycles). This docking was monitored by the energy level of the system until a plateau was reached, where the ligand hardly moved and seemed stable in the cleft. Once the molecule docked, the all system’s energy was minimised using molecular mechanics (MMFF94X) and by electronic algorithms (PM3). Then, the ligand was docked in this less cluttered active site using the same parameters as the previous docking until one result was obtained. The stability of this ligand docked in the protein could be assessed by applying molecular dynamics on the entire complex, and checking on any fluctuations of the ligand. As the ligand hardly moved, one could assume that the docking was successful.

